CHIRAL PROTON CATALYSIS: DESIGN AND DEVELOPMENT OF ENANTIOSELECTIVE AZA-HENRY AND DIELS-ALDER REACTIONS

Ryan A. Yoder

Accepted by the Graduate Faculty, Indiana University, in partial fulfillment of the
requirements for the degree of Doctor of Philosophy.

Doctoral Committee

_____

Jeffrey N. Johnston, Ph.D.

_____

Daniel J. Mindiola, Ph.D.

_____

David R. Williams, Ph.D.

_____

Jeffrey Zaleski, Ph.D.

April 24, 2008

DEDICATION

This work is dedicated to my parents, David and Doreen Yoder, and my sister, LeeAnna Loudermilk. Their unwavering love and support provided the inspiration for me to pursue my dreams. The sacrifices they have made and the strength they have shown continue to motivate me to be a better person each and every day. Thank you mom, dad, and little sis for being the rocks that I can lean on and the foundation that allowed me to find the happiness I have today. Without you, none of this would have been possible.

ACKNOWLEDGEMENTS

ABSTRACT

Ryan A. Yoder

CHIRAL PROTON CATALYSIS: DESIGN AND DEVELOPMENT OF ENANTIOSELECTIVE AZA-HENRY AND DIELS-ALDER REACTIONS

The proton (H+) is arguably Nature's most common Lewis acid and is utilized by many enzymes to carry out asymmetric transformations. These "natural" Brønsted acid catalysts have served as an inspiration to synthetic organic chemists for the development of both regioselective and stereoselective bond forming reactions. Inspired by Nature's elegance and motivated by the demand for inexpensive, robust and environmentally friendly catalysts, a Brønsted acid catalyst called the chiral proton was developed. This catalyst relies upon polar ionic hydrogen bonding for substrate activation and as a primary control element for enantioselection. The catalyst system was based on a coordination complex between a proton and a chiral, C2-symmetric BisAMidine ligand (BAM).

This complex has demonstrated the ability to both activate and control the absolute and relative stereochemistry in the addition of silyl nitronates to Boc-protected imines. It was further demonstrated that nitroalkanes could be used in place of silyl nitronates (aza-Henry reaction), eliminating the need for preformation of the nucleophile. In the latter reaction, the amount of catalyst could be reduced to as low as 1 mol% without loss of enantioselectivity, attesting to the BAM ligand's ability to sequester protons from bulk solvent. The products of this reaction provide access to enantioenriched 1,2-diamines.

Furthermore, this catalyst system has been successfully applied to the enantioselective synthesis of both syn and anti α,β-diamino acids.

The chiral BAM-protic acid complexes were further applied to the stereoselective intramolecular hetero-Diels-Alder reactions of azadienes. These catalysts were found to influence both the endo/exo selectivity, as well as the facial selectivity of the [4+2] cycloadditions. The azadienes used in this study were modeled after the putative Diels-Alder precursors in the biosynthesis of the brevianamide class of natural products. In addition, a novel Diels-Alder reaction was hypothesized as an alternative route to the synthesis of oseltamivir phosphate (Tamiflu). A model system was chosen to examine the effectiveness of this route. The chiral proton catalyst was shown to catalyze this model reaction to produce the desired exo Diels-Alder adduct.

_____

_____

_____

_____

TABLE OF CONTENTS

LIST OF TABLES

LIST OF FIGURES

LIST OF CHARTS

LIST OF SCHEMES

xiv

Chapter 1. Chiral Proton Catalysis and Activation Using Hydrogen Bonds: An Overview

1.1. How Nature Serves as an Inspiration for Asymmetric Catalysis

Understanding the biosynthesis of natural products provides chemists a glimpse at how nature establishes complexity into large molecules. This process and its typical complexity can guide the synthetic chemist in the discovery of new bond forming reactions that are both regioselective and stereoselective. Understanding how nature is able to build these complex molecules can also provide insight into unique methods for small molecule activation.

Among biosynthetic reactions, the cascade cyclization of squalene to various triterpene natural products is a prominent example of a complexity-generating, asymmetric chemical transformation that is unmatched by any synthetic catalyst/reaction combination. Since Woodward and Bloch's proposal in 1953,[1] and the introduction of the Stork-Eschenmoser hypothesis soon thereafter,[2,3] biomimetic cascade cyclizations have been an inspiration for synthetic chemists. In the past 10 years, biochemists have made significant progress in the understanding of how nature converts squalene to hopene enantioselectively in bacteria.[4] There have been equally outstanding developments in the area of non-enzymatic enantioselective π-cation cascade cyclizations over the past decade. These remarkable mechanistic and synthetic accomplishments have been recently reviewed[5] and will be highlighted in Sections 1.1.1 and 1.1.2.

1.1.1. Probing the Role of the Enzyme

Biochemists have recently employed sophisticated tools to elucidate how an enzyme's active site can control a cascade cyclization (Figure 1). Among them is the site-

---

[1] Woodward, R. B.; Bloch, K. *J. Am. Chem. Soc.* **1953**, *75*, 2023.
[2] Stork, G.; Burgstahler, A. W. *J. Am. Chem. Soc.* **1955**, *77*, 5068.
[3] (a) Gamboni, G.; Schinz, H.; Eschenmoser, A. *Helv. Chim. Acta* **1954**, *37*, 964. Note: translation of original text provided by Professor Eschenmoser (ETH), private communication. (b) Eschenmoser, A.; Ruzika, L.; Jegger, O.; Arigoni, D. *Helv. Chim. Acta.* **1955**, *38*, 1890.
[4] It should be noted that the corresponding process in eukaryotes (the cascade cyclization of oxidosqualene to lanosterol) is a diastereoselective process.
[5] Yoder, R.A.; Johnston, J. N. *Chem. Rev.* **2005**, *105*, 4730.

directed mutagenesis studies initially reported by Poralla in 1996.[6] The following year (1997) Schulz reported the first X-ray crystal structure of squalene-hopene cyclase (SHC) refined to 2.9 Å resolution[7] and later to 2.0 Å resolution.[8] In 2004 Schulz successfully cocrystallized SHC with the known inhibitor 2-azasqualene in the active site.[9] In conjuction with site-directed mutagenesis, the key residues and the role they play can now be better understood.

Figure 1. Enzymatic control over cascade cyclization
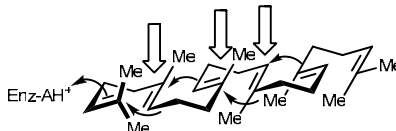
In order to probe the SHC active site for key residues, Poralla mutated Asp376, the residue believed to initiate cyclization by protonation of squalene (Figure 2). Replacement of Asp376 with Glu significantly diminished the relative activity of the cyclase to just 10% of the wild-type, while replacement of Asp376 with Gln or Arg resulted in complete loss of all enzyme activity. Although replacement with Gly showed some activity, it was 0.1% that of wild-type. Furthermore, Asp377 was also exchanged with Glu, Gln, Gly, and Arg, dropping activities to less than 1% in all cases.

Figure 2. X-Ray crystal structure of 2-azasqualene-bound SHC illustrating residues necessary for activation (protonation)
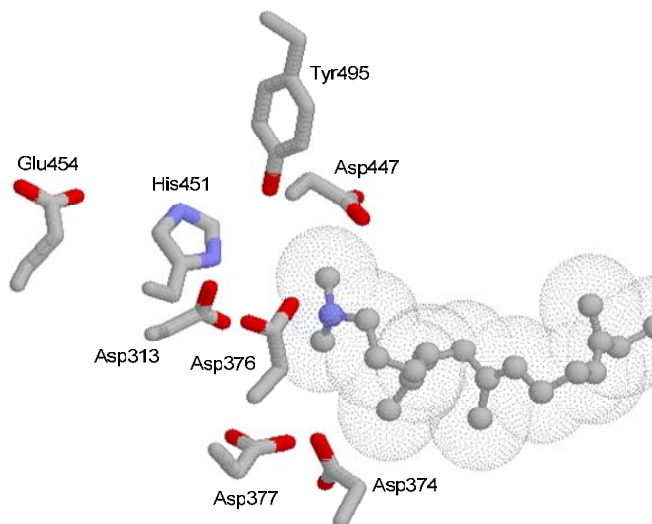
[6] Feil, C.; Sussmuth, R.; Jung, G.; Poralla, K. *Eur. J. Biochem.* **1996**, *242*, 51.
[7] Wendt, K. U.; Poralla, K.; Schulz, G. E. *Science* **1997**, *277*, 1811.
[8] Wendt, K. U.; Lenhart, A.; Schulz, G. E. *J. Mol. Biol.* **1999**, *286*, 175.
[9] Reinert, D. J.; Balliano, G.; Schulz, G. E. *Chem. Biol.* **2004**, *11*, 121.

At the front of the active site cavity are Asp374 and Asp377 which are important to catalysis and conserved throughout the cyclases. These residues are believed to bear a negative charge to balance the positive charge of Asp376 and His451. Moreover, the role of the protonated histidine is to activate the aspartic acid residue by increasing its acidity, and therefore the electrophilicity of the proton for C3 of squalene. The resulting positive charge at squalene C2 is in turn stabilized by the squalene 6,7-olefin that has already arranged conformationally for the cascade reaction.

Rohmer and Poralla also determined the importance of the His451 residue using site-directed mutagenesis in 1999.[10] Replacement of His451 with Ala provided the same product pattern as the wild-type, but at a much slower rate. This presumably follows from the acid-strengthening effect of His451 on Asp376 but its otherwise innocuous steric influence. It is significant to note that His451 is not a conserved residue among SHCs, so complete inactivation was not expected by this mutation. It is often replaced by Arg in other cyclases and believed to function analogously.

Site-directed mutagenesis has also indicated the existence of a secondary support mechanism that provides activation of residues along the front line. For example, substitution of Tyr495 by Phe resulted in complete loss of activity due simply to removal of the hydroxyl group. However, when Tyr495 is replaced with Ala, the mutant activity was attenuated by 48% relative to native enzyme, despite the lack of a hydrogen-bond donor.[11] The suggestion then followed that Tyr495 activates Asp376 prior to the initial protonation through hydrogen bonding between the phenolic hydroxyl group, a water molecule, and the aspartic acid residue.[12,13]

Although the existence of discrete carbenium ion intermediates has yet to be unequivocally confirmed or eliminated from consideration, the large number of aromatic residues resident in the active site has led to the suggestion that they may stabilize any positive charge(s) that develops (Figure 3). Loss of this stabilization might lead to

[10] Merkofer, T.; Pale-Grosdemange, C.; Wendt, K. U.; Rohmer, M.; Poralla, K. *Tetrahedron Lett.* **1999**, *40*, 2121.
[11] Sato, T.; Hoshino, T. *Biosci. Biotechnol. Biochem.* **2001**, *65*, 2233.
[12] Wendt, K. U.; Schulz, G. E.; Corey, E. J.; Liu, D. R. *Angew. Chem. Int. Ed.* **2000**, *39*, 2812.
[13] Füll, C.; Poralla, K. *FEMS Microbiol. Lett.* **2000**, *183*, 221.

truncated polycycles that result from premature termination of the carbenium ion. The role of these aromatic residues was examined by Poralla as well as Hoshino.[14]

Figure 3. X-Ray crystal structure of 2-azasqualene-bound SHC illustrating residues necessary for charge stabilization during polycyclization
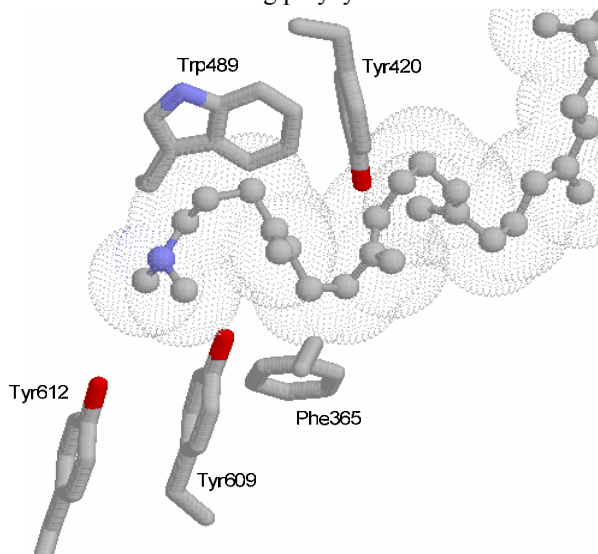
Phe365 is highly conserved among both prokaryotic and eukaryotic species of cyclase enzymes. When Phe365 is mutated to Ala, bicyclic products are obtained, presumably from loss of stabilization of the bicyclic carbocation. In order to test this hypothesis, Hoshino replaced Phe365 with the more electron rich Tyr and observed a 41-fold acceleration in rate compared to the wild-type.[15]

Tyr609 is also positioned in the active site to stabilize the bicyclic carbenium ion. Mutagenesis experiments that replaced Tyr609 with Ala produced bicyclic compounds, suggesting that Tyr609 may in fact also serve to stabilize the bicyclic carbocation. However, mutation of Tyr609 with Ala only produced these bicyclic products in 50% yield, whereas Phe365 replacement by Ala formed them in 96% yield. Furthermore, replacement of Tyr609 with Phe does not stop the cascade process at the bicyclic carbocation. This suggests that the aromatic π-electrons, rather than the hydroxyl group, are necessary for stabilization of the bicyclic carbenium ion by Phe365.

Phe601 is also a highly conserved residue in both species of squalene cyclases (Figure 4). This residue is believed to stabilize the C19 carbenium ion that results from a

---

[14] Hoshino, T.; Sato, T. *Chem. Commun.* **2002**, 291.
[15] Hoshino, T.; Sato, T. *Chem. Commun.* **1999**, 2005.

5-*exo* Markovnikov D-ring closure. This stabilization allows for ring expansion, followed by E-ring closure.

Figure 4. X-Ray crystal structure of 2-azasqualene-bound SHC illustrating residues necessary for charge stabilization during polycyclization
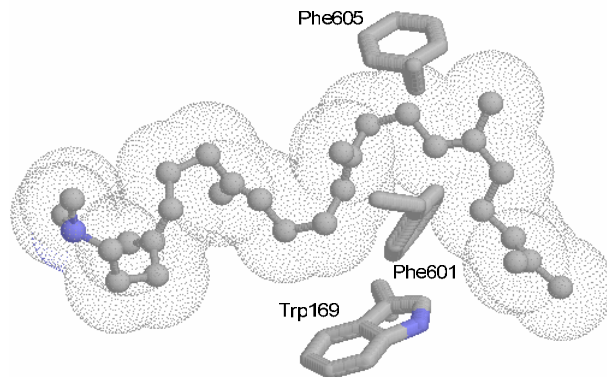
Poralla and Hoshino[16] replaced Phe601 by Ala and the resulting product distribution was significantly different from that of the native enzyme. There was a significant increase in the formation of the 5-*exo* D-ring closure product, supporting the theory that the D-ring closure is initially a 5-*exo* process followed by ring expansion and E-ring closure.

Phe605 is present in all prokaryotic squalene-hopene cyclases that form the pentacyclic hopene skeleton, but it is not conserved in lanosterol synthase in which a tetracyclic skeleton is formed. When Phe605 was mutated to Ala, the activity decreased by 67% relative to the native enzyme.[17] However, when Phe605 was mutated to either of the more electron rich Tyr and Trp residues, the relative activity increased by 165% and 256%, respectively. This increase in rate was interpreted as Phe605's facilitation of the 5-membered D-ring expansion to the 6-membered D-ring. Moreover, Phe605 may be involved in stabilization of the hopanyl cation prior to loss of proton and formation of the neutral product.

1.1.2. Enantioselective Biomimetic Organic Syntheses

"Can truly enantioselective biomimetic cyclization of isoprenoids be achieved in vitro?"[18] This question was raised by de la Torre and Sierra in their recent review on

[16] Hoshino, T.; Kouda, M.; Abe, T.; Ohashi, S. *Biosci. Biotechnol. Biochem.* **1999**, *63*, 2038.
[17] Hoshino, T.; Kouda, M.; Abe, T.; Sato, T. *Chem. Commun.* **2000**, 1485.
[18] De la Torre, M. C.; Sierra, M. A. *Angew. Chem. Int. Ed.* **2004**, *43*, 160.

biomimetic organic synthesis. The best answer to that question to date can be found in the work of Yamamoto using a Lewis acid-assisted chiral Brønsted acid (LBA, Figure 5).

Figure 5. Yamamoto's LBA catalysts
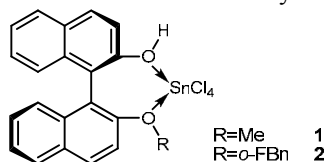
In 1999, Yamamoto developed the first enantioselective biomimetic cyclization of a polyprenoid using LBA **1** as an artificial cyclase to synthesize (-)-ambrox (**4**).[19] The cyclization of homofarnesol (**3**) promoted by LBA **1** proceeded with 42% ee (Scheme 1, eq 1). This enantioselective cyclization was further improved in 2002 using LBA **2** as the promoter.[20] The ether (-)-**4** was obtained in 54% yield with 75% ee and 3:1 dr from **3** utilizing an enantioselective cyclization, silylation, and diastereoselective cyclization sequence.

Scheme 1. Yamamoto's enantioselective olefin protonation-initiated polycyclization
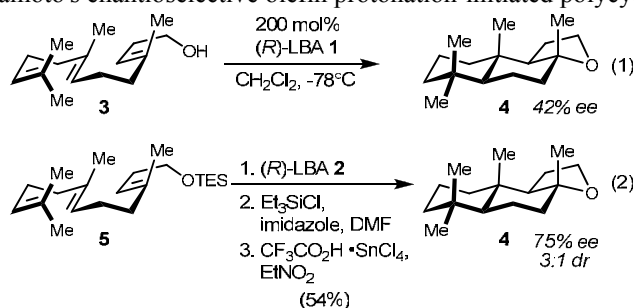
Yamamoto also applied LBA **2** to the enantioselective cyclization of polyprenoids in which the terminating group is an aromatic ring instead of the more nucleophilic hydroxyl terminator which was present in homofarnesol. LBA **2** promotes the cyclization of **6** to a mixture of **7** and **8** (Scheme 2).

---

[19] Ishihara, K.; Nakamura, S.; Yamamoto, H. *J. Am. Chem. Soc.* **1999**, *121*, 4906.
[20] Ishihara, K.; Ishibashi, H.; Yamamoto, H. *J. Am. Chem. Soc.* **2002**, *124*, 3647.

Scheme 2. Yamamoto's enantioselective synthesis of (5*S*,10*S*)-**7**
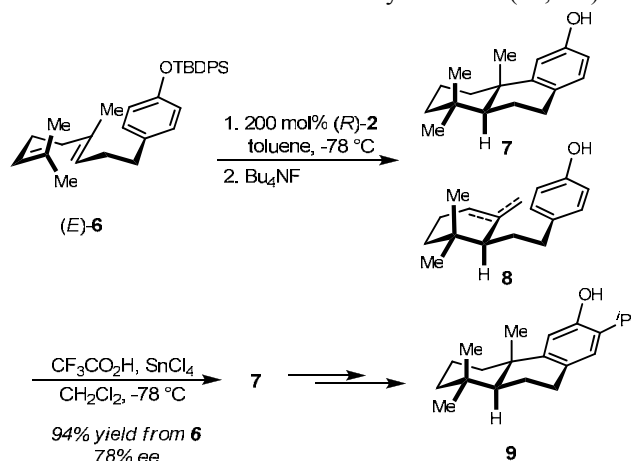
The mixture was then treated with an achiral Lewis acid (boron trifluoride etherate) in order to complete the cyclization to tricycle **7**. The first two rings are formed in approximately 78% ee. Since (±)-**7** had previously been reported by King[21] and Ghatak en route to the total synthesis of ferruginol (**9**),[22] this marked the first formal synthesis of enantioenriched ferruginol.

In an early review by van Tamelen, he defined a biogenetic-type or biomimetic synthesis as "an organic synthesis designed to follow, in at least its major aspects, biosynthetic pathways proved, or presumed, to be used in the natural construction of the end product."[23] In the spirit of this definition, Yamamoto *et al.* have completed biomimetic, and for the first time enantioselective, formal syntheses of several natural products. Although not all LBA catalyzed total syntheses will be listed here,[24,25,26,27] perhaps Yamamoto's most impressive enantioselective cyclization to date was on substrate **10** (Scheme 3). Again, he utilized his two-step procedure of initial enantioselective formation of the A ring, followed by diastereoselective formation of the B ring. This sequence provided product **14** in a remarkable 89% yield and 75% ee. This compound is easily converted to **15** which is an intermediate in the total syntheses of isophyllocladene, phyllocladene, hibaone, manool, sclareol, manoyl oxide, isoabienol,

[21] King, F. E.; King, T. J.; Topliss, J. G. *J. Chem. Soc.* **1957**, 573.

[22] Banik, B. K.; Chakraborti, A. K.; Ghatak, U. R. *J. Chem. Res. (S)* **1986**, 3391.

[23] Van Tamelen, E. E. *Fortscr. Chem Org. Naturst.* **1961**, *19*, 242.

[24] Nakamura, S.; Ishihara, K.; Yamamoto, H. *J. Am. Chem. Soc.* **2000**, *122*, 8131.

[25] Ishihara, K.; Ishibashi, H.; Yamamoto, H. *J. Am. Chem. Soc.* **2001**, *123*, 1505.

[26] Ishibashi, H.; Ishihara, K.; Yamamoto, H. *Chem. Rec.* **2002**, *2*, 177.

[27] Kumazawa, K.; Ishihara, K.; Yamamoto, H. *Org. Lett.* **2004**, *6*, 2551.

trans-abienol, and anticopelic acid.[28] Remarkably, this represents the enantioselective formal syntheses of nine naturally occurring compounds.

Scheme 3. Yamamoto's enantioselective synthesis of (5*S*,10*S*)-**14**
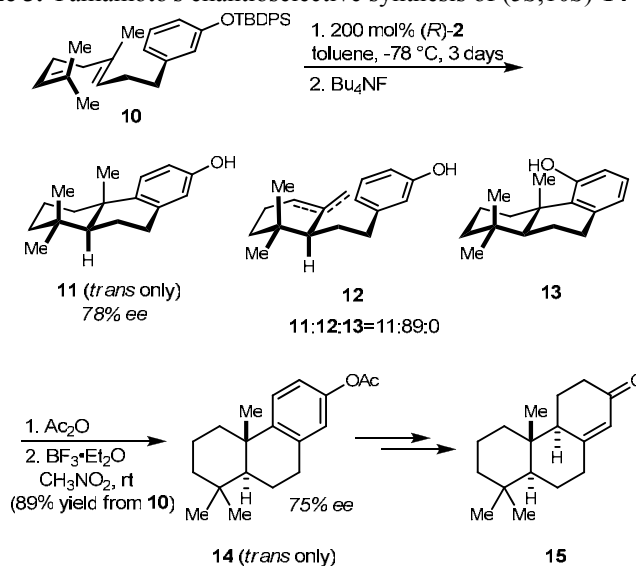
The realization of a truly enantioselective biomimetic cyclization is arguably among the greatest contributions to this field to date. The idea that induction from a noncovalently-bound source of asymmetry could control an entire cascade of events leading to multiple ring formation as well as controlling several asymmetric centers may have been previously thought to be unachievable without the size and complexity of a protein. This concept also goes a long way toward supporting the theory of minimal enzymatic assistance, which states that the enzyme may only activate the substrate for cyclization and prevent alternative modes of cyclization from occurring.[29]

This new frontier is presented to us by the same chemistry that inspired chemists for decades. Incredible advances have been made in the last ten years both in the understanding of how nature performs such elegant reactions, as well as in the laboratory in the development of nonenzymatic enantioselective total syntheses. Fifty years after the Stork-Eschenmoser hypothesis, chemists continue to be inspired by the complex molecules made by Nature as well as by the catalysts which enable Nature to make those molecules.

---

[28] Jannsen, C. G.; Godefroi, E. F. *J. Org. Chem.* **1982**, *47*, 3274.

[29] Abe, I.; Rohmer, M.; Prestwich, G. D. *Chem. Rev.* **1993**, *93*, 2189.

1.2. Asymmetric Brønsted Acid Catalysis

Through the process of evolution, Nature has developed sophisticated protein catalysts to produce a seemingly unlimited library of chiral complex molecules. As mentioned in Section 1.1.1, Nature has established hydrogen bonding as a powerful method to both activate and orient substrates for a chemical reaction. Perhaps inspired by Nature's elegant peptide catalysts, chemists have dramatically increased the successful use of hydrogen bonds in asymmetric catalysis. In large part, this interest stems from the ability to accelerate a reaction in the same way as traditional Lewis acids, but without the need of a heavy metal. As such, these so-called organic catalysts (or 'organocatalysts') are both environmentally friendly and cost-effective alternatives to traditional Lewis acid catalysts. Although Brønsted acids have been known to catalyze many organic reactions since the 19th century, the area of metal-free asymmetric Brønsted acid catalysis has remained unexplored until recent years.

The history of chiral organocatalysis can be traced back to the pioneering work of Hajos and Parrish at Hoffmann La Roche,[30] and Eder, Sauer, and Wiechert at Schering.[31] During the 1970's, these two industrial groups discovered that proline was an effective enantioselective catalyst in classic aldol condensations. More recently others have expanded this methodology to a number of reactions including Michael additions, Diels-Alder cycloadditions, and Mannich reactions.[32] These catalysts have been shown to function by covalently bonding to the substrate, forming chiral intermediates such as enamines and iminium ions, which in turn facilitate diastereoselective reactions. Although there has been extensive research in the area of proline-catalyzed asymmetric reactions, the focus here will remain on chiral Brønsted acid catalysis, as this relates more directly to our research efforts. Specifically, the discussion will focus on the use of hydrogen bonds to both accelerate the rate of a reaction as well as serve as the primary source of stereocontrol.

---

[30] Hajos, Z. G.; Parrish, D. R. *J. Org. Chem.* **1974**, *39*, 1615.
[31] Eder, U.; Sauer, G.; Wiechert, R. *Angew. Chem., Int. Ed. Engl.* **1971**, *10*, 496.
[32] For reviews of proline asymmetric catalysis see (a) List, B. *Tetrahedron* **2002**, *58*, 5573. (b) Dalko, P.; Moisan, L. *Angew. Chem. Int. Ed.* **2001**, *40*, 3726. (c) Dalko, P.; Moisan, L. *Angew. Chem. Int. Ed.* **2004**, *43*, 5138. (d) Jarvo, E.; Miller, S. *Tetrahedron* **2002**, *58*, 2481. (e) Groger, J.; Wilken, J. *Angew. Chem. Int. Ed.* **2001**, *40*, 529.

1.2.1. Brønsted Acids in Enantioselective Protonations

In 1977 Dunhamel *et al.* reported the enantioselective protonation of lithium enolate **17** using chiral Brønsted acid **18** in 58% ee (eq 3).[33]
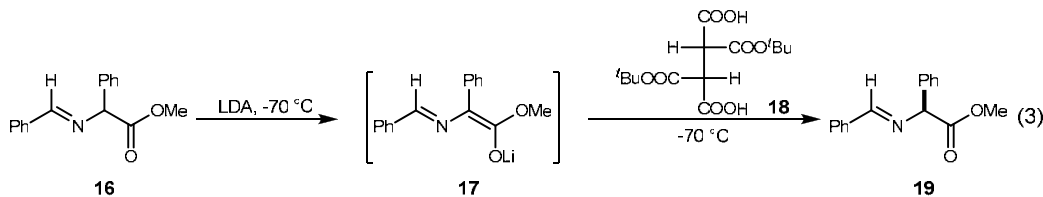
Although many reports have described asymmetric protonation, the focus here will be on enantioselective Brønsted acid catalyzed reactions. Specifically outlined here will be the use of hydrogen bonds to accelerate the rate of a reaction, while at the same time controlling enantioselection. Hydrogen bonding has been evoked as a secondary control element in several enantioselective reactions.[34] However, this again falls outside the scope of what is to be described here, *i.e.* hydrogen bonds as the primary source of asymmetric induction.

This young field was pioneered by Yamamoto in the mid-1990's using his Lewis acid assisted chiral Brønsted acid (LBA) (Chart 1). This is similar to his earlier work when he used Brønsted acid assisted chiral Lewis acids (BLA).

Chart 1. Yamamoto's chiral BLA and LBA complexes
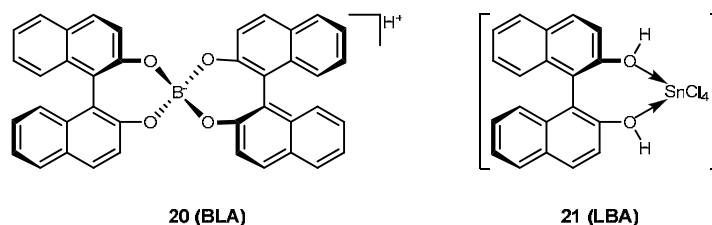
There is an important distinction between the two chiral complexes. A BLA is presumed to both activate and direct a substrate using the chiral Lewis acid center, while the Brønsted acid acts as a secondary control element. In contrast, an LBA activates the

---

[33] (a) Duhamel, L.; Plaquevent, J. *Tetrahedron Lett.* **1977**, *26*, 2285-2288. (b) Duhamel, L.; Plaquevent, J. *J. Am. Chem. Soc.* **1978**, *100*, 7415.

[34] (a) Ishihara, K.; Yamamoto, H. *J. Am. Chem. Soc.* **1994**, *116*, 1561. (b) Ishihara, K.; Miyata, M.; Hattori, K.; Tada, T.; Yamamoto, H. *J. Am. Chem. Soc.* **1994**, *116*, 10520.

substrate through the chiral Brønsted acid, while the Lewis acid serves only as a means by which the Brønsted acid is activated.

Yamamoto began using LBA **21** in the enantioselective protonation of silyl enol ethers and later ketene disilyl acetals.[35] Shortly thereafter, **21** was shown to protonate prochiral allyltrimethyltins with up to 89% ee (eq 4).[36]
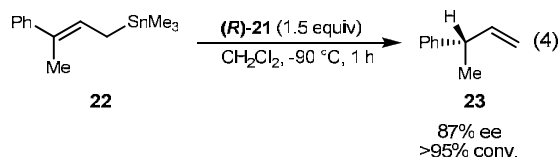
Yamamoto further developed the LBA concept and in 1999 published his landmark report of biomimetic polyprenoid cyclizations as discussed in detail in Section 1.1.2.

1.2.2. O-H Based Chiral Brønsted Acid Catalysts

Since Yamamoto's pioneering work, several chiral alcohols have been used as asymmetric hydrogen bond donors. In 2003, Schaus reported an enantioselective Morita-Baylis-Hillman reaction using a chiral Brønsted acid.[37,38] Although BINOL only provided minimal enantioselection (32% ee), modification of the asymmetric hydrogen bond donor to **24** afforded excellent enantioselection (Chart 2).

Chart 2. Schaus' BINOL-Derived Chiral Brønsted Acid
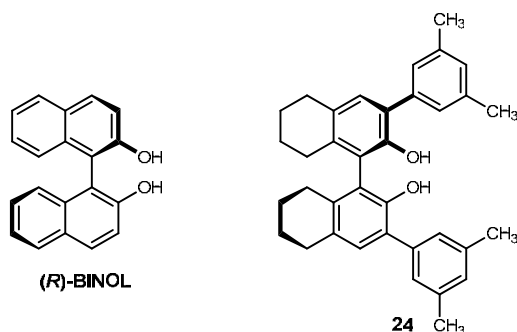
[35] (a) Ishihara, K.; Kaneeda, M.; Yamamoto, H. *J. Am. Chem. Soc.* **1994**, *116*, 11179. (b) Nakamura, S.; Kaneeda, M.; Ishihara, K.; Yamamoto, H. *J. Am. Chem. Soc.* **2000**, *122*, 8120. (c) Ishihara, K.; Nakashima, D.; Hiraiwa, Y.; Yamamoto, H. **2003**, *125*, 24.

[36] Ishihara, K.; Ishida, Y.; Nakamura, S.; Yamamoto, H. *Synlett* **1997**, 758.

[37] (a) McDougal, N. T.; Schaus, S. E. *J. Am. Chem. Soc.* **2003**, *125*, 12094. (b) McDougal, N. T.; Trevellini, W.; Rodgen, S. A.; Kliman, L. T.; Schaus, S. E. *Adv. Synth. Catal.* **2004**, *346*, 1231.

[38] In 2004 Nagasawa reported a bis-thiourea catalyst that afforded MHB products with moderate ee. Sohtome, Y.; Tanatani, A.; Hashimoto, Y.; Nagasawa, K. *Tetrahedron Lett.* **2004**, *45*, 5589.

While aromatic aldehydes provided moderate enantioselection, aliphatic aldehydes typically gave better enantiomeric excess, as high as 96% ee (eq 5).
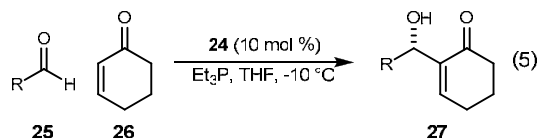
Also inspired by the BINOL framework was a novel phosphoric acid catalyst discovered independently by Akiyama[39] and Terada[40] in 2004. By substituting the 3-position of the naphthyl ring with aromatic groups, both investigators were able to achieve excellent enantioselection in their respective Mannich reactions (Scheme 4).

Scheme 4. Initial Reports by Akiyama and Terada of Chiral Phosphoric Acids in Asymmetric Catalysis

Mannich reaction (Akiyama):
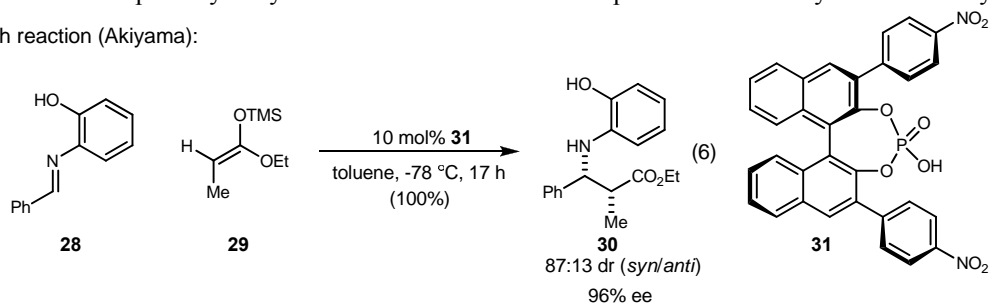
Mannich reaction (Terada):
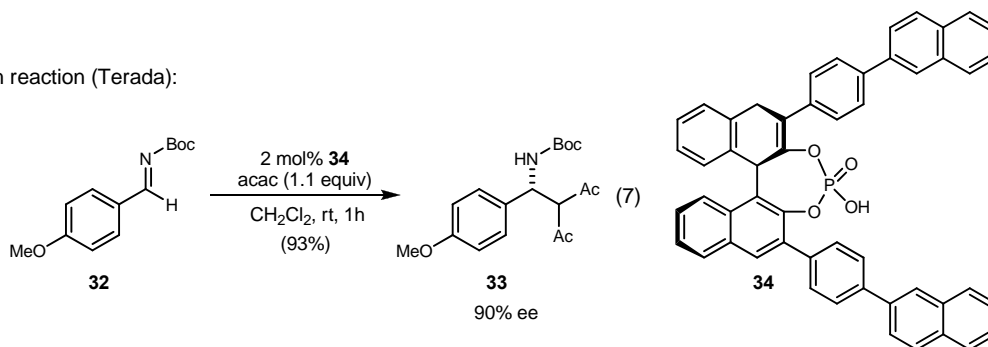
Since these initial reports, both authors have expanded the applications of these relatively more acidic Brønsted acid catalysts to a number of asymmetric transformations (Scheme 5 and Scheme 6).

[39] Akiyama, T.; Itoh, J.; Yokata, K.; Fuchibe, K. *Angew. Chem. Int. Ed.* **2004**, *43*, 1566.
[40] Uraguchi, D.; Terada, M. *J. Am. Chem. Soc.* **2004**, *126*, 5356.

Scheme 5. Chiral Phosphoric Acid Catalyzed Asymmetric Reactions Reported by Akiyama

10 mol% **38**
m-xylene, rt
(86%)   (8)

35   **36**   **37**   **38**
                                                  90% ee

CH$_3$CO$_2$H (1.2 equiv)
5 mol% **42**
toluene, -78 °C   (9)
(99%)

39   **40**   **41**   **42**
                                                  80% ee   Ar = C$_6$H$_2$[2,4,6-(^{i}Pr)$_3$]

1. 3 mol% **46**
   mesitylene, -40 °C
2. PhCO$_2$H (1.0 equiv)   (10)
   (72%)

43   **44**   **45**   **46**
                                                  92% ee   Ar = 9-Anthryl

10 mol% **46**
toluene, -10 °C   (11)
(89%)

47   **48**   **49**   **46**
                                                  99:1 cis/trans   Ar = 9-Anthryl
                                                  94% ee

13

Alkylation of α-diazoester:

(12)

50   **51**

52
97% ee

46
Ar = 9-Anthryl
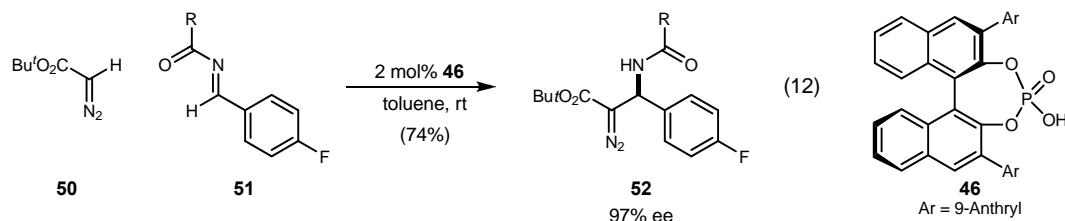
Friedel-Crafts Reaction of Furan:

(13)

53   **54**

55
97% ee

56
Ar = 3,5-dimesitylphenyl

Aza-Ene-Type reaction:

1. **56**
   S/C 1000:1
   toluene, rt
2. $H_3O^{\oplus}$
   (90%)

(14)

57   **58**

59
95% ee
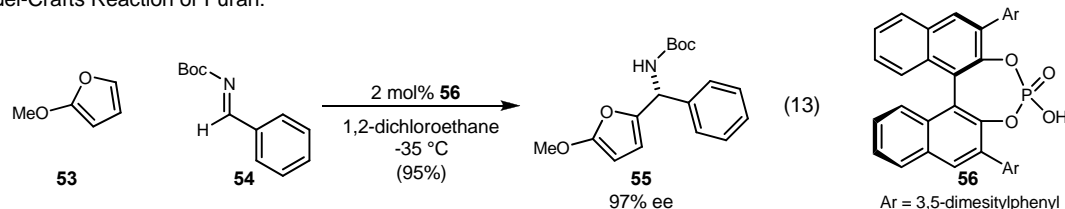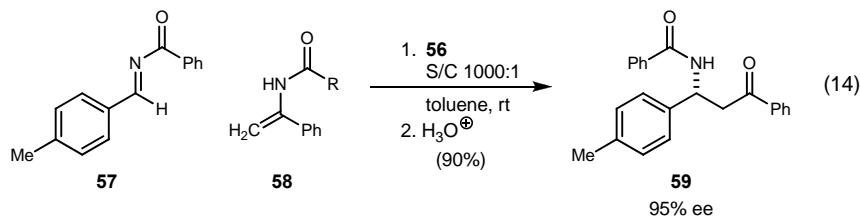
Among the most notable transformations effected by asymmetric hydrogen bond catalysis is the enantioselective hetero-Diels-Alder reaction reported by Rawal in 2003.[41] Using chiral alcohol **62**, asymmetric hetero-Diels-Alder reactions provided products **64** in good yields and excellent enantioselectivity for a variety of substrates (eq 15).

60 **61**   **63**   **64**

(15)
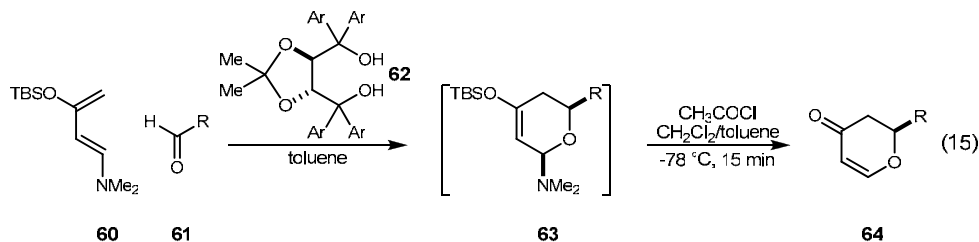
Rawal compares this type of catalysis to enzymatic catalysis, suggesting that the above transformation is a more biomimetic form of traditional Lewis acid catalysis. Since reporting the asymmetric hetero-Diels-Alder reaction, Rawal has extended the use of

---

[41] Huang, Y.; Unni, A. K.; Thadani, A. N.; Rawal, V. H. *Nature*, **2003**, *424*, 146.

these TADDOL catalysts to the asymmetric Mukaiyama aldol reaction in which he is able to achieve good diastereo- and enantioselection.[42]

1.2.3. N-H Based Chiral Brønsted Acid Catalysts

As organic catalysts became popularized in asymmetric catalysis, one reaction in particular served as an inspiration for new catalyst design. The Strecker reaction, which is the hydrocyanation of imines leading to α-amino acids, had not been asymmetrically catalyzed until the mid-1990s.

$$(16)$$
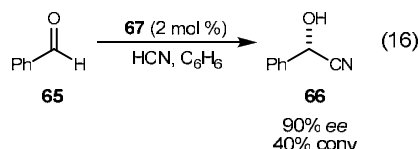
Prior to the hydrocyanation of imines, Inoue reported that dipeptide **67** (Chart 3) was able to catalyze the asymmetric addition of hydrogen cyanide to benzaldehyde (eq 16). Remarkably, after 30 minutes the cyanohydrin product **66** was obtained in 90% ee. However, if allowed to react longer, the cyanohydrin product would racemize. For example, after 72 hours only a 12% ee was obtained with 80% conversion.

Chart 3. Inoue and Lipton's Dipeptide Catalysts
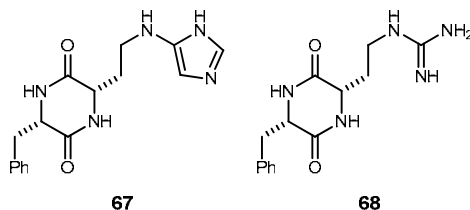
In 1996 Lipton *et al.* reported the first enantioselective catalyst for the Strecker reaction, dipeptide **68** (Chart 3). Lipton was able to achieve excellent enantioselectivity, greater than 99% ee for several substrates, but the generality was low (eq 17).

$$(17)$$
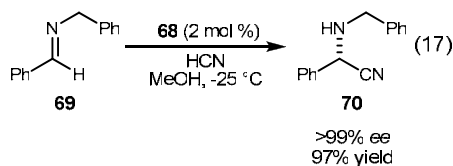
[42] (a) McGilvra, J. D.; Unni, A. K, Modi, K.; Rawal, V. H. *Angew. Chem. Int. Ed.* **2006**, *45*, 6130. (b) Gondi, V. B.; Gravel, M.; Rawal, V. H. *Org. Lett.* **2005**, *7*, 5657.

In the years following Lipton's initial efforts in this area, Corey and Grogan (**71**),[43] as well as Sigman and Jacobsen (**72** and **73**),[44] reported novel organocatalysts for the Strecker reaction (Chart 4).

Chart 4. Corey's Guanidine and Jacobsen's Urea / Thiourea Chiral Catalysts

71

72 R = polystyrene, X = S
73 R = Ph, X = O
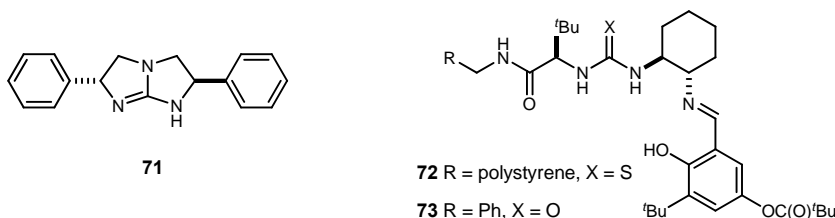
These catalysts afforded the α-aminonitriles in high yield and excellent enantioselectivity. In 2000 Vachal and Jacobsen extended the use of catalyst **72** from aldimines to ketimines.[45]

Intrigued by the increased activation of substrate provided by catalyst **72**, Vachal and Jacobsen studied the effect of structural changes on **72** in 2002.[46] Their investigation revealed that the thiourea moiety played a large role in substrate binding and thus activation. After modifying the catalyst design based on their mechanistic insights, catalyst **74** was identified as "the most enantioselective Strecker catalyst prepared to date" (Figure 6).

Figure 6. Jacobsen's Improved Thiourea Catalyst

74
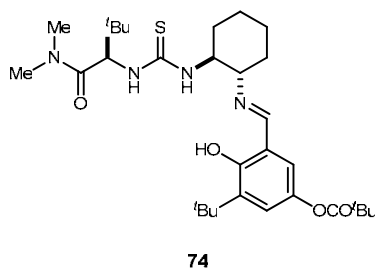
[43] Corey, E. J.; Grogan, M. J. *Org. Lett.* **1999**, *1*, 157.
[44] (a) Sigman, M. S.; Jacobsen, E. N. *J. Am. Chem. Soc.* **1998**, *120*, 4901. (b) Sigman, M.S.; Vachal, P.; Jacobsen, E. N. *Angew. Chem. Int. Ed.* **2000**, *39*, 1279.
[45] Vachal, P.; Jacobsen, E. N. *Org. Lett.* **2000**, *2*, 867.
[46] Vachal, P.; Jacobsen, E. N. *J. Am. Chem. Soc.* **2002**, *124*, 10012.

With only minor structural changes, Jacobsen has continued to use the thiourea motif of catalyst **74** to adapt this organocatalyst to a number of asymmetric reactions (Scheme 7).[47]

Scheme 7. Asymmetric Reactions Catalyzed by Jacobsen's Thiourea Derivatives

Nitro-Mannich Reaction:
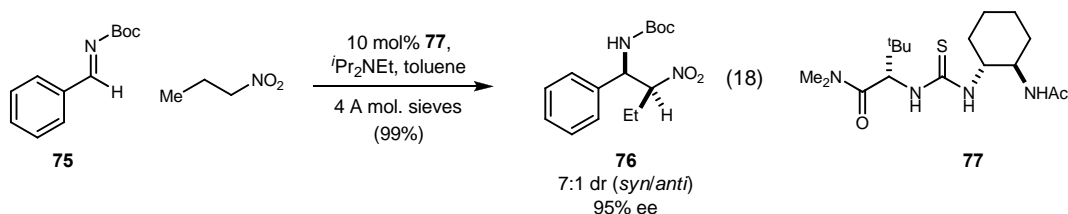
Hydrophosphonylation:
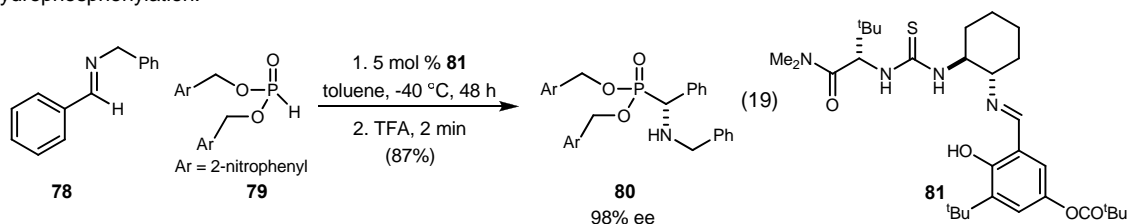
Acyl Pictet-Spengler Reaction:
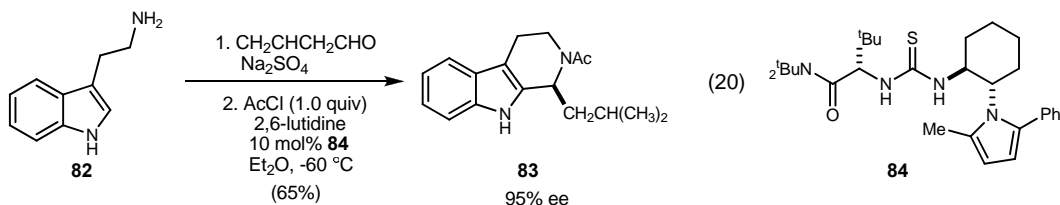
Mannich Reaction:

---
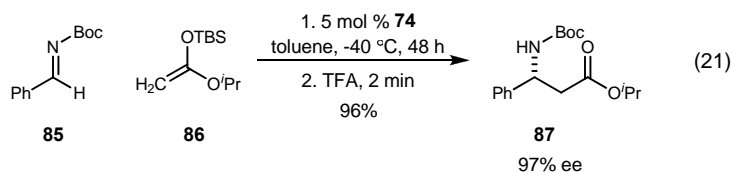
[47] (a) Wenzel, A. G.; Jacobsen, E. N. *J. Am. Chem. Soc.* **2002**, *124*, 12964. (b) Wenzel, A. G.; Lalonde, M. P.; Jacobsen, E. N. *Synlett* **2003**, *12*, 1919. (c) Joly, G. D.; Jacobsen, E. N. *J. Am. Chem. Soc.* **2004**, *126*, 4102. (d) Taylor, M. S.; Jacobsen, E. N. *J. Am. Chem. Soc.* **2004**, *126*, 10558.

Acyl-Mannich Reaction:

$$(22)$$

88 → **89**
86% ee
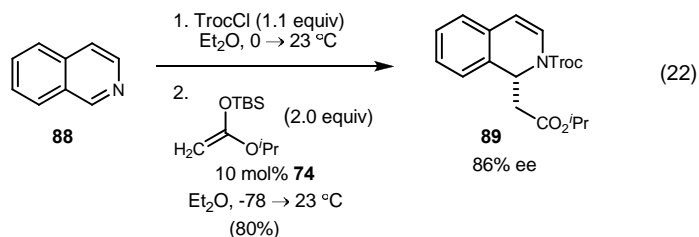
Conjugate Addition of Ketones to Nitroalkenes:

$$(23)$$

90   **91**   **92**   **93**
99% ee
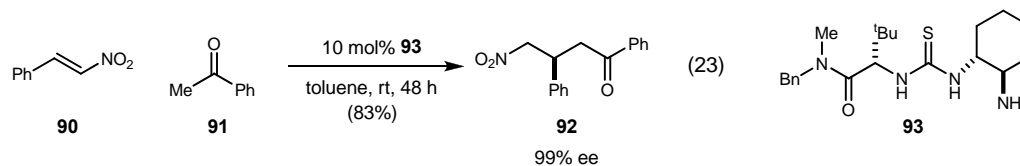
Conjugate Addition of α,α-disubstituted Aldehydes to Nitroalkenes:

$$(24)$$

94   **95**   **96**   **97**
> 50:1 dr (*syn:anti*)
97% ee
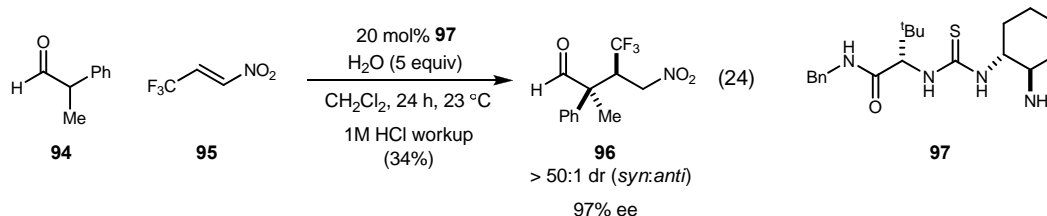
Cyanosilylation of Ketones:

$$(25)$$

98   **99**   **100**
97% ee
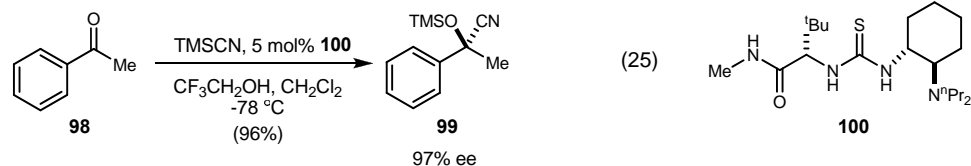
Aza-Baylis-Hillman:

$$(26)$$

101   **102**   **103**   **104**
95% ee
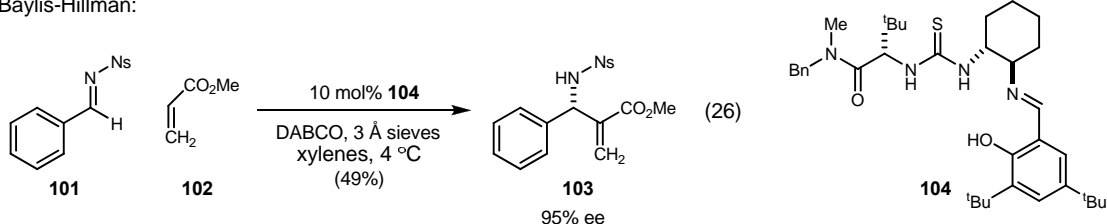
In only a few years, Jacobsen has shown that these chiral thioureas can efficiently accelerate and enantioselectively direct a variety of reactions to produce enantiomerically enriched amines (eq 18 – 26). Recently, Jacobsen reported the enantioselective catalytic acyl-Pictet-Spengler reaction using modified thiourea catalyst **84**. In a one-pot reaction,

he was able to convert indole **82** to tetrahydro-β-carboline **83** in good yield with high enantioselectivity (eq 20).

Shortly after Jacobsen's initial reports using thioureas in asymmetric catalysis, Takemoto *et al.* described a new achiral thiourea **107**, which they used to catalyze the addition of cyanide to nitrones (eq 27).[48]
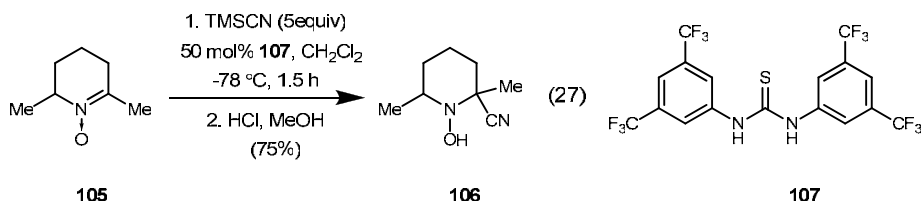
This thiourea was converted into chiral bifunctional catalyst **111** and used in the Michael addition of malonates to nitroolefins (eq 28).[49] They achieved high enantioselectivity in good yields for a broad range of substrates.
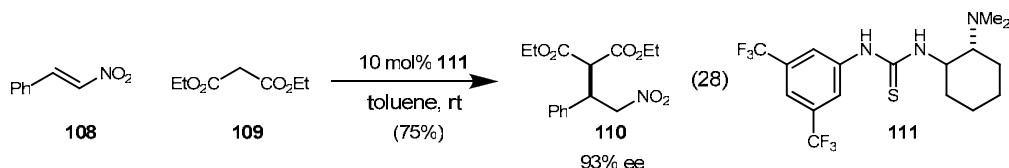
The same catalyst **111** was used in a 2004 report by Takemoto *et al.* on the aza-Henry reaction.[50] Again they believed that the catalyst had a bifunctional role, activating both the electrophile and nucleophile. This reaction will be further discussed in Section 2.1.

Recently, Schaus has reported that a hydroquinine derived thiourea was a very effective general catalyst for the addition of stabilized nucleophiles to acyl imines. The nucleophiles studied included nitromethane, nitroethane and dimethyl malonate (eq 29).[51]

---

[48] Okino, T.; Hoashi, Y.; Takemoto, Y. *Tetrahedron Lett.* **2003**, *44*, 2817.
[49] Okino, T.; Hoashi, Y.; Takemoto, Y. *J. Am. Chem. Soc.* **2003**, *125*, 12672.
[50] Okino, T.; Nakamura, S.; Furukawa, T.; Takemoto, Y. *Org. Lett.* **2004**, *6*, 625.
[51] Bode, C. M.; Ting, A.; Schaus, S. E. *Tetrahedron* **2006**, *62*, 11499.

$$(29)$$
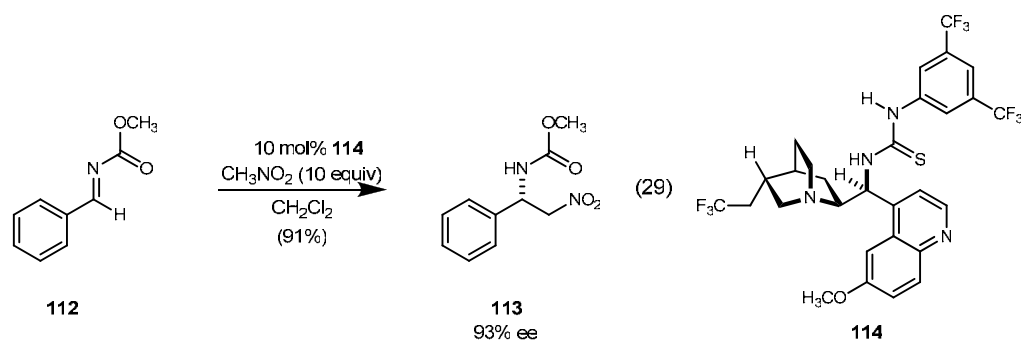
1.3. Polar Ionic Hydrogen Bonds

As discussed in Section 1.1.2, hydrogen bonding has recently witnessed great success in the area of asymmetric catalysis. These so-called organocatalysts have received special recognition in recent years. Although these catalysts have already been shown to accelerate reactions with high enantioselectivity, improvements can still be made. In order to advance upon the chiral non-metal catalysts that are already available, we noted the potential differences between polar covalent and polar ionic hydrogen bonds (Figure 7).

Figure 7. A Comparison of Polar Covalent and Polar Ionic Hydrogen Bond Solvation
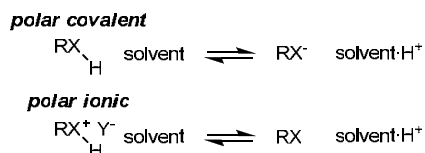
Specifically, the former employs a chiral anion, whereas the latter makes use of an uncharged chiral ligand for the proton. In essence, the requirement is a chiral solvating agent. It is for this reason that bulk solvation effects are a critical consideration in the proposal below.

The same advantages that polar covalent hydrogen bonds have over traditional Lewis acid catalysts exist for polar ionic hydrogen bonds as well. We hypothesize that the benefits of using a polar ionic hydrogen bond over a polar covalent hydrogen bond are increased activation as well as increased turnover. This increase in activation will be discussed in more detail in Section 2.1.3.

Experimentally, it is easier to purify a neutral organic product from a salt than it is from a neutral catalyst, by column chromatography or aqueous extraction. Furthermore, the salts that are formed upon protonation by strong acid are more likely to be crystalline compounds that are bench stable. In order to utilize polar ionic hydrogen bonding in asymmetric catalysis, we began with the straightforward premise that a new ligand must be designed to both hold the proton throughout a reaction as well as impose its chirality onto the substrate.

1.3.1. BAM Ligands

The premise that a ligand must bind a proton and effectively transfer asymmetry to the substrate led to several key design elements. First, and perhaps most important, the ligand must be sufficiently Brønsted basic such that the proton will remain bound at all times and not transferred to achiral solvent, substrate, or product. Second, the ligand must provide a chiral environment while binding to the proton complex, presenting only one prochiral face of the substrate to the nucleophile. Third, the ligand should be readily available in enantiopure form and should be easily modified to allow a library of diverse structures to be created. Finally, we hypothesized that a bidentate ligand may prove more effective than a monodentate ligand. These principles of design led us to target **115** (Figure 8).

Figure 8. Chiral Ligand Designed For A Proton

115
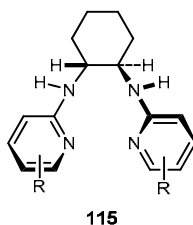
The design of **115** is similar to the *N,N'*-bis-(2-pyridyl-methyl)-*N,N'*-dimethyl-1,2-cyclohexanediamine **116** (BPMCN) ligand that Que and coworkers described in 2001.[52] A crystal structure of this ligand bound to Fe(II) revealed a bidentate binding mode where

---

[52] Costas, M.; Tipton, A. K.; Chen K.; Jo, D.; Que, L. *J. Am. Chem. Soc.* **2001**, *123*, 6722-6723.

the two pyridine rings were *trans* to each other (Figure 9). It should be noted that the complex is C_2-symmetric with the pyridyl rings twisting out of planarity.

Figure 9. ORTEP Plot for Que's BPMCN·Fe(ClO$_4$)$_2$
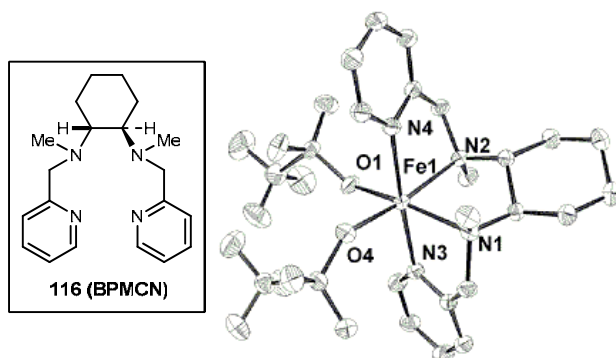
When the 6-Me$_2$-BPMCN ligand (**117**) was used, which placed methyls at the 6-position of the pyridyl ring, the pyridine rings were no longer *trans* to one another. This simple modification provided an unexpectedly large change in conformation and coordination geometry (Figure 10).

Figure 10. ORTEP Plot for Que's 6-Me$_2$-BPMCN
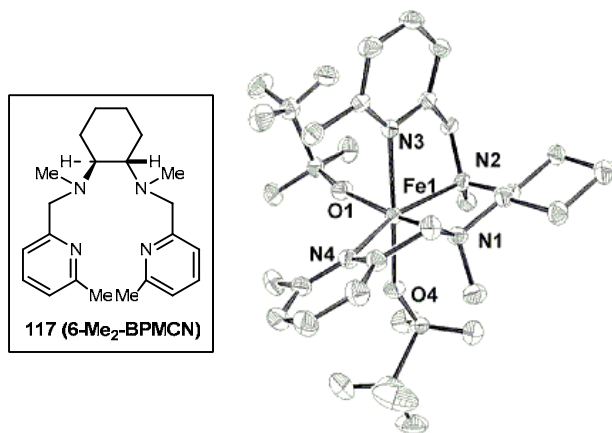
This change in conformation had a large impact in the *cis*-dihydroxylation of olefins, where the ee rose from 29% using BPMCN to 82% using 6-Me$_2$-BPMCN. The change in conformation also increased the ratio of diol to epoxide formation as well.

In proposing **115**, the lower homolog of Que's BPMCN, a potentially more conformationally rigid ligand should result, as well as a Brønsted base whose strength approximates that of DMAP. Utilizing 1,2-(*R,R*)-*trans*-diaminocyclohexane as a backbone combined with substituted pyridines reveals the BisAMidine (**BAM**) moiety (eq 30).[53] It should be noted that many BAM ligands that have been synthesized, as well as their triflic acid salts, are bench stable, crystalline solids.

$$(30)$$
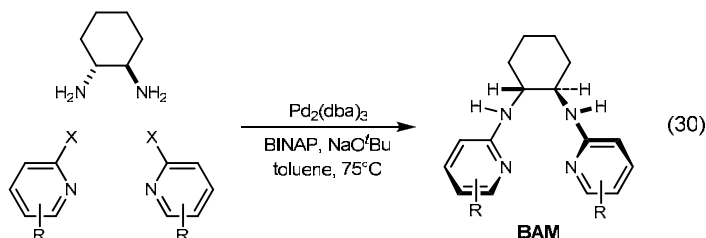
The basicity of the BAM was initially estimated by comparison to the pK_a of dimethylaminopyridine (DMAP), which has been measured at 9.5.[54] The BAM can be viewed as a chiral *ortho*-DMAP derivative and thus the pK_a should be similar; however, this does not take into consideration the bidentate nature of the ligand which may have an increasing effect on the pK_a of the protonated species. For comparison, the pK_a of pyridinium has been measured at 5.2. Given the basicity of the BAM ligand, many strong acids can be used to form the protonated complex, **118** (eq 31).

$$(31)$$
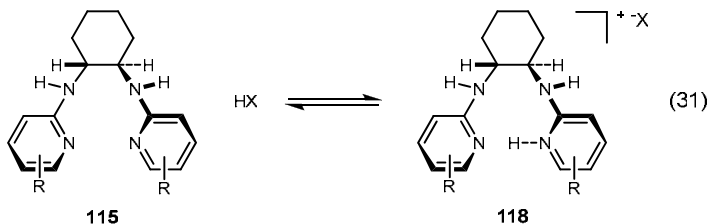
A naming system was adopted to more easily communicate structural differences in the BAM ligand motif. Using the numbering system below (Chart 5) for the R_2 pyridine substituent, in conjuction with R_1 as the cyclohexane diamine substituent, **115a** would be called H,^{3}Me-BAM, while **115k** would be called Me,^{6}Me-BAM.

[53] Nugent, B. N.; Yoder, R. A.; Johnston, J. N. *J. Am. Chem. Soc.* **2004**, *126*, 3418.
[54] Perrin, D. D. *Dissociation Constants of Organic Bases in Aqueous Solution*; Butterworths: London, 1965.

Chart 5. Shorthand Notation for BAM ligands.

$R_1,^{R2}$BAM (**115**)   H,^{3}Me-BAM (**115a**)   Me,^{6}Me-BAM (**115k**)
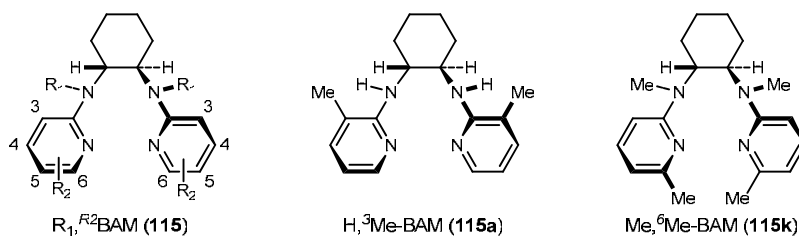
A complete list of all BAM ligands and their abbreviations can be found in Appendix 1.

Modeling studies were used to determine the lowest energy conformations of the protonated complex. These studies were performed using PCModel; however, PCModel forces a proton onto one atom prior to minimization. By doing this, it was not possible to generate the desired C_2-symmetric complex for some ligands. The views below were obtained by fixing the angle of the N-H-N of the protonated pyridine system at 180º. The models below used the 5,6-disubstituted (quinoline) BAM proton complex, which was minimized with only the restriction mentioned above.

Figure 11. 3D Views of BAM-Proton Complex Generated by PCModel

Front View   *Side View*
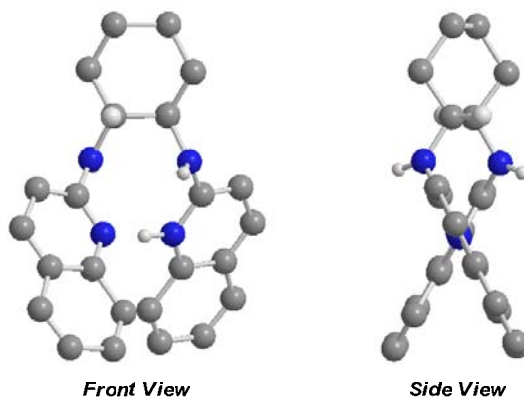
This low energy conformation is the expected C_2-symmetric conformation of the active complex (Figure 11). From the modeling studies, it appeared that the 6-position on the pyridine ring would be most beneficial in terms of distinguishing faces of attack by the nucleophile.

24

Two crystal structures were obtained of the protonated BAM complexes. The first was using H,^{6}Me-BAM (Figure 12). N-H bond distances are included, but the triflate counterion is omitted for clarity.

Figure 12. X-ray Crystal Structure of H,^{6}Me-BAM·HOTf complex
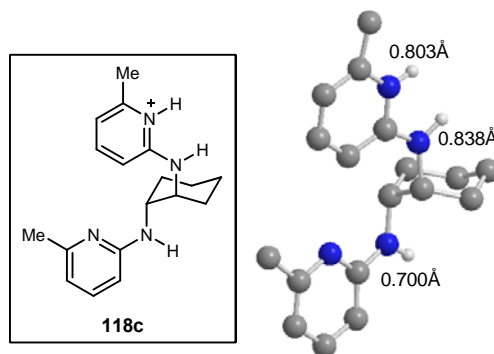
The complex appears to prefer a 'swung-out' conformation in the solid state in which no intramolecular hydrogen bonding is present. Also, notice that the cyclohexyldiamine chair is in a diaxial conformation. A possible reason for these deviations from the expected conformation is the stabilization of intermolecular hydrogen bonding in the solid state structure. Indeed, there are multiple intermolecular hydrogen bonds to bridging triflates.

A second crystal structure was obtained using H,Quin-BAM·HOTf (Figure 13).

Figure 13. X-ray Crystal Structure of H,Quin-BAM·HOTf complex
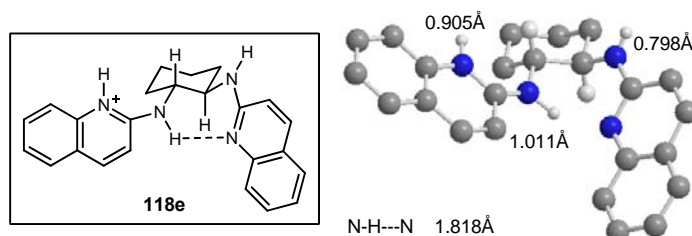
This X-ray showed an internal hydrogen bond between the N-H of the cyclohexyl diamine and the opposing quinoline N. Again the appropriate N-H bond lengths are displayed and it should be noted that the N-H---N distance is indicative of a medium-

strong H-bond,[55] at 1.82 Å. This can be compared to the crystal structure of the chiral (racemic) proton sponge obtained by Lloyd-Jones in 1998 which showed the N-H---N bond distance to be 1.72 Å (Figure 14).[56]

Figure 14. X-ray Crystal Structure of Lloyd-Jones' Chiral Proton Sponge
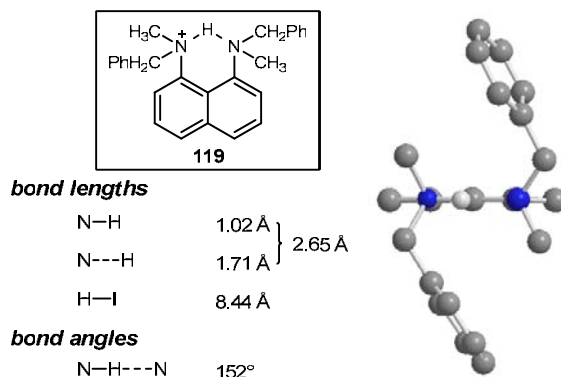
The H,Quin-BAM X-ray does in fact show that the cyclohexyl diamine chair is in the di-equatorial position as expected. The deviation in this X-ray from the expected C_2-symmetric complex described above can again be attributed to the intermolecular hydrogen bonds which are present throughout the crystal lattice. The direct relevance of these solid state structures to their solution chemistry remains a question.

1.3.2. Reaction Development

The basis for developing a variety of chiral proton-catalyzed enantioselective reactions began from the general catalyst-substrate complex **120b** (Figure 15).

---

[55] Jeffrey, G. A. *An Introduction to Hydrogen Bonding*; Oxford University: New York, 1997.
[56] Charmant, Jonathan P. H.; Lloyd-Jones, Guy C.; Peakman, Torren M.; Woodward, Robert L. *Tetrahedron Lett.* **1998**, *39*, 4733.

Figure 15. Binding of Imine to Bidentate Proton Complex

120a   120b
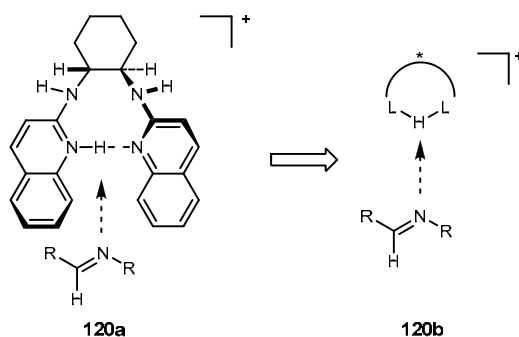
Although carbonyl compounds are attractive electrophiles, the basicity of the carbonyl oxygen is low[57] and as such may lead to a long O---H*L bond in the transition state. The more basic imine[58] might lead to a tighter bound electrophile in the transition state, hopefully leading to higher stereoselection. As our model advanced it became clear that stereochemical induction may be more difficult using a monodentate catalyst (Figure 16). The undefined coordination geometry of the proton allows for a multitude of binding modes.

Figure 16. Binding of Imine to Monodentate Proton Complex

121a   121b
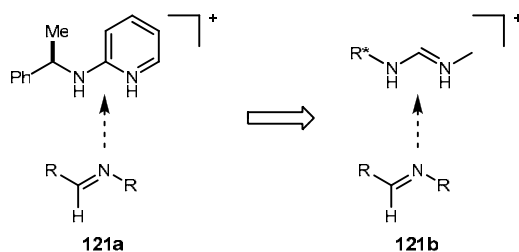
We hypothesized that a bidentate ligand would force the substrate into a more defined position in the chiral proton complex (Figure 15). We turned to modeling to better rationalize how the ligand might shield one face of the substrate from attack, thereby leading to enantioselection. Chem 3D was used to dock a representative imine into the PCModel minimized protonated BAM, ultimately arriving at the complex shown below

---

[57] pK_a has been determined several times, with values ranging from -4 to -8 (see: Arnett, E. M.; Quirk, R. P.; Larsen, J. W. *J. Am. Chem. Soc.* **1970**, *92*, 3977.)

[58] pK_a (*N*-benzylidenebenzylamine) ~ 7 (see: Koehler, K.; Sandstrom, W.; Cordes, E. H. *J. Am. Chem. Soc.* **1964**, *86*, 2413. Cordes, E. H.; Jencks, W. P. *J. Am. Chem. Soc.* **1963**, *85*, 2843.)

(Figure 17). An imine bound in this way would only be accessible to attack from one face, leading to high enantioselection.

Figure 17. Proposed Catalyst - Substrate Complex
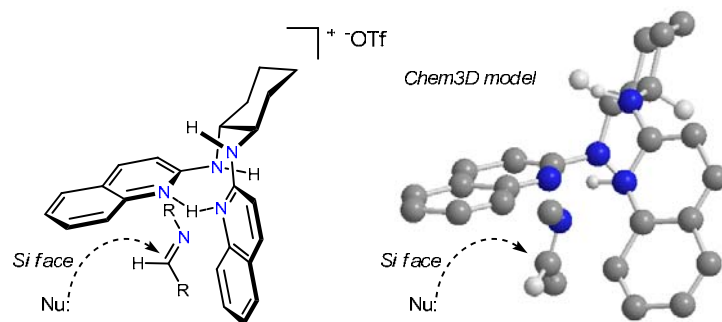
The diagram above suggests that an imine bound to the chiral proton complex will react with a nucleophile stereoselectively. To avoid the possibility of a strong nucleophile simply getting protonated by the catalyst, we hypothesized that neutral nucleophiles would provide a better starting point. Silyl nitronates are readily available neutral nucleophiles which could be used to test this hypothesis.

Chapter 2. Chiral Proton Catalyzed Additions to Imines: Silyl Nitronate and Nitronic Acid Nucleophiles

2.1. Determination of the BAM Acidity Constant

2.1.1. Background on pK_a Values

When talking about chiral Brønsted acids, it is useful to be able to compare their relative acidities. When the acid dissociation constant for an acid and its conjugate base (K_a) is known, this equilibrium constant can be converted to a pK_a, where pK_a = -log$_{10}K_a$. Taking the logarithim to base 10 of the value creates a convenient scale for comparing relative acidities over a much smaller range since K_a varies over many degrees of magnitude. Chemists use this absolute scale for acidity as a tool for both comparing two compounds with known acidity constants as well as for predicting the pK_a for a compound in which the acid dissociation constant is unknown.

$$A{-}H \ + \ H_2O \ \underset{}{\overset{K_a}{\rightleftharpoons}} \ A^- \ + \ H_3O^+ \quad (32)$$
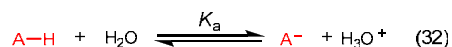
For polar covalent H-bonds, the acidity constant for a compound is a reflection of that compound's ability to stabilize the resulting negative charge upon deprotonation (eq 32). The more stable a polar-covalent H-bond is upon loss of that proton, the lower the pK_a value is for that compound. It then follows that HCl has a pK_a of -6 compared to H_2O which has a value of 15. The rationale is that the more electronegative chloride can better stabilize the resulting negative charge than hydroxide can.

$$A^+{-}H \ + \ H_2O \ \underset{}{\overset{K_a}{\rightleftharpoons}} \ A \ + \ H_3O^+ \quad (33)$$
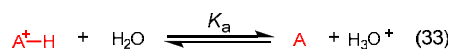
The corresponding acidity constant for a compound which has a polar ionic H-bond is a reflection of that compound's inability to stabilize the resulting positive charge upon protonation (eq 33). Stabilization of the resulting positive charge causes an increase in the pK_a, thus making the protonated complex a weaker acid. By way of example, the pK_a for an ammonium ion is approximately 10. However, the addition of a phenyl group, to make the correspoinding anilinium ion, drops the pK_a to 5. The anilinium is more acidic because of the electron withdrawing effect of the phenyl group.

There are two main influences that contribute to an acid-ionization constant. First there is a resonance effect (also known as the mesomeric effect, **M**), which describes the electron withdrawing (**-M**) or electron donating (**+M**) properties of the corresponding functional group based on the relevant resonance structures. Acetyl, phenyl, and nitro are examples of electron withdrawing groups (**-M**), while alcohols and amines are examples of electron donating groups (**+M**).

The second major contributor to the overall electron flow to or from a substituent is the inductive effect. The inductive effect is based soley on the electronegativity of the individual atoms and their structural connectivity. The electron cloud that forms the bond between two atoms with different electronegativities is not uniform and as a result chemists describe the more electronegative element as having a partial negative (δ^-) charge and the other atom as having a partial positive charge (δ^+).

Figure 18. Example of Inductive Effect on the Acidity Constant

	122	123	124	125
pK_a (H$_2$O) =	4.76	0.23	3.02	4.16
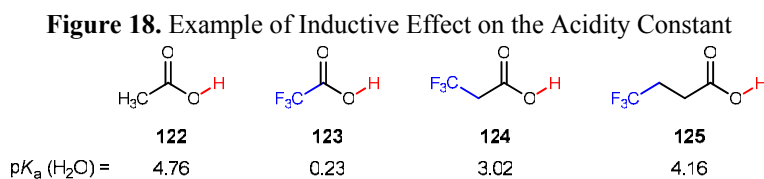
Although the inductive effect is strongest when the electronegative atom is directly connected to the functional group in question, it can be transferred through a chain of atoms. However, since the induced polarity through the chain is less than the original bond polarity and decreases with each bond, the inductive effect is only significant over short distances. Using acetic acid as an example, substitution of a trifluoromethyl group in place of the methyl group drops the pK_a by 4.5 units due to the increased stabilization of the resulting anion provided by the electronegative fluorides (Figure 18). However replacement of the methyl by trifluoroethyl or trifluoropropyl groups only drops the pK_a by 1.7 units and 0.6 units respectively. This demonstrates how significantly the bond polarization decreases over short distances.

Figure 19. Acidity Constants of Methoxy-Substituted Pyridines

	126	**127**	**128**	**129**
pK_a (H_2O) =	5.23	6.62	4.88	3.28
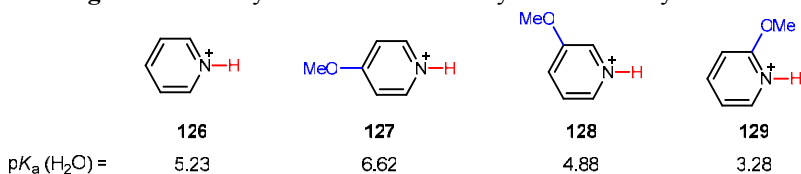
Although it is typical for a resonance donating effect (**+M**) to outweigh an inductive decreasing effect (**-I**) in cases where orbital overlap is good for pi-bonding, in large part due to the decreasing effect over short distances mentioned above, it is important to note that there are examples where the inductive effect overrides the resonance effect. One such example can be found in the chemistry of protonated methoxy-substituted pyridines (Figure 19). As mentioned above, oxygen can have a **+M** effect as a substituent, but due to its high electronegativity, it also has a significant **–I** contribution as well. When substituted at the 4-position of the pyridine ring, the inductive effect is minimized and a 1.4 unit increase in pK_a is observed over unsubstituted pyridine. However, when the methoxy is moved to the 2-position, the inductive effect is at its strongest. The resonance contribution (**+M**) has not changed, but the large decrease in **I** causes a net *decrease* in pK_a by nearly 2 full units.

Figure 20. Acidity Constants of Amino-Substituted Pyridines

	126	**130**	**131**	**132**
pK_a (H_2O) =	5.23	9.17	5.98	6.86
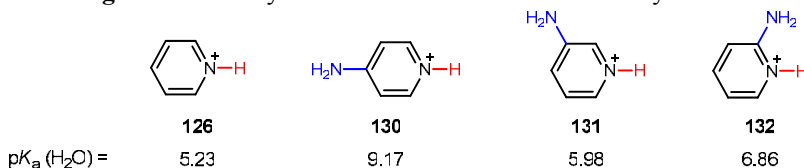
Since our efforts are primarily concerned with amino-substituted pyridines, it should be mentioned that a similar effect has been observed as in the methoxy-substituted pyridines. The large increase of almost 4 pK_a units between pyridine and 4-amino pyridine can be attributed to the expected large **M** contribution (Figure 20). However, this effect is suppressed to some degree when the amino group is moved to the 2-position. This follows from a more pronounced decreasing contribution to the acidity constant from **I**. It should be noted that this **I** contribution does not cause a net decrease in pK_a between pyridine and 2-aminopyridine as in the 2-methoxypyridine case above. This can

be rationalized from the decreased electronegativity of nitrogen relative to oxygen. As a result, amino substituents have larger **M** contributions and smaller **I** contributions as compared to their oxygen counterparts. Hence, protonated 2-aminopyridine has a lower pK_a than that of protonated 4-aminopyridine resulting from an increase in the **-I** contribution, but is still greater than that of unsubstituted pyridine.

2.1.2. Determining pK_a Values For Protonated BAM Complexes

In hopes of unraveling some of the mechanistic complexity associated with the chiral proton catalyzed aza-Henry reaction discussed below in Section 2.2.3, we set out to determine the pK_a of the H,Quin-BAM·HOTf complex. Perrin has developed a titration procedure which utilizes the change in chemical shifts when titrating two bases with a Brønsted acid in a deuterated solvent. The result of Perrin's method is the difference in pK_a between two (or more) compounds as well as which compound is the most basic. This method would allow us to answer one question that arose early in the design stage of the BAM ligands. Does the bidentate nature of the catalyst have a base-strengthening effect similar to that of proton sponge (Figure 21)?

Figure 21. Comparison of BAM and Proton Sponge Salts

HQuin-BAM (115e)·H⁺ ⁻OTf
(118e)

Proton sponge (133)·H⁺ ⁻X
(134)
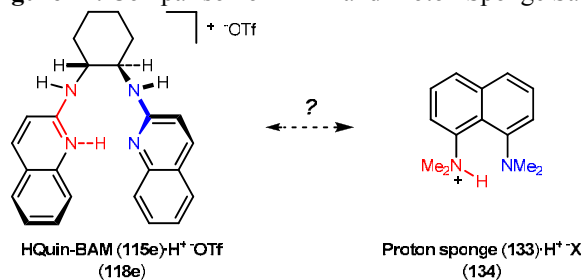
Although we initially had hoped to obtain the pK_a in H_2O, poor solubility of the free ligand (**115e**) forced us to use another solvent. We chose DMSO in part because it has been used as a solvent for the determination of many pK_a values spanning a vast library of compounds. Furthermore, all protonation states of catalyst **115e** have been shown to be soluble in DMSO which also makes it an operationally suitable choice. We found that when using Perrin's method, it is advisable to choose an appropriate base such that the

difference in pK_a is not greater than 2 units. We narrowed our window to range from 2-aminopyridine to proton sponge (Figure 22).[59]

Figure 22. Acidity Constants for Protonated Compounds in DMSO

	135	**134**	**132**
pK_a (DMSO) =	2.4	7.5	6.1
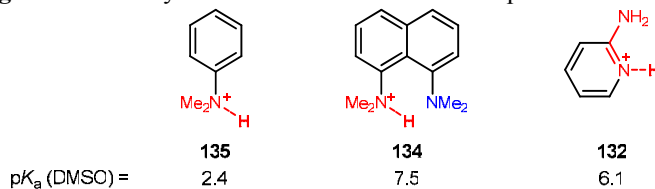
Given that the base-strengthening effect of proton sponge over its functional component dimethyl aniline is over 5 units, we expected the pK_a of H,Quin-BAM·HOTf (**118e**) to be between 6 and 11 in DMSO. Titration of H,Quin-BAM with 2-aminopyridine determined that the ΔpK_a was 0.34 with 2-aminopyridine being the more basic compound of the pair. This gave a pK_a value of 5.78 for H,Quin-BAM·HOTf (**118e**) in DMSO. This shows that there is in fact no base-strengthening effect as observed in proton sponge. This is most likely due to the flexibility of the ligand in solution to change conformations where proton sponge is constrained in such a way as to force both lone pairs from nitrogen to participate in hydrogen bonds.

	135	**136**	**118e**; 1st proton = 5.78	**138**	**126**
pK_a (DMSO) =	6.14	5.93	**137**; 2nd proton = 4.2 / 4.4	4.1	3.4
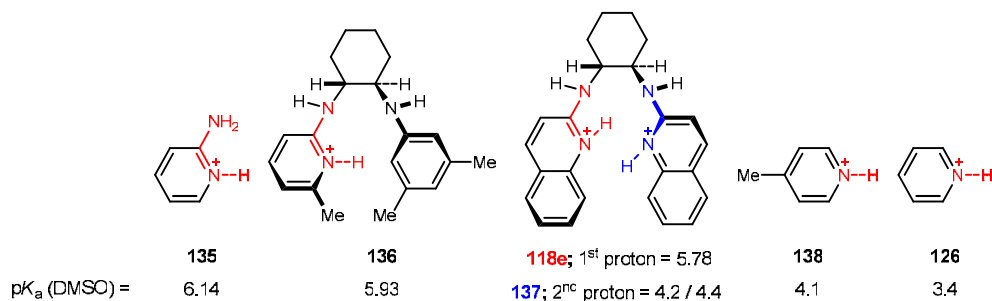
We were also interested in determining the pK_a of the diprotonated salt, which is inactive in the aza-Henry reaction as mentioned in Section 2.2.3. We were able to obtain the acidity constant by comparing it to two different bases, pyridine and lutidine. When the pK_a was measured in a competition with pyridine, the value was determined to be 4.2. In a competition with picoline, a pK_a of 4.4 was determined, emphasizing the importance of the accuracy of the absolute pK_a chosen as a comparison. As expected, the inductive

---

[59] Hess, A. S.; Yoder, R. A.; Johnston, J. N. *SynLett* **2006**, *1*, 147.

effect produced by having a protonated quinoline ring in close proximity to the second basic site, caused a decrease in pK_a of **137** by 1.4-1.6 units.

Finally, we confirmed that there was in fact no base increasing effect from the fact that **115e** was a bidentate ligand. The pK_a of **136** was determined to be 5.93, which clearly demonstrates that **118e** does not possess any special base-strengthening properties. Although the bidentate nature is still believed to play a role in the stereochemical determining step in the aza-Henry reaction, this kinetic property does not translate to the thermodynamic acidity constant. Thus it appears that proton sponge is unique in its base-strengthening effect over its component functionality.

2.2. Enantioselective Aza-Henry Reaction

2.2.1. Background

The aza-Henry reaction is a powerful C-C bond forming reaction in which a nitroalkane is added to an imine, typically using an acid or base catalyst (eq 34).
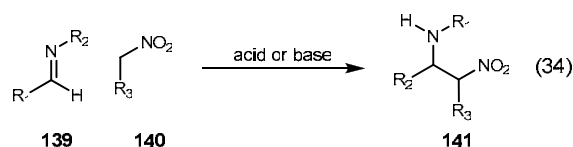
The direct products of the reaction are α-nitro amines (**141**), and these products can be transformed into a number of synthetically useful intermediates such as *vicinal* diamines (**143**) or α-amino acids (**142**) (eq 35).
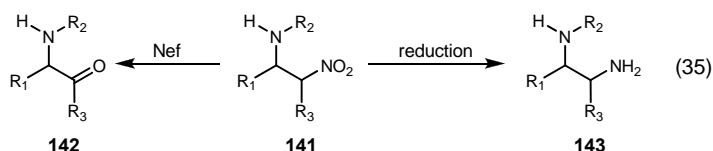
Historically, the aza-Henry can be traced back to Henry who discovered the first example of a nitroalkane addition to an aldehyde in 1896.[60,61] In that same work, Henry also described what could be considered the first example of an aza-Henry by using a nitroalkane and two equivalents of a hemi-aminal (eq 36).

---

[60] Henry, L. *Chem. Ber.* **1905**, *38*, 2027.
[61] Henry, L. *Bull. Acad. Roy. Belg.* **1896**, *32*, 33.

$$\text{Me}_2\text{N}\text{-}\text{CH}_2\text{-OH} \quad \xrightarrow{\text{MeNO}_2} \quad \text{product} \quad (36)$$

144 → **145**
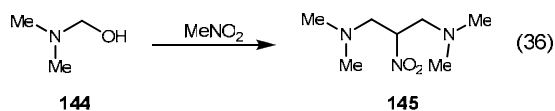
This transformation is a traditional Mannich reaction using a nitroalkane as the nucleophile and as such has been referred to as a nitro-Mannich reaction. Although other examples of the aza-Henry emerged,[62] it wasn't until 1937 that Cerf extended the scope of the reaction.[63] However, Cerf made claims that only two equivalents of **144** will react with nitromethane and only one equivalent of **144** will react with any other nitroalkane. This led to Senkus[64] publishing work to the contrary in 1946 using primary amines and formaldehyde and Johnson[65] in the same issue using seconday amine formation of the hemiaminal precursors. The work of Senkus was the first example of a nitro-Mannich using primary amines.

Much of this work was left undeveloped for several years until mechanistic studies into the Mannich reaction were investigated in the late 1950's and early 1960's. Butler speculated that prior to attack by the nitroalkane, the hemiaminal actually formed the *gem*-diamine **147** (eq 37).[66]

$$R_2N\text{-}OH \quad \xrightarrow[R_2NH]{-H_2O} \quad R_2N\text{-}NR_2 \quad (37)$$

146 → **147**
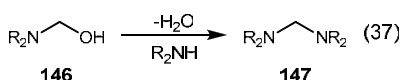
This was followed by Fernandez who put forth that the *aci*-nitroalkane, which is similar to the enol tautomer of a ketone and now more commonly called nitronic acid, was the active form involved in the transition state (eq 38).[67,68]

148 **147** **149** **150**
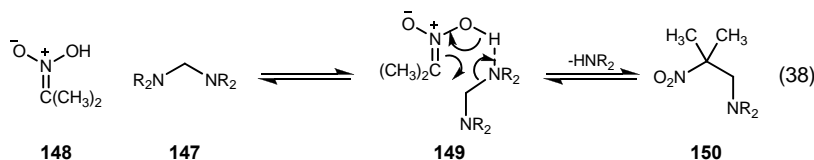
The aza-Henry as it is thought of today was not attempted using a traditional imine and nitroalkane until 1950.[69] Hurd and Strong published the addition of nitromethane into *N*-phenylbenzylimine affording the aza-Henry product in 65% yield. The authors also

[62] Duden; Bock; Reid, *Ber.* **1905**, *38*, 2036.
[63] Cerf de Mauney, H. *Bull. Soc. Chim. France* **1937**, *4*, 1451.
[64] Senkus, M. *J. Am. Chem. Soc.* **1946**, *68*, 10.
[65] Johnson, H. *J. Am. Chem. Soc.* **1946**, *68*, 12.
[66] Butler, G. *J. Am. Chem. Soc.* **1955**, *78*, 482.
[67] Fernandez, J. E.; Fowler, J. S. *J. Am. Chem. Soc.* **1964**, *29*, 402.
[68] Fernandez, J. E.; Fowler, J. S.; Glaros, S. J. *J. Am. Chem. Soc.* **1965**, *30*, 2787.
[69] Hurd, C. D.; Strong, J. S. *J. Am. Chem. Soc.* **1950**, *72*, 4813.

used nitroethane achieving a 35% yield, but there was no comment on diastereoselectivity.[70] Similarly, Kozlov and Fink used nitropropane with the very same imine to also yield the α-nitro amine product in a 35% yield, again without comment on diastereoselectivity.[71]

In 1998 Anderson *et al.* revisited the aza-Henry reaction as a viable way to stereoselectively make *vicinal* diamines.[72] Their investigations led them to a variety of *vic*-diamines (**151**) in high yields with diastereoselection as high as 15:1 (eq 39).
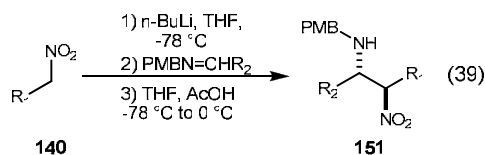
Anderson continued this work and in 2001 published a catalytic variant using Sc(OTf)$_3$ as the Lewis acid catalyst. To improve the rate of the reaction, they employed silyl-nitronates, similar to silyl enol ethers.[73] In their best example, they were able to achieve a 99% yield after 2 hours at 0 ºC, with a 9:1 diatereomeric ratio.

The following year, Qian, Gao, and Chen showed that TiCl$_4$ alone or KO^{i}Pr alone did not catalyze the addition of nitromethane into *N*-tosyl imines.[74] However, a mixture of the two gave a 34% yield of product. This led them to survey lanthanide alkoxides to see if the direct aza-Henry could be performed without an additional base. This screen revealed that Yb(O^{i}Pr)$_3$ could in fact catalyze the aza-Henry reaction with excellent yields using as little as 1 mol% of the Lewis acid.

A significant advancement in this area came in 1999, prior to the Chen work, when Shibasaki reported the first catalytic enantioselective aza-Henry reaction.[75] Using a heterobimetallic complex prepared from Yb(O^{i}Pr)$_3$, KO^{t}Bu, and (*R*)-binaphthol, the reaction was catalyzed with enantioselection as high as 91% ee (eq 40).

---
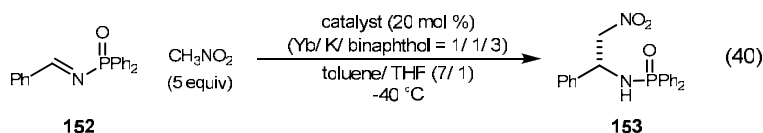
[70] Our own work in this area has shown that these products undergo the retro process on the GC, making it difficult to assay the diastereoselectivity without NMR.

[71] Kozlov, L. M.; Fink, E. F. *Trudy Kazan. Khim. Tekhnol. Inst. Im. S. M. Kirova* **1956**, *21*, 163.

[72] Adams, H.; Anderson, J. C.; Peace, S.; Pennell, A. M. K. *J. Org. Chem.* **1998**, *63*, 9932.

[73] Anderson, J. C.; Peace, S.; Pih, S. *Synlett* **2000**, *6*, 850.

[74] Qian, C.; Gao, F.; Chen, R. *Tetrahedron Lett.* **2001**, *42*, 4673.

[75] Yamada, K.; Harwood, S. J.; Gröger, H.; Shibasaki, M. *Angew. Chem. Int. Ed.* **1999**, *38*, 3504.

This was followed in 2001 by the first example of an enantioselective and diastereoselective catalytic nitro-Mannich reaction, again by Shibasaki.[76,77] This time the catalyst had to be modified to what he called a second-generation heterobimetallic complex. This is because the YbKH$_2$[(R)-binaphthoxide]$_3$ catalyst, which catalyzed the addition of nitromethane, did not catalyze the addition of nitroethane into the imine. By changing to an AlLi[(R)-binaphthoxide]$_2$ complex, the reaction was efficient with 10 mol%, giving high yields with enantioselection as high as 83% ee and a 7:1 diastereomeric ratio. In 2002, two biologically active compounds, ICI-199441 (**154**) and CP-99994 (**155**), were synthesized using this methodology.[78] Previously these compounds were only made using readily available chiral compounds such as amino acids, followed by functional group transformation to afford the *vicinal* diamine. Asymmetric catalysis provided a more straightforward and flexible approach to these targets and derivatives thereof (Chart 6).

Chart 6. Biologically Active Compounds Containing 1,2-Diamines
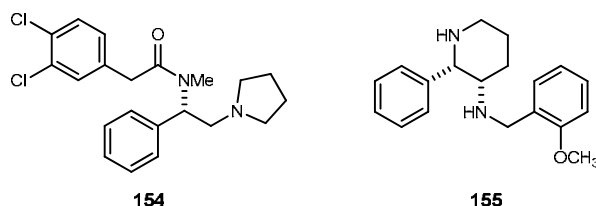
Jørgensen *et al.* published the first catalytic asymmetric aza-Henry reaction of silyl nitronates with α-imino esters in 2001 (eq 41).[79]
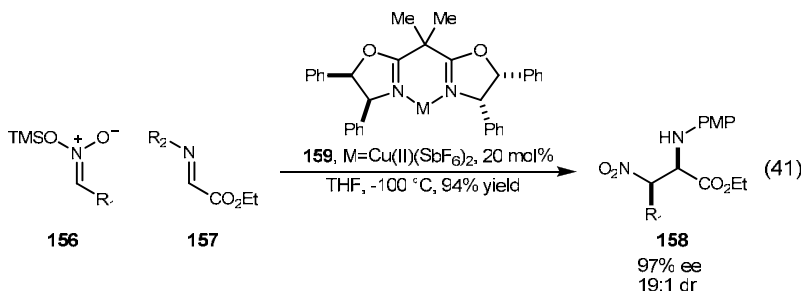
[76] Yamada, K.; Moll, G.; Shibasaki, M. *Synlett* **2001**, *SI*, 980.
[77] Shibasaki, M.; Kanai, M. *Chem. Pharm. Bull.* **2001**, *49*, 511.
[78] Tsuritani, N.; Yamada, K.; Yoshikawa, N.; Shibasaki, M. *Chemistry Letters* **2002**, *3*, 276.
[79] Knudsen, K. R.; Risgaard, T.; Nishiwaki, N.; Gothelf, K. V.; Jørgensen, K. A. *J. Am. Chem. Soc.* **2001**, *123*, 5843.

The reaction proceeds well using a variety of Cu(II) Box salts, affording the products in high yields, excellent enantioselectivities, and very good diastereomeric ratios. The stereoselection was surprisingly insensitive to differences in the chiral ligand as well as different counterions. Shortly after this publication, Jørgensen published a direct variant in which an external base was used in addition to the chiral Cu(II) Box catalyst (eq 42).[80]

$$(42)$$
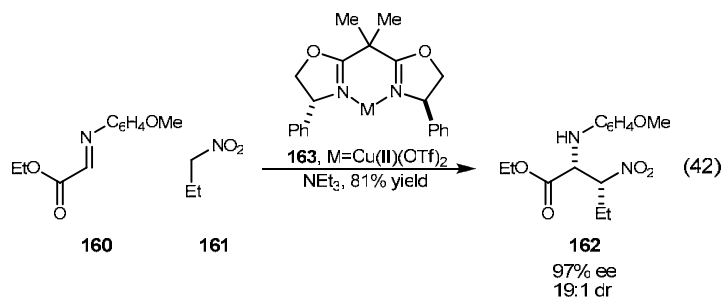
The additional base allowed direct addition of nitroalkane, rather than preformation of the nucleophile as was done previously. Again, the stereoselection was excellent and the conversion was high using 20 mol% of catalyst.

Early in 2004, concurrent with the work in our group, Takemoto *et al.* published an enantioselective aza-Henry reaction catalyzed by a bifunctional organocatalyst. The reaction proceeded to good conversion, with the enantioselectivity reaching as high as 76% ee. Only one diastereoselective example was reported, with a ratio of 3:1. As mentioned in Section 1.1.2, the catalyst employed was thiourea **111**, similar to Jacobsen's hydrogen-bonding catalyst **74** (Chart 7).

Chart 7. Jacobsen and Takemoto's Thiourea Catalysts
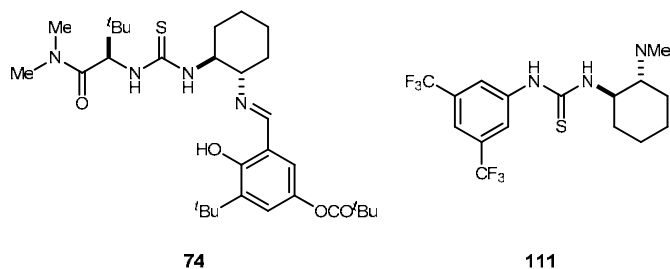
[80] Nishiwaki, N.; Knudsen, K. R.; Gothelf, K. V.; Jørgensen, K. A. *Angew. Chem. Int. Ed* **2001**, *40*, 2992.

The authors suggest possible bifunctionality stemming from the basic site of the dimethylamine allowing for deprotonation of the nucleophile while the thiourea can activate through hydrogen bonding.

Although the aza-Henry reaction has been increasingly active in recent years,[81] many opportunities for development remain. In particular, reported methods for high enantioselection in the nitro-Mannich involve organometallic complexes. Furthermore, readily available imines and nitroalkanes provide a good starting point for the development of a new asymmetric Brønsted acid catalyst.

2.2.2. Silyl Nitronate Additions

As discussed in Section 2.2.1, the aza-Henry reaction is a C-C bond forming reaction that yields *vic*-diamine products.
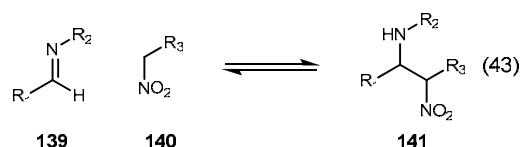
This reaction is both acid and base catalyzed, and can also be a reversible process (eq 43). As discussed previously, the enantioselective reaction has been catalyzed using chiral Lewis acids by Shibasaki and Jørgensen. Following the plan outlined in Section 1.3.2, an imine will be activated by the chiral proton complex to render it more electrophilic, and therefore more reactive toward addition by a neutral nucleophile to afford the aza-Henry product (eq 44).
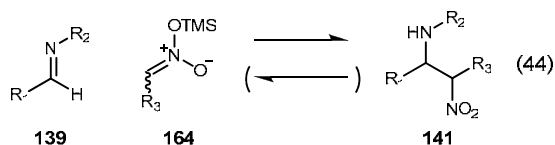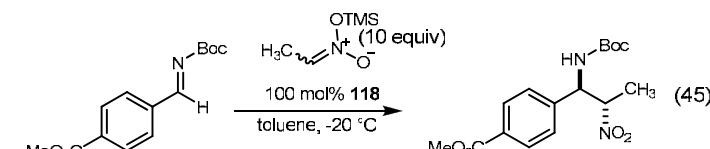
The aza-Henry reaction provided an opportunity to test several of the hypotheses about chiral proton catalysis. First and foremost, we expected the chiral proton to effect rate-acceleration of the reaction, the hallmark of catalysis. We were pleased to discover that reactions with catalyst were in fact faster than the background rate of the reaction (without catalyst). For example, after 70 h the protonated H,^{6}Me-BAM complex furnished the product in 47% conversion compared to just 22% for the uncatalyzed

---

[81] Westermann, B. *Angew. Chem. Int. Ed.* **2003**, *42*, 151.

reaction.[82] This indicates that the chiral proton is activating the electrophile (a Boc-imine) for attack by the nucleophile (a silyl-nitronate). Our second hypothesis was that the chiral proton could effectively shield one face of the substrate from attack by the nucleophile, assuming that the binding pocket would be formed by the two quinoline rings binding simultaneously to the proton. To test this hypothesis, we varied the position of methyl substitution on the pyridine ring of the BAM complex (Table 1).[83]

Table 1. Effect of Stereoelectronics of BAM Ligand on the Chiral
Proton-Catalyzed Silyl Nitronate Addition to Azomethine[a]

entry	R	time (h)	% yield	dr	% ee
1	3-Me (**118a**)	88	85	3:1	1
2	5-Me (**118b**)	88	77	8:1	64
3	6-Me (**118c**)	163	56	12:1	70

[a]Diastereomeric ratios determined by GC. Enantiomeric excess determined by HPLC using a chiral stationary phase. Isolated yield after chromatography.
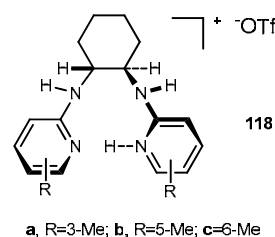
For example, substitution at the six-position of the pyridine ring proved vital for stereoselectivity (entry 3), while enantioselectivity dropped as substution moved to the five (entry 2) and three positions (entry 1). This behavior is consistent with azomethine binding to the proton proximal to the 6-position of each pyridine ring.

---

[82] Percent conversion determined by GC analysis.
[83] With Ben Nugent.

Table 2. Effect of Stereoelectronics of BAM Ligand on the Chiral

Proton-Catalyzed Silyl Nitronate Addition to Azomethine[a]

entry	R	time (h)	% yield	dr	% ee
1	quinoline (**118e**)	48	99	14:1	86
2	lepidine (**118f**)	68	74	16:1	85
3	isoquinoline (**118d**)	68	67	4:1	19

[a]Diastereomeric ratios determined by GC. Enantiomeric excess determined by HPLC using a chiral stationary phase. Isolated yield after chromatography.

Using the basic assumption that bidentate ligand binding to the proton our stereochemical model to guide catalyst design, H,Quin-BAM (**118e**), was synthesized from 2-chloroquinoline. We hypothesized that this ligand could provide even greater facial discrimination than H,^{6}Me-BAM due to the greater shielding capability of the extension of the 5 and 6 positions outward. We were pleased to see that H,Quin-BAM·HOTf exhibited a significant increase in both enantioselectivity and diastereoselectivity (Table 2, entry 1).

The isoquinoline, which substitutes only the 3 and 4 positions of the pyridine ring, again saw a dramatic loss in enantioselectivity (entry 3). This data was consistent with our hypothesis that the 6-position of the pyridine ring was critical for enantioselection (Figure 23). The 4-methyl substituted quinoline, or lepidine (**118f**), was also synthesized. This supported the notion that the distal carbons of the pyridine ring (positions 3 and 4) were not important to the stereoselective pathway as no change in ee was observed (entry 2). This also suggests that the 4-position could be substituted with both electron donating as well as electron withdrawing groups to probe electronic effects of the BAM ligands without additional steric complications.

Figure 23. Proposed Catalyst-Substrate Complex
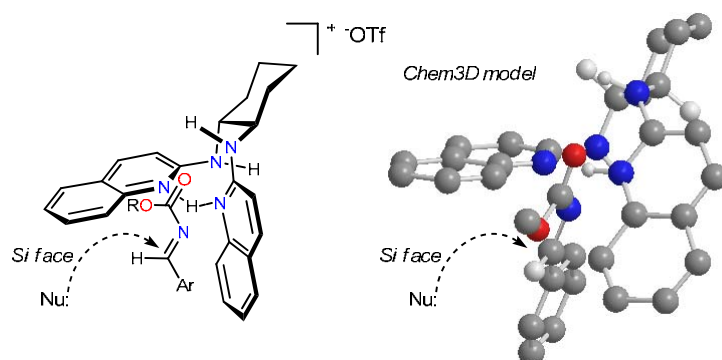
The importance of the 6-position of the pyridine ring is clearly shown in the above model. This model was created by minimizing the protonated catalyst using PC Model. In order to provide a C_2-symmetric representation of the catalyst, the N-H-N bond angle was fixed at 180 degrees. The Boc-imine was then docked into the model to provide the proposed complex above. The conformation of the complex provides significant obstruction from the *re* face to the approaching nucleophile.

Structurally, a very interesting change in enantioselectivity was observed when the cyclohexane diamine was tri-substitiuted (Table 3).

Table 3. Effect of Cyclohexane Diamine Substitution on the
Chiral Proton-Catalyzed Silyl Nitronate Addition to Azomethine[a]

entry	R	time (h)	% yield	dr	% ee
1	H (**118c**)	163	56	12:1	70
2	H,Me (**118i**)	144	22	5:1	44
3	Me (**118k**)	144	54	4:1	1
4	H,COPh (**118j**)	70	65	5:1	3
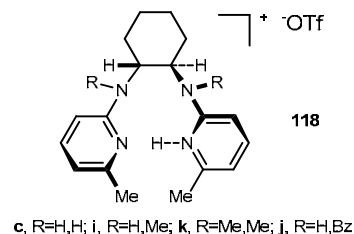
[a]Diastereomeric ratios determined by GC. Enantiomeric excess determined by HPLC using a chiral stationary phase. Isolated yield after chromatography.

Tetra-substitution of the diamine unexpectedly afforded racemic product (entry 3). With the importance of the N-H bond in question, the unsymmetrical BAM **118i** was synthesized. Surprisingly, this afforded some enantioselection, above that of **118k**, but

below that of **118c** (entry 2). Changes in the overall conformation of the catalyst were expected to lead to changes in stereoselection. However, the role of the N-H in the asymmetric pathway is still not clearly understood. Further experiments are needed to probe the possible importance of the additional hydrogen bond donors.

Perhaps even more striking is the drop in enantiomeric excess from 44% with **118i** (entry 2) to 3% with **118j** (entry 4). The substitution of the diamine backbone in each case is similar; however, the electron-withdrawing effect that the Bz group has on **118j** appears to cause the significant decrease in ee. However, we cannot rule out the possibility that this is at least partially the result of a change in conformation.

Table 4. Electronic Effect of BAM Ligand on the Chiral
Proton-Catalyzed Silyl Nitronate Addition to Azomethine^{a}

entry	R^1	R^2	time (h)	% yield	dr	% ee
1	H	6-Me (**118c**)	163	56	12:1	70
2	H	6-OMe (**118h**)	192	12	5:1	4
3	H,COPh	6-Me (**118j**)	70	65	5:1	3

^{a}Diastereomeric ratios determined by GC. Enantiomeric excess determined by HPLC using a chiral stationary phase. Isolated yield after chromatography.
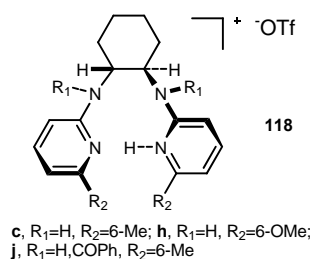
This electron-withdrawing effect led us to a survey of electronic effects of the BAM ligands on enantioselection in the aza-Henry reaction (Table 4). The H,^{6}MeO-BAM (**118h**) was expected to have similar enantiomeric excess to the H,^{6}Me-BAM (**118c**) based on sterics, but have an additional electon-donating effect on the BAM ligand. It wasn't until much later that we discovered that 2-methoxypyridine actually has a lower pK_a than pyridine. This is discussed in more detail in Section 2.1.1. Although the products afforded were racemic, it is interesting to note the significant drop in the rate of this reaction (entry 2). Not surprisingly, the aza-Henry is sensitive to the electronics of the BAM ligand and adjustments in either direction have an effect on enantioselectivity.

43

Table 5. Effect of Additional Basic Sites on the BAM Ligand on the Chiral Proton-Catalyzed Silyl Nitronate Addition to Azomethine[a]

entry	R	time (h)	% yield	dr	% ee
1	quinoline (**118e**)	48	99	14:1	86
2	pyrazine (**118l**)	24	66	4:1	2
3	pyrimidine (**118m**)	120	70	4:1	7
4	quinoxaline (**118n**)	24	63	4:1	1
5	quin, naph (**118o**)	68	68	5:1	3
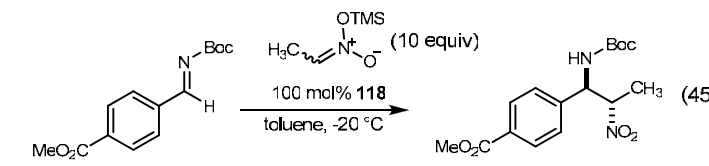
[a]Diastereomeric ratios determined by GC. Enantiomeric excess determined by HPLC using a chiral stationary phase. Isolated yield after chromatography.

In order to investigate the importance of the Lewis basic pyridine nitrogen, several ligands were made containing two nitrogens per pyridine ring (Table 5). In all cases a substantial decrease in enantioselection was observed (entries 2, 3, and 4). Similarly, the removal of a basic site in the case of the unsymmetrical **118o** led to the formation of racemic product. This implies that the second quinoline is not merely shielding one face of the substrate from attack; rather the quinoline *nitrogen* is a prerequisite for the asymmetric pathway. There are two explanations for this unusual result. First, both quinoline nitrogens are bound to the proton in the transition state along with the substrate. The finding that H,Quin(^{2}Nap)-BAM leads to racemic product supports this notion, and at a minimum suggests that the conformation of the second cyclohexane diamine substituent is important for enantioselection, regardless of whether it is ligated to the proton in the transition state. Second, there is also the possibility that the quinoline nitrogen is directing the nucleophile to the substrate in the transition state. Both of these stereochemical models will be further evaluated in Section 2.2.3.

Regardless of how the H,Quin(^{2}Nap)-BAM is affecting the transition state, it is likely that there has been a change in the overall conformation of the chiral proton complex. As discussed in Section 1.3.2, changes to the conformation could have drastic effects on the stereoselection of the chiral proton catalyzed aza-Henry reaction. These changes in the chiral pocket or cavity of the BAM ligand are most striking in the H,^{2}Quin(^{3}Quin)-BAM (**118q**) catalyzed reaction (Table 6).

Table 6. Effect of Cavity Shape in the BAM Ligand on the
Chiral Proton-Catalyzed Silyl Nitronate Addition to Azomethine[a]

entry	R	% yield	dr	% ee
1	2-quinoline (**118e**)	99	14:1	86
2	3-quinoline (**118p**)	55	3:1	5
3	2-quin, 3-quin (**118q**)	63	8:1	-70

[a]Diastereomeric ratios determined by GC. Enantiomeric excess determined by HPLC using a chiral stationary phase. Isolated yield after chromatography.

3-Chloroquinoline was used to make H,^{3}Quin-BAM and it was evaluated in the aza-Henry reaction. The enantiomeric excess was found to be 5% which is not surprising considering the extreme change in catalyst structure (entry 2). However, when unsymmetrical BAM **118q** is used, the *opposite* enantiomer is formed with nearly the same enantioselection as **118e**. It is reasonable to conclude that this catalyst is either a simple chiral amidinium ion complex **165** in which the 3-quinoline ring acts soley as a steric force, or that the cyclohexane diamine nitrogen becomes the second donor ligand, resulting in a chiral complex with the Schiff-base that exposes the opposite prochiral face relative to complex **165** (Figure 24).

Figure 24. Visualization for Catalyst Binding Site

165
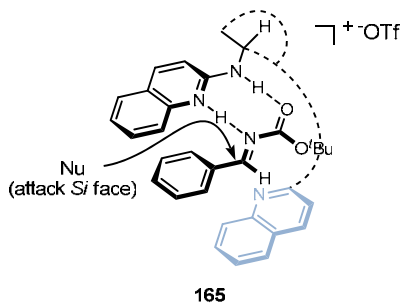
Given the weak Brønsted basicity of a naphthyl amino nitrogen, we favor the first of the possibilities, and rationalize the difference between naphtholine and quinoline as a conformational preference by the latter to minimize dipoles.

45

2.2.3. Development of a Chiral Proton Catalyzed Direct Aza-Henry Reaction

The chiral proton-catalyzed silyl nitronate additions to imines a simplified picture of the BAM ligand and chiral proton complex in which Lewis acidity is clearly identified as the activation means. And within this context, variations in structure were evaluated by their effect on enantioselection to arrive at a stereochemical model for asymmetric induction. Silyl nitronate additions, however, are not ideal in that the nucleophile must be preformed. A more attractive approach would involve addition of a nitroalkane to an imine mediated by a catalyst that can in some way activate both the electrophile (as before) and the nucleophile, while maintaining enantiocontrol. However, this would be a greater challenge due to the loss in activation of the nitroalkane nucleophile. Although nitromethane is in equilibrium with its more reactive tautomer, the equilibrium constant is only 1.1×10^{-7} (eq 46). [84]
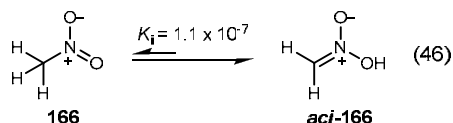
The equilibrium constant K_i reflects the degree of tautomerization for nitromethane from **166** to *aci*-**166**. This rate appears to be too small to account for an appreciable formation of the active nucleophile, which in turn could lead to product. Under our standard reaction conditions, using 0.4 mL of CH_3NO_2, there would only be 0.044 nL (less than 0.01 equivalents) of *aci*-**166** at equilibrium. A mechanism in which the rate determining step, the tautomerization of the nitroalkane, happens prior to attack of the activated electrophile is proposed below (Scheme 8).

---

[84] Turnbull, D.; Maron, S. H. *J. Am. Chem. Soc.* **1943**, *65*, 212.

Scheme 8. Chiral Proton Catalyzed Aza-Henry Mechanism Using *aci*-nitromethane Tautomer
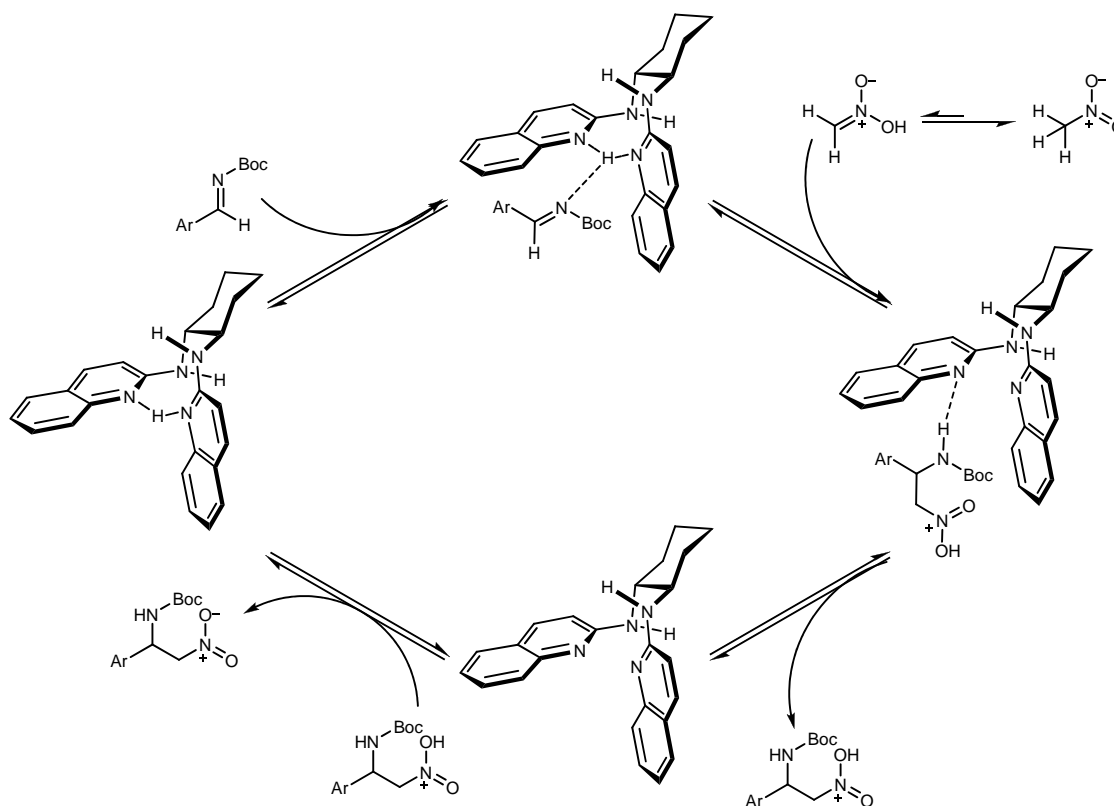
The stoichiometry of conversion alone suggests that the reaction could be catalytic in the chiral proton complex. In order for this to be true, the catalyst must have one of two roles. First the ligand could hold onto the same proton throughout the course of the reaction serving just as an activator, similar to a traditional Lewis acid complex. Another possibility is that the proton which activates the substrate is released during the C-C bond forming step to the product. In turn the enolized proton from the nitroalkane would be returned to the free ligand resulting in formation of the neutral product and regeneration of the catalyst (Scheme 8).

Our hypothesis was that the direct aza-Henry would be comparable to the indirect variant in terms of enantioselectivity, but slower due to the loss of activation in the electrophile. There is an added benefit to this loss in activation of the nucleophile, *i.e.* a slower background rate and therefore a greater possibility to employ substoichiometric amounts of the chiral proton promoter. In order to test our hypothesis, a Boc-imine was added to a solution of catalyst **118e** in nitromethane (Table 7).

Table 7. Effect of Catalyst Loading on the Chiral Proton-
Catalyzed Direct Nitromethane Addition to Azomethine[a]

entry	mol%	time (h)	% conv	% ee
1	100	3	81	81
2	25	6	76	81
3	10	24	81	79
4	5	48	81	81
5	1	96	78	81

[a]Diastereomeric ratios determined by GC. Enantiomeric excess determined by HPLC using a chiral stationary phase. Isolated yield after chromatography.

The reaction with a full equivalent of promoter proceeded rapidly at room temperature and with good enantiomeric excess. Gratifyingly, the stereoselection was maintained with as little as 1 mol% of catalyst (entry 5). The observation that ee translates well between the silyl nitronate additions and nitronic acid additions suggests a common model for enantioselection. Although it was shown that the catalyst loading could be as low as 1 mol%, in order to minimize reaction times 10 mol% would be used as the standard catalyst loading.

Table 8. Effect of Nitroalkane on the Chiral Proton-
Catalyzed Direct Nitroalkane Addition to Azomethine[a]

entry	R	time (d)	% yield	dr	% ee
1	H	9	65	–	95
2	CH3	11	51	11:1	89
3	Et	37	34	10:1	89
4	^{n}Pr	37	18	13:1	90

[a]Diastereomeric ratios determined by GC. Enantiomeric excess determined by HPLC using a chiral stationary phase. Isolated yield after chromatography.

To study the effect of substitution on the nucleophile in the direct aza-Henry reaction, a variety of nitroalkanes were surveyed (Table 8). Cooling to -20 °C allowed for higher

enantioselectivities than had previously been obtained, reaching as high as 95% ee (entry 1). The use of nitroethane led to product with good diastereoselectivity and high enantioselectivity (entry 2). Although larger nitroalkanes such as nitropropane and nitrobutane were equally selective, the rate of the reaction was slower (entries 3 and 4), leading to 34% and 18% yields of nitroethane and nitropropane adducts, respectively, after 37 days. Disubstituted nitroalkanes such as 2-nitropropane, nitrocyclohexane, and nitrocyclopentane did not form any product after several weeks even at room temperature.

Table 9. Chiral Proton-Catalyzed Direct Nitromethane Addition to Azomethine[a]

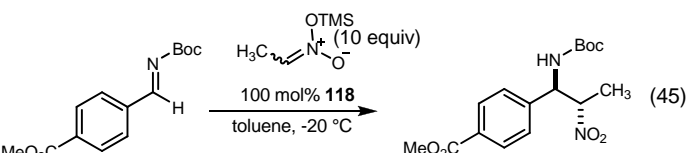| entry	Ar	prod	% yield	% ee
1	p-CH$_3$OC$_6$H$_4$ (**167a**)	**168a**	64	25
2	p-CH$_3$C$_6$H$_4$ (**167b**)	**168b**	49	50
3	2-naphthyl (**167c**)	**168c**	60	42
4	1-naphthyl (**167d**)	**168d**	73	64
5	C$_6$H$_5$ (**167e**)	**168e**	57	60
6	p-ClC$_6$H$_4$ (**167f**)	**168f**	52	79
7	p-AcOC$_6$H$_4$ (**167g**)	**168g**	46	65
8	p-CF$_3$OC$_6$H$_4$ (**167h**)	**168h**	42	67
9	2-NO$_2$-5-ClC$_6$H$_3$ (**167i**)	**168i**	46	61
10	3,4-Cl$_2$C$_6$H$_3$ (**167j**)	**168j**	47	76
11	3,4-F$_2$C$_6$H$_3$ (**167k**)	**168k**	80	84
12	p-CF$_3$C$_6$H$_4$ (**167l**)	**168l**	60	78
13	m-CF$_3$C$_6$H$_4$ (**167m**)	**168m**	66	71
14	o-CF$_3$C$_6$H$_4$ (**167n**)	**168n**	90	73
15	p-MeO$_2$CC$_6$H$_4$ (**167o**)	**168o**	62	80
16	o-NO$_2$C$_6$H$_4$ (**167p**)	**168p**	57	70
17	m-NO$_2$C$_6$H$_4$ (**167q**)	**168q**	65	95
18	p-NO$_2$C$_6$H$_4$ (**167r**)	**168r**	61	82

[a]Diastereomeric ratios determined by GC. Enantiomeric excess determined by HPLC using a chiral stationary phase. Isolated yield after chromatography.

The substrate scope was examined first using nitromethane and a variety of Boc-imines under the aforementioned optimized conditions (Table 9). The stereoselectivity of the aza-Henry appears to be sensitive to the electronics of the Schiff base. In the case of the p-MeOPh imine, the enantioselectivity was very poor at 25% ee (entry 1). Furthermore, the amine derived from p-tolyl imine was produced with 40% ee, suggesting the need for electron withdrawing groups on the Schiff base to achieve high

enantioselectivity. Yields were as high as 90% for the *o*-CF$_3$Ph imine (entry 14). Excellent enantioselection was achieved in the *m*-NO$_2$Ph imine, reaching 95% ee (entry 17).

Table 10. Chiral Proton- Catalyzed Direct Nitroethane Addition to Azomethine^a

entry	Ar	prod	% yield	dr	% ee
1	2-naphthyl (**167c**)	**169c**	62	9:1	44
2	1-naphthyl (**167d**)	**169d**	71	6:1	56
3	C$_6$H$_5$ (**167e**)	**169e**	69	14:1	59
4	*p*-ClC$_6$H$_4$ (**167f**)	**169f**	59	17:1	82
5	*p*-AcOC$_6$H$_4$ (**167g**)	**169g**	95	13:1	77
6	*p*-CF$_3$OC$_6$H$_4$ (**167h**)	**169h**	53	19:1	84
7	3,4-F$_2$C$_6$H$_4$ (**167k**)	**169k**	65	18:1	86
8	*p*-CF$_3$C$_6$H$_4$ (**167l**)	**169l**	53	19:1	84
9	*m*-CF$_3$C$_6$H$_4$ (**167m**)	**169m**	84	12:1	69
10	*o*-CF$_3$C$_6$H$_4$ (**167n**)	**169n**	64	6:1	83
11	*p*-MeO$_2$CC$_6$H$_4$ (**167o**)	**169o**	49	20:1	88
12	*o*-NO$_2$C$_6$H$_4$ (**167p**)	**169p**	62	7:1	82
13	*m*-NO$_2$C$_6$H$_4$ (**167q**)	**169q**	51	11:1	89
14	*p*-NO$_2$C$_6$H$_4$ (**167r**)	**169r**	60	7:1	90

^{a}Diastereomeric ratios determined by GC. Enantiomeric excess determined by HPLC using a chiral stationary phase. Isolated yield after chromatography.

Nitroethane was also screened as the nucleophile against a variety of Boc-imines using the optimal conditions (Table 10). The *p*-AcOPh had the highest yield at 95% of any direct aza-Henry (entry 5). The diastereoselection was typically greater than 10:1, reaching as high as 19:1 in the *p*-CF$_3$Ph imine (entry 6). Enantioselection was very high on average, with *p*-NO$_2$Ph attaining a 90% ee (entry 14). The stereoselection was expected to increase in the nitroethane reactions with the additional methyl substituent able to provide additional gauche interactions in the transition state to limit the number of low energy transition states.

In an effort to increase the rate of the reaction without sacrifice of enantioselection, several counterions were screened in the aza-Henry reaction (Table 11).

Table 11. Effect of Counterion on Conversion and Enantioselectivity of the Chiral Proton-Catalyzed Direct Nitromethane Addition to Azomethine[a]

entry	X⁻	% conv	% ee
1	O_2CCH_3	30	31
2	O_3STol	64	53
3	Cl	30	45
4	PF_6	25	20
5	O_3SCF_3	76	75
6	SbF_6	15	70

[a]Diastereomeric ratios determined by GC. Enantiomeric excess determined by HPLC using a chiral stationary phase. Isolated yield after chromatography.
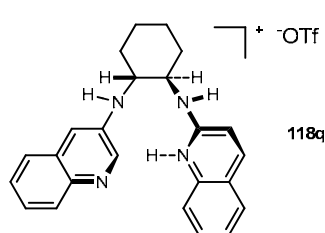
The trifluoromethanesulfonate appears to be the best counterion in terms of both reactivity and stereoselectivity (entry 5). The data suggests that the weakly-coordinating, dissociative counterions are better for enantioselection in the chiral proton catalyzed aza-Henry than the more associative counterions such as acetate (entry 1).

Since it appears that the best counterion was already chosen with triflate, several additives were employed to see if the nitroalkane could be activated either by a base through deprotonation, or by an acid that might increase the concentration of nitronic acid (Table 12).

Table 12. Effect of Additive on the Chiral Proton-Catalyzed Direct Nitromethane Addition to Azomethine[a]

entry	additive	% conv	% ee
1	-	35	95
2	Et_3N	84	0
3	$^iPr_2NEt$	81	0
4	pyridine	36	-
5	DMAP	74	0
6	AcOH	0	-
7	phenol	5	-

[a]Diastereomeric ratios determined by GC. Enantiomeric excess determined by HPLC using a chiral stationary phase. Isolated yield after chromatography.

The addition of a base whose pK_a was similar to or higher than our catalyst gave a faster, base-catalyzed reaction, but afforded racemic product (entries 2, 3, and 5). The addition of pyridine, which has a pK_a of 5.2, lower than that of our catalyst, had no effect on the rate of the reaction (entry 4). Finally, the addition of a hydrogen bond donor had a negative effect on the rate of reaction, completely inhibiting it (entries 6 and 7). This could be due to the fact that the BAM·HOTf complex is now inhibited by the additive. However, this is not likely because the phenol is much less nucleophilic than pyridine which had no effect on the reaction. More likely, the acidic proton is being at least partially transferred to the free quinoline on the BAM ligand.

If the transfer of a proton to the free quinoline of the complex is shutting down the reaction, then the quinoline must be playing an important role not only in the asymmetric step, but also in the activation. This data lends itself to a new mechanistic picture than the one previously described in which the rate determining step is no longer simply self-tautomerization of nitromethane, but rather an assisted deprotonation of nitromethane by the free quinoline of the catalyst (Scheme 9).
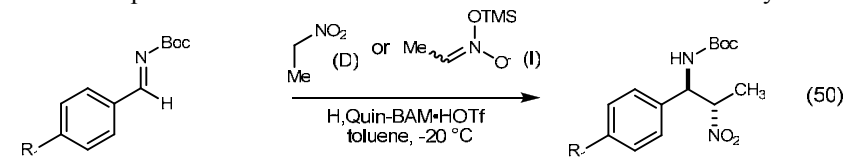
Scheme 9. Chiral Proton Catalyzed Aza-Henry Mechanism Using Bifunctional Catalyst
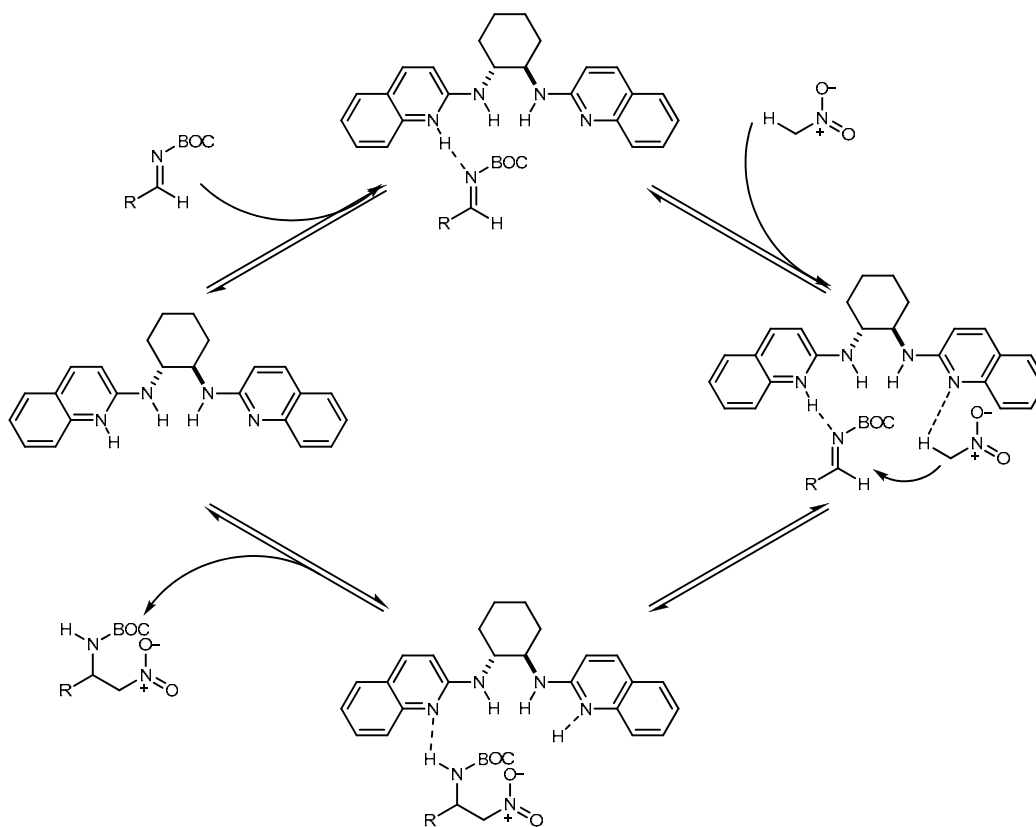
This data suggests the chiral proton complex is bifunctional in the aza-Henry reaction, i.e. it activates the electrophile and also activates the nucleophile. Although it was not our intent to gather direct mechanistic evidence in the investigation as to what may improve the rate of the reaction, it was discovered that a second equivalent of triflic acid shuts down product formation. This also supports the theory that the catalyst is bifunctional in the aza-Henry reaction.

There is one piece of data that does not fit into the mechanistic picture depicted in Scheme 9. The products obtained from the indirect (**I**) aza-Henry show the same level and direction of stereochemical induction as the products from the direct (**D**) aza-Henry (Table 13).[85] Using the same substrate in each reaction produces similar levels of enantioselection (Table 13, entries 6 and 7). While this finding may be coincidental, an unavoidable possibility is that both variants share a stereochemical model in the enantioselectivity-determining step.

---

[85] With Anand Singh.

Table 13. Comparison of Enantioselection in Direct and Indirect aza-Henry Reaction.

entry	R₁	catalyst (mol%)	D/I	dr[a]	%ee[b]	yield[c] (%)
1	^{p}Cl	10	D	18:1	78	71
2	^{p}Cl	100	D	12:1	84	76
3	^{p}Cl	100	I	14:1	95	82
4	H	10	D	17:1	78	65
5	H	100	I	17:1	93	71
6	^{p}CO$_2$Me	10	D	19:1	86	81
7	^{p}CO$_2$Me	100	I	14:1	88	86

[a]Diastereomeric ratios determined by GC. [b]Enantiomer ratios were measured using chiral stationary phase HPLC. [c]Isolated yield after chromatography.

Since the stereochemical determining step in the indirect aza-Henry reaction can only be through Lewis acid activation of the electrophile (the nucleophile is preformed), we again revised the mechanistic picture to that proposed below (Figure 25). Figure 25 represents two possible scenarios in which catalyst **118e** can activate both the electrophile and the pronucleophile. Activation of both the electrophile and pronucleophile by a *single catalyst* is depicted on the right side of Figure 25 and was also depicted in Scheme 9. Another possibility is depicted on the left side of Figure 25, whereby both the electrophile and pronucleophile are activated simultaneously, but by *two catalysts*. This mechanism best fits all of the data that we currently have regarding the mechanism. We know that the activation of the electrophile is the stereochemical determining step and that the stereochemical step must be conserved between the indirect and direct mechanisms. However, we also needed to account for the rate limiting step being the deprotonation of the nitroalkane by the catalyst. This is best explained by a second molecule of catalyst being involved in the deprotonation step.

Figure 25. Two Possible Activation Scenarios for Bifunctional Catalysis
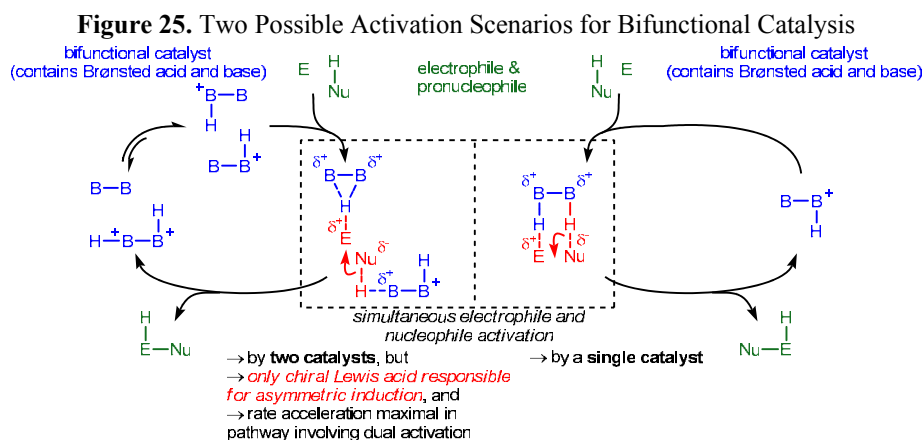
Further clarification of the mechanism turned us to an investigation of non-Boc Schiff bases to examine the effect of the Boc group on the rate as well as on the enantioselection of the direct aza-Henry reaction (Table 14).

Table 14. Chiral Proton-Catalyzed Direct Nitromethane Addition to Azomethine[a]

entry	R_1	R_2	time (h)	% conv	% ee
1	Ph	2-pyridyl	14	95	11
2	p-(NO$_2$)Ph	2-pyridyl	36	95	22
3	2-pyridyl	DPM	2.5	100	25
4	2-pyridyl	CPh$_3$	no rxn	-	-
5	p-(NO$_2$)Ph	CPh$_3$	no rxn	-	-
6	p-ClPh	CPh$_3$	no rxn	-	-
7	Ph	BOC	48	25	29
8	p-ClPh	BOC	84	50	54
9	Ph	CBz	96	80	14
10	p-ClPh	CBz	60	50	48
11	Ph	p-(OCH$_3$)Ph	8	100	11
12	2-pyridyl	p-(OCH$_3$)Ph	1	100	11
13	2-pyridyl	m-(OCH$_3$)Ph	1	100	4
14	2-pyridyl	o-(OCH$_3$)Ph	1	100	6

[a]Enantiomeric excess determined by HPLC using a chiral stationary phase.

The Boc and CBz protected imines were the least reactive, but afforded the highest enantiomeric excess (entries 7-10). This seems to indicate an importance of the Boc group in the stereochemical determing step. The Boc group does allow for a bidentate mode of binding, but that may not be the only factor which leads to high enantioselection

for these substrates. The diphenylmetyhl (DPM) imines appeared to be the next most promising in terms of fastest conversion and highest enantioselectivity (entry 3). In order to evaluate the effect that the DPM group has on the aza-Henry reaction, a series of DPM imines were screened for enantiomeric excess (Table 15).

Table 15. Chiral Proton-Catalyzed Direct Nitromethane Addition to Azomethine[a]

(54)

entry	R	time (h)	% conv	% ee
1	2-pyridyl	2.5	100	25
2	Ph	14	85	10
3	C_6H_{11}	24	>50	2
4	^tBu	72	35	6
5	o-(OCH$_3$)Ph	8	25	<10
6	p-(OCH$_3$)Ph	8	25	7
7	3-pyridyl	8	95	30-35
8	4-pyridyl	60	0	-
9	p-(NO$_2$)Ph	36	50	4
10	o-BrPh	24	75	9
11	p-ClPh	24	85	0

[a]Enantiomeric excess determined by HPLC using a chiral stationary phase.

The 2-pyridyl was considerably faster than any other DPM imine, affording the product in 25% ee (entry 1). This substrate again has the possibility for a bidentate mode of coordination to the catalyst. However, it was discovered that over time, the DPM products would undergo complete racemization. For example, a sample of the enantioenriched product would be racemized to 0% ee within 18-24 hours in ethanol or in 72 hours in dichloromethane. This is presumably due to the retro-process forming the iminium ion and nitronate, which in turn recombine nonselectively to afford the racemic product (eq 55).

(55)
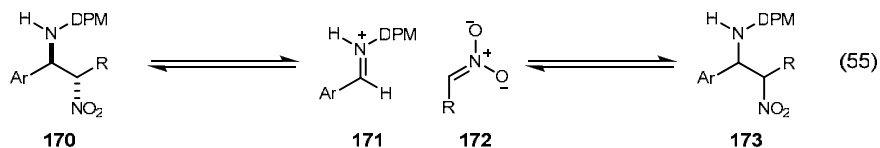
Perhaps this is one reason the Boc-imines are so much more stereoselective than other imines screened in the aza-Henry reaction. The carbamate functionality withdraws the lone pair of electrons on the nitrogen such that they become less nucleophilic toward

regeneration of the iminium ion. Due to this electron withdrawing effect of the carbamate, no racemization was ever observed in any Boc-protected products.

There are many additional factors that may contribue to the high stereoselection of the Boc-imines, not the least of which is their possibility for bidentate coordination mentioned above. In order to maintain the high enantioselectivity as well as increase the rate of the reaction, we reexamined our bifunctional mechanism hypothesis (Figure 25). If the rate-limiting step of the reaction is in fact the deprotonation of the nitroalkane by the free quinoline of the BAM ligand, then the rate would be substantially higher by dropping the pK_a of the pronucleophile's proton. With this in mind, ethyl nitroacetate was combined with the Boc-imine and BAM·HOTf complex to yield the new aza-Henry product **175** (eq 56).
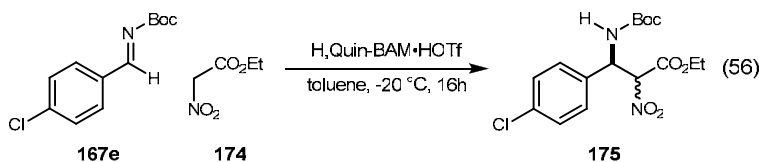
For the first time, only one equivalent of the nucleophile was necessary as opposed to its use as solvent in the previous cases. This is attributed to the dramatic increase in the rate of the reaction due to the more acidic proton as previously mentioned. The enantiomeric excess of **175** can be compared to the nitromethane and nitroethane enantioselectivities using the same substrate. When nitromethane was used as solvent, the product was afforded in 52% yield and 79% ee (Table 9 entry 6). When nitroethane was the nucleophile, the product was afforded in 59% yield, 17:1 diastereomeric ratio, and 82% ee (Table 10 entry 4). These can now be compared directly to ethyl nitroacetate which was obtained in 75% yield using only one equivalent and in a fraction of the time. The diastereomeric ratio was found to be 1:1 by HPLC; GC could not be used in this case as the product appeared to undergo the retro process on the column. HPLC separation of **175**, gratifyingly showed an enantiomeric excess of 80% for both diastereomers. Thus it appears not only that the rate greatly improved, but the enantioselection was at least maintained if not enhanced. However, the low diastereoselection would need to be addressed before nitroacetates could be used effectively in a new methodology. This will be addressed in greater detail in Section 2.3.1.

2.3. Application of the Asymmetric Aza-Henry Reaction to the Synthesis of Enantioenriched α-Amino Acids

The enantioselective synthesis of α-amino acids is an actively pursued area of asymmetric catalysis.[86] At the forefront of this field is the phase-transfer catalysis pioneered by O'Donnell (eq 57).[87]

$$Ph_2C=N\diagup CO_2{}^tBu \quad \xrightarrow[\substack{\textbf{178} \text{ (10 mol\%)} \\ \text{BEMP, CH}_2\text{Cl}_2 \\ -78\,°C, 23h}]{RBr} \quad Ph_2C=N\diagup \underset{\underset{R}{\vdots}}{}CO_2{}^tBu \quad (57)$$

$$\textbf{176} \hspace{7cm} \textbf{177}$$

As his source of asymmetry, O'Donnell used the cinchonidine-derived phase-transfer catalysts of type **178** (Chart 8). In 1994, they improved the enantioselectivity by using second generation catalysts of type **179**. In 1997, Lygo[88] and Corey[89] independently developed the so-called third generation cinchona-derived phase-trnasfer catalysts of type **180**.

Chart 8. First, Second, and Third Generation Cinchonidine-Derived Phase Transfer Catalysts

cinchonidine **178** **179** **180**
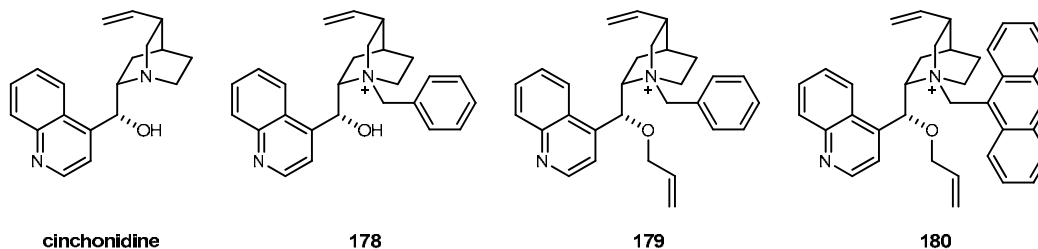
Nitroacetic acid derivatives have also been used as masked amino acids in a variety of transformations,[90] but their use in enantioselective transformations is presently limited to only three recent cases[91] that produce non-epimerizable nitroacetate derivatives. At the end of Section 2.2.3, it was shown that chiral proton catalyst **118e** could successfully

---

[86] For a recent review, see: O'Donnell, M. J. *Acc. Chem. Res.* **2004**, *37*, 506 and references therein.
[87] O'Donnell, M. J.; Eckrich, T. M. *Tetrahedron Lett.* **1978**, 4625.
[88] Lygo, B.; Wainwright, P.G. *Tetrahedron Lett.* **1997**, *38*, 8595.
[89] Corey, E. J.; Xu, F.; Noe, M. C. *J. Am. Chem. Soc.* **1997**, *119*, 12414.
[90] (a) Shipchandler, M. T. *Synthesis* **1979**, 666. (b) Rosini, G.; Ballini, R. *Synthesis* **1988**, 833. (c) Charette, A. B.; Wurz, R. P.; Ollevier, T. *Helv. Chim. Acta* **2002**, *85*, 4468. (d) Fornicola, R. S.; Oblinger, E.; Montgomery, J. *J. Org. Chem.* **1998**, *63*, 3528.
[91] (a) Li, H.; Wang, Y.; Tang, L.; Wu, F.; Liu, X.; Guo, C.; Foxman, B. M.; Deng, L. *Angew. Chem. Int. Ed.* **2005**, *44*, 105. (b) Knudsen, K. R.; Jorgensen, K. A. *Org. Biomol. Chem.* **2005**, *3*, 1362. (c) Charette: Moreau, B.; Charette, A. B. *J. Am. Chem. Soc.* **2005**, *127*, 18014.

catalyze the addition of ethyl nitroacetate into Boc-imines with good enantioselection (eq 56). We hypothesized that nitroacetate **185** could be converted to enantiomerically enriched α-amino acids **186** (eq 59). A side by side comparison of the Brønsted base and Brønsted acid approaches to the synthesis of enantioenriched α-amino acids is provided in Scheme 10.

Scheme 10. Brønsted Base and Brønsted Acid Approaches to the Synthesis of Enantioenriched α-Amino Acids
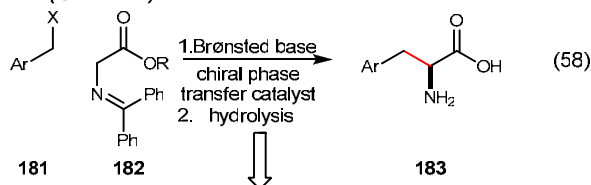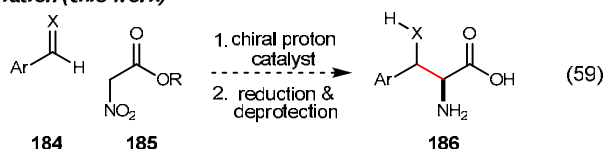
The addition of nitroacetates into N-Boc-imines, which was demonstrated in Section 2.2.3, produces α,β-diamino acids which are protected orthogonally, allowing the underlying amino acid to be revealed with a high degree of chemoselectivity.[92]

2.3.1. Enantioselective Synthesis of *Anti*-α,β-diamino Acids

Although high enantioselectivity had been observed in our initial addition of ethyl nitroacetate to an N-Boc imine, we set out to optimize this procedure for the large-scale synthesis of these α,β-diamino acids. Among our initial goals was to use an easily removable protecting group on the ester functionality that masked the carboxylic acid. We thought benzyl and *tert*-butyl would both be beneficial to others interested in this methodology. Screening the ester substituent also provided us with a good starting point for the optimization of yield, enantioselection, and diastereoselection (Table 16).

---

[92] Viso, A.; de la Pradilla, R. F.; Garcia, A.; Flores, A. *Chem. Rev.* **2005**, *105*, 3167.

Table 16. Effect of Nitroacetate Ester Substitution on Stereoselection

$$ \text{167e} \quad + \quad \text{185} \quad \xrightarrow[\text{toluene, -20 °C}]{10 \text{ mol\% 118e}} \quad \text{187} \quad (60) $$
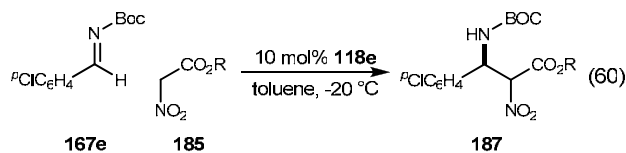
entry	R	time (h)	dr^b	%ee^b cis	trans	yield (%)^c
1	Me	16	1:1	82	nd	70
2	Et	16	1:1	80	80	75
3	Bn	36	1:1	71	nd	80
4	^{t}Bu	36	2:1	84	84	80

^{a}All reactions were 0.3 M in substrate and proceeded to complete conversion. ^{b}Diastereomer and enantiomer ratios were measured using chiral stationary phase HPLC. ^{c}Isolated yield.

The rate was unaffected by the change in substituent and only small changes were observed in enantioselection. We chose *tert*-butyl nitroacetate as the optimal nucleophile for this reaction because of its high enantioselectivity as well as the ease with which it can be cleaved (entry 4). The low diastereoselection observed was unexpected in light of nitroethane products that resulted in diastereomeric ratios of >20:1 (Section 2.2.3). Initially it was believed that a change in catalyst structure could provide an increase in diastereoselection. As a result, several BAM ligands were surveyed in this reaction as well as similar motifs that lack the Bis-Amidine core (Chart 9).

Chart 9. Structural Variations on Bis-Amidine Motif (without the bis-amidine)
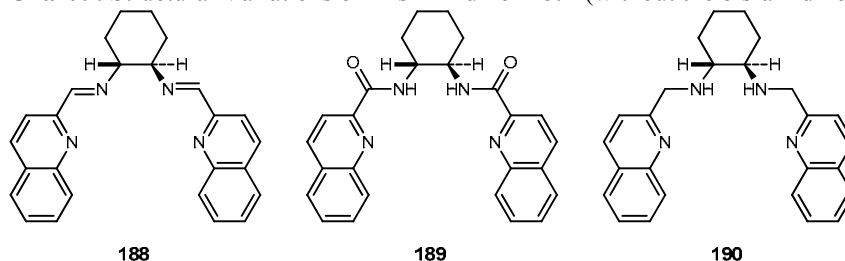
The triflic acid complexes of ligands **188**, **189**, and **190** did not catalyze the reaction. In **188** and **189**, the pyridines are less basic than the corresponding bis-amidines. Ligand **190** has an alkyl amine which is more basic than the bis-amidines, but is expected to be very different conformationally.

The same trends found in the ligand screen with silyl nitronates were consistent in the screen with nitroacetates. First, the position of substitution on the pyridine ring proved to be critical to enantioselection (Table 17 entries 1, 3, and 4).

Table 17. Effect of Pyridine Substitution on Nitroacetate Additions

entry	BAM	%yield	dr	%ee
1	H,^{6}Me (**118c**)	50	1:1	57,55
2	H,^{6}MeO (**118h**)	-	-	-
3	H,^{3}Me (**118a**)	40	1:1	6,10
4	H,^{5}Me (**118b**)	60	1:1	60,62
5	H,^{6}(Ph$_2$COH) (**118r**)	25	1:1	-18,-17

The more acidic H,^{6}MeO-BAM did not catalyze the reaction (entry 2); however, the larger H,^{6}(Ph$_2$COH)-BAM provided low enantiomeric excess for the opposite enantiomer (entry 5).

The quinoline derived bis-amidines proved to have various effects on the enantioselection (Table 18). H,Quin-BAM and H,Lep-BAM again proved to be the most selective affording 83% and 87% ee respectively (entries 1 and 6). As expected, H,Isoquin-BAM afforded racemic product due to lack of substitution at the 5 or 6 position (entry 5).

Table 18. Effect of Ligand Conformation of Enantioselection

entry	BAM	%yield	dr	%ee
1	H,Quin (**118e**)	75	1:1	81,83
2	H,^{3}Quin (**118p**)	45	1:1	-24,-20
3	H,^{2}Quin(^{3}Quin)-BAM (**118q**)	55	1:1	-50,-49
4	H,Quin(^{2}Nap)-BAM (**118o**)	35	1:1	-17,-7
5	H,^{1}Isoquin-BAM (**118d**)	50	1:1	-2,3
6	H,Lep (**118f**)	70	1:1	83,87
7	H,Quinox (**118n**)	-	-	-

The enantioselection was again reversed with H,^{2}Quin(^{3}Quin)-BAM (entry 3). Interestingly, H,^{3}Quin was found to provide some enantioselection, but also for the opposite enantiomer (entry 2). H,Quinox-BAM did not afford any product, which is consistent with the trend of more acidic ligands not catalyzing the reaction (entry 7).

Anand Singh identified unsymmetrical H,Quin(^{6}(^{9}Anth)^{2}Pyr)-BAM complex **118oo** as a catalyst for the highly *anti*-diastereoselective and enantioselective nitroacetate additions. In order to isolate the aza-Henry adduct with high diastereoselection, the product needed to be reduced before warming to room temperature. It was observed that these adducts would epimerize on warming to room temperature, which will be discussed in more detail in Section 2.3.2. To avoid any loss in diastereoselection, Bo Shen developed a method for the cold reduction of the nitro group following a Ganem protocol.[93] Table 19 summarizes their work.

Table 19. Chiral Proton Catalyzed Additions of α-Nitroesters to Azomethines: Scope^a

entry	Ar		catalyst	dr^b (5)	dr^b (6)	%ee^b (6)	yield^c
1	^{p}Cl	a	**118e**	1:2	1:2	84	80
2	^{p}Cl	a	**118oo**	5:1	5:1	95	88
3	^{p}AcO	b	**118e**	2.5:1	2.2:1	85	76
4	^{p}AcO	b	**118oo**	11:1	11:1	89	74
5	^{2}Np	c	**118e**	4:1	4:1	78	69
6	^{2}Np	c	**118oo**	12:1	11:1	91	80
7	^{p}F	d	**118e**	-	1:1	67	80
8	^{p}F	d	**118oo**	-	7:1	93	81
9	^{p}CF$_3$	e	**118oo**	7:1	7:1	88	83
10	^{p}Me	f	**118oo**	6:1	6:1	95	81
11	^{m}PhO	g	**118oo**	6:1	6:1	87	84
12	^{m}Cl	h	**118oo**	10:1	10:1^d	87	70
13	^{p}MeO$_2$C	i	**118oo**	8:1	8:1	95	84

^{a}All reactions were 0.30 M in substrate and proceeded to complete conversion. ^{b}Diastereomer ratios were measured by ^{1}H NMR (a reliable measurement was not possible for the addition product for entries 7-8). Enantiomer ratios were measured using chiral stationary phase HPLC. ^{c}Isolated yield (two steps). ^{d}Measured by GC.
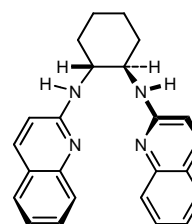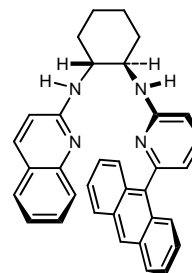
With a reliable two step procedure in hand, we surveyed a variety of N-Boc imines with catalyst **118oo** (Table 19).[94] Use of sodium borohydride/cobalt(II) chloride allows

[93] Satoh, T.; Suzuki, S.; Suzuki, Y.; Miyaji, Y.; Imai, Z. *Tet. Lett.* **1969**, 4555. Heinzman, S. W.; Ganem, B. *J. Am. Chem. Soc.* **1982**, *104*, 6801.
[94] Singh, A.; Yoder, R. A.; Shen, B.; Johnston, J. N. *J. Am. Chem. Soc.* **2007**, *129*, 3466.

for an effective reduction of the adducts without epimerization at the α-position. Alternatives that were investigated resulted in either lowering of the diastereomeric ratio, or reduction of halogenated adducts.[95] These issues are cleanly avoided in the protocol described here, and over two steps, high yields are consistently observed. It is also important to note that using catalyst **118oo** with nitroacetates, we did not observe any effect on enantioselection from the substituent on the aromatic ring of the imine as was observed in the addition of nitroalkanes (see Section 2.2.3). Excellent enantioselection and high diastereoselection were demonstrated for a variety of substrates isolated in good yield after two steps.
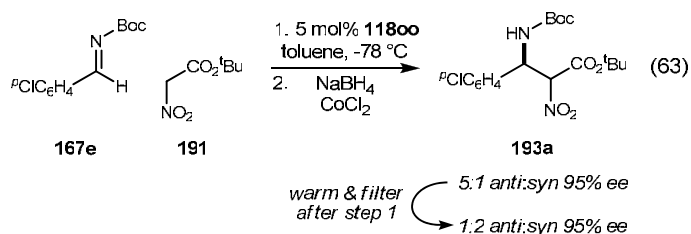
It was estabilished that the *anti* diastereoselection represents a kinetic selectivity by subjecting the product to conditions that favor epimerization (eq 63).[85] It was observed that a 5:1 (*anti*:*syn*) mixture resulted in a 1:2 (*anti*:*syn*) mixture after warming and filtering the reaction mixture through silica gel.[96] This post addition epimerization also highlights the fact that this catalyst can selectively deprotonate **191** in a mixture of **191** and **193**. We hypothesized that this post addition epimerization could allow access to enantioenriched *syn*-α,β-diamino acids.

2.3.2. Enantioselective Synthesis of *Syn*-α,β-diamino Acids

As mentioned in the previous section, it was discovered that the products obtained from nitroacetate addition into N-Boc imines would epimerize upon warming to room temperature (eq 63). Initial experiments were carried out examining the degree to which this thermodynamic epimerization could be used to increase diastereoselection favoring the *syn* product (Table 20).

---

[95] Shen, B.; Johnston, J. N. unpublished results.
[96] Note: Silica gel is not necessary for the epimerization but it accelerates the process.

Table 20. Effect of Time and Temperature on Diastereoselection

entry	time	temperature	dr
1	1 h	-78 °C	1:1
2	4 h	-78 °C	1:1
3	2 h	rt	1.2:1
4	1 d	rt	1.4:1
5	2 d	rt	2.1:1
6	3 d	rt	2.4:1
7	6 d	rt	3:1

Monitoring the reaction of ethyl nitroacetate by NMR showed an increase in diastereoselection to 3:1 (entry 7). The same experiment was conducted with methyl nitroacetate, but the diastereoselection only increased to 1.5:1. Since it appears to be a thermodynamically driven isomerization, *tert*-butyl nitroacetate was expected to give the highest diastereselection. In fact, after stirring for 6 days at room temperature, the diastereoselection rose to 4:1. Since the enantioselection is conserved as these changes in diastereomeric ratios were observed, we can rule out a retro-aza-Henry mechanism leading to the observed epimerization. Therefore, the increased acidity of the hydrogen atom on the nitroacetate could be used as a tool in selective epimerization leading to the *syn*-diastereomers.
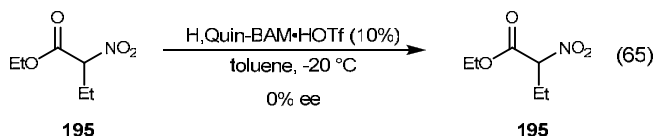
These experiments suggested that catalyst-mediated epimerization led to a thermodynamic ratio of 3-4:1 *syn*:*anti*-α,β-diamines. An alternative rationale for the ratio involves a stereoselective reprotonation mediated by the chiral catalyst. We therefore examined whether the catalyst could enantioselectively protonate a similar compound (**195**). Since no enantioselection was observed under these conditions, it is unlikely that the catalyst is deprotonating and diastereoselectively reprotonating the product with facial selectivity. More likely, the catalyst is serving as a general base allowing for the epimerization of the kinetic (*anti*) product to the thermodynamically favored *syn* product.

In fact, it was found that the purified nitro compound would isomerize upon standing at room temperature and that silica gel catalyzes that process.

Scheme 11. *Syn* Selective Synthesis of Nitroacetate adducts using Recrystallization

(66)

167e   191   193a   193a
                          5:1 syn:anti   >99:1 syn:anti
                            86% ee   >99% ee
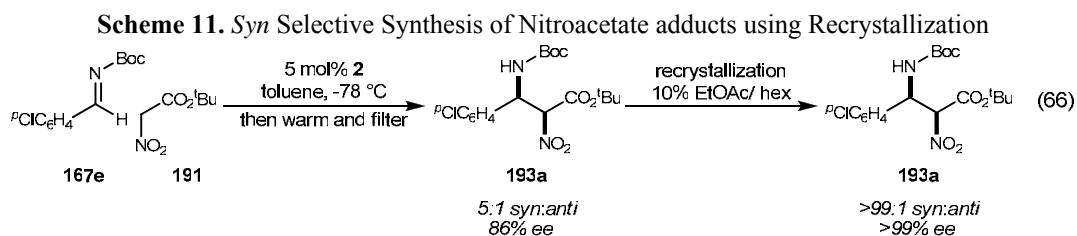
We thought that recrystallization could be used as a means to obtain highly *syn*-enriched product. As illustrated in Scheme 11, it was possible to get material with high optical purity but it turned out that the recrystallization was exceedingly difficult to reproduce.[97] It should be noted that this highly *syn*-enriched material was also found to epimerize over time, eventually resulting in a 4:1 mixture of diastereomers (*syn:anti*). However, it was possible to obtain material consistently in 60-70% yield and 7:1 dr using the recrystallization process. An X-Ray crystal structure of *syn*-**193a** was obtained which showed a hydrogen bond between the NH of the Boc-amine and the nitro group (Figure 26).

Figure 26. X-Ray Crystal Structure of *syn*-**193a**
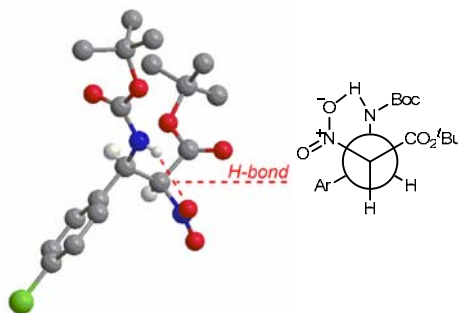
Our initial efforts in optimizing a protocol for a highly enantioselective and diastereoselective nitroacetate addition to yield *syn*-enriched products began with H,Quin-BAM·HOTf (**118e**).

---

[97] With Bo Shen.

Table 21. Substrate Scope of **118e** Catalyzed Nitroacetate Additions to N-Boc Imines

entry	R		dr[b]	%ee[b]	yield(%)[c]
1	p-OAc	d	3:1	85	74
2	p-CO$_2$Me	c	2:1	85	82
3	p-Cl	a	2:1	86	81
4	p-Me	e	2:1	81	81
5	Ar=2-naphthyl	f	2:1	78	84
6	p-F	g	2:1	67	79
7	o-CF$_3$	h	2:1	70	80
8	Ar=1-naphthyl	i	2:1	62	83

[a]All reactions were 0.30 M in substrate and proceeded to complete conversion. [b]Diastereomer and enantiomer ratios were measured using chiral stationary phase HPLC. [c]Isolated yield after two step.

The results of a substrate screen using H,Quin-BAM·HOTf as the catalyst were somewhat surprising (Table 21). Although enantioselection was good for several substrates (entries 1-3), they were uncharacteristically low for several other substrates (entries 6-8). The ligand screen reported in Section 2.3.1 demonstrated that H,Quin(^{6}(^{9}Anth)^{2}Pyr)-BAM provided the α,β-diamino acid products with higher enantioselection.

Table 22. Substrate Scope of **118oo** Catalyzed Nitroacetate Additions to N-Boc Imines
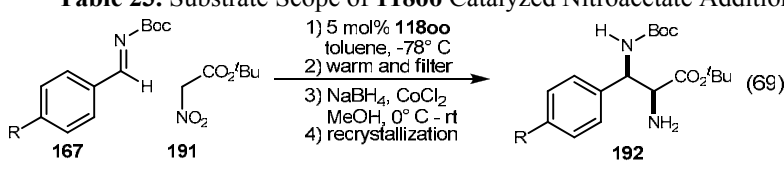
entry	R		dr[b]	%ee[b]	yield(%)[c]
1	p-OAc	d	3:1	99	74
2	p-CO$_2$Me	c	2:1	95	83
3	p-Cl	a	5:1	95	86
4	p-Me	e	2:1	93	85
5	Ar=2-naphthyl	f	2:1	91	80
6	p-F	g	4:1	93	85
7	o-CF$_3$	h	2:1	80	80
8	Ar=1-naphthyl	i	2:1	83	71

[a]All reactions were 0.30 M in substrate and proceeded to complete conversion. [b]Diastereomer and enantiomer ratios were measured using chiral stationary phase HPLC. [c]Isolated yield after two step.

By comparison, we were pleased to discover that the reactions catalyzed by **118oo** gave consistently higher enantioselectivities for all substrates (Table 22). Excellent
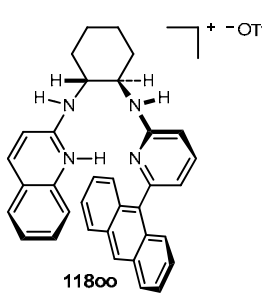
enantioselectivities were obtained for a variety of substrates (entries 1-6). Product **192g** was obtained with 93% ee, 26% higher than the analogous reaction catalyzed by H,Quin-BAM·HOTf (entry 6). Recrystallization of these adducts could provide access to highly enantioenriched *syn*-α,β-diamino acids.

Table 23. Substrate Scope of **118oo** Catalyzed Nitroacetate Additions to N-Boc Imines

entry	R		dr[b]	%ee[b]	yield(%)[c]
1	*p*-OAc	d	8:1	92	68
2	*p*-Cl	a	10:1	93	86
3	*p*-Me	e	8:1	90	81
4	*o*-Me	j	16:1	70	80
5	*p*-F	g	8:1	90	85
6	*p*-CF$_3$	k	3:1	80	69

[a]All reactions were 0.30 M in substrate and proceeded to complete conversion. [b]Diastereomer and enantiomer ratios were measured using chiral stationary phase HPLC. [c]Isolated yield after two step.

Recrystallization of the products before reduction allows for a substantial increase in diastereoselection for most substrates (Table 23).[95] These numbers now approach the desired level of stereoselection necessary for this to be a useful methodology to access the *syn*-α,β-diamino acids. Therefore, using the same reaction and the same catalyst, both *syn*- and *anti*-α,β-diamino acids can be obtained with very good stereoselection and in good yield. The key difference being allowing the initial nitroacetate adduct to warm to room temperature and recrystallized before employing the reduction procedure.

2.3.3. Rationale for Stereoselection of the Nitroacetates

Variations to each component of a highly stereoselective chiral proton catalyzed reaction provide insight into our evolving stereochemical model. The proposed stereochemical model was first introduced in Figure 17 in Section 1.3.2. Support for this model was obtained when an increase in rate was observed with the catalyst in the silyl-nitronate addition to imines in Section 2.2.2. Furthermore, the importance of substitution at the six-position of the pyridine ring was verified in that section. The importance of the Boc group of the N-Boc imines was shown in Section 2.2.3. In addition, experiments

suggest that the direct aza-Henry reaction proceeds via bifunctional catalysis even though the activation of the electrophile and the nucleophile are not believed to occur simultaneously. Just as each of these examples helped evolve the stereochemical model, using nitroacetates as nucleophiles has also provided additional information which can contribute to the overall picture of the stereochemical model.

One key difference in the addition of nitroacetates was the discovery that catalyst **118oo** achieved better enantioselection and diastereoselection than H,Quin-BAM·HOTf (**118e**). Because the structure of the unsymmetrical **118oo** is significantly different from that of the symmetrical **118e**, it is remarkable that the catalyst provided an *increase* in enantioselection. Furthermore, the fact that the products produced by these two catalysts have the *same* sense of stereoinduction lends further support to the stereochemical model's proposal of bidentate chelation by the ligand.

Figure 27. One Alternative to the Proposed Stereochemical Model
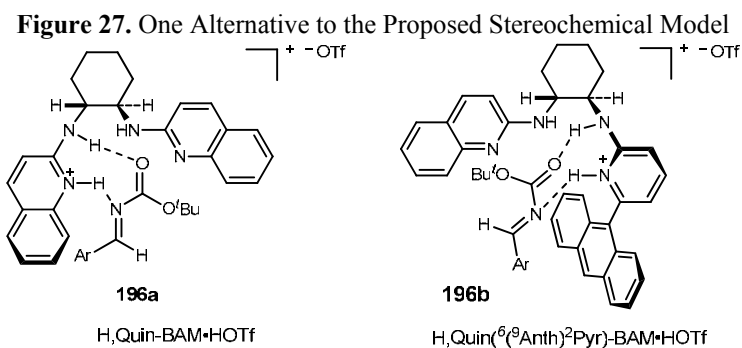
One alternative to the proposed stereochemical model is binding of the N-Boc imine to a monodentate amidinium ion as depicted in **196a** (Figure 27). The implications of this transition state in the enantiodetermining step are very different for the symmetrical **118e** and the unsymmetrical **118oo**. H,Quin-BAMHOTf (**118e**) offers equivalent binding sites to the substrate whereas H,Quin(^{6}(^{9}Anth)^{2}Pyr)-BAM (**118oo**) provides competing recognition motifs. The fact that there is a shared sense of stereoinduction between these two very different catalysts lends support to the bidentate nature of the catalyst in the enantiomer-determining step.

Catalysts **118e** and **118oo** also have the unique ability of providing highly diastereoselective reactions, both yielding the *anti* diastereomer as their respective kinetic products (nitroalkanes for **118e** and nitroacetates for **118oo**). This indicates that the

catalyst plays an important role in determining the diastereoselection of the products. Furthermore, although catalyst **118e** can effect high diastereoselectivity for nitroalkanes, it produces 1:1 mixtures of *syn* and *anti* when nitroacetates are used. Therefore, catalyst **118oo** must be perturbing the transition state to regain the preferential selectivity for the *anti* diastereomer.

Figure 28. Newman Projections for Nitroalkane and Nitroacetate Additions to N-Boc Imines
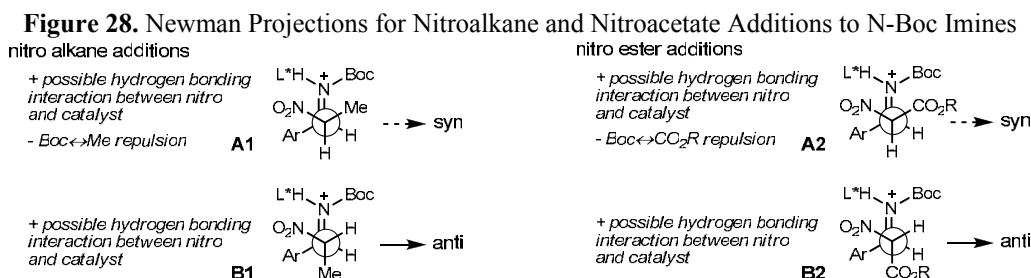
A closer examination of the diastereoselection in these reactions led to the Newman projections depicted above (Figure 28). These pictures can be simplified by the assumption that the nitro group is influenced in some way by the catalyst, perhaps in a secondary hydrogen bonding interaction. Fixing the nitro group to that quadrant only gives the R group two options. First, the methyl could be up (leading to the *syn* product), but in this orientation there is repulsion from the Boc group. Alternatively and more likely, the R group could be pointed down, thus minimizing the steric repulsion while still allowing for the secondary control element that holds the nitro near the catalyst. Although this clearly explains why the *anti* diastereomer is favored in both reactions, it does not account for the dramatic decrease in dr when catalyst **118e** is used with nitroacetates.

Figure 29. Alternative Newman Projection Leading to *syn* Product
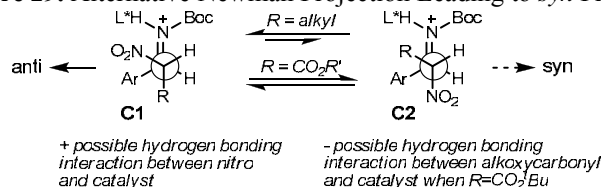
In order to provide a unified rationale for observed diastereoselection in all highly selective chiral proton catalyzed aza-Henry variants, two main issues must be addressed.

First, the loss of diastereoselection when using H,Quin-BAM·HOTf (**118e**) with nitroacetates as opposed to nitroalkanes must be explained. Also the recovery of diastereoselection with nitroacetates when catalyst **118oo** was used instead of **118e** must be addressed by the same model. This data can best be explained by an alternative transition state only accessible to the nitroacetates and not the nitroalkanes (Figure 29). The ester group of the nitroacetates has the ability to interact with the catalyst as a Lewis base (hydrogen bond acceptor) in the same manner invoked for the nitro group. This in turn allows for alternate Newman projection **C2**, which accounts for the drop in diastereoselection by catalyst **118e** when going from nitroalkanes to nitroacetates. Furthermore, changes in the ligand could allow for better discrimination between the ester group and the nitro group of the nitroacetates. In this way, it is believed that catalyst **118oo** causes a steric repulsion with the *tert*-butyl ester group and disfavors transition state **C2**. This would select for formation of the *anti* diastereomer through transition state arrangement **C1** and effectively recover the high diastereoselection observed in the nitroalkane chemistry with **118e**.

Chapter 3. Chiral Proton Catalyzed Diels-Alder Reactions

3.1. Brevianamide

3.1.1. Background

The brevianamide class of natural products possess a structurally unique diazabicyclo[2.2.2] octane core which has stimulated interest in its proposed biosynthesis as well as in its laboratory synthesis. Birch and Wright first isolated brevianamide A in 1969 from the culture extracts of the fungus *Penicillium brevicompactum*.[98] Structure elucidation by spectroscopic methods (UV, IR, 1H NMR, MS), and derivative studies, revealed a diketopiperazine bicyclic core and a spiro-indoxyl center (Figure 30). X-ray analysis of a single crystal of the semisynthetic derivative 5-bromo-brevianamide A by Coetzer in 1974 confirmed the proposed structure and at the same time established the relative and absolute stereochemistry of brevianamide A.[99] Since its initial isolation in 1969, brevianamide A has also been isolated from *Penicillium viridicatum*[100] and *Penicillium ochraceum*.[101]

Figure 30. Stucture of Brevianamide A
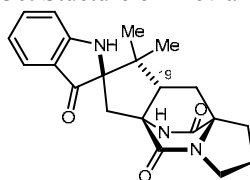
(+)-brevianamide A

Minor metabolites were also isolated from the extracts of *Penicillium brevicompactum* and were subsequently named brevianamides B-F (Chart 10).[102] It was later discovered that irradiation of brevianamide A with white light produced

---

[98] (a)Birch, A. J.; Wright, J. *J. Chem. Soc. Chem. Comm.* **1969**, 644-645. (b) Birch, A. J.; Wright, J. *Tetrahedron* **1970**, *26*, 2329. (c) Birch, A. J. *J. Agr. Food Chem.* **1971**, *19*, 1088-1092.

[99] Coetzer, J. *Acta Cryst.* **1974**, B30, 2254.

[100] Wilson, B. J.; Yang, D. T.; Harris, T. M. *Appl. Microbiol.* **1973**, *26*, 633.

[101] Robbers, J. E.; Straus, J. W.; Tuite, J. *Lloydia* **1975**, *38*, 355.

[102] Birch, A. J.; Russell, R. A. *Tetrahedron* **1972**, *28*, 2999.

brevianamides C and D and thus their isolation was concluded to be an artifact of culture conditions. The relative and absolute stereochemistry of the proposed structure **201** for brevianamide E was later confirmed by total synthesis. Brevianamide F (**202**) was determined to be *cyclo*(L-tryptophyl-L-proline), which was later determined to be a biosynthetic precursor of brevianamide A using feeding experiments.

Chart 10. The Brevianamide Family of Natural Products

brevianamide A (**197**)   brevianamide B (**198**)   brevianamide C(**199**)

brevianamide D (**200**)   brevianamide E (**201**)   brevianamide F (**202**)
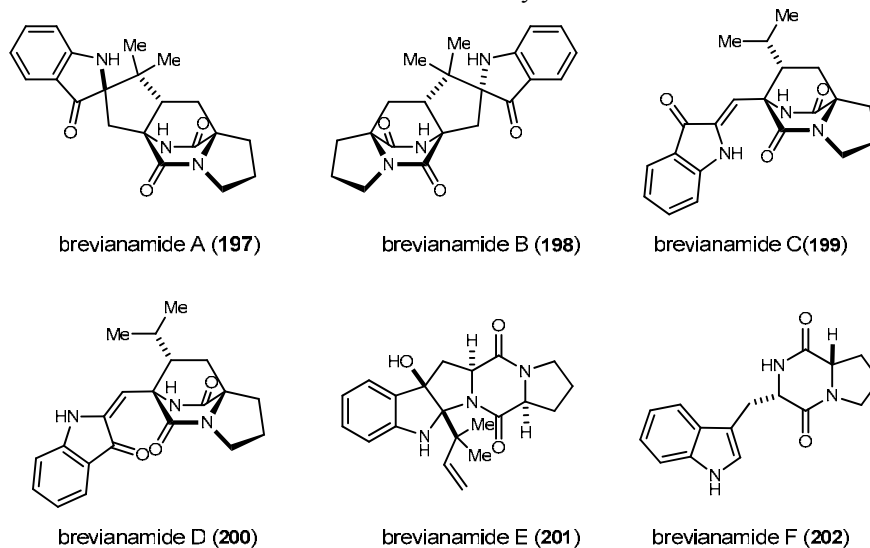
Upon the initial isolation of brevianamide B, the structure was hypothesized to be epimeric to that of brevianamide A at the indoxyl spirocyclic center (C2). The rationale for this assignment was that brevianamide B could be made from brevianamide A via a three-step reduction/oxidation sequence (Scheme 12), a procedure that proved useful in obtaining sufficient quantities of this minor metabolite for studies. However, in 1988 Williams and coworkers completed the total synthesis of brevianamide B which revealed its true absolute stereochemistry (Chart 10).[103] Surprisingly, the structures for naturally occurring brevianamides A and B were found to be enantiomorphic with respect to their diazabicyclo[2.2.2] octane core and possess identical configuration at the C2 spiroindoxyl center. This discovery had major implications on the ensuing debate over the biosynthesis

---

[103] (a) Williams, R. M.; Glinka, T.; Kwast, E. *J. Am. Chem. Soc*. **1988**, *110*, 5927. (b) Williams, R. M.; Glinka, T.; Kwast, E.; Coffman, H.; Stille, J. K. *J. Am. Chem. Soc*. **1990**, *112*, 808. (c) Williams, R. M.; Glinka, T. *Tetrahedron Lett.* **1986**, *27*, 3581.

of brevianamides A and B. These implications will be the focus of the following discussion.

Scheme 12. Three-Step Synthesis of Brevianamide B from Brevianamide A

(+)-brevianamide A   deoxybrevianamide A   (-)-brevianamide B
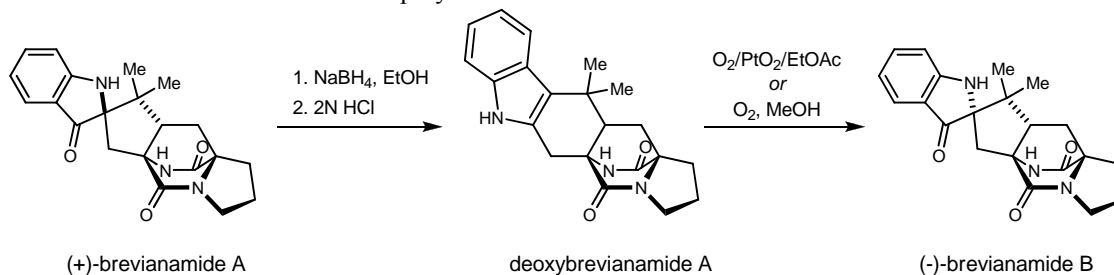
A great deal of interest has been generated by the possible biosynthetic origin of the bicyclo[2.2.2] pyrazinedione core, which in large part has fueled studies on this family of natural products.[104] Shortly after the structure of brevianamide A was published, Sammes put forth a provocative hypothesis for the formation of the bicyclo[2.2.2] pyrazinedione core, suggesting it could arise from an intramolecular [4+2] cycloaddition reaction of a hydroxypyrazinone moiety and the tethered prenyl alkene (Figure 31).[105] At the time, Diels-Alder reactions on these systems were unknown; however, Sammes supported this proposal with experimental results on model pyrazine systems (*vide infra*).

Figure 31. Proposed Biological Diels-Alder Reaction

203   204
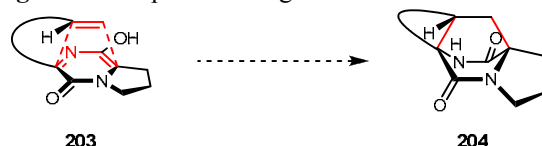
By proposing a biological Diels-Alder reaction for the formation of the brevianamide bicyclic core, Sammes was able to account for the formation of both enantiomorphic forms embodied by brevianamides A and B. Approach of the prenyl alkene dienophile from one face of the relatively planar prochiral hydroxypyrazinone diene would produce

---

[104] For reviews, see (a) Williams, R. M.; Cox, R. J. *Acc. Chem. Res*. **2003**, *36*, 127. (b) Williams, R. M *Chem. Pharm. Bull*. **2002**, *50*, 711.
[105] Porter, A. E. A; Sammes, P. G. *Chemical Communications* **1970**, 1103.

the bicyclic core of brevianamide A, while approach from the opposite face would produce the core of brevianamide B (Figure 32).

Figure 32. Diels-Alder Reaction Leading to Brevianamides A and B
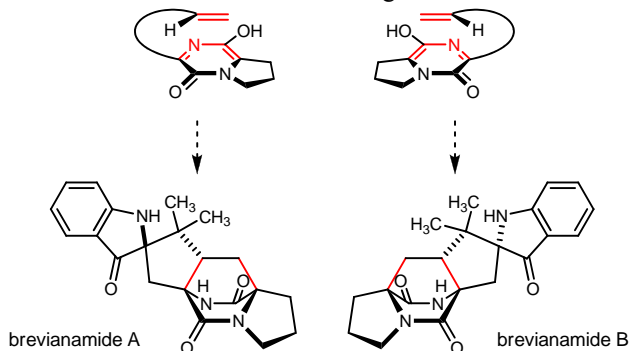
Combining the elucidation of the absolute stereochemistry of brevianamide B with Sammes hypothesized hetero-Diels-Alder reaction, Williams developed a more detailed biosynthetic proposal (Scheme 13).[106] In this pathway, two electron oxidation of the known biological precursor brevianamide F forms the achiral hydroxypyrazinone **206**, which serves as the azadiene for the intramolecular hetero-Diels-Alder reaction. As mentioned above, approach of the prenyl alkene (dienophile) from either face of the 2-hydroxypyrazinone (diene) would furnish adducts **207** or **208**. Oxidation at the 3-position of the indole would produce hydroxylindolenines **209** and **210**, which could then undergo a well-precedented stereospecific Pinicol rearrangement to furnish both naturally occurring Brevianamides A and B.

[106] Williams, R. M.; Kwast, E.; Coffman, H.; Glinka, T.; *J. Am. Chem. Soc.* **1989**, *111*, 3064.

Scheme 13. Proposed Biosynthesis of Brevianamides A and B via Enantioselective [4+2] Cycloaddition
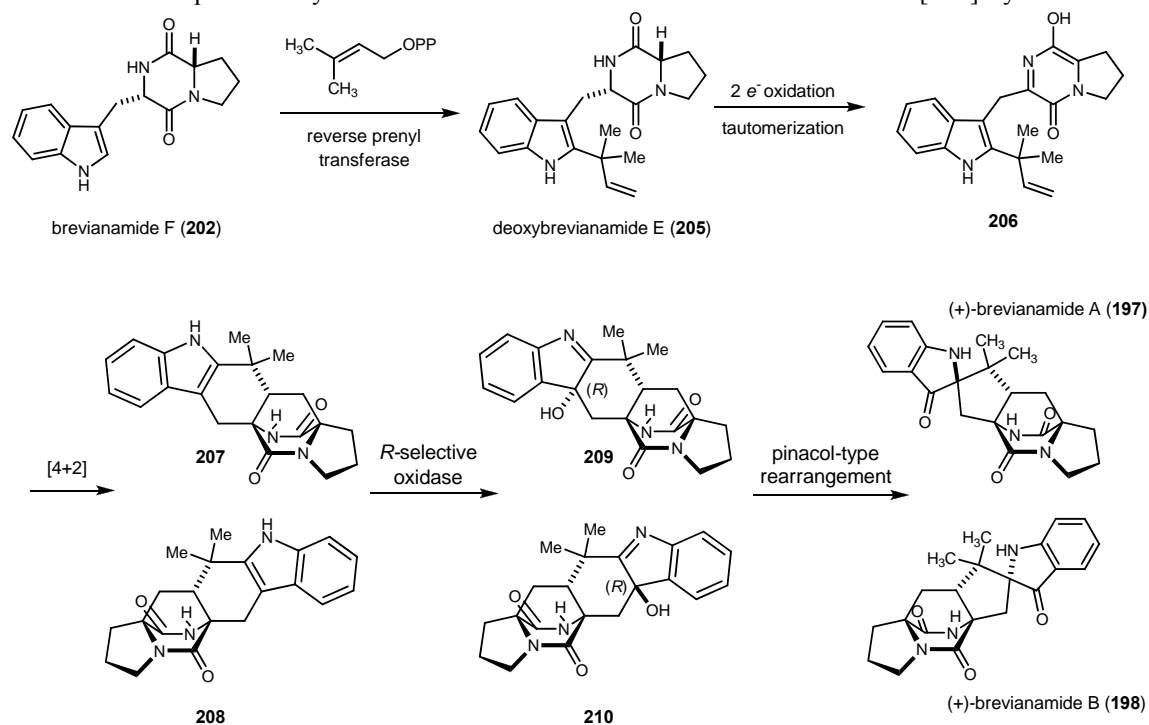
The above biosynthetic proposal outlined by Williams has several major implications. First, since brevianamide A is produced naturally in a greater quantity than brevianamide B (~20:1), either (1) the Diels-Alder reaction produces adducts **207** and **208** in unequal, nonracemic form favoring **207**, or (2) a kinetic resolution takes place in the oxidation of racemic **207**. If the former were true, intervention of an enzyme capable of stereoselectively effecting a [4+2] cycloaddition reaction (the so-called Diels-Alderase) would be necessary. Moreover, the involvement of a Diels-Alderase would explain the complete diastereoselectivity observed in the biosynthesis, which only produces the *anti*-C-19 configuration, a diastereomer that is not favored in the thermal Diels-Alder reaction of **206** (*vide infra*).

Second, since both brevianamides A and B share the same stereochemistry at the indoxyl spirocenter (*R*), the oxidation of **208** would take place from the less hindered face for brevianamide B (**198**) and the *more hindered face* for brevianamide A (**197**). As was shown above, the preferred facial selectivity of this oxidation has been established experimentally in the semisynthesis of brevianamide B from A (Scheme 12). An (*R*)-selective indole oxidase was proposed to explain the diastereoselectivity of the oxidation

step by recognizing the binding orientation of the indole moiety. However, no enzyme responsible for mediating the Diels-Alder or indole oxidation has been characterized for *Penicillium brevicompactum*.

On the contrary, feeding experiments of radio-labeled *d,l*-[8-^{13}C]-**202** into cultures of *Penicillium brevicompactum* resulted in no observable incorporation into brevianamides A or B, which would have been expected based on the above proposal.[107] As a result, Williams proposed a revised biosynthetic pathway shown below (Scheme 14).[108] In this pathway, deoxybrevianamide E is first diastereoselectively oxidized by an (*R*)-selective indole oxidase, producing hydroxyindolenine **211**. This intermediate can then undergo nucleophilic addition from the pyrazinedione nitrogen to form brevianamide E, or a stereospecific pinacol rearrangement could take place to form **212**. Indoline **212** must then undergo a 2 electron oxidation to give the putative hydroxypyrazinone which can then undergo the hetero-Diels-Alder reaction.

Scheme 14. Proposed Biosynthesis of Brevianamides A and B via Diastereoselective [4+2] Cycloaddition
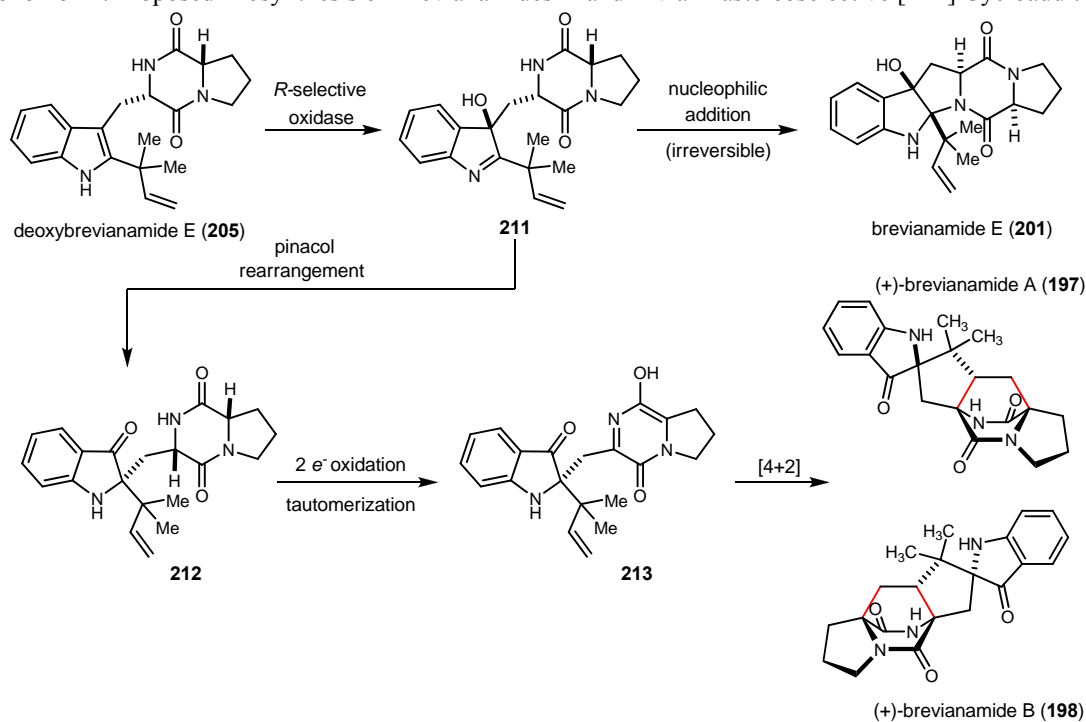
[107] Sanz-Cervera, J. F.; Glinka, T.; Williams, R. M. *Tetrahedron* **1993**, *49*, 8471.
[108] Sanz-Cervera, J. F.; Glinka, T.; Williams, R. M. *J. Am. Chem. Soc.* **1993**, *115*, 347.

Feeding experiments were again conducted in an effort to test the revised proposal for the biosynthesis of the brevianamides. These results indicated significant incorporation of [8-^{3}H]-deoxybrevianamide E into brevianamides A (7.8%), B (0.9%) and E (24.9%). However, no incorporation was observed when [8-^{3}H]-brevianamide E was used in the feeding experiments.[107] Furthermore, it was shown that brevianamide E could be made directly from photooxidation of deoxybrevianamide E. This led Williams to conclude that brevianamide E is a shunt metabolite that is not an intermediate in the biosynthesis of brevianamides A or B. Unfortunately, attempts to synthesize **211** for feeding experiments to validate this pathway have been unsuccessful.

3.1.2. Previous Total Syntheses of the Brevianamides

In 1988, Williams completed the first total synthesis of (-)-Brevianamide B (Scheme 15).[103] Starting from known pivaldehyde acetal **214**, amide **215** was formed after opening the lactone functionality with lithium *p*-methoxybenzylamide salt. Acylation of the proline nitrogen with bromoacetylbromide, followed by alkylative ring closure formed pyrazinedione **216**. **217** was then formed by ozonolysis of the terminal olefin, Wittig olefination of the resulting aldehyde and alkylation of the pyrazinedione with gramine. Formation of the bicyclo[2.2.2]diazaoctane ring of the natural product was accomplished in the key step using a stereoselective S$_N$2' cyclization. Optimization of the solvent and as well as of an additive for the cyclization revealed that the addition of several equivalents of 18-crown-6 to a reaction of **217** with sodium hydride in THF gave the desired diastereomer **219** in a 4.9:1 ratio. Williams' proposed that association of the crown ether with the sodium cation generated a sterically demanding environment around the enolate oxygen, which in turn favored transition state **218**, with the allylic chloride facing away from the enolate. Ring closure and Boc deprotection was achieved by treatment of **219** with aqueous HCl to give **220**. Oxidation of **220** gave a single diastereomer of hydroxyindolenine **221.** This was then treated with NaOMe in methanol to effect the stereospecific pinacol rearrangement to (-)-brevianamide B. X-ray crystallographic analysis was obtained to confirm the relative stereochemistry of the synthetic product.

Scheme 15. Williams' Total Synthesis of (-)-Brevianamide B
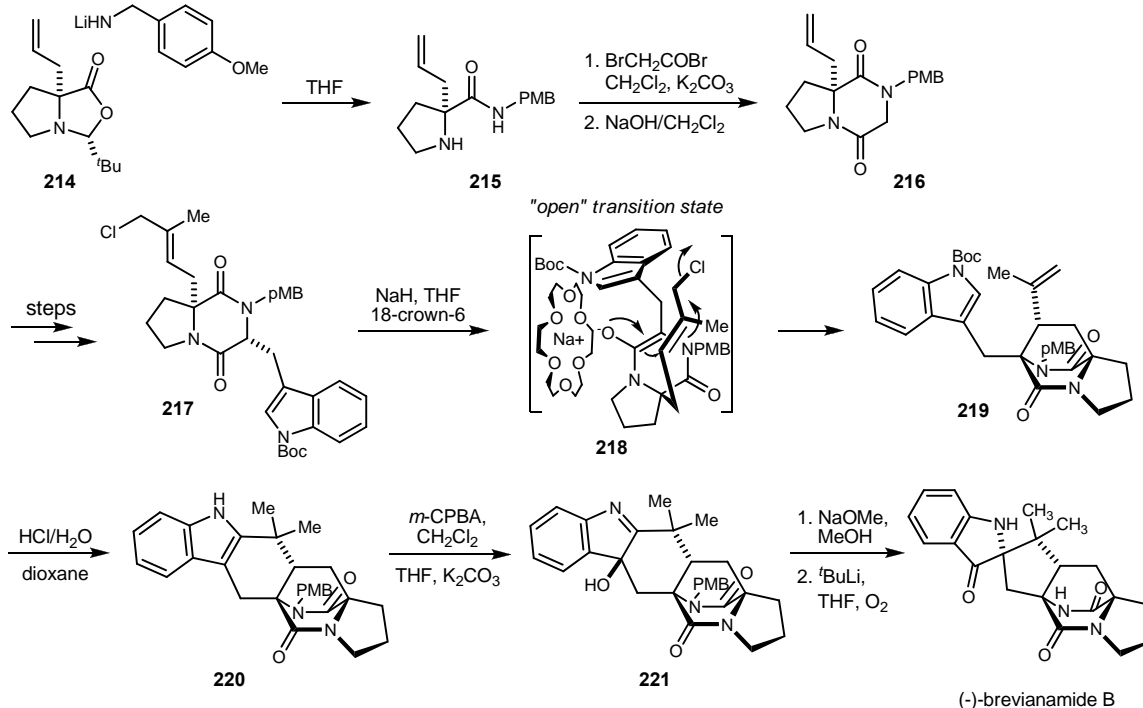
Ten years after his initial synthesis of (-)-brevianamide B, Williams employed an intramolecular hetero-Diels-Alder reaction in the racemic synthesis of C-19-*epi*-brevianamide A and brevianamide B (Scheme 16).[109] Beginning with epi-deoxybrevianamide E as reported by Kametani (*vide infra*), treatment with Me₃OBF₄ furnished the amidate **222**. **222** was then oxidized with DDQ to afford **223**, which upon treatment with methanolic KOH produced the desired Diels-Alder precursor, achiral azadiene **224**. **224** could not be purified due to spontaneous [4+2] cyclization at room temperature, producing **225** in a 2:1 ratio respectively. The major diastereomer, which possessed the incorrect *syn* stereochemistry at C-19, was carried on to the nonnatural C-19-*epi*-brevianamide A as described earlier. In the same way, the minor diastereomer was used to form brevianamide B (not shown). With this study, Williams effectively demonstrated the viability of an intramolecular Diels-Alder reaction of a

[109] (a) Williams, R. M.; Sanz-Cervera, J. F.; Sancenon, F.; Marco, J. A.; Halligan, D. *J. Am. Chem. Soc.* **1998**, *120*, 1090. (b) Williams, R. M.; Sanz-Cervera, J. F.; Sancenon, F.; Marco, J. A.; Halligan, D. *Bioorg. Med. Chem.* **1998**, *120*, 1233.

hydroxypyrazinone intermediate in the biosynthesis of the bicyclo[2.2.2]diazaoctane core of the brevianamides.

Scheme 16. Williams' Total Synthesis of C-19-*epi*-Brevianamide E
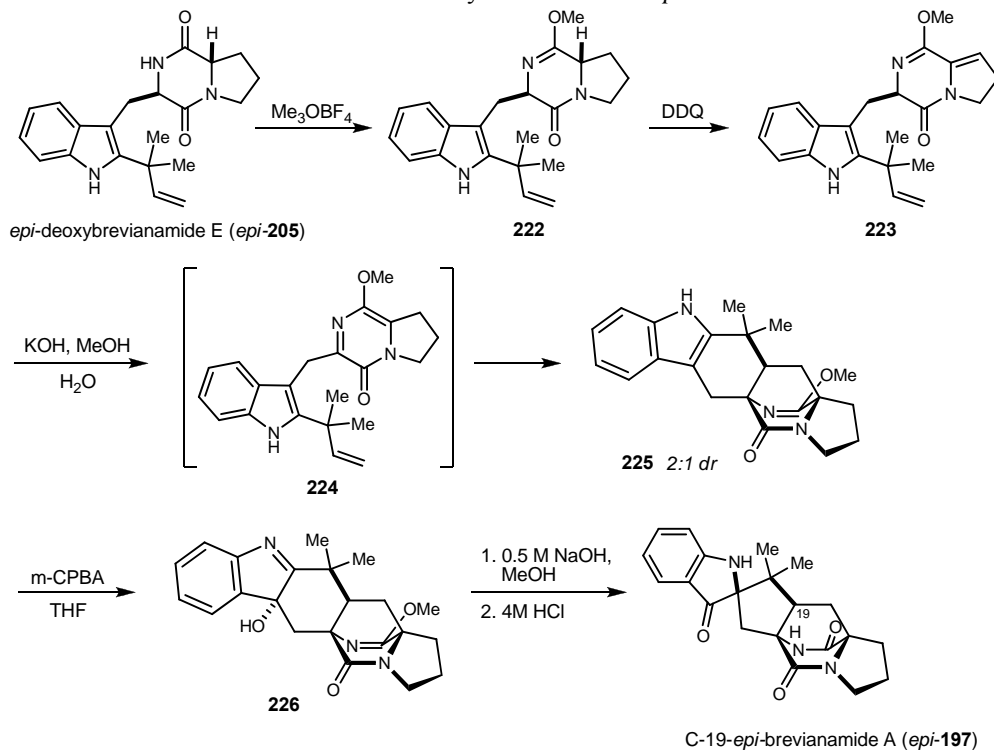
In 1988, Dunkerton and co-workers reported efforts toward the synthesis of brevianamides A and B (Scheme 17).[110] His synthetic approach utilized an Ireland ester enolate Claisen rearrangement of indole **227** to reverse-prenylated indoline **230**. After transforming **230** to aldehyde **231**, condensation with *N-para*-methoxybenzyl-protected *cyclo*-Gly-L-Pro gave **233**. Unfortunately, there were no reports on an attempted hetero-Diels-Alder reaction with compound **233**.

---

[110] Dunkerton, L. V.; Chen, H.; Mc Killican, B. P. *Tetrahedron Lett.* **1988**, *29*, 2539.

Scheme 17. Dunkerton's Partial Synthesis of the Brevianamides
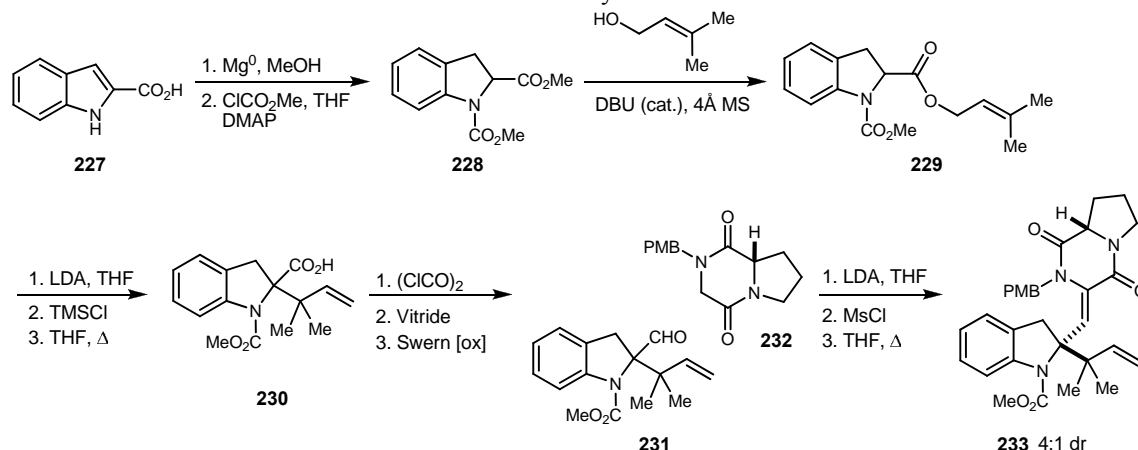
In 1980, Kametani completed the first total synthesis of (-)-brevianamide E.[111] Amide **235** was formed by Schotten-Baumann reaction of the acid chloride of CBz-protected proline with dimethyl aminomalonate (Scheme 18). Hydrogenation to remove the CBz protecting group, followed by hydroxypyridine catalyzed cyclization, produced diketopiperazine **236**. Condensation of **236** with gramine **237** afforded **238**, which after saponification and decarboxyation gave deoxybrevianamide E. Oxidation of **205** by irradiation in the presence of O_2 and Rose Bengal in MeOH followed by treatment with dimethyl sulfide furnished (-)-brevianamide E and its isomer in a 2:1 ratio.

Scheme 18. Kametani's Synthesis of (-)-Brevianamide E
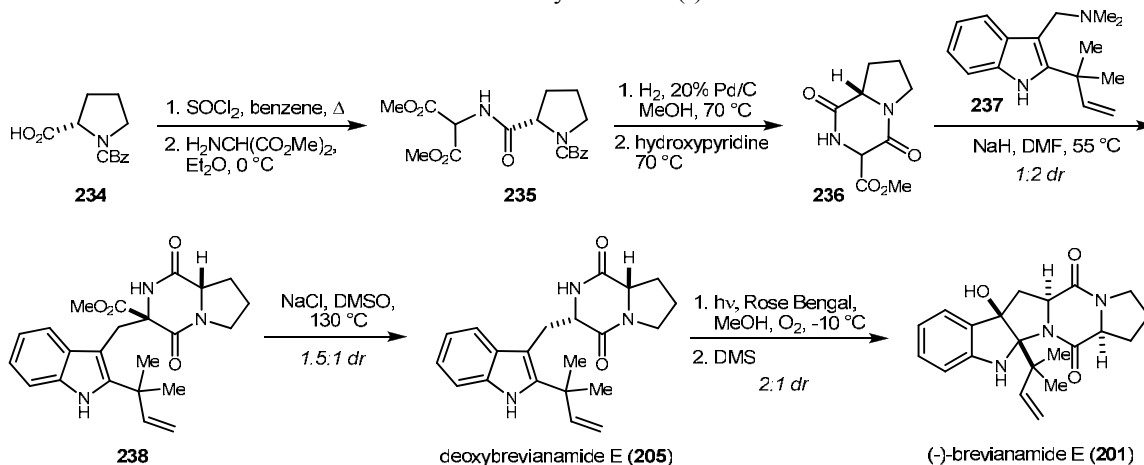
[111] (a) Kametani, T.; Kanaya, N.; Ihara, M. *J. Am. Chem. Soc* **1980**, *102*(11), 3974. (b) Kametani, T.; Kanaya, N.i; Ihra, M. *J.C.S. Perkin I* **1981**, 959.

In 1999, Danishefsky accomplished the most concise and efficient synthesis of deoxybrevianamide E and brevianamide E.[112] During the course of his total synthesis of gypsetin, Danishefsky developed a novel methodology to reverse prenylate the 2-position of indoles (Scheme 19). This had an obvious application to the synthesis of brevianamide E and as such it served as the key step. Starting with *N*-phthaloyltryptophan methyl ester, treatment with *tert*-butylhypochlorite gave the unstable 3-chloroindolenine which was immediately reacted with prenyl-9-BBN to give **241** in 95% yield over the two steps. Deprotection of the phthaloyl nitrogen with hydrazine followed by coupling with *N*-Boc-protected *L*-proline furnished amide **242**. Nitrogen deprotection and cyclization afforded deoxybrevianamide E. In contrast to Kametani's oxidation of **205** with O$_2$ above, treatment of **205** with dimethyldioxirane actually favored the undesired, nonnatural bis-*epi*-brevianamide to brevianamide E (~5:1).

Scheme 19. Danishefsky's Synthesis of Deoxybrevianamide E and Brevianamide E
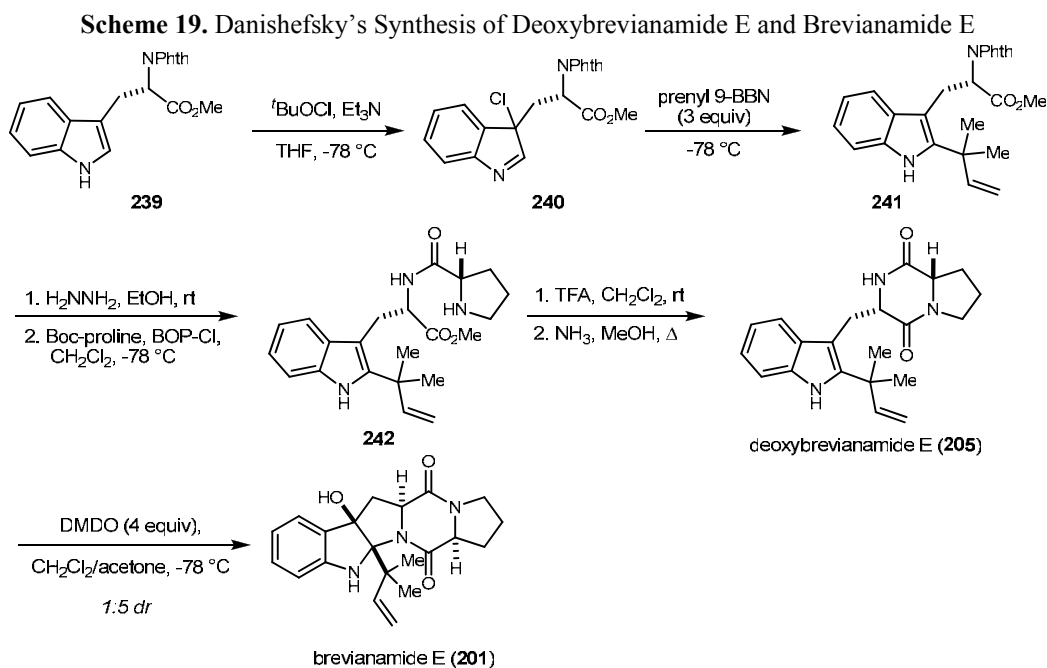
[112] Schkeryantz, J. M.; Woo, J. C. G.; Siliphaivanh, P.; Depew, K. M.; Danishefsky, S. J. *J. Am. Chem. Soc.* **1999**, *121*, 11964.

3.1.3. Chiral Proton Catalyzed Hetero-Diels-Alder Reaction

The success of the chiral proton catalyst in the enantioselective aza-Henry reaction led us to consider other reactions for its application. One such reaction was the hetero-Diels-Alder reaction, specifically the intramolecular variant that forms the bicyclo[2.2.2]diazaoctane core of the brevianamides as discussed above. The recent success of organocatalysts to promote a variety of transformations suggests that small molecules may be able to approach the selectivity and efficiency of their much larger enzymatic counterparts. Our efforts in this pseudo-biomimetic total synthesis could lend support to the notion that an enzyme is involved in the biosynthetic cycloaddition reaction that forms the bicyclo[2.2.2]diazaoctane core of the brevianamides. However, it is not suggested that disclosure of a chiral proton catalyzed [4+2] reaction of the brevianamide putative intermediate would unequivocally prove the existence of a Diels-Alderase in *Penicillium brevicompactum*. Rather, such a discovery would add to the growing amount of experimental evidence supporting the intervention of such an enzyme and shed additional light onto the biosynthesis of this fascinating family of alkaloids.

Based on information learned in developing the aza-Henry reaction, the brevianamide Diels-Alder precursor **206** appears to be a suitable candidate for catalysis with chiral proton complexes. The relative planarity of the 2-hydroxypyrazinone moiety, analogous to the Boc Schiff bases, should allow binding in the sterically demanding BAM chiral pocket. Furthermore, the additional Lewis basic sites offered by **206** are also encouring as that was a key feature in achieving high enantioselectivity in the aza-Henry reaction (Figure 33). In addition, Brønsted acids have already been shown to activate identical azadiene systems by lowering the LUMO-HOMO energy gap for the corresponding [4+2] cycloaddition.[113]

---

[113] (a) Domingo, L. R.; Sanz-Cervera, J. F.; Williams, R. M.; Picher, M. T.; Marco, J. A. *J. Org. Chem.* **1997**, *62*, 1662. (b) Jin, S.; Wessig, P.; Liebscher, J. *Eur. J. Org. Chem.* **2000**, 1993. (c) Shangde, J.; Wessig, P.; Liebscher, J. *J. Org. Chem.* **2001**, *66*, 3984-3997.

Figure 33. Comparison of 2-Hydroxypyrazinone and Boc Shiff Base Coordination
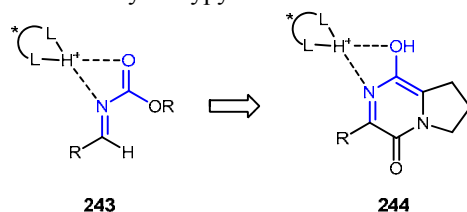
In order to efficiently synthesize the brevianamide core, the chiral proton catalyst must be able to direct both enantio- and diastereocontrol of the hetero-Diels-Alder reaction. A simplified depiction of the azadiene intermediate **206** bound to H,Quin-BAM·HX is shown below with the indole omitted for clarity (Figure 34). This figure is only intended to show the anticipated substrate coordination sites and the approach of the dieonophile necessary for obtaining each product enantiomer. This figure is not intended as a predictive tool for enantioselection in the [4+2] cycloaddition. Chelation of the pyrazinone amidate to the BAM-protic acid complex is envisioned to occur in a bidentate manner, analogous to the stereochemical model developed for N-Boc imines that was adopted for the aza-Henry reaction (Figure 17). The BAM ligand must effectively destabilize the transition state formed by approach of the tethered dieneophile from one face of the 2-hydroxypyrazinone relative to the opposite face in order to achieve enantioselection. If facial discrimination is accomplished, then use of the opposite enantiomer of the BAM catalyst (*S*,*S*-BAM) would also furnish the opposite enantiomer of the Diels-Alder adduct, thus providing access to cores of both brevianamide A and B.

Figure 34. H,Quin-BAM·HX Azadiene Complex
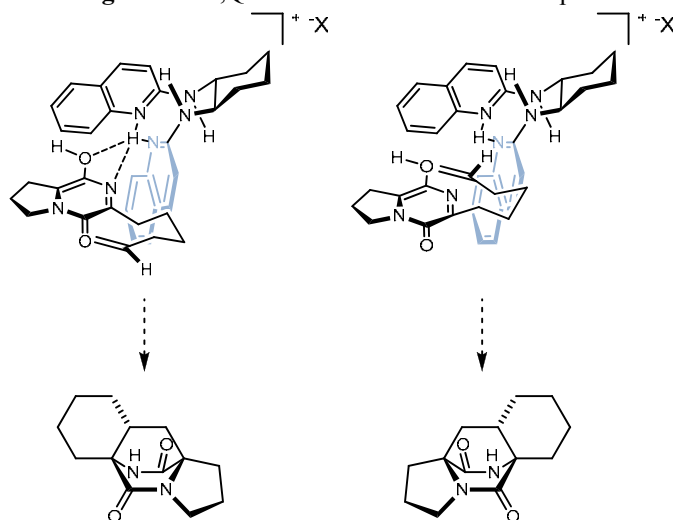
The diastereoselectivity of the hetero-Diels-Alder reaction is determined by the intrinsic preference for *endo* or *exo* orientation of the prenyl olefin in the transition state (Figure 35). As discussed in Section 3.1.2, the *endo* transition state is favored in the thermal Diels-Alder reaction of **206**, which produces the *syn* configuration at C19.[109] Therefore, the catalyst will be required to not enhance, but completely reverse the *endo*:*exo* selectivity of the Diels-Alder reaction with respect to the thermal process. This will be critical to allow access to the brevianamide core.

Figure 35. Endo vs Exo Selectivity
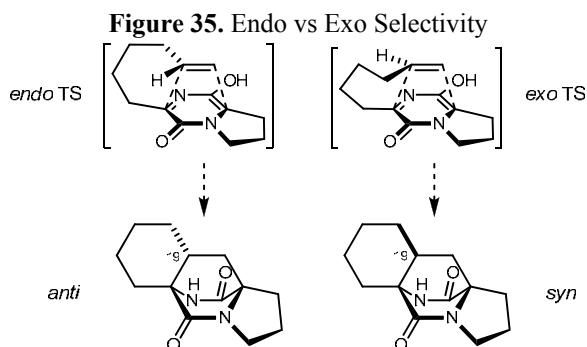
For the initial synthesis of the Diels-Alder precursor in our labs, Ben Nugent used a combination of Williams' and Kametani's total syntheses described above.[114] As discussed earlier, Williams had previously synthesized the achiral Diels-Alder precursor

---

[114] Nugent, B. M. *PhD Dissertation*, **October 2005**.

(**224**) from *epi*-deoxybrevianamide E (**205**). Kametani's convergent synthesis of intermediate **205** was adopted, which involves the coupling of reverse-prenylated indole **237** and pyrazinedione **236** (Scheme 20).

Scheme 20. Retrosynthetic Analysis of Achiral Diels-Alder Precursor

224   *epi*-deoxybrevianamide E (**205**)   **237**
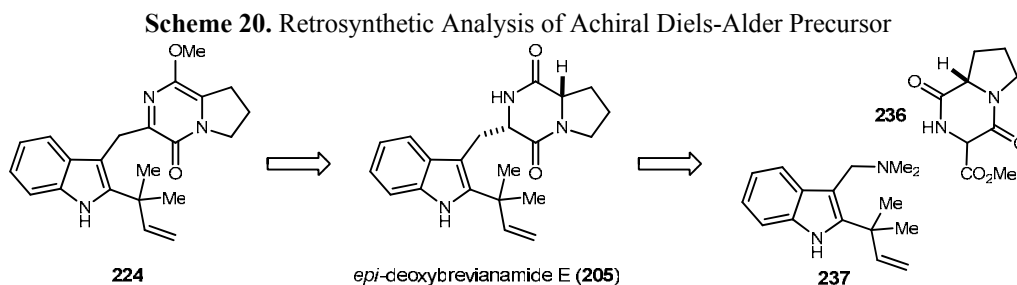
Reverse-prenylated indole **237** was synthesized in three steps starting from indole and known sulfide **245**, which is made from the corresponding allyl chloride (Scheme 21).[115] Warming a solution of indole and sulfide **245** with NCS generated the thio-Claisen product **247**, albeit in low yield. Strictly following the literature procedure proved to be extremely problematic for this reverse-prenylation process, resulting in yields ranging from 1-9%. However, Nugent found that yields could be significantly improved by cooling the solution of NCS to -40 °C before adding the sulfide (**245**) and indole. Using this protocol, higher yields were achieved reproducibly, however; the reaction was still difficult to scale-up, losing significant yield on 10 g scale and even 5 g scale. Heating an acetic acid solution of **247** with zinc powder effected the removal of the sulfide group and gave reverse-prenylated indole **248**. This was followed by subsequent Mannich alkylation with dimethylamine/formaldehyde under acidic conditions furnishing gramine **237** in good yield.

---

[115] Tomita, K.; Terada, A.; Tachikawa, R. *Heterocycles*, **1976**, *4*, 733-737.

Scheme 21. Synthesis of Intermediate **237** from Indole
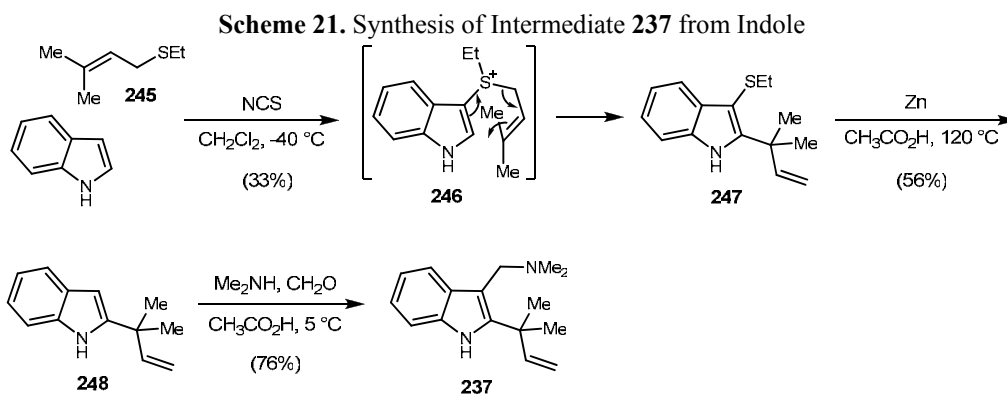
In an attempt to optimize the reverse-prenylation protocol outlined by Nugent above, several temperatures were surveyed for this reaction (Table 24). It should be noted that - 40 °C does in fact appear to be the optimal temperature for this reaction, with cooling an additional 10 °C adversely affecting the yield. The sensitivity to temperature was surprising and may explain, at least partially, the difficulty of this reaction to effectively produce **247** on larger scale.

Table 24. Effect of Scale and Temperature on Reverse-Prenylation

entry	T (°C)	scale (g of indole)	% yield
1	-50	1.00	21
2	-45	1.00	32
3	-40	1.00	34
4	-35	1.00	25
5	-30	1.00	18
6	-40	5.00	14
7	-40	10.00	6

Pyrazinedione **236** was synthesized in three steps from *L*-proline (Scheme 22). The proline nitrogen was protected with a benzyloxycarbonyl (CBz) group followed by coupling with dimethylaminomalonate using EDC and DMAP to produce diester **250**. Removal of the CBz protecting group under hydrogenation conditions was immediately followed by thermal cyclization to form pyrazinedione **236**.

Scheme 22. Synthesis of Intermediate **236** from Proline
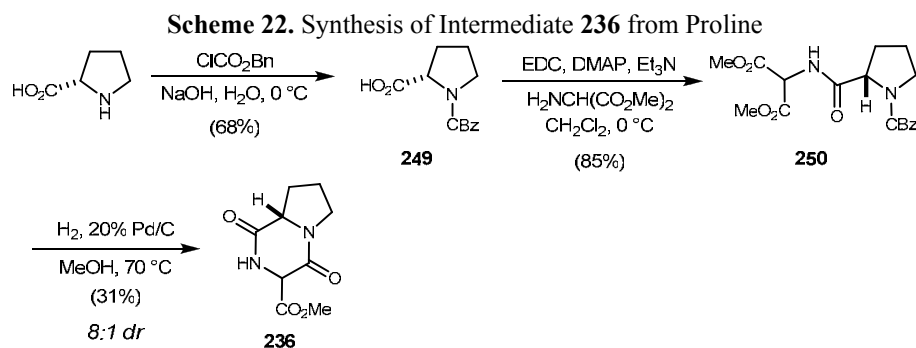
The desired coupled product **251** was produced from fragments **236** and **237** using tri-*n*-butylphosphine, but again in low yield (Scheme 23). Saponification of the methyl ester followed by decarboxylation gave *epi*-deoxybrevianamide E (**205**) as the major diastereomer (9:1 ratio). Using Williams' protocol for alkylation of the amide oxygen with Me$_3$OBF$_4$ produced **222**, which was then oxidized with DDQ to provide azadiene **223**, albeit in low yield.

Scheme 23. Synthesis of Azadiene Precursor **223** via Coupling of **236** and **237**
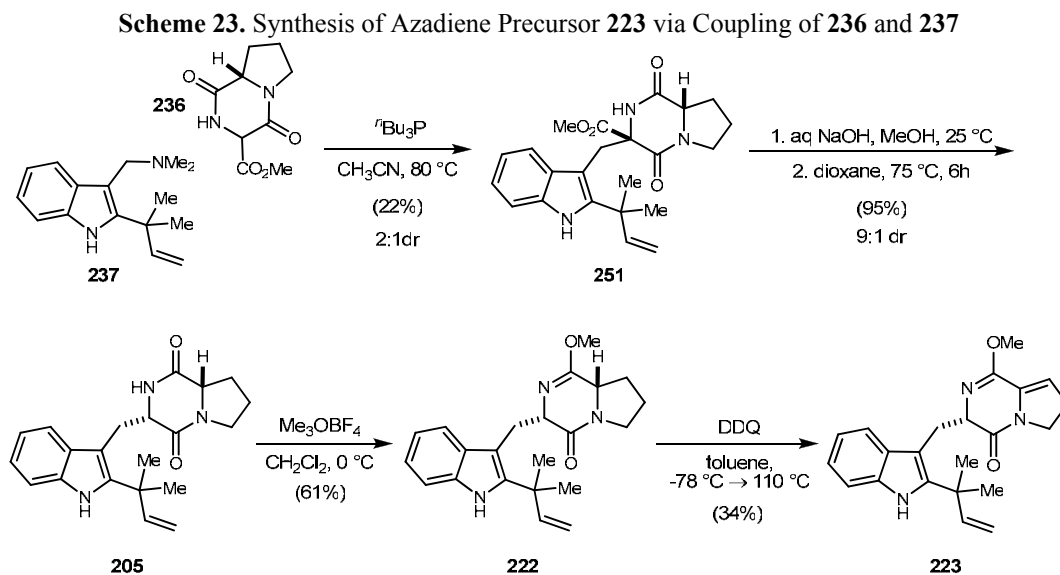
The problematic step in the above synthetic route has always been the reverse prenylation of the indole ring (Scheme 21). Although some optimization, such as a lower temperature (-40 °C instead of -30 °C), was found to increase yield, scale-up attempts were still coupled with significantly decreased yields. Furthermore, this problem was coupled with additional key steps, such as the convergent coupling, also producing very

low yields. These synthetic challenges proved to be too large of an obstacle to overcome with brute force and as a result a new pathway was desired.

As discussed in Section 3.1.2, the most concise and efficient synthesis of deoxybrevianamide E (**205**) has been accomplished by Danishefsky. Starting from *L*-Tryptophan, the synthesis is six steps, of which four are protections/deprotections and one is a routine peptide coupling. The only step which caused concern at the outset was the reverse prenylation using prenyl 9-BBN (Scheme 24). After synthesizing *N*-phthaloyltryptophan methyl ester (**239**), the Danishefsky protocol was tested. The reaction proceeded exactly as reported and provided the desired reverse prennylation product (**241**) in 65% yield. The scale of this reaction did not provide any additional issues; reaction of 57.5 g of substrate produced the desired product in 57% yield. The effectiveness of this procedure to produce the desired product provided access to **223** in much greater amounts than achieved previously.

Scheme 24. Danishefsky's Reverse-Prenylation of *N*-Protected *L*-Tryptophan Methyl Ester
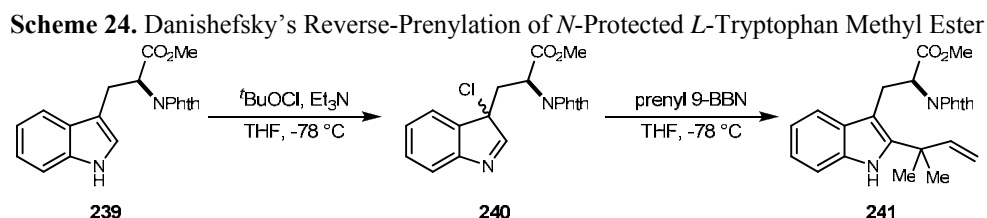
241 is only three steps from deoxybrevianamide E (**205**) as reported by Danishefsky (Scheme 25). The phthalimide deprotection proceeds smoothly, however, the purification is complicated by the extreme polarity of the primary amine on standard silica gel. Danishefsky reported the use of silica gel pretreated with HMDS, but a MeOH/ CH_2Cl_2 column on standard silica gel was also effective. Further optimization of this reaction was attempted by increasing the temperature to 60 °C for several hours. Unfortunately, the crude NMR showed complete loss of the methyl ester, presumably from dimerization of the desired product to form the dipeptide.

Scheme 25. Final Steps of Danshefsky's Synthesis of Deoxybrevianamide E
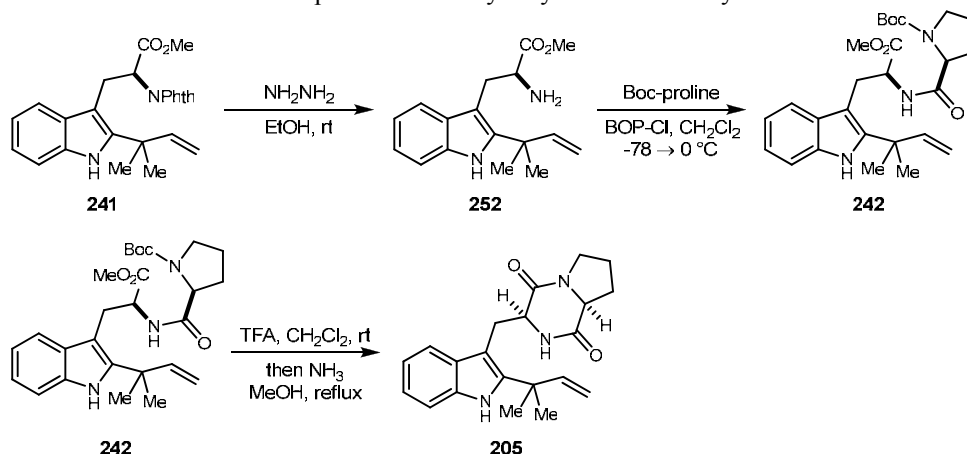
The remaining steps from **252** to deoxybrevianamide E (**205**) are done sequentially without purification of the intermediates. After workup of the peptide coupling reaction, the crude product is dissolved in dichloromethane and an excess of trifluoroacetic acid is added. After stirring at room temperature, a 7M solution of NH_3 in MeOH is added and the solution is allowed to continue stirring until cyclization appeared complete. After purification, this afforded deoxybrevianamide E (**205**) in a 45% yield over the final three steps.

From deoxybrevianamide E (**205**), there are two remaining steps before reaching the Diels-Alder precursor (Scheme 26). Formation of the lactim ether was performed using Me_3OBF_4 as reported by Williams and described above. Lactim ether (**222**) was converted to azadiene (**223**) using DDQ, also as reported by Williams and described above. The yield over these two steps is typically around 15-20% due to the low yielding DDQ reaction. This product is stored and only deprotonated with KOH to reveal the Diels-Alder precursor (**224**) when performing the enantioselective Diels-Alder reaction.

Scheme 26. Synthesis of Azadiene Precursor **223** from Deoxybrevianamide E (**205**)
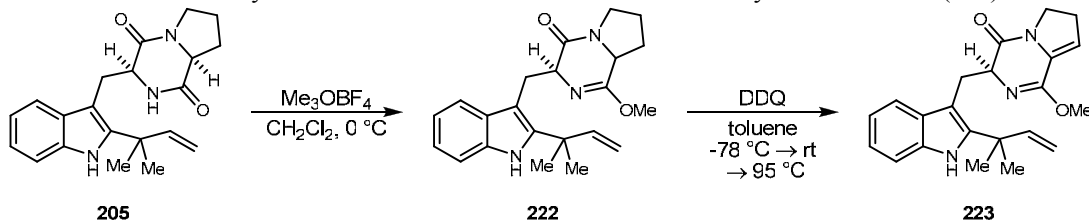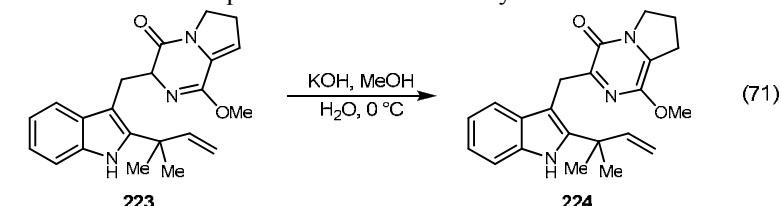
The Meerwein salt reaction proved to be very sensitive to the reagent itself. Several attempts were made to scale-up this reaction, but regardless of how many equivalents of the oxonium salt were used, the reaction would not proceed in any appreciable yield. Finally, fresh salt was ordered and tested and the reaction proceeded to approx. 4:1 conversion by NMR. This reaction was further optimized by changing the order of addition. When **205** was cooled to -78 °C and added to the Meerwein salt, the reaction proceeded to complete conversion by NMR. Since it was suspected that some yield may have been lost during purification, and having pushed the reaction to complete conversion, the crude material was taken on without further purification to the final oxidation step.

The DDQ reaction, which is unfortunately the last step of the synthesis of the azadiene precursor, has proven to be the most difficult. The reaction is carefully controlled from the point of addition at -78 °C, allowed to stir for 8 hours, then warmed to room temperature overnight, then heated to reflux for approx. 3 hours or until starting material is completely consumed. Unfortunately the crude NMR shows a 1:1 ratio of product to byproduct which leads to a 31% yield of the desired product after isolation.
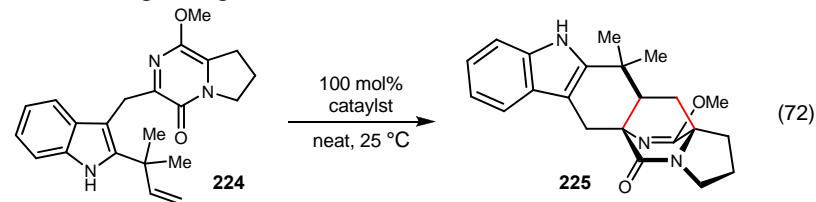
Optimization of the potassium hydroxide catalyzed isomerization of azadiene **223** to form Diels-Alder precursor **224** was performed (Table 25). Previously, entry 1 was used as the standard conditions in which the diene was formed prior to addition of catalyst. This consistently left 30-40% of azadiene precursor **223** unreacted. Varying the reaction time at 0 °C, followed by warming to room temp, again for a controlled period of time, led to the optimal results in entry 2. Diels-Alder product was avoided which is essential to obtain an accurate picture of the catalyst's effect on the reaction. Furthermore, the conversion of **223** to **224** has been increased to 90% which allows for greater amount of Diels-Alder product to be formed after being treated with BAM·HOTf catalysts.

Table 25. Optimization of Base Catalyzed Isomerization
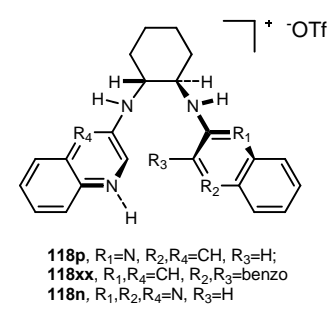
entry	time @ 0 °C (min)	time @ rt (min)	%conv **224**	%conv **225**
1	30	30	60	0
2	45	45	90	0
3	60	60	90	10
4	30	240	60	40

The [4+2] cycloaddition was found by Williams to occur spontaneously in the absence of solvent which was confirmed in our hands. Unfortunately the hetero-Diels-Alder reaction was not catalyzed by H,Quin-BAM·HOTf in solvent, however; Nugent found that the reaction was catalyzed with a small degree of stereoselection when performed neat. Expanding on this initial result, Nugent performed a ligand screen which is summarized below (Table 26).[114] Enantioselectivity was generally minimal with the exception of one ligand, H,³Quin-BAM·HOTf (**118p**), which afforded an appreciable increase to 35% ee (entry 4). The structurally similar H,Quinox-BAM·HOTf also gave similar enantioselection with a small increase in de (entry 12).

Table 26. Nugent Ligand Screen on Hetero-Diels-Alder Reaction of **224**

entry	catalyst	time(h)[a]	%de (dr)[b]	% ee[c]
1	H,Quin-BAM·HOTf (**118e**)	21	47	13
2	H,^{6}Me-BAM·HOTf (**118a**)	24	41	1
3	H,Isoquin-BAM·HOTf (**118d**)	42	20	14
4	H,^{3}Quin-BAM·HOTf (**118p**)	48	36	35
5	H,^{5}Me-BAM·HOTf (**118b**)	48	13	5
6	H, ^{2}Quin, Napth-BAM·HOTf (**118o**)	48	37	0
7	H,^{5}CF$_3$-BAM·HOTf (**118cc**)	48	13	11
8	H,^{6}MeO-BAM·HOTf (**118h**)	48	33	5
9	H,Me-^{6}Me-BAM·HOTf (**118i**)	48	46	2
10	H,^{2,3}Quin-BAM·HOTf (**118q**)	42	49	6
11	H,^{3}Quin,Phen-BAM·HOTf (**118xx**)	48	49	12
12	H,Quinox-BAM·HOTf (**118n**)	48	56	35
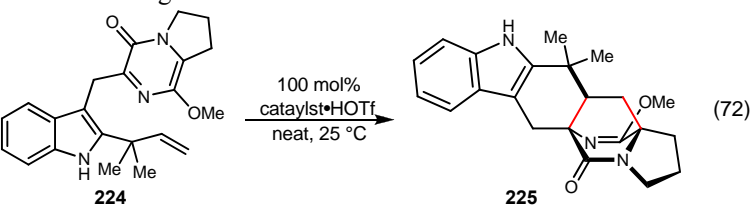
[a]Reactions carried out to complete conversion. [b]Diastereomeric excess determined by ^{1}H NMR.
[c]Enantiomeric excess determined by HPLC using OD-H column.

The H,^{3}Quin-BAM·HOTf result was followed up by Nugent with two important experiments. First, the enantioselection was verified by reaction of (*S*,*S*)-H,^{3}Quin-BAM·HOTf producing the opposite enantiomer of the product with 25% ee. Second, the importance of the proton was established by demonstrating that free H,^{3}Quin-BAM ligand alone catalyzed the addition with -9% ee. This provided preliminary circumstantial evidence for the proton as a primary stereocontrol element.

After modifying the synthetic route to the Diels-Alder precursor, the goal was to expand upon these initial results in hopes of identifying a more selective chiral proton catalyst (Table 27). Regrettably there was no increase in enantioselection for those ligands that afforded the cycloaddition product. Many of these ligands were complicated by hydrolysis of the product to form the amide byproduct. In some cases this side reaction prevented the determination of enantioselection with that catalyst. In the cases of entries 6-8, it appeared that some other side-reaction may have taken place. The resulting crude NMR spectra did not have any major identifiable peaks. This is similar to the reaction observed by Nugent using IAN-amines in that both examples do not posess the bis-amidine motif that has successfully catalyzed the reaction.

Table 27. Ligand Screen on Hetero-Diels-Alder Reaction of **224**

entry	catalyst	time(h)[a]	%de (dr)[b]	% ee[c]
1	H,3-Quin-BAM (**118p**)	48	36	35
2	H,^{8}Me^{3}Quin-BAM (**118t**)	24	49	-[d]
3	H,Quinox(^{2}Quin)-BAM (**118v**)	36	45	8
4	H,^{3,6}Me$_2$^{2}Pyrimidine-BAM (**118w**)	48	51	12
5	H,^{4,6}Me$_2$Pyrazine-BAM (**118aa**)	48	39	2
6	2-Quin-Trost (**189**)	96	-	-[d]
7	2-Quin-Jacobson (**188**)	96	-	-[d]
8	2-Quin-Que (**190**)	96	-	-[d]
9	H,^{6}Ph-BAM (**118x**)	48	17	-2
10	H,Quin(^{6}Ph)-BAM (**118z**)	48	53	-[d]
11	H,Quin(^{6}(^{9}Anth)^{2}Pyr)-BAM (**118oo**)	48	45	15
12	H,^{4}CF$_3$-Quin-BAM (**118**)	36	32	7
13	H,^{4}MeOQuin-BAM (**118ii**)	72	35	0
14	H,^{6}MeO-BAM (**115h**)	36	-	-[d]
15	miracle-BAM™ (**115hh**)	48	-	-[d]

[a]Reactions carried out to complete conversion. [b]Diastereomeric excess determined by ^{1}H NMR. [c]Enantiomeric excess determined by HPLC using an OD-H column. [d]Complex mixture resulted; unable to determine.

Although the synthetic route to the Diels-Alder precursor (**224**) was improved, no ligands were identified that could improve the overall selectivity of the [4+2] cycloaddition. The difficulties associated with the development of an enantioselective reaction in which the substrate requires over ten steps to produce proved to be too great of a challenge to be done in a time efficient manner. In order to optimize the enantioselective hetero-Diels-Alder reaction, smaller model cases will be used by Anand Singh before returning to the pseudo-biomimetic substrate.

3.2. Tamiflu

3.2.1. Background

While it is likely that influenza has been a serious disease to mankind for thousands of years, the first well-documented report of a worldwide influenza pandemic was in 1580.[116] After originating in Asia, the virus was able to spread to Africa and then Europe

---

[116] Garmana, E.; Laver,G. *Current Drug Targets* **2004**, *5*, 119.

before finally reaching America.[117] Since then, influenza pandemics have occurred at varying intervals with unpredictable degrees of severity. Perhaps the most famous global outbreak of influenza occurred during the fall and winter of 1918-1919. An exceptionally virulent form of influenza, the so-called Spanish influenza, spread globally killing at least 20 million and possibly more than 40 million people worldwide.[118] At the time, the cause of the disease was unknown and there were no effective preventive or curative measures available that had scientific evidence to support such claims. The virus caused epidemics again in 1957 and 1968, foreshadowing the high risk for future epidemics as well as pandemics. Today, influenza is responsible for the deaths of 20,000 to 40,000 Americans each year.[119] However, the lethality of this disease historically increases the likelihood of influenza becoming a pandemic once again. Fortunately, science has begun to make significant progress towards combatting the next influenza outbreak with respect to a century ago.[120]

Although isolated over half a century earlier, the fowl plague virus was not identified to be an influenza virus until 1955. This led many to believe that the first influenza virus isolated was a swine influenza virus in 1931.[121] This was follwed in 1933 by the first isolation of the human influenza virus by Smith and coworkers.[122] Interestingly, another human influenza virus was isolated in 1940 and found to be completely unrelated, serologically, to the known human influenza virus.[123] In order to distinguish these viruses, they were labeled Type A and for the new strain Type B. It should be noted that both influenza A and B viruses are RNA viruses. Using subtypes based on the structure of the two surface proteins, the influenza A virus can be classified as haemagglutinin (H) and neuraminidase (N). Furthermore, the influenza A virus is unique in that it contains the M2 protein, which has been found to act as a proton channel. This M2 protein is not

---

[117] Pyle, G.F. *The Diffusion of Influenza: Patterns and Paradigms*; Rowan and Littlefield: New Jersey, 1986.
[118] Taubenberger, J. K.; Reid, A. H.; Fanning, T. G. *Virology* **2000**, *274*, 241.
[119] (a) Wang, G. T. *Expert Opin. Ther. Pat.* **2002**, *12*, 845. (b) Klumpp, K. *Expert Opin. Ther. Pat.* **2004**, *14*, 1153.
[120] Farina, V.; Brown, J. D. *Angew. Chem. Int. Ed.* **2006**, *45*, 7330.
[121] Shope, R.E. *J. Exp. Med.* **1931**, *54*, 373.
[122] Smith, W.; Andrewes, C.H.; Laidlaw, P.P. *Lancet* **1933**, *2*, 66.
[123] Francis, T. Jr. *Science* **1940**, *92*, 405.

present in the type B virus, but another protein called BM2, may function as an ion channel.[124]

Once the human influenza virus had been isolated, it did not take long to prove that it was antigenically unstable.[125] Several years later, this discovery was confirmed mercilessly by the infamous epidemic of 1946-47 in which people immunized with the then available flu vaccine were not protected at all against the new strain. Since then science has shown that the virus continues to change gradually and continually, commonly referred to as antigenic drift. However, the virus has also undergone sudden and complete changes known as major antigenic shifts. Although there are believed to have been many of these major antigenic shifts in the long history of the influenza virus, there are three recorded occurrences which happened at irregular intervals over the last 50 years. In 1957, the circulating H1N1 strains, which were related to the type A virus originally isolated in 1933, were replaced by a never before isolated H2N2 strain. Similarly, in 1968 H3N2 replaced the aforementioned H2N2 strains and in 1977 the H1N1 subtype from 1950 reappeared.

Since vaccinations were developed by the United States military in the 1940s, immunization has been an invaluable tool to battle the constant threat of flu epidemics. However, constant and unpredictable antigenic variation in the human influenza viruses caused by error-prone RNA replication has made vaccine production difficult. Vaccination against influenza virus is complicated by a reduced effectiveness due to the constant antigenic variation, which as a result requires continuous updates of vaccines. Since vaccines against a new pandemic strain would almost certainly take 6 months to a year before becoming available to the public, small-molecule antiviral agents offer a novel alternative for effective prevention and therapy of the influenza viruses. It is no wonder that with the widespread commonality and ability to cause worldwide human affliction influenza is among the best studied of all the viruses. However, it is surprising that despite the fact that no reliable vaccine exists and despite the pharmaceutical industries best efforts in the combinatorial screening of many thousands of compounds for anti influenza activity, there has only very recently been anti-viral drugs discovered

---

[124] Mould, J.A.; Paterson, R.G.; Takeda, M.; Ohigashi, Y.; Venkataraman Lamb, R.A.; Pinto, L.H. *Developmental Cell*, **2003**, *5*, 175.
[125] Hirst, G. K. *J. Exp. Med.* **1943**, *78*, 407.

which were effective against all strains of influenza, including both Type A and Type B.[116]

One potential therapeutic method for treating influenza was developed in the 1960s, which targeted the M2 protein of the Type A influenza viruses. The M2 protein spans the lipid bilary and functions as an ion channel, allowing the entry of H+ into the virus. The inhibitors of this M2 proton pump have been known for decades since their discovery in 1964.[126] Amantadine, and its derivative, rimantadine, the two marketed, clinically effective inhibitors, have been used therapeutically against Type A influenza. However, these drugs are useless against Type B influenza, which is a serious limitation.[127] This is because they function by blocking the M2 ion channel which is not present in the Type B viruses.[128] Furthermore, these drugs have been plagued by the emergence of drug resistant strains as well as by toxic side effects. Until very recently, however, amantadine and rimantadine were the only drugs which had been approved for worldwide use against influenza.

In the 1940s, a series of key discoveries ranging from the observation that influenza virus appeared to have an enzyme which destroyed receptors for the virus on red blood cells,[129] to the identification by Alfred Gottschalk and others that this enzyme was a sialidase or neuraminidase. This in turn led to the realization by McFarlane Burnet in 1948, long before anything was known about the molecular biology of the influenza viruses, that inhibitors of the recently discovered and isolated neuraminidase enzyme might be useful as anti-viral therapies. "An effective competitive poison for the virus enzyme might be administered which, when deposited on the mucous film lining the respiratory tract would render this an effective barrier against infection, both initial infection from without and the spreading surface infection of the mucosa which follows the initiation of infection."[130]

---

[126] Davies, W.L.; Grunert, R.R.; Haff, R.F.; McGahen, J.W.; Neumayer, E.M.; Paulshock, M.; Watts, J.C.; Wood, T.R.; Hermann, E.C. and Hoffmann, C.E. *Science* **1964**, *144*, 826.

[127] Oxford, J. S.; Bossuyt, S.; Balasingam, S.; Mann, A.; Novelli, P.; Lambkin, R. *Clin. Microbiol. Infect.* **2003**, *9*, 1.

[128] (a) Hay, A. J.; Wolstenholme, A. J.; Skehel, J. J.; Smith, M. H. *EMBO Journal* **1985**, *4*, 3021. (b) Pinto, L. H.; Holsinger, L. J. and Lamb, R. A. *Cell* **1992**, *69*, 517.

[129] Hirst, G.K. *Science* **1994**, *94*, 22.

[130] Burnet, F. M. *Australian J. Exp. Biol and Med. Sci.* **1948**, *26*, 410.

The function of this neuraminidase was determined in 1966 by Seto and Rott to be the release of virus particles from infected cells.[131] By directing an antibody exclusively against the neuraminidase, it was fount that the virus, while not prevented from infecting cells, was prevented from releasing newly formed virus particles.[132] This determination of how the neuraminidase works is critical to understanding in what capacity inhibitors of the viral enzyme may be able to function as therapeutic agents. Clearly, an inhibitor will be most effective when administered as close as possible to the onset of the infection.

It should also be emphasized that neuraminidase is an essential enzyme for viral replication in all classes of influenza. By solving the X-ray crystal structure for this enzyme, it was learned that the enzyme is a tetramer made up of identical subunits. Furthermore this enyme has also been characterized crystallographically as a complex with sialic acid.[133] This complexation helped identify the active site, which turns out to be highly conserved across all strains of the influenza A and B viruses. This suggests that the neuramidase enzyme could make a very attractive target for inhibiting all strains of the influenza viruses with one drug. The structural data that has been obtained about the active site has, in turn, stimulated the proposal of potent inhibitors.[119] Two of these inhibitors have already reached the market, while two others, developed by Biocryst and Abbott, have not yet been approved for use in humans.[134] The first of the two aforementioned neuramidase inhibitors to reach the market was zanamivir (**253**), marketed by GSK as Relenza and released in July 1999. Unforunately, Relenza is not capapble of being submitted orally to the patient. Instead it is administered as a powder which is puffed into the lungs by inhalation, which can cause problems in patients with underlying respiratory disease. Obviously the attractiveness of an orally bioavailable drug left something to be desired.

---

[131] Seto, J. T.; Rott, R. *Virology* **1966**, *30*, 731.
[132] Webster, R. G.; Laver, W. G. *J. Immunology* **1967**, *99*, 49.
[133] (a) Colman, P. M.; Varghese, J. N.; Laver, W. G. *Nature* **1983**, *303*, 41. (b) Varghese, J.N.; McKimm-Breschkin, J. L.; Caldwell, J. B. *Proteins Struct. Funct. Genet.* **1992**, *14*, 327.
[134] Kati, W.M.; Montgomery, D.; Maring, C.; Stoll, V.S.; Giranda, V.; Chen, X.; Laver, W.G.; Kohlbrenner, W.; Norbeck, D.W. *Antimicrob. Agents Chemother.* **2001**, *45*, 2563.

Figure 36. Structures of Relenza (**253**) and Tamiflu (**254**).

253 (zanamivir)   254 (oseltamivir phosphate)
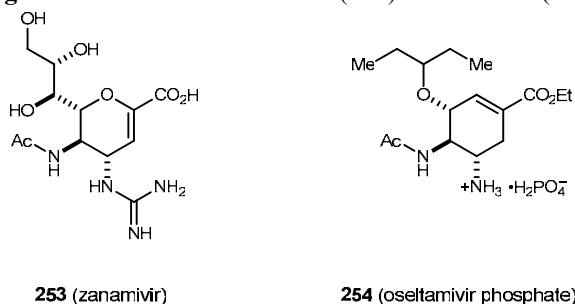
In October 1999, oseltamivir phosphate (**254**) was released to the market as Tamiflu, developed by Gilead Sciences and also marketed by Roche. Tamiflu was in fact orally bioavailable, stemming from the carboxylic acid moiety which is revealed after hydrolysis of the ethyl ester pro-drug by the liver.[135] Both Tamiflu as well as Relenza were successful in Phase 1, 2 and 3 clinical trials and are currently being administered for the treatment of influenza world-wide. While their success in preventing death in cases of severe influenza has not yet been determined, anecdotal evidence suggests that this could very well be an important property of these drugs. Identifying these effective therapeutic agents was a spectacular scientific breakthrough. The challenge now is to develop a low-cost and readily scalable synthesis for the orally bioavailable Tamiflu, the best protection that humankind has against an influenza pandemic.

3.2.2. Synthesis

The intial total synthesis developed by Roche and Gilead Sciences for the prodrug tamiflu used shikimic acid as a precursor (Scheme 27). Unfortunately, this precursor has limited the largescale production of the prodrug due to its scarcity, for the most part obtained from the extraction of plants. Shikimic acid (**256**) is an intermediate in the biosynthetic pathways leading to essential aromatic amino acids. In plants, it is also a precursor to lignins and phenols[136] and is accumulated to some extent, especially in gymnosperms and woody dicotyledons.

---

[135] Kim, C. U.; Williams, M. A.; Lui, H.; Zhang, L.; Swaminathan, S.; Bischofberger, N.; Chen, M. S.; Mendel, D. B.; Tai, C. Y.; Laver, W. G.; Stevens, R. C. *J. Amer. Chem. Soc.* **1997**, *119*, 681.

[136] (a) Boudet, A. *Phytochemistry* **1973**, *12*, 363. (b) Möller, B.; Herrmann, K. *Phytochemistry* **1983**, *22*, 477.

Scheme 27. Retro-synthetic route of **254** starting from shikimic acid (**256**).
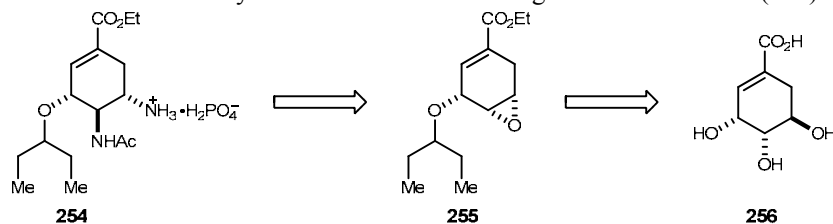
The most abundant source of shikimic acid is in the Illicium family, which is a small tree or shrub of known herbal value. Although shikimic acid was first isolated from a member of this family, I. religiosum in 1885,[137] star anise (I. verum), which is found in four provinces of Southern China, was found to be a rich natural source for shikimic acid. Starting from 30 kg of dried plant, approximately 1 kg of shikimic acid can be produced.[138] This fact alone causes concern to the US government's goal of storing 300 million doses of Tamiflu, each dose being approximately 75 mg. This would require 23 tons of the prodrug substance and assuming a yield of 35% from shikimic acid to oseltamivir phosphate, the amount of shikimic acid needed would require about 840 tons of star anise.[138] An alternative source of shikimic acid has been driven by the demand from the United States alone. One possible solution to this problem was reported by Frost and co-workers at Michigan State University. Using genetically modified E. coli, they were able to produce shikimic acid by recombinant microbial biocatalysis.[139] Currently, this fermentation approach supplies approximately 30% of the present requirements.[138]

Although scientists at Roche were able to improve the yield of the synthesis from epoxide **255** to Tamiflu (**254**) by over 30%, the improved synthetic route still relied on shikimic acid.[140] The desire for an alternative approach to Tamiflu, which does not rely on the relatively scarce shikimic acid, has stimulated interest throughout the synthetic community.

Scientists at Roche did make an effort to move away from shikimic acid as a raw material, which proved to be more challenging, but attempts to this end can be found in

---

[137] Jiang, S.; Singh, G. *Tetrahedron* **1998**, *54*, 4697; this review also describes approaches to shikimic acid by total chemical synthesis.
[138] Flores, G. *The Scientist*, Published online: January 4, 2006.
[139] Draths, K. M.; Knop, D. R.; Frost, J. W. *J. Am. Chem. Soc.* **1999**, *121*, 1603.
[140] (a) Karpf, M.; Trussardi, R. *J. Org. Chem.* **2001**, *66*, 2044. (b) Harrington, P. J.; Brown, J. D.; Foderaro, T.; Hughes, R. C. *Org. Process Res. Dev.* **2004**, *8*, 86.

the patent literature. The first of which utilized a Lewis acid activated Diels–Alder reaction of ethyl acrylate and furan as the first step of the synthesis (Scheme 28).[141] This reaction resulted in a 9:1 mixture of racemic exo/endo adducts. This racemic adduct (**258**) underwent an effective resolution using an esterase (Chirazyme L-2). After the [4+2] cycloaddition, the resulting was combined with phosphoryl azide to give two regioisomeric [3+2] exo products, which were found to decompose thermally to aziridine **259**. This intermediate underwent transesterification with ethanol and base elimination to give **260**, which is a key precursor to **254**.[142]

Scheme 28. Diels-Alder Approach to Tamiflu (**254**) Avoiding Shikimic Acid
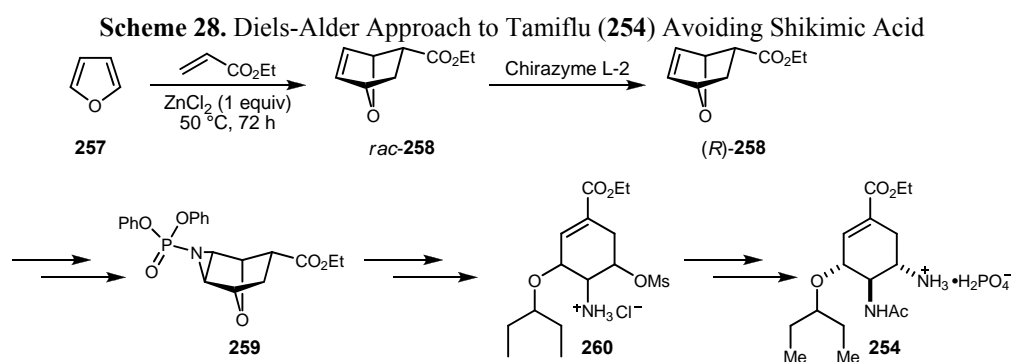
There were several flaws in this initial attempt to eliminate shikimic acid from the Tamiflu synthesis. First and perhaps most adverse to product throughput is the fact that several steps required high dilution. Also, the resolution of the cycloaddition product catalyzed by Chirazyme L-2 was not efficient, with a yield of only 20%. This led to a revised synthesis by the scientists at Roche in which they utilized a very inexpensive starting material, 1,6-dimethoxyphenol (**261**) (Scheme 29).[143] The key hydrogenation to give an all-cis diether was catalyzed by Ruthenium, and was followed by deprotection of the methyl ethers using in situ generated trimethylsilyl iodide. The resulting dihydroxy diester **263** was desymmetrized by using inexpensive pig-liver esterase to give **264** in very high yield (96%) as well as excellent enantiomeric excess (96–98% ee). **264** was then subjected to a Yamada–Curtius degradation using diphenylphosphoryl azide, which

[141] Abrecht, S.; Karpf, M.; Trussardi, R.; Wirz, B. US Patent 6,403,824, **2002**.

[142] Abrecht, S.; Harrington, P.; Iding, H.; Karpf, M.; Trussardi, R.; Wirz, B.; Zutter, U. *Chimia* **2004**, *58*, 621.

[143] Iding, H.; Wirz, B.; Zutter, U. US Patent 6,518,048, **2003**.

produced oxazolidinone **265**. Reaction with NaN$_3$ gave the **266**, which was transformed into **254** in four additional steps with good overall yield (30%).

Scheme 29. Desymmetrization Approach to Tamiflu (**254**) Starting From Phenol **261**.
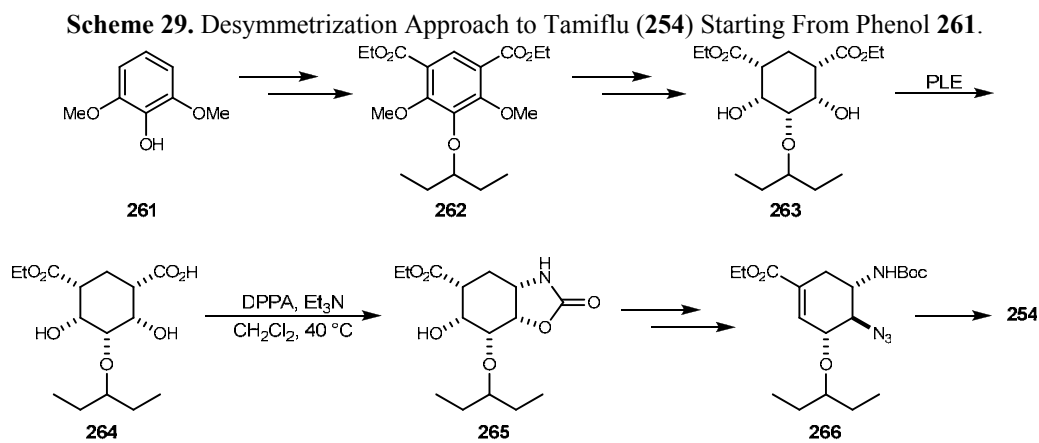
This approach avoids the use of shikimic acid while still maintaining high throughput and good yields as compared to the manufacturing process. On the downside, the synthesis still requires sodium azide late in the process, which from a reaction safety standpoint is undesirable. More recently, the demand for Tamiflu has attracted the attention of academic chemists, who have reported several new approaches.

In 2006 Corey reported a twelve step synthesis of oseltamivir phosphate (Tamiflu) which began with the enantioselective Diels-Alder reaction of 1,3-butadiene and trifluoroethyl acrylate (Scheme 30).[144] After conversion to amide **271**, bicyclic copound **272** was formed in 84% yield. Protection of the amide with Boc was followed by elimination of the iodine to form compound **274**. After bromination and alkene isomerization, the lactam was opened with Cs$_2$CO$_3$ and EtOH to form diene **276**. Acyl aziridine **278** was formed in two steps and was opened under Lewis Acidic conditions with 3-pentanol to reveal compound **279**. Subjecting this compound to H$_3$PO$_4$ in EtOH served to both deprotect the Boc group as well as form the desired phosphate salt (**254**).

---

[144] Yeung, Y-Y.; Hong, S.; Corey, E. J. *J. Am. Chem. Soc.* **2006**, *128*, 6310.

Scheme 30. Corey's Synthesis of oseltamivir phosphate (Tamiflu).
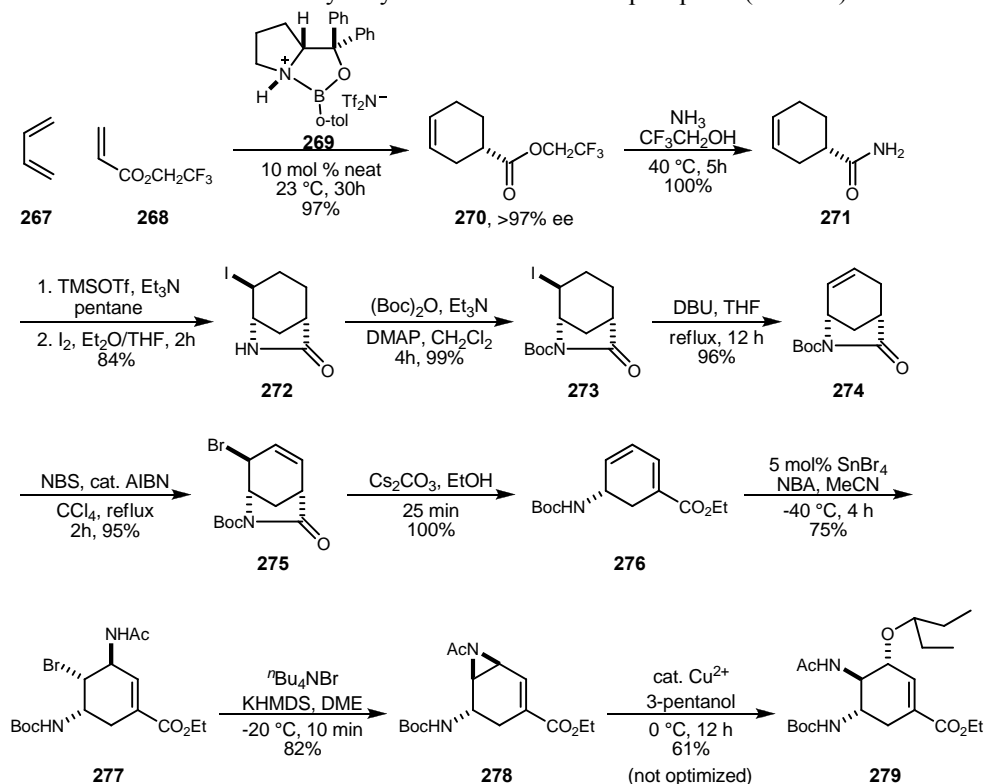
Concurrent with Corey's report, Shibasaki also published a synthesis of Tamiflu in 2006.[145] Shibasaki's synthesis utilized an enantioselective ring-opening of *meso*-aziridine **280** with TMSN$_3$. The resulting diamine **282** is obtained in 96% yield with 91% ee, but can be recrystallized from ^{i}PrOH to >99% ee in 72% yield.
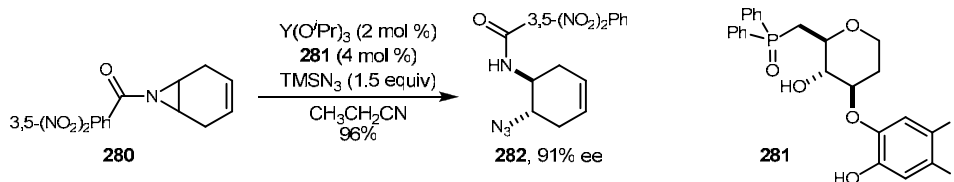
Transformation of azide **282** to the *bis*-Boc protected diaminocyclohexene (**284**) was performed in four steps (Scheme 31). Conversion of the alkene to the enone, followed by Michael addition of a cyano group afforded compound **286** in four steps. This was then reduced to the allylic alcohol using LiAlH(O^{t}Bu)$_3$ in 20:1 dr favoring the desired product

---

[145] Fukuta, Y.; Mita, T.; Fukuda, N.; Kanai, M.; Shibasaki, M. *J. Am. Chem. Soc.* **2006**, *128*, 6312.

287. Conversion to the aziridine followed by BF$_3$·OEt$_2$ catalyzed ring-opening with 3-pentanol afforded **288** in good yield with a net retention of stereochemistry. Protecting group manipulation followed by conversion of the nitrile to the ethyl ester afforded compound **279** in four steps. This intermediate is converted directly to Tamiflu upon addition of H$_3$PO$_4$.

Scheme 31. Shibasaki's synthesis of oseltamivir phosphate (Tamiflu).
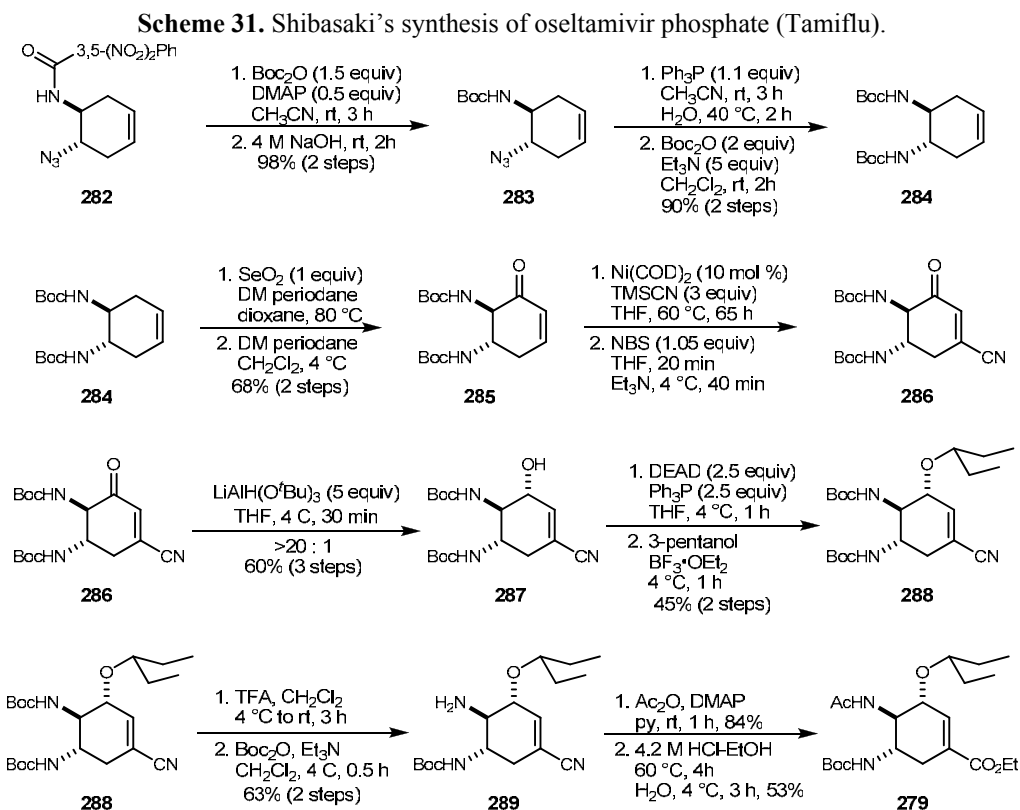
Also in 2006, Yao reported his synthesis of the active pharmaceutical ingredient (**279**) which utilized a ring-closing methathesis as the key transformation (Scheme 32).[146] Starting from L-serine, an inexpensive commercially available chiral starting material, they were able to form intermediate **290** in short order using known chemistry.[147] This intermediate was able to be converted into the metathesis precursor (**297**) in good yield, albeit low diastereoselectivity (3:1). The key ring-closing metathesis step gave the desired product **298** in a remarkable 98% yield. Deprotection to reveal the primary

---

[146] Cong, X.; Yao, Z.-J. *J. Org. Chem.* **2006**, *71*, 5368.
[147] (a) Cong, X.; Liao, Q.-J.; Yao, Z.-J. *J. Org. Chem.* **2004**, *69*, 5314. (b) Mckillop, A.; Taylor, R. J. K.; Waston, R. J.; Lewis, N. *Synthesis* **1994**, 31. (c) Dondoni, A.; Perrone, P. *Synthesis* **1997**, 527.

alcohol (**299**), followed by oxidation and esterification gave intermediate **300**. Finally, protecting group removal afforded the active pharmaceutical ingredient **279** in good yield. The synthesis was completed in 18 steps from intermediate 290 with an overall yield of 16.5%.

Scheme 32. Yao's Synthesis of **279** Starting From L-Serine-derived **290**.
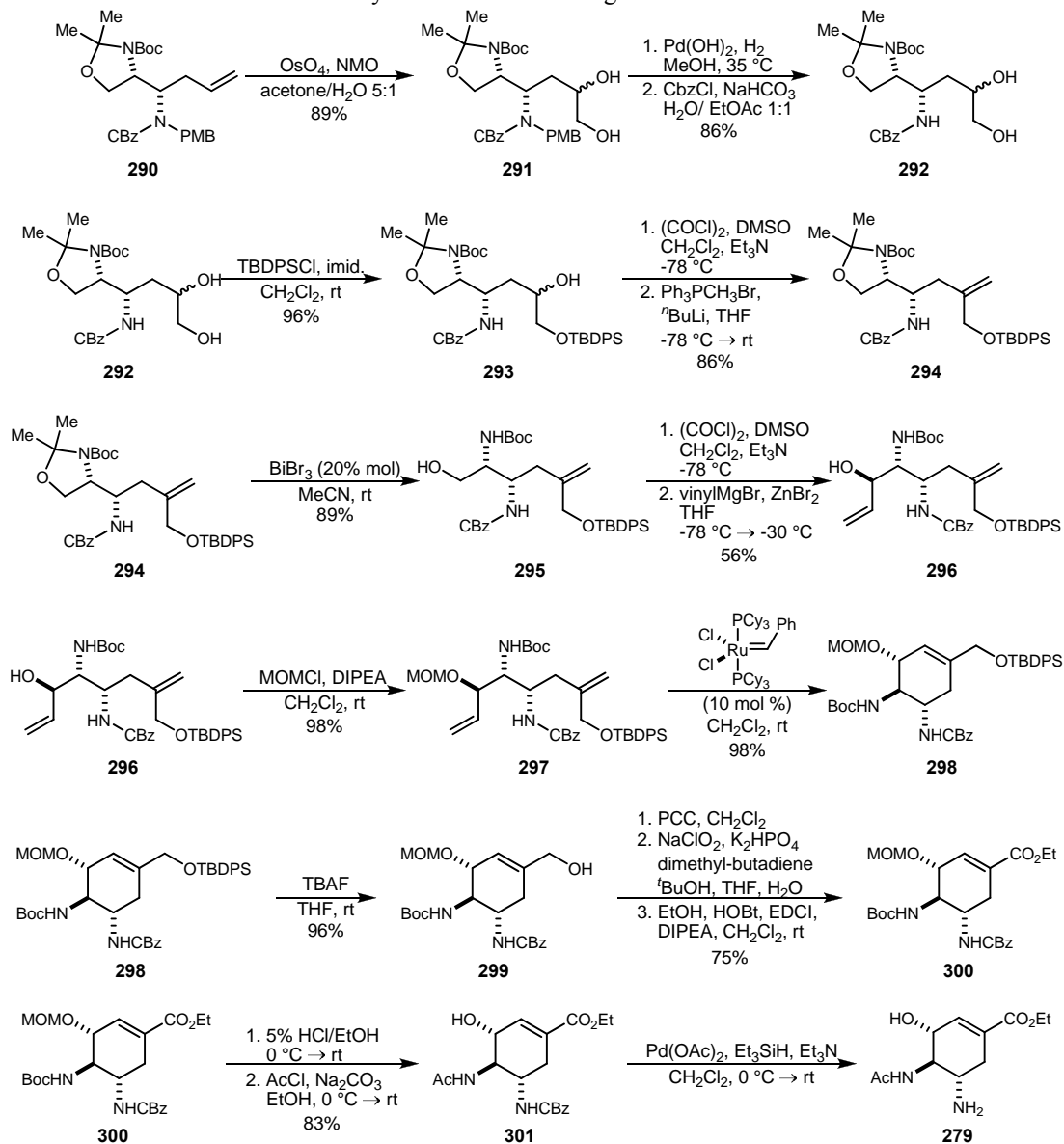
In 2007, Shibasaki and coworkers reported an improved synthesis of Tamiflu (**254**) (Scheme 33),[148] building off of their previous work (*vide supra*). Intermediate **283** was again synthesized using their previously reported catalytic enantioselective *meso*-aziridine desymmetrization methodology. However, rather than forming symmetrical cyclohexene **284** as previously reported, they instead converted intermediate **283** into carbamate **302**. After conversion to enone **304**, a cyanophosphorylation was used to generate intermediate **305** with excellent diastereoselection. The key allylic rearrangement produced **306** in 78% yield over two steps. Although more direct routes were attempted, the authors found the conversion of **306** to **308** to be most effective using a series of Mitsunobu reaction, aziridination formation, and aziridine opening with 3-pentanol. This intermediate was then converted to Tamiflu (**254**) in 60% yield over two steps. This second-generation synthesis is only 15 steps from aziridine **280**, in part due to the elimination of protecting group shuffling at the beginning of the synthesis.

Scheme 33. Shibasaki's Second-Generation of Tamiflu (**254**).
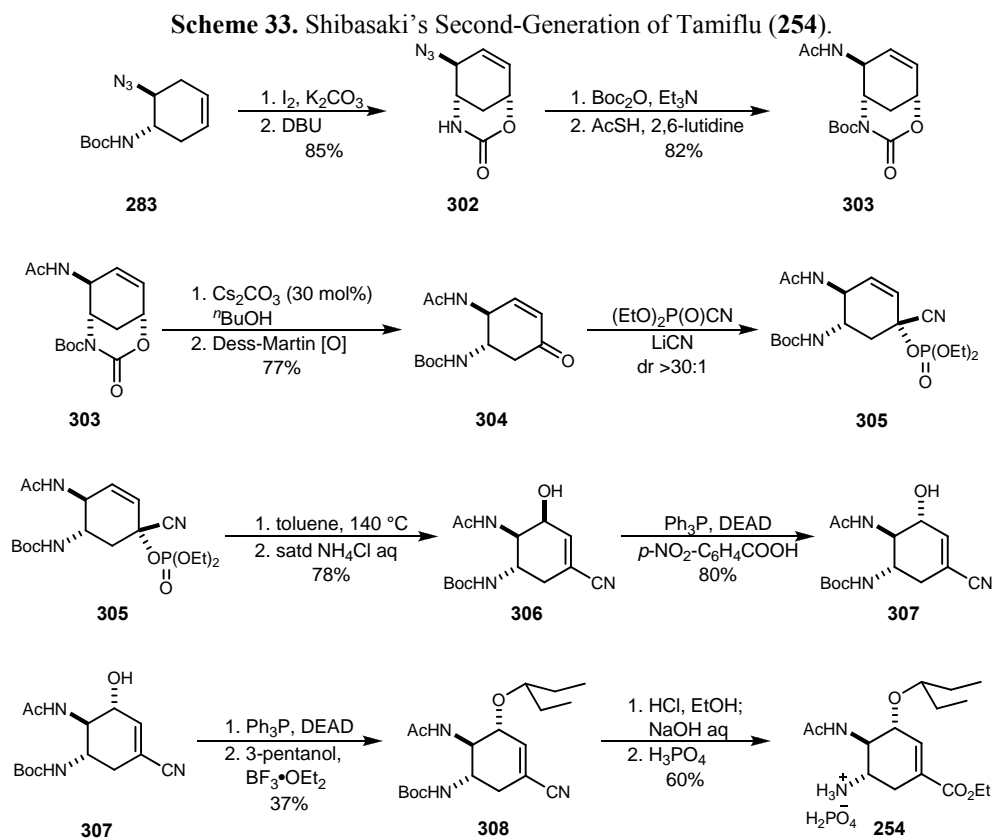
[148] Mita, T.; Fukuda, N.; Roca, F. X.; Kanai, M.; Shibasaki, M. *Org. Lett.* **2007**, *9*, 259.

Also in 2007, concurrent with our work, Shibasaki reported his third-generation synthesis of Tamiflu (**254**) in *Tetrahedron Letters*.[149] This time he chose to abandon the catalytic enantioselective *meso*-aziridine desymmetrization methodology. His synthetic strategy was obviously inspired by intermediate **307** in his second-generation synthesis. Arguably, the most concise method to reach intermediate **307** would utilize a Diels-Alder reaction to build the cyclohexene ring. Shibasaki found that diene **309** and dienophile **310** successfully underwent a [4+2] cycloaddition to give the desired product in 55% yield after the removal of the TMS protecting group. The free hydroxyl group underwent the designed reaction with the intermediate isocyanate formed during the Curtius rearrangement to give intermediate **312**. Once converted to cyclohexenone **314**, the racemic material was resolved using chiral HPLC. The enantiomerically enriched material was taken forward first undergoing a 1,4-addition of TMSCN to give intermediate **315**, followed by reduction of the ketone with $LiAl(O^tBu)_3H$ to give the desired diastereomer of **307** in 44% yield over 3 steps. Shibasaki used the same procedure to convert **307** to Tamiflu (**254**) here as in his second-generation synthesis, although with an improved yield. Utilizing a Diels-Alder reaction followed by a Curtius rearrangement allowed for rapid access to Tamiflu (**254**), 12 steps in 4% overall yield.

[149] Yamatsugu, K.; Kamijo, S.; Suto, Y.; Kanai, M.; Shibasaki, M. *Tetrahedron Lett.* **2007**, *48*, 1403.

Scheme 34. Shibasaki's Third-Generation Synthesis of Tamiflu (**254**).
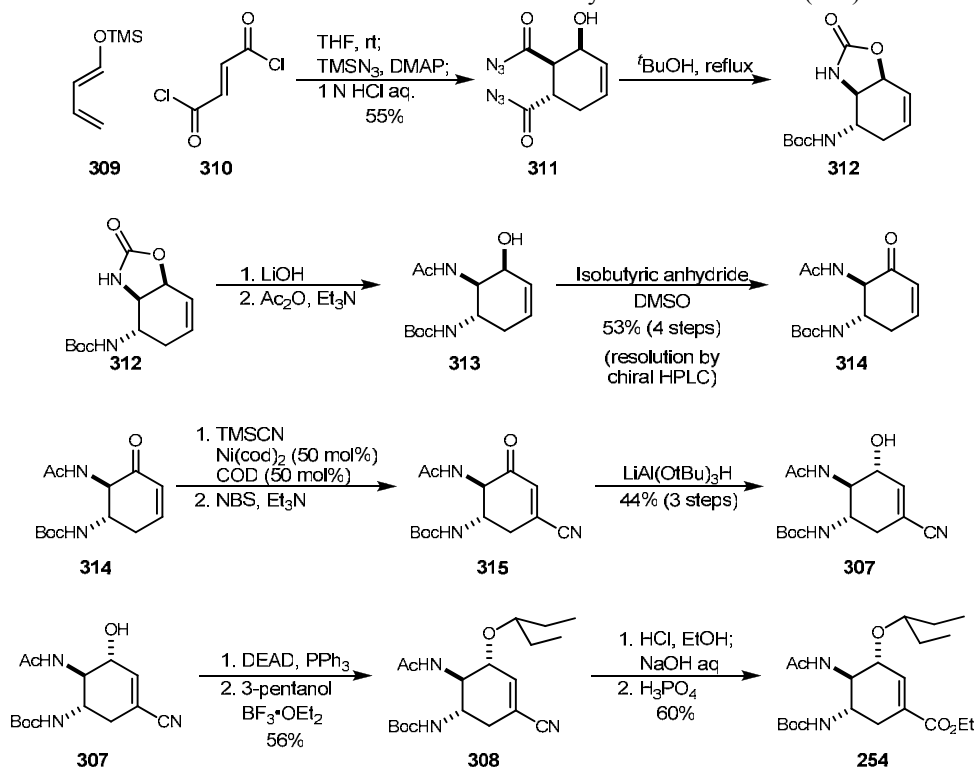
3.2.3. Retro-synthetic Analysis of Tamiflu

The proposed retro-synthesis of oseltamivir phosphate (Tamiflu), **254**, is shown below (Scheme 35). The key step is a Diels-Alder reaction which in one step generates all three stereocenters with proper relative configuration. The starting materials are cheap and available in large quantities and the overall synthesis is highly atom economic. However, neither the diene nor the dienophile have been previously synthesized, let alone used in a [4+2] cycloaddition reaction.

Scheme 35. Retro-synthetic analysis of oseltamivir phosphate (Tamiflu).
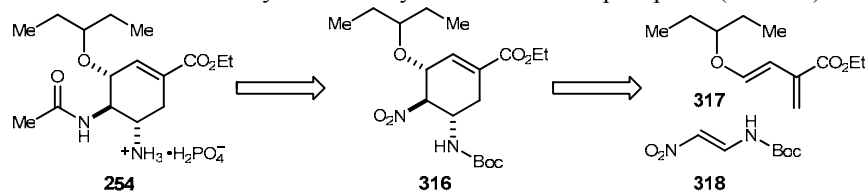
After formation of the novel diene and dienophile, the remaining steps in the proposed synthesis consist of the key Diels-Alder step mentioned above as well as functional group transformation of the nitro to the acylated amine present in **254** (Scheme 36).

Scheme 36. Proposed End Game for synthesis of oseltamivir phosphate (Tamiflu).
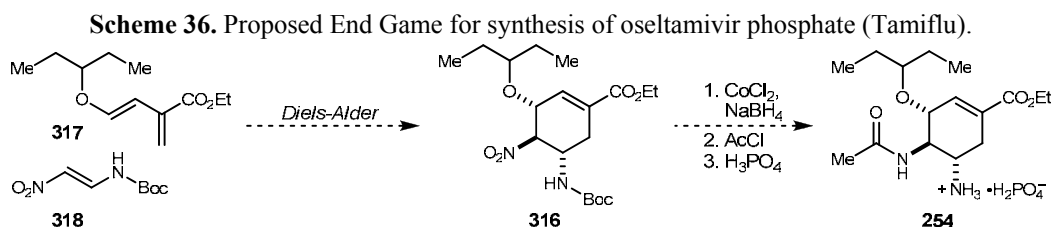
Our group has experience in reducing the nitro group chemoselectively in the presence of other functionality. The final two steps have been previously reported to proceed in high yield, acylation and Boc deprotection concurrent with forming the phosphate salt **254**. Therefore the only questionable step of the synthesis appears to be the Diels-Alder reaction. Further investigation into the literature has shown that there are very few examples using either a diene or dienophile of the types described here. However, there are three precedents which lend a great deal of support to the proposed reaction.

First the only example of an *N*-acyl,*N*-Boc-diaminoethylene (**321**) in a Diels-Alder reaction was reported in 1999 by chemists at Gilead Sciences Inc. and Roche Discovery Welwyn.[150] This Diels-Alder reaction was used to generate a new series of potential influenza neuramidase inhibitors with a Tamiflu like structure. However, the synthesis of the dienophile proved to be inefficient, yielding only 8% over two steps. Furthermore, the regioselectivity of the Diels-Alder reaction favored the undesired isomer in a 3:1 ratio. Although the synthesis was not efficient, it did show that a Diels-Alder using dienophile **321** could be performed in 87% yield (Scheme 37).

---

[150] Zhang, L.; Williams, M. A.; Mendel, D. B.; Escarpe, P. A.; Chen, X.; Wang, K-Y.; Graves, B. J.; Lawton, G.; Kim, C. U. *Bioorg. Med. Chem. Lett.* **1999**, *9*, 1751.

Scheme 37. Diels-Alder reaction of **321** to make Tamiflu-like compounds.
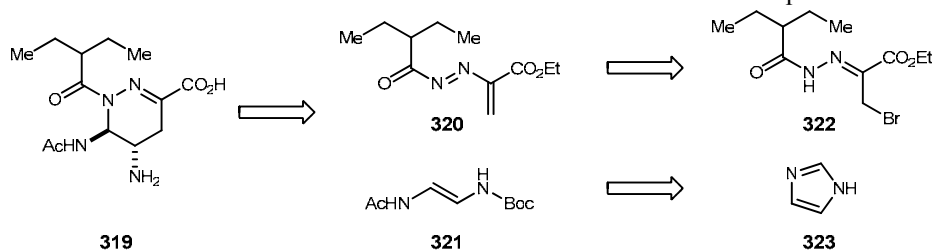
Kraus reported a Diels-Alder reaction using unsaturated benzoyloxy, nitro compound **324** in 1988.[151] The products were found to give *endo/exo* ratios of 1:1 to 6:1 depending on the R group of the diene (eq 73). However, the paper does not mention how the *endo/exo* ratio was determined and there is no experimental section. Furthermore, rapid decomposition of the Diels-Alder products to the aromatic nitrobenzenes was found to occur in the presence of a slight excess of base.
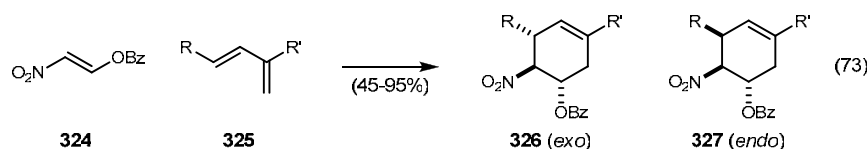
In 1996 Node and coworkers published an interesting *exo* selective Diels-Alder reaction using nitroolefins and Danishefsky's diene.[152] Using various substituents on the nitroolefin, they found the cyclohexenes generated from reaction with Danishefsky's diene consistently favored the *exo* product in ratios from 2:1 to 10:1 (eq 74).
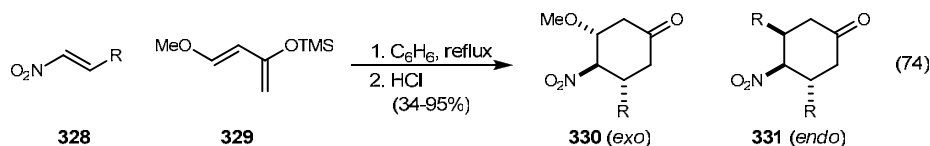
The authors did suggest a possible explanation for the unusual *exo* stereoselectivity that resulted. There are two interactions, one electrostatic and one steric, which could favor either the *exo* or *endo* transition state respectively (Figure 37).

[151] Kraus, G. A.; Thurston, J.; Thomas, P. J. *Tetrahedron Lett.* **1988**, *29*, 1879.
[152] Node, M.; Nishide, K.; Imazato, H.; Kurosaki, R.; Inoue, T.; Ikariya, T. *Chem. Commun.* **1996**, 2559.

Figure 37. Rationale for observed exo selectivity in the Diels-Alder reaction.
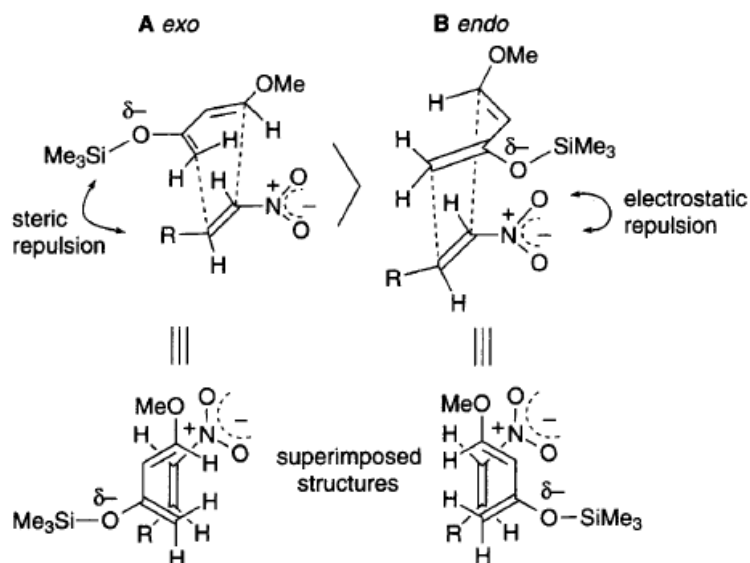
Extrapolating this to the expected outcome of the proposed Diels-Alder reaction, it is hypothesized that the ethyl ester group can cause an electrostatic repulsion in the same way as the OTMS does in Danishefsky's diene (Figure 38). This repulsion in turn should provide high *exo* selectivity if the group on the nitroolefin does not cause too much of a steric repulsion with the ester group on the diene (or OTMS as shown in Figure 37).

Figure 38. Proposed exo and endo transition states.

110
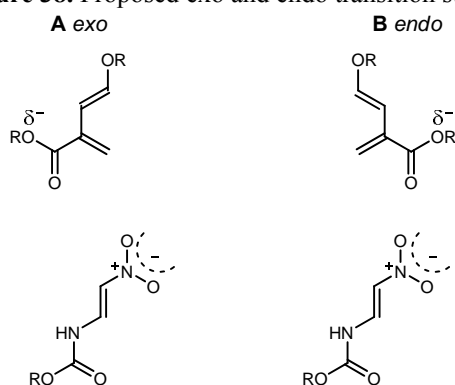
3.2.4. Synthetic Studies toward Tamiflu

At first glance, the synthesis of the diene appeared to be straight forward starting from commercially available dimethoxyacetaldehyde (**332**) and commercially available triethyl 2-phosphonopropionate (**333**). Using a *Horner-Emmons* reaction as reported by Pfander in 1999, unsaturated aldehyde **334** was isolated in 78% yield (Scheme 38).[153] The next step to make the acetal proceeds smoothly with 10 equivalents of 3-pentanol in toluene over 4 Å molecular sieves at 60 °C. However, attempts to eliminate the resulting acetal that forms diene **317** were unsuccessful. Further research into the literature of 3-ester-butadienes revealed that they are unstable even at cold temperatures and quickly dimerize or polymerize to produce complex mixtures. It was hypothesized that this diene may have potential if generated *in situ* with the dieneophile present so as to trap the diene in a [4+2] cycloaddition upon formation.

Scheme 38. Synthesis of the diene precursor to oseltamivir phosphate (Tamiflu).
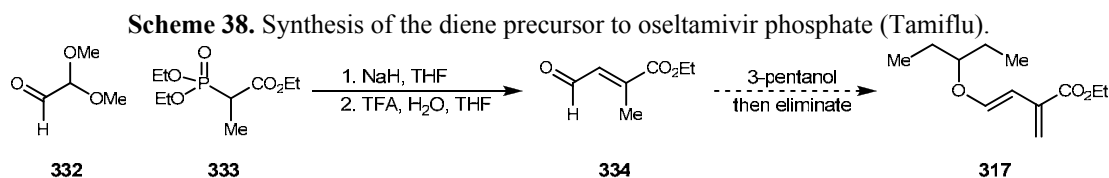
Turning to the synthesis of the dienophile, commercially available *N,N*-dimethyl formamide dimethyl acetal (**335**) and commercially available *tert*-butyl carbamate (**336**) were initially chosen as starting materials (Scheme 39). Compound **337** was formed in 88% yield using Lin's general procedure[154] as described by Helmchen.[155] It was hypothesized that this intermediate could then be treated with nitromethane to form the desired product **318**.

Scheme 39. Synthesis of the dienophile precursor to oseltamivir phosphate (Tamiflu).
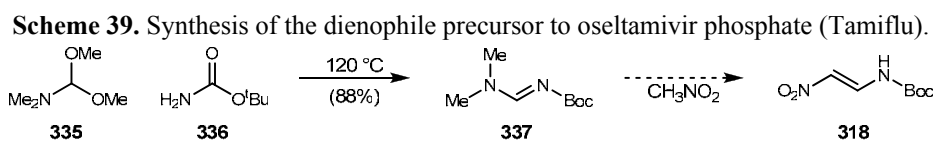
[153] Häberli, A.; Pfander, H. *Helv. Chim. Act.* **1999**, *82*, 696.
[154] Lin, Y.; Lang, Jr., S. A. *Synthesis* **1980**, 119.
[155] Weihofen, R.; Tverskoy, O.; Helmchen, G. *Angew. Chem. Int. Ed.* **2006**, *45*, 5546.

However, heating in nitromethane provided the over-addition product (**338**) in which a second equivalent of nitromethane was added to the desired product (Scheme 40). Intermediate **338** was refluxed in xylenes in the presence of DMAP, however; the additional nitromethane equivalent was unable to be removed. Formation of **338** goes through the desired product **318**, but the addition of the second equivalent of nitromethane is faster than the addition of the first equivalent. Hence at various points during the course of the reaction, only starting material **337** and over-addition product **338** could be observed.

Scheme 40. Attempted Synthesis of Dienophile **318** from Amidine **337**.
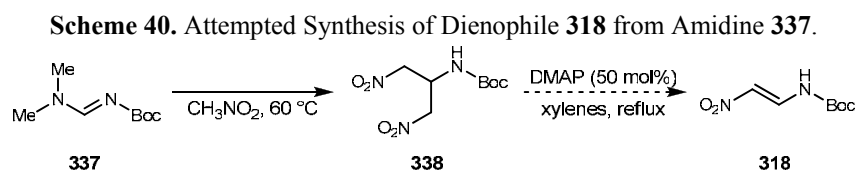
Similarly, if acetic acid and water is used to make the Boc-protected formamide (**337**), the same over-addition product (**338**) is obtained after treatment with nitromethane (Scheme 41). Again it is presumed that the intermediate (**318**) in route to the over-addition product is formed, but reacts faster with nitromethane than the starting Boc-protected formamide (**339**).

Scheme 41. Attempted Synthesis of Dienophile **318** from Formamide **339**.
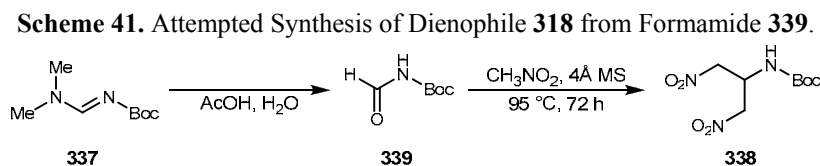
Our next approach was to intercept methazonic acid, a precursor to nitroacetonitrile, which has been shown to react with aniline to form nitro-olefin **341** (Scheme 42). Unfortunately the analogous reaction using *tert*-butylcarbamate was unsuccessful. Gas evolution was observed during the reaction suggesting decarboxylation of the Boc preotecting group.

Scheme 42. Attempted Synthesis of Dienophile **318** from Methazonic Acid (**340**).
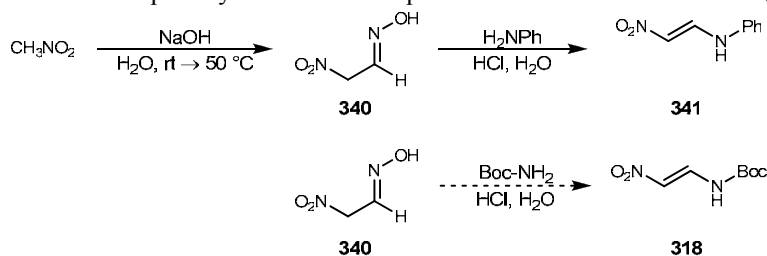
Finally, we hypothesized that it might be possible to displace thiophenol in an analogous matter to what had been previously reported using *N*-methylaniline to form nitro-olefin **346** (Scheme 43).[156] After forming the nitro-olefin (**345**) from intermediate **344** using sulfuryl chloride,[157] the desired reaction using *tert*-butylcarbamate did not proceed, presumably due to the lower nucleophilicity of the carbamate nitrogen.

Scheme 43. Attempted Synthesis of Dienophile **318** from Nitroethanol **342**.
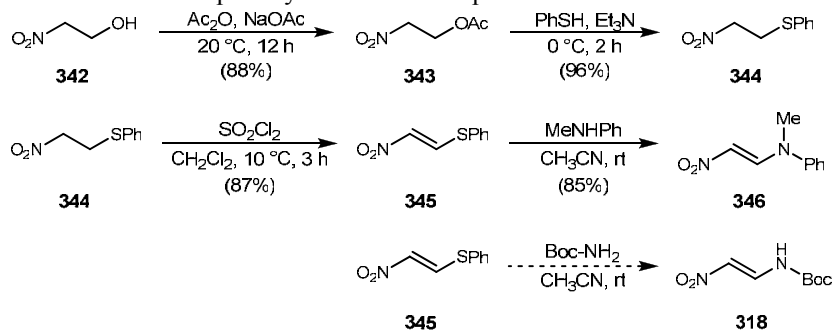
While work continued to generate the desired dienophile, we turned our attention to the possibility of using the commercially available nitro-olefin **347** and Danishefsky's diene (**329**) to study the Diels-Alder reaction. Unfortunately no product was formed after refluxing in toluene for several days. Although no thermal reaction was observed, the possibility to catalyze the reaction with a Lewis acid still exists. Several Lewis acids were screened in dichloromethane at room temperature (eq 75). Regrettably, there was again no cycloaddition reaction observed eventually leading to decomposition of the diene in the cases of the stronger Lewis acids. Presumably, the captodative nature of the dienophile (**347**) is playing a large role in its poor reactivity. This problem is avoided in

---

[156] Kamimura, A.; Ono, N. *Synthesis* **1988**, *11*, 921.
[157] Ono, N.; Kamimura, A.; Kaji, A. *J. Org. Chem.* **1986**, *51*, 2139.

the proposed dienophile (**318**) as the electron-withdrawing nature of the Boc protecting group should increase its reactivity.

Lewis acid = Ti(OiPr)$_4$, TiCl$_4$, ZnCl$_2$, BF$_3$OEt$_2$, thiourea, H,Quin-BAM·HOTf (**118e**)
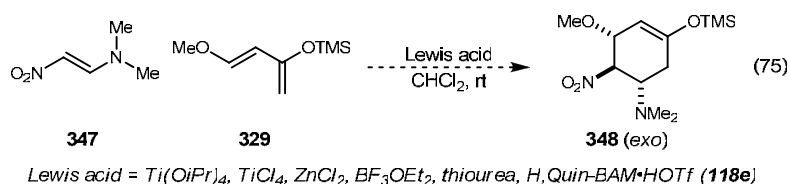
Turning to the literature, it was discovered that the Diels-Alder reaction could be examined using Danishefsky's diene (**329**) and commercially available nitro-styrene (**349**).[152] The goal of this model study was to better simulate this unique cycloaddition reaction with a dienophile more similar electronically to the proposed dienophile (**318**) than the above nitro-olefin (**347**). Using nitrostyrene, the thermal Diels-Alder reaction produced the product in 60% yield favoring the desired *exo* adduct in a 9:1 ratio over the *endo* isomer (eq 76).
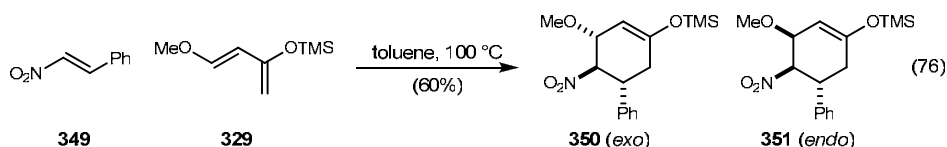
With this result in hand, we next investigated the effectiveness of a Lewis acid catalyzed cycloaddition. Since no reaction was observed at room temperature, our concern at the outset was to find a catalyst to improve the rate of the reaction at lower temperatures while not diminishing the already favorable *exo* selectivity. We were surprised to see that reaction with BF$_3$·OEt$_2$ at -78 °C in dichloromethane led to decomposition of Danishefsky's diene before any reaction could take place (eq 77).

114
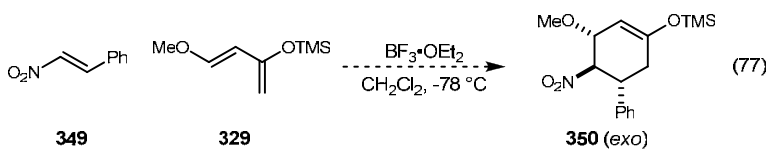
Suspecting that a weaker catalyst may be more effective at catalyzing the cycloaddition reaction without decomposing the starting diene, H,Quin-BAM·HOTf (**118e**) was examined. The reaction was found to proceed, albeit in very low conversion (<10%), at -20 °C in toluene (eq 78). The product was isolated in such a small amount that it is difficult to comment on the *exo*:*endo* ratio with a high degree of certainty. After purification, only peaks corresponding to the *exo* product were observed by NMR. This product was examined by HPLC to determine if there was any enantioselection, however; the product was racemic. Although there was no enantiomeric excess, this result does suggest that it may be possible to develop a catalyst for this cycloaddition reaction.
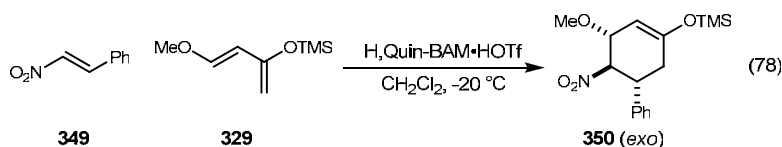
In conclusion, although we were not able to demonstrate the capability of this method as a viable route to Tamiflu, we have determined several key factors that may one day lead to a powerful new synthetic route. First, the dienophile can not be so captodative so as to become unreactive. This can be accomplished by substituting the enamine nitrogen with an electron withdrawing protecting group such as Boc or CBz. Second, although the diene appears to be extremely reactive, so much so that it rapidly leads to dimerization and polymerization, it has the potential to be trapped given a sufficiently reactive dienophile. Finally, the proposed Diels-Alder reaction has been shown to produce the desired *exo* cyclohexene in useful ratios for model compounds. Furthermore, this reaction can be catalyzed using a Brønsted acid catalyst at low temperatures. This opens the door for enantioselective catalysts such as H,Quin-BAM·HOTf to be used in the enantioselective synthesis of Tamiflu.

Chapter 4. Experimental Section

Flame-dried (under vacuum) glassware was used for all reactions. All reagents and solvents were commercial grade and purified prior to use when necessary. Diethyl ether (Et_2O), tetrahydrofuran (THF), dichloromethane (CH_2Cl_2), and benzene (C_6H_6) were dried by passage through a column of activated alumina as described by Grubbs.[158] Benzene was additionally passed through a column containing activated Q-5 reactant. Methanol was distilled from Mg under N_2 immediately before use. The aldimines[159] and Pd(dba)$_2$[160] were prepared as reported in literature. Palladium-mediated aryl amination was executed using a Buchwald protocol.[161]

Thin layer chromatography (TLC) was performed using glass-backed silica gel (250 μm) plates and flash chromatography utilized 230–400 mesh silica gel from Scientific Adsorbents. UV light, and/or the use of ceric ammonium molybdate and potassium iodoplatinate solutions to visualize products.

IR spectra were recorded on a Nicolet Avatar 360 spectrophotometer and are reported in wavenumbers (cm^{-1}). Liquids and oils were analyzed as neat films on a NaCl plate (transmission), whereas solids were applied to a diamond plate (ATR). Nuclear magnetic resonance spectra (NMR) were acquired on either a Varian INOVA-400 (400 MHz) or VXR-400 (400 MHz) instrument. Chemical shifts are measured relative to residual solvent peaks as an internal standard set to δ 7.26 and δ 77.1 (CDCl$_3$) and δ 7.15 and δ 128.1 (d_6-benzene). Mass spectra were recorded on a Kratos MS-80 spectrometer by use of chemical ionization (CI). Atlantic Microlabs, GA, performed combustion analyses.

[158] Pangborn, A. B.; Giardello, M.A.; Grubbs, R. H.; Rosen, R. K.; Timmers, F. J. *Organometallics* **1996**, *15*, 1518-1520
[159] Kanazawa, A. M.; Denis, J.; Greene, A.E. *J. Org. Chem.* **1994**, *59*, 1238-1240.
[160] Rettig, M.F.; Maitlis, P.M. *Inorg. Synth.* **1992**, *28*, 110.
[161] Wagaw, S.; Rennels, R.; Buchwald, S. *J. Am. Chem. Soc.* **1997**, *119*, 8451-8458.
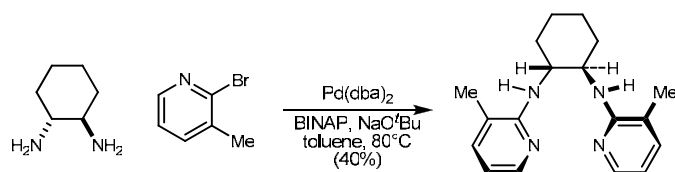
H,^{3}Me-BAM (115a). Pd(dba)$_2$ (14.4 mg, 50.0 μmol), BINAP (31.1 mg, 50.0 μmol), and NaO^{t}Bu (288.3 mg, 3.0 mmol) were combined in a round-bottomed flask in a glove box. Toluene (10 mL, 0.10 M) was added to the mixture, followed by 1,2-(R,R)-*trans*-diaminocyclohexane (114.2 mg, 1.0 mmol), and 2-bromo-3-methylpyridine (344.1 mg, 2.0 mmol) as a solution in toluene. The reaction was heated to 80 °C and stirred until TLC suggested complete conversion. The reaction was cooled to room temperature, concentrated, and purified by flash chromatography (SiO$_2$, 25% ethyl acetate in hexanes) to afford the desired diamine as a white solid (120 mg, 40%); [α]$_D^{25}$ +186.7 (*c* 1.0, CHCl$_3$); mp = 132-134 °C; R$_f$ = 0.25 (20% EtOAc/hexanes); IR (neat) 3339, 2930, 2855, 1603, 1505, 1418 cm^{-1}; ^{1}H NMR (400 MHz, CDCl$_3$) δ 7.95 (d, *J* = 3.9 Hz, 1H), 7.10 (d, *J* = 6.7 Hz, 1H), 6.43 (dd, *J* = 5.1, 1.9 Hz, 1H), 5.04 (d, *J* = 4.3 Hz, 1H), 4.07-4.04 (m, 1H), 2.30 (d, *J* = 12.9 Hz, 1H), 1.87 (s, 3H), 1.81 (d, *J* = 6.7 Hz, 1H), 1.52-1.38 (m, 2H); ^{13}C NMR (100 MHz, CDCl$_3$) ppm 157.8, 145.4, 137.0, 116.9, 112.3, 56.6, 34.0, 25.7, 17.5; HRMS (EI) Exact mass calculated for C$_{18}$H$_{24}$N$_4$ [M+H]$^+$ 297.2074. Found 297.2074.
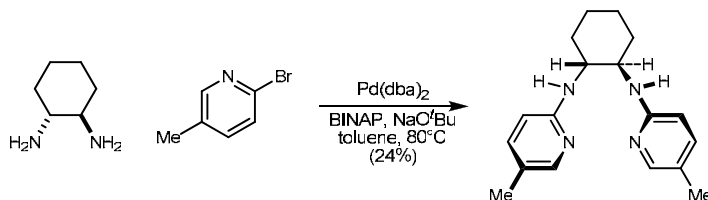
H,^{5}Me-BAM (115b). Pd(dba)$_2$ (14.4 mg, 50.0 μmol), BINAP (31.1 mg, 50.0 μmol), and NaO^{t}Bu (288.3 mg, 3.0 mmol) were combined in a round-bottomed flask in a glove box. Toluene (10 mL, 0.10 M) was added to the mixture, followed by 1,2-(R,R)-*trans*-diaminocyclohexane (114.2 mg, 1.0 mmol) and 2-bromo,5-methylpyridine (344.1 mg, 2.0 mmol) as a solution in toluene. The reaction was stirred at 80 °C until TLC indicated complete conversion. The reaction was cooled to room temperature, concentrated, and purified by flash chromatography (SiO$_2$, 25% ethyl acetate in hexanes) to provide the desired diamine as a white solid (70 mg, 24%); [α]$_D^{25}$ +593.0 (*c* 0.5, CHCl$_3$); mp = 126-128 °C; R$_f$ = 0.33 (40% EtOAc/hexanes); IR (neat) 3283, 3006, 2928, 2858, 1616, 1500

cm^{-1}; ^{1}H NMR (400 MHz, CDCl$_3$) δ 7.84 (s, 1H), 7.07 (dd, *J* = 8.4, 2.0 Hz, 1H), 6.12 (d, *J* = 8.4 Hz, 1H), 4.89 (s, 1H), 3.69 (d, *J* = 3.3 Hz, 1H), 2.19 (d, *J* = 13.1 Hz, 1H), 2.10 (s, 3H), 1.72 (dd, *J* = 3.5, 3.5 Hz, 1H), 1.41 (dd, *J* = 6.4, 3.5 Hz, 1H), 1.37-1.26 (m, 1H); ^{13}C NMR (100 MHz, CDCl$_3$) ppm 157.2, 147.2, 138.2, 121.0, 108.4, 56.3, 33.3, 25.1, 17.6; HRMS (EI): Exact mass calculated for C$_{18}$H$_{24}$N$_4$ [M+H]$^+$ 297.2074. Found 297.2079.
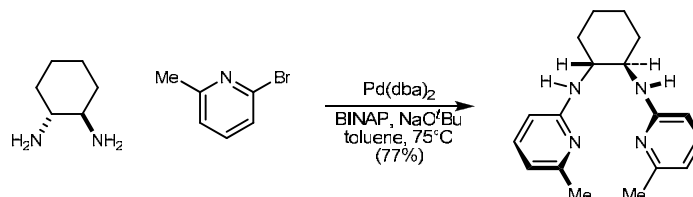
H,^{6}Me-BAM (115c). Pd(dba)$_2$ (10.1 mg, 17.5 μmol), BINAP (21.8 mg, 35.0 μmol), and NaO^{t}Bu (286.4 mg, 2.98 mmol) were loaded into a round bottom flask in a glove box. Toluene (10 mL, 0.10M) was added to the mixture followed by the 1,2-(*R*,*R*)-*trans*-diaminocyclohexane (100.0 mg, 876.0 μmol). 2-Bromo,6-methylpyridine (301.5 mg, 1.75 mmol) was added as a solution in toluene. The reaction was allowed to stir at 80 °C and monitored by TLC. The reaction was then cooled to room temperature, concentrated, and purified by flash column chromatography on silica gel (5% Et$_3$N, 10% EtOAc in hexanes) affording **115c** as a white solid (200 mg, 77%); [α]$_D$^{25} +111.1 (*c* 1.0, CHCl$_3$); mp 126-128 °C; R$_f$ =0.17 (5% Et$_3$N, 10% EtOAc, 85% hexanes); IR (neat) 3256 3051 2927 2855 1559 cm^{-1}; ^{1}H NMR (400 MHz, CDCl$_3$) δ 7.17 (dd, *J* = 8.2, 7.3 Hz, 1H), 6.33 (d, *J* = 7.3 Hz, 1H), 6.09 (d, *J* = 8.2 Hz, 1H), 5.08 (m, 1H), 3.66 (dd, *J* = 7.3, 7.0 Hz, 1H), 2.34 (s, 3H), 2.20 (dd, *J* = 10.7, 6.7 Hz, 1H), 1.70-1.72 (m, 1H), 1.23-1.43 (m, 2H); ^{13}C NMR (100 MHz, CDCl$_3$) δ 158.4, 156.8, 137.5, 111.6, 104.6, 55.3, 32.3, 24.7, 24.5; HRMS (EI) Exact mass calculated for C$_{18}$H$_{24}$N$_4$ [M]$^+$ 296.2001, found 296.1994.
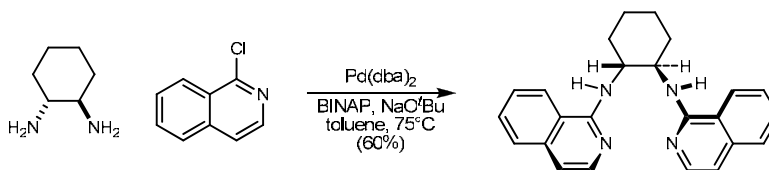
H,Isoquin-BAM (115d). Pd(dba)$_2$ (118.9 mg, 130.0 μmol), BINAP (161.9 mg, 260.0 μmol), and NaO^{t}Bu (2.15 g, 22.3 mmol) were loaded into a round bottom flask in a glove box. Toluene (65 mL, 0.10M) was added to the mixture followed by the 1,2-(*R*,*R*)-*trans*-diaminocyclohexane (750.0 mg, 6.6 mmol). 1-Chloroisoquinoline (2.1 g, 13.1 mmol) was

added as a solution in toluene. The reaction was allowed to stir at 80 °C and monitored by TLC. The reaction was then cooled to room temperature, concentrated, and purified by flash column chromatography on silica gel (5% Et_2O in hexanes) affording **115d** as a white solid (1.75 g, 60%). $[\alpha]_D^{25}$ -240.0 (*c* 1.0, $CHCl_3$); Mp 141-142 °C; IR (film) 3315, 3048, 2931, 2855, 1594, 1522, 1427, 1409 cm^{-1}; ^1H NMR (400 MHz, $CDCl_3$) δ 7.98 (d, *J* = 5.8 Hz, 1H), 7.65 (d, *J* = 8.2 Hz, 1H), 7.52 (d, *J* = 7.9 Hz, 1H), 7.45 (dd, *J* = 7.3, 6.7 Hz, 1H), 7.32 (dd, *J* = 8.2, 7.9 Hz, 1H), 6.81 (d, *J* = 5.8 Hz, 1H), 6.50 (s, 1H), 4.26 (s, 1H), 2.42 (d, *J* = 10.7 Hz, 1H), 1.85 (d, *J* = 6.7 Hz, 1H), 1.54-1.17 (m, 2H); ^{13}C NMR (100 MHz, $CDCl_3$) δ 155.9, 141.1, 137.9, 137.2, 129.8, 127.0, 125.8, 122.2, 110.6, 56.8, 33.3, 25.3; HRMS (EI): Exact mass calcd for $C_{24}H_{24}N_4$ $[M]^+$ 368.2001, found 368.2009.
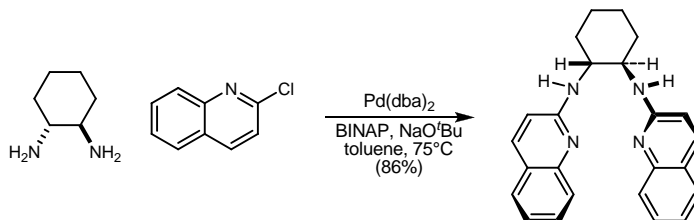
H,Quin-BAM (115e). $Pd(dba)_2$ (800.0 mg, 880.0 μmol), BINAP (1.1 g, 1.76 mmol), and NaO^tBu (14.3 g, 148.9 mmol) were loaded into a round bottom flask in a glove box. Toluene (250 mL, 0.18M) was added to the mixture followed by the 1,2-(*R,R*)-*trans*-diaminocyclohexane (5.0 g, 43.8 mmol). 2-Chloroquinoline (14.3 g, 87.6 mmol) was added as a solution in toluene. The reaction was allowed to stir at 80 °C and monitored by TLC. The reaction was then cooled to room temperature, concentrated, and purified by flash column chromatography on silica gel (5% Et_2O in hexanes) affording **115e** as a white solid (13.9 g, 86%); $[\alpha]_D^{25}$ +686.2 (*c* 1.0, $CHCl_3$); mp 156-158 °C; R_f=0.13 (20% EtOAc/hexanes); IR (neat) 3410, 3297, 2931, 1618, 1524, 1486, 1421, 1401, 817, 755 cm^{-1}; ^1H NMR (400 MHz, $CDCl_3$) δ 7.68 (d, *J* = 8.2 Hz, 1H), 7.55 (d, *J* = 8.9 Hz, 1H), 7.47-7.51 (m, 2H), 7.14 (dd, *J* = 7.0, 7.9 Hz, 1H), 6.28 (d, *J* = 8.9 Hz, 1H), 5.86 (s, 1H), 4.12 (s, 1H), 2.37 (d, *J* = 12.5 Hz, 1H), 1.81-1.83 (m, 1H), 1.40-1.52 (m, 2H); ^{13}C NMR (100 MHz, $CDCl_3$) δ 169.9, 157.3, 136.9, 129.6, 127.6, 126.1, 123.5, 121.9, 113.2, 56.3, 33.1, 25.1; HRMS (CI, CH_4) Exact mass calculated for $C_{24}H_{24}N_4$ $[M]^+$ 368.2001, found 368.1992.
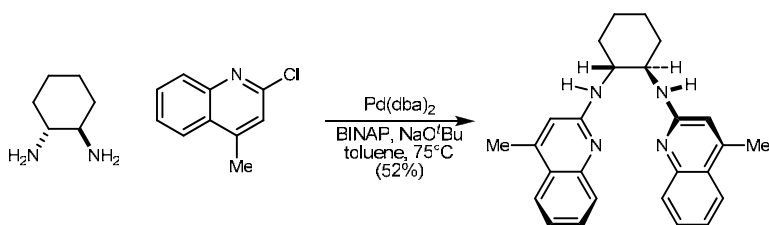
H,Lep-BAM (**115f**). Pd(dba)$_2$ (165.0 mg, 320.0 μmol), BINAP (39.9 mg, 640.0 μmol), and NaO^{t}Bu (3.69 g, 38.4 mmol) were combined in a round-bottomed flask in a glove box. Toluene (250 mL, 0.05 M) was added to the mixture, followed by 1,2-(R,R)-*trans*-diaminocyclohexane (1.46 g, 12.8 mmol) and 2-chlorolepidine (4.54 g, 25.6 mmol) as a solution in toluene. The reaction was allowed to stir at 85 °C and monitored by TLC. The reaction was then cooled to room temperature, concentrated, and purified by flash chromatography (SiO$_2$, 15% ether in hexanes) to afford the desired diamine as a white solid (3.90 g, 77%); [α]$_D^{25}$ +706.6 (*c* 1.0, CHCl$_3$); mp = 168-170 °C; R$_f$ = 0.19 (40% EtOAc/hexanes); IR (film) 3252, 3058, 2931, 2855, 1622, 1538, 1505, 1447, 1416 cm^{-1}; ^{1}H NMR (400 MHz, CDCl$_3$) δ 7.74-7.68 (m, 2H), 7.53 (dd, *J* = 14.0, 8.0 Hz, 1H), 7.21 (dd, *J* = 8.0, 7.2 Hz, 1H), 6.13 (s, 1H), 5.73 (s, 1H), 4.14 (s, 1H), 2.35 (s, 3H), 1.85 (d, *J* = 7.6 Hz, 2H), 1.59-1.32 (m, 2H); ^{13}C NMR (100 MHz, CDCl$_3$) ppm 157.3, 148.2, 144.2, 129.3, 126.5, 123.9, 123.7, 121.6, 113.4, 56.3, 33.2, 25.3, 18.6; HRMS (EI): Exact mass calcd for C$_{26}$H$_{28}$N$_4$ [M+H]$^+$ 396.2308. Found 396.2310.

H,^{6}OMe-BAM (**115h**). Pd(dba)$_2$ (14.4 mg, 25.0 μmol), DPPF (27.7 mg, 50.0 μmol), and NaO^{t}Bu (288.3 mg, 3.0 mmol) were loaded into a round bottom flask in a glove box. Toluene (10 mL, 0.10M) was added to the mixture followed by the 1,2-(R,R)-*trans*-diaminocyclohexane (114.2 mg, 1.0 mmol). 2-Bromo,6-methoxy-pyridine (376.0 mg, 2.0 mmol) was added as a solution in toluene. The reaction was allowed to stir at 80 °C and monitored by TLC. The reaction was then cooled to room temperature, concentrated, and purified by flash column chromatography on silica gel (5% Et$_2$O in hexanes) affording **115h** as a white solid (215 mg, 65%); Mp 70-72 °C; R$_f$ = 0.33 (25% Et$_2$O/hexanes). IR (film) 3389, 3325, 3051, 3002, 2936, 2855, 1615, 1505, 1456, 1425, 1405, 1332, 1248,

1147, 1059 cm^{-1}; ^{1}H NMR (400 MHz, CDCl$_3$) δ 7.25 (dd, J = 7.9, 7.9 Hz, 1H), 5.97 (d, J = 7.7 Hz, 1H), 5.84 (d, J = 7.9 Hz, 1H), 5.11 (d, J = 4.0 Hz, 1H), 3.91 (s, 3H), 3.70-3.66 (m, 1H), 2.30 (d, J = 13.0 Hz, 1H), 1.81-1.79 (m, 1H), 1.44-1.30 (m, 2H); ^{13}C NMR (100 MHz, CDCl$_3$) δ 163.8, 158.0, 140.0, 99.2, 96.6, 56.5, 53.4, 33.4, 25.2; HRMS (CI, CH$_4$) Exact mass calculated for C$_{18}$H$_{24}$N$_4$O$_2$ [M]$^+$ 329.1972, found 329.1973.
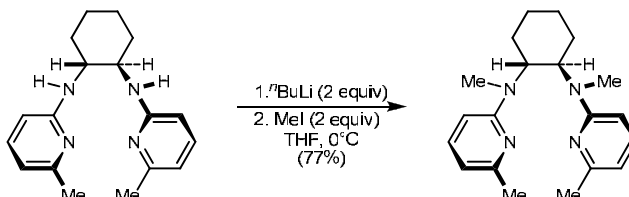
Me,^{6}Me-BAM (115k). To a solution of H,^{6}Me-BAM (250.0 mg, 843.0 μmol) in THF (10 mL, 0.08M) was added *n*-butyl lithium (697.0 μL, 2.42M in hexanes, 1.7 mmol) via syringe at 0 °C. Methyl iodide (105.0 μL, 1.7 mmol) was added and the reaction was warmed to room temperature. The reaction was allowed to stir at room temperature and monitored by TLC. The reaction was then quenched with water, the organic phase separated and the aqueous phase back-extracted with EtOAc. The combined organic phases were dried over MgSO$_4$, filtered, and concentrated. Purification by flash column chromatography on silica gel (5% Et$_2$O in hexanes) afforded **115k** as a white solid (210 mg, 77%); R$_f$ = 0.70 (20% EtOAc/hexanes). IR (film) 2927, 2851, 1589, 1481, 1428, 1314, 772 cm^{-1}; ^{1}H NMR (400 MHz, CDCl$_3$) δ 7.21 (dd, J = 8.5, 7.3 Hz, 1H), 6.30 (d, J = 7.0 Hz, 1H), 6.04 (d, J = 8.5 Hz, 1H), 4.98-4.96 (m, 1H), 2.62 (s, 3H), 2.35 (s, 3H), 1.81-1.75 (m, 2H), 1.61-1.41 (m, 2H); ^{13}C NMR (100 MHz, CDCl$_3$) ppm 158.6, 156.3, 137.4, 110.3, 102.4, 54.7, 30.3, 30.0, 25.9, 25.0; HRMS (EI): Exact mass calcd for C$_{20}$H$_{28}$N$_4$ [M]$^+$ 324.2314, found 324.2286.
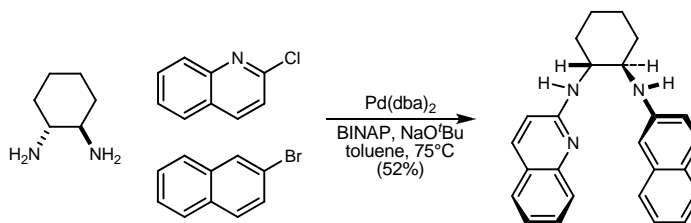
H,Quin(^{2}Nap)-BAM (115o). Pd(dba)$_2$ (14.4 mg, 25.0 μmol), BINAP (31.1 mg, 50.0 μmol), and NaO^{t}Bu (336.4 mg, 3.5 mmol) were loaded into a round bottom flask in a glove box. Toluene (20 mL, 0.05M) was added to the mixture followed by the 1,2-(R,R)-

trans-diaminocyclohexane (114.2 mg, 1.0 mmol). 2-Chloroquinoline (163.6 mg, 1.0 mmol) was added as a solution in toluene and monitored by TLC. 2-Bromonaphthalene (207.1 mg, 1.0 mmol) was added as a solution in toluene. The reaction was allowed to stir at 80 °C and monitored by TLC. The reaction was then cooled to room temperature, concentrated, and purified by flash column chromatography on silica gel (20% EtOAc in hexanes) affording **115o** as a white solid (190 mg, 52%). $[\alpha]_D^{25}$ +698.4 (*c* 1.0, CHCl$_3$); Mp 124-126 °C; IR (film) 3406, 3280, 3051, 2932, 2848, 1627, 1524, 1486, 1401 cm^{-1} ^{1}H NMR (400 MHz, CDCl$_3$) δ 7.85 (d, *J* = 8.2 Hz, 1H), 7.72 (d, *J* = 8.8 Hz, 1H), 7.65-7.54 (m, 4H), 7.44 (d, *J* = 8.8 Hz, 1H), 7.34-7.27 (m, 2H), 7.13 (dd, *J* = 7.7, 7.1 Hz, 1H), 6.68 (bs, 1H), 6.59 (d, *J* = 8.8 Hz, 1H), 6.47 (d, *J* = 9.0 Hz, 1H), 6.09 (bs, 1H), 4.55 (d, *J* = 7.0 Hz, 1H), 4.36-4.31 (m 1H), 3.30-3.28 (m, 1H), 2.52 (d, *J* = 12.3 Hz, 1H), 2.22 (d, *J* = 9.2 Hz, 1H), 1.88 (bs, 1H), 1.56-1.38 (m, 4H); ^{13}C NMR (100 MHz, CDCl$_3$) δ 157.4, 147.8, 146.3, 137.4, 135.6, 130.0, 129.0, 127.8 (2C), 127.1, 126.3, 126.2, 125.8, 123.8, 122.5, 121.5, 118.6, 112.9, 103.0, 61.1, 54.1, 33.9, 32.6, 25.6, 24.7. HRMS (CI): Exact mass calcd for C$_{25}$H$_{25}$N$_3$ [M]$^+$ 368.2127, found 368.2123.
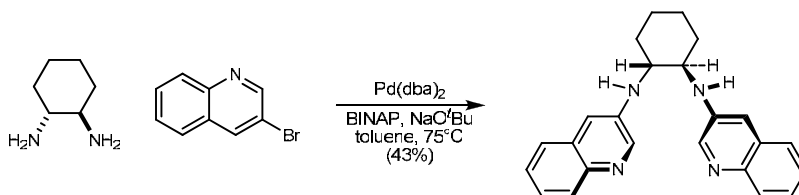
H,^{3}Quin-BAM (115p). Pd(dba)$_2$ (14.4 mg, 25.0 μmol), BINAP (31.1 mg, 50.0 μmol), and NaO^{t}Bu (288.3 mg, 3.0 mmol) were loaded into a round bottom flask in a glove box. Toluene (10 mL, 0.10M) was added to the mixture followed by the 1,2-(*R,R*)-*trans*-diaminocyclohexane (114.2 mg, 1.0 mmol). 3-Bromoquinoline (268.8 μL, 2.0 mmol) was added and the reaction was allowed to stir at 80 °C and monitored by TLC. The reaction was then cooled to room temperature, concentrated, and purified by flash column chromatography on silica gel (25% EtOAc in hexanes) affording **115p** as a white solid (158 mg, 43%); Mp 128-130 °C; R$_f$ = 0.15 (50% EtOAc/hexanes). IR (film) 3259, 3048, 2935, 2851, 1608, 1538, 1487, 1392, 1221 cm^{-1}; ^{1}H NMR (400 MHz, CDCl$_3$) δ 8.46 (s, 1H), 7.89 (d, *J* = 7.1 Hz, 1H), 7.43-7.38 (m, 3H), 6.61 (s, 1H), 4.99 (s, 1H), 3.15 (s, 1H), 2.35 (d, *J* = 12.8 Hz, 1H), 1.82 (d, *J* = 6.8 Hz, 1H), 1.43 (dd, *J* = 9.5, 9.3 Hz, 1H), 1.28-

1.24 (m, 1H); ^{13}C NMR (100 MHz, CDCl$_3$) ppm 143.9, 141.9, 141.2, 129.8, 129.0, 127.0, 126.3, 124.9, 109.7, 56.4, 31.8, 24.8.
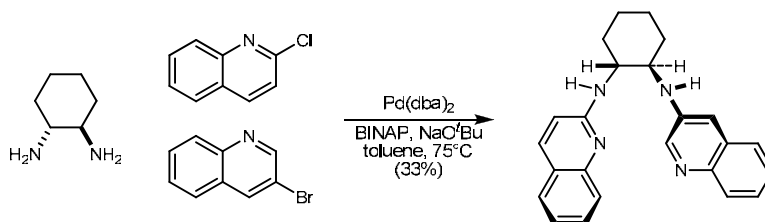
H,^{2}Quin(^{3}Quin)--BAM (115q). Pd(dba)$_2$ (14.4 mg, 25.0 μmol), BINAP (31.1 mg, 50.0 μmol), and NaO^{t}Bu (288.3 mg, 3.0 mmol) were loaded into a round bottom flask in a glove box. Toluene (10 mL, 0.10M) was added to the mixture followed by the 1,2-(*R,R*)-*trans*-diaminocyclohexane (114.2 mg, 1.0 mmol). 2-Chloroquinoline (163.6 mg, 1.0 mmol) was added as a solution in toluene and monitored by TLC. 3-Bromoquinoline (134.4 μL, 1.0 mmol) was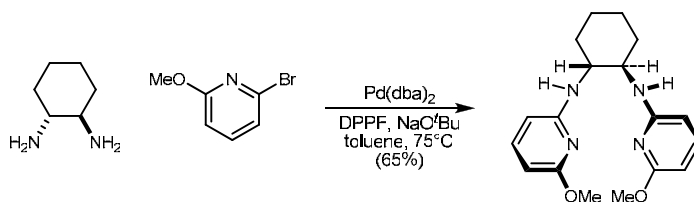 added and the reaction was allowed to stir at 80 °C and monitored by TLC. The reaction was then cooled to room temperature, concentrated, and purified by flash column chromatography on silica gel (25% EtOAc in hexanes) affording **115q** as a white solid (120mg, 33%); Mp 98-100 °C; R$_f$ = 0.13 (50% EtOAc/hexanes). IR (film) 3410, 3255, 3048, 2932, 2855, 1609, 1522, 1484, 1420, 1401 cm^{-1}; ^{1}H NMR (400 MHz, CDCl$_3$) δ 8.08 (d, *J* = 2.7 Hz, 1H), 7.83 (dd, *J* = 8.2, 4.8 Hz, 1H), 7.80 (s, 1H), 7.72 (d, *J* = 8.8 Hz, 1H), 7.63-7.58 (m, 2H), 7.52 (dd, *J* = 8.1, 8.1 Hz, 1H), 7.35 (ddd, *J* = 6.8, 6.8, 1.1 Hz, 1H), 7.31-7.25 (m, 2H), 6.95 (bs, 1H), 6.83 (d, *J* = 2.6 Hz, 1H), 6.49 (d, *J* = 8.8 Hz, 1H), 4.60 (d, *J* = 6.8 Hz, 1H), 4.37-4.30 (m 1H), 3.22-3.17 (m, 1H), 2.46 (m, 1H), 2.18 (d, *J* = 10.4 Hz, 1H), 1.91-1.87 (m, 2H), 1.79 (bs, 1H), 1.55-1.50 (m, 4H); ^{13}C NMR (100 MHz, CDCl$_3$) ppm 157.3, 147.4, 144.2, 142.1, 141.5, 137.7, 130.3, 130.0, 129.1, 127.8, 126.8, 126.0, 125.7, 124.1, 123.8, 122.8, 112.7, 108.1, 61.8, 54.0, 33.7, 32.2, 25.5, 24.5.
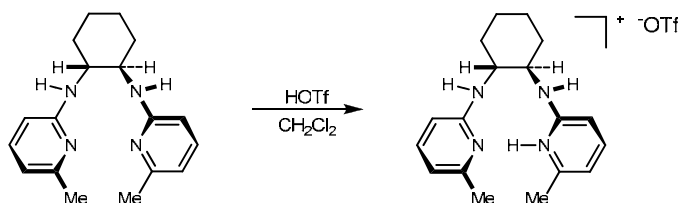
H,6-Me-BAM·HOTf (118c). To a solution of BAM in CH$_2$Cl$_2$ was added freshly distilled trifluoromethanesulfonic acid via syringe at room temperature. The reaction was allowed to stir for 20-30 minutes and was concentrated to afford **118c** as a white solid.

$[\alpha]_D^{25}$ -103.0 (*c* 1.0, CHCl$_3$); mp 142-144°C; IR (neat) 3290, 3122, 2938, 2862, 1652, 1602, 1516, 1464, 1283, 1243, 1225, 1163, 1029, 782 cm^{-1}; ^{1}H NMR (400 MHz, CDCl$_3$) δ 10.75 (bs, 1H), 7.53 (dd, *J* = 7.9, 7.9 Hz, 1H), 6.68-6.80 (m, 2H), 6.42 (d, *J* = 7.3 Hz, 1H), 3.67 (m, 1H), 2.38 (s, 3H), 2.08 (d, *J* = 13.1 Hz, 1H), 1.79 (d, *J* = 6.1 Hz, 1H), 1.42-1.50 (m, 2H); ^{13}C NMR (100 MHz, CDCl$_3$) δ156.6, 153.3, 139.9, 111.8, 106.1, 55.6, 31.7, 24.1, 22.8; ^{19}F NMR (376 MHz, CDCl$_3$) δ −79.09; HRMS (FAB) Exact mass calculated for C$_{19}$H$_{25}$F$_3$N$_4$O$_3$S [M]$^+$ 297.2079, found 297.2072.
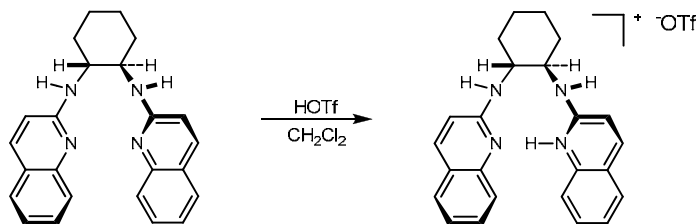
H,Quin-BAM·HOTf (118e). To a solution of BAM in CH$_2$Cl$_2$ was added freshly distilled trifluoromethanesulfonic acid via syringe at room temperature. The reaction was allowed to stir for 20-30 minutes and was concentrated to afford **118e** as a white solid; $[\alpha]_D^{25}$ +450.7 (*c* 1.0, CHCl$_3$); mp 134-136°C; IR (neat) 3276, 3164, 3069, 2942, 2866, 1661, 1652, 1616, 1532 cm^{-1}; ^{1}H NMR (400 MHz, CDCl$_3$) δ 8.03 (bs, 1H), 7.81 (m, 2H), 7.61 (dd, *J* = 7.0, 8.2 Hz, 1H), 7.55 (d, *J* = 7.9 Hz, 1H), 7.31 (dd, *J* = 7.6, 7.6 Hz, 1H), 6.82 (bs, 1H), 4.19 (m, 1H), 2.18 (d, *J* = 13.4 Hz, 1H), 1.86 (d, *J* = 8.5 Hz, 1H) 1.72 (d, *J* = 9.8 Hz, 1H) 1.50-1.58 (m, 1H); ^{13}C NMR (100 MHz, CDCl$_3$) δ 154.2, 141.4, 132.4, 128.7, 124.9, 122.0, 120.6, 118.8, 113.2, 56.7, 31.8, 24.1; ^{19}F NMR (376 MHz, CDCl$_3$) δ −78.67; HRMS (FAB) Exact mass calculated for C$_{25}$H$_{25}$F$_3$N$_4$O$_3$S [M]$^+$ 369.2079, found 369.2079.
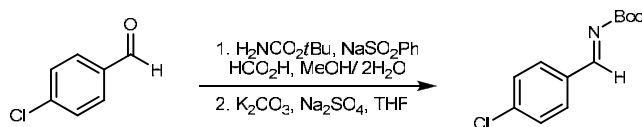
(*E*)-*tert*-butyl 4-chlorobenzylidenecarbamate (167f). Following the Greene protocol, the Schiff base was obtained as a white solid; Mp = 60-62 °C; IR (film) 2976, 1715, 1268, 1154 cm^{-1}; ^{1}H NMR (400 MHz, CDCl$_3$) δ 8.85 (s, 1H), 7.87 (d, *J* = 8.5 Hz, 2H), 7.47 (d, *J* = 8.5 Hz, 2H) 1.61 (s, 9H); ^{13}C NMR (100 MHz, CDCl$_3$) ppm 168.5, 162.6,

140.1, 132.8, 131.5, 129.5, 82.8, 28.2; HRMS (CI): Exact mass calcd for $C_{12}H_{14}NO_2Cl$ [M]$^+$, 239.0713, found 239.0706.
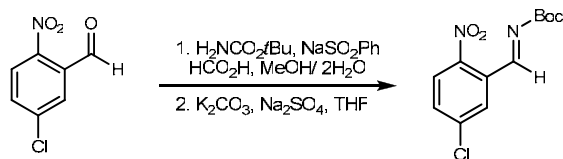
(*E*)-*tert*-butyl 5-chloro-2-nitrobenzylidenecarbamate (167i). Following the Greene protocol, the Schiff base was obtained as a white solid; IR (film) 2976, 1702, 1571, 1527, 1369, 1337, 1179, 841 cm^{-1}; ^{1}H NMR (400 MHz, CDCl$_3$) δ 9.42 (s, 1H), 8.40 (d, *J* = 2.1 Hz, 1H), 8.29 (d, *J* = 8.8 Hz, 1H) 7.85 (dd, *J* = 8.7, 2.3 Hz, 1H) 1.80 (s, 9H); HRMS (CI): Exact mass calcd for $C_{12}H_{14}ClN_2O_4$ [M+H]$^+$, 285.0642, found 285.0635.
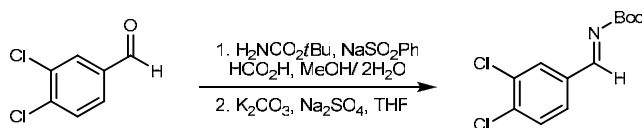
(*E*)-*tert*-butyl 3,4-dichlorobenzylidenecarbamate (167j). Following the Greene protocol, the Schiff base was obtained as a white solid; IR (film) 2982, 1680, 1397, 1364, 1190 cm^{-1}; ^{1}H NMR (400 MHz, CDCl$_3$) δ 8.79 (s, 1H), 8.06 (d, *J* = 1.7 Hz, 1H), 7.74 (dd, *J* = 8.2, 1.7 Hz, 1H) 7.58 (d, *J* = 8.2, 1H) 1.61 (s, 9H); HRMS (CI): Exact mass calcd for $C_{12}H_{14}NO_2Cl_2$ [M+H]$^+$, 274.0402, found 274.0397.
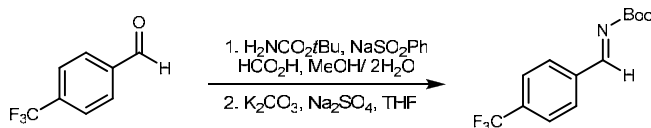
(*E*)-*tert*-butyl 4-(trifluoromethyl)benzylidenecarbamate (167l). Following the Greene protocol, the Schiff base was obtained as a white solid; IR (film) 3325, 2982, 1696, 1500, 1326, 1168 cm^{-1}; ^{1}H NMR (400 MHz, CDCl$_3$) δ 8.88 (s, 1H), 8.04 (d, *J* = 8.2 Hz, 2H), 7.75 (d, *J* = 8.2 Hz, 2H) 1.62 (s, 9H); ^{13}C NMR (100 MHz, CDCl$_3$) ppm 167.7, 162.4, 137.4, 134.8, 130.4, 126.9, 126.1, 83.1, 28.1; HRMS (CI): Exact mass calcd for $C_{13}H_{15}F_3NO_2$ [M+H]$^+$, 274.1055, found 274.1060.
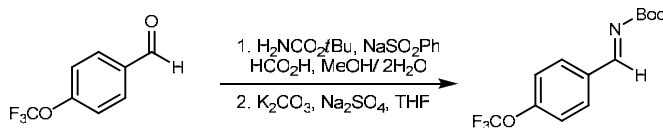
 (*E*)-*tert*-butyl 4-(trifluoromethoxy)benzylidenecarbamate (167n). Following the Greene protocol, the Schiff base was obtained as a clear oil; IR (film) 3330, 2982, 1701,

1507, 1369, 1263, 1223, 1164, 1015 cm^{-1}; ^{1}H NMR (400 MHz, CDCl$_3$) δ 8.86 (s, 1H), 7.98 (d, J = 8.5 Hz, 2H), 7.32 (d, J = 8.3 Hz, 2H) 1.61 (s, 9H); ^{13}C NMR (100 MHz, CDCl$_3$) ppm 167.9, 162.5, 153.1, 132.7, 132.0, 128.0, 121.0, 82.8, 28.1; HRMS (CI): Exact mass calcd for C$_{13}$H$_{15}$F$_3$NO$_3$ [M+H]$^+$, 290.1004, found 290.1007.
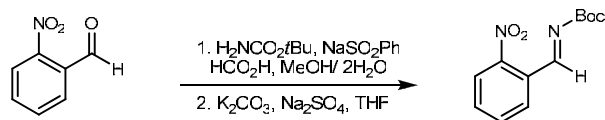
(E)-tert-butyl 2-nitrobenzylidenecarbamate (167p). Following the Greene protocol, the Schiff base was obtained as a yellow oil; IR (film) 2981, 1721, 1635, 1530, 1369, 1347, 1253, 1155 cm^{-1}; ^{1}H NMR (400 MHz, CDCl$_3$) δ 9.21 (s, 1H), 8.17 (d, J = 7.0 Hz, 1H), 8.07 (dd, J = 7.6, 0.9 Hz, 1H) 7.71-7.67 (m, 2H) 1.57 (s, 9H); ^{13}C NMR (100 MHz, CDCl$_3$) ppm 164.4, 161.8, 150.1, 133.9, 133.2, 130.0, 129.4, 124.9, 83.3, 28.1; HRMS (CI): Exact mass calcd for C$_{12}$H$_{15}$N$_2$O$_4$ [M+H]$^+$, 251.1032, found 251.1033.
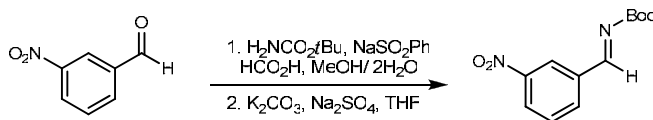
(E)-tert-butyl 3-nitrobenzylidenecarbamate (167q). Following the Greene protocol, the Schiff base was obtained as a yellow oil; IR (film) 3083, 2978, 2928, 1717, 1533, 1352, 1255, 1155 cm^{-1}; ^{1}H NMR (400 MHz, CDCl$_3$) δ 8.89 (s, 1H), 8.76 (s, 1H), 8.41 (d, J = 6.7 Hz, 1H) 8.25 (d, J = 7.7 Hz, 1H) 7.70 (dd, J = 7.9 Hz, 1H) 1.61 (s, 9H); ^{13}C NMR (100 MHz, CDCl$_3$) ppm 166.5, 162.0, 148.9, 136.0, 135.4, 130.3, 127.7, 124.8, 83.4, 28.1; HRMS (CI): Exact mass calcd for C$_{12}$H$_{14}$N$_2$O$_4$ [M+H]$^+$, 251.1032, found 251.1026.
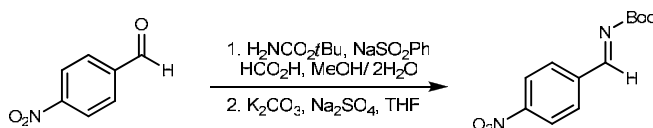
(E)-tert-butyl 4-nitrobenzylidenecarbamate (167r). Following the Greene protocol, the Schiff base was obtained as a yellow solid; Mp = 102-105 °C; IR (film) 2976, 1707, 1522, 1348, 1157, 852 cm^{-1}; ^{1}H NMR (400 MHz, CDCl$_3$) δ 8.89 (s, 1H), 8.34 (d, J = 8.7 Hz, 2H), 8.10 (d, J = 8.9 Hz, 2H) 1.62 (s, 9H); ^{13}C NMR (100 MHz, CDCl$_3$) ppm 166.5, 162.0, 139.6, 130.9, 124.3, 123.7, 83.5, 28.3; HRMS (CI): Exact mass calcd for C$_{12}$H$_{15}$N$_2$O$_4$ [M+H]$^+$, 251.1032, found 251.1037.

H,Quin-BAM•HOTf
CH$_3$NO$_2$, -20 °C
(60%)
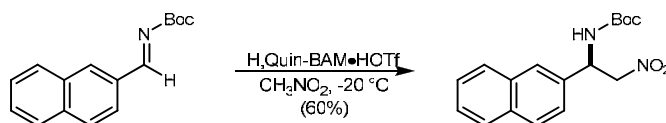
(1-Naphthalen-2-yl-2-nitro-ethyl)-carbamic acid tert-butyl ester (168c). A solution of imine (25.0 mg, 100.0 μmol) and H,Quin-BAM•TfOH (5.2 mg, 10.0 μmol) in nitromethane (0.4 mL, 0.25M) was stirred at -20 °C. The solution was concentrated and purified by flash chromatography (Al$_2$O$_3$, 25% ethyl acetate in hexanes) to furnish the product as a white solid (19.0 mg, 60 %) and was determined to be *42% ee* by chiral HPLC analysis (Chiralcel® AD, 90:10 hexanes:*i*-PrOH, 1 mL/min, t_r(major) = 15.0 min, t_r(minor) = 18.1 min); Mp = 128-130 °C; R$_f$ = 0.55 (50% EtOAc/hexanes); IR (film) 3358, 3059, 2976, 2930, 1695, 1556, 1509, 1368, 1166 cm^{-1}; ^{1}H NMR (400 MHz, CDCl$_3$) δ 8.08-7.97 (m, 4H), 7.73-7.70 (m, 2H), 7.60 (dd, *J* = 8.4, 1.5 Hz, 1H), 5.76-5.72 (m, 1H), 5.61 (d, *J* = 7.3 Hz, 1H), 5.13-4.97 (m, 2H), 1.66 (s, 9H); ^{13}C NMR (100 MHz, CDCl$_3$) ppm 155.2, 134.6, 133.7, 133.6, 129.7, 128.5, 128.2, 127.2, 127.1, 126.0, 124.2, 79.3, 67.3, 53.8, 28.7; HRMS (EI): Exact mass calcd for C$_{17}$H$_{21}$N$_2$O$_4$ [M]$^+$, 317.1501, found 317.1511.

H,Quin-BAM•HOTf
CH$_3$NO$_2$, -20 °C
(73%)
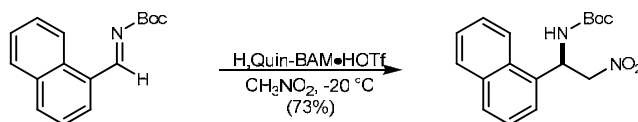
(1-Naphthalen-1-yl-2-nitro-ethyl)-carbamic acid tert-butyl ester (168d). A solution of imine (25.0 mg, 100.0 μmol) and H,Quin-BAM•TfOH (5.2 mg, 10.0 μmol) in nitromethane (0.4 mL, 0.25M) was stirred at -20 °C. The solution was concentrated and purified by flash chromatography (Al$_2$O$_3$, 25% ethyl acetate in hexanes) to furnish the product as a white solid (23.1 mg, 73 %) and was determined to be *64% ee* by chiral HPLC analysis ([α]$_D^{25}$ -4.0 (*c* 1.0, CHCl$_3$) Chiralcel® AD, 90:10 hexanes:*i*-PrOH, 1 mL/min, t_r(major) = 13.7 min, t_r(minor) = 19.7 min); Mp = 158-160 °C; R$_f$ = 0.44 (50% EtOAc/hexanes); IR (film) 3357, 2980, 2360, 2342, 1685, 1542, 1526, 1167, 775 cm^{-1}; ^{1}H NMR (400 MHz, CDCl$_3$) δ 8.10 (d, *J* = 8.2 Hz, 1H), 7.88 (d, *J* = 7.9 Hz, 1H), 7.84-7.82 (m, 1H), 7.59 (ddd, *J* = 8.2, 7.0, 1.5 Hz, 1H), 7.52 (dd, *J* = 7.0, 7.0 Hz, 1H), 7.42-7.46 (m, 2H), 6.25 (d, *J* = 6.4 Hz, 1H), 5.30 (d, *J* = 7.0 Hz, 1H), 4.87 (bm, 2H), 1.41 (s, 9H); ^{13}C NMR (100 MHz, CDCl$_3$) ppm 154.9, 134.3, 132.8, 130.5, 129.7, 129.5, 127.5,

126.5, 125.4, 123.4, 122.4, 81.0, 78.5, 49.5, 28.4; HRMS (EI): Exact mass calcd for $C_{17}H_{20}N_2O_4$ [M]$^+$, 316.1423, found 316.1411.
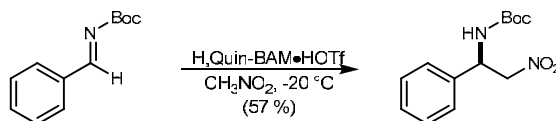
tert-butyl (*R*)-2-nitro-1-phenylethylcarbamate (168e). A solution of imine (100.0 mg, 487.0 μmol) and H,Quin-BAM•TfOH (25.3 mg, 48.7 μmol) in CH_3NO_2 (0.4 mL, 0.25M) was stirred at -20 °C. The solution was concentrated and purified by flash chromatography (Al_2O_3, 20% ethyl acetate in hexanes) to furnish the product as a white solid (74.0 mg, 57 %) which was determined to be 60% ee by chiral HPLC analysis (Chiralcel® AD, 95:5 hexanes:*i*-PrOH, 1 mL / min, t_r(major) = 24.9 min, t_r(minor) = 23.3 min); Mp = 116-118 °C; R_f = 0.33 (30% EtOAc/hexanes); IR (film) 3331, 2984, 1682, 1553 cm^{-1}; ^{1}H NMR (400 MHz, CDCl$_3$) δ 7.30-7.40 (m, 5H), 5.37 (m, 1H), 5.29 (bs, 1H), 4.85 (m, 1H), 4.71 (dd, *J* = 12.4, 5.2 Hz, 1H), 1.44 (s, 1H); ^{13}C NMR (100 MHz, CDCl$_3$) ppm 154.9, 137.0, 129.4, 128.9, 126.5, 80.9, 79.1, 53.0, 28.4; HRMS (EI): Exact mass calcd for $C_{13}H_{19}N_2O_4$ [M+H]$^+$, 267.1345, found 267.1343.
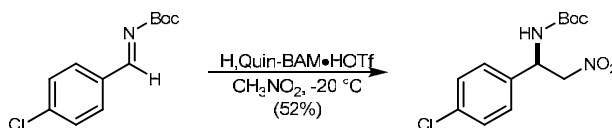
tert-butyl (*R*)-1-(4-chlorophenyl)-2-nitroethylcarbamate (168f). A solution of imine (100.0 mg, 417.0 μmol) and H,Quin-BAM•TfOH (21.6 mg, 41.7 μmol) in CH_3NO_2 (0.4 mL, 0.25M) was stirred at -20 °C. The solution was concentrated and purified by flash chromatography (Al_2O_3, 20% ethyl acetate in hexanes) to furnish the product as a white solid (65.4 mg, 52 %) which was determined to be 79% ee by chiral HPLC analysis (Chiralcel® AD, 90:10 hexanes:*i*-PrOH, 1 mL / min, t_r(major) = 14.9 min, t_r(minor) = 11.8 min); Mp = 128-130 °C; R_f = 0.33 (30% EtOAc/hexanes); IR (film) 3330, 2977, 2926, 1680, 1553 cm^{-1}; ^{1}H NMR (400 MHz, CDCl$_3$) δ 7.36 (d, *J* = 8.2 Hz, 2H), 7.25 (d, *J* = 8.2 Hz, 2H), 5.33 (m, 2H), 4.83 (m, 1H), 4.69 (dd, *J* = 12.5, 4.3 Hz, 1H), 1.44 (s, 1H); ^{13}C NMR (100 MHz, CDCl$_3$) ppm 154.9, 135.7, 134.8, 129.6, 127.9, 81.1, 78.9, 52.4, 28.4; HRMS (EI): Exact mass calcd for $C_{13}H_{17}ClN_2O_4$ [M+H]$^+$, 301.0955, found 301.0956.
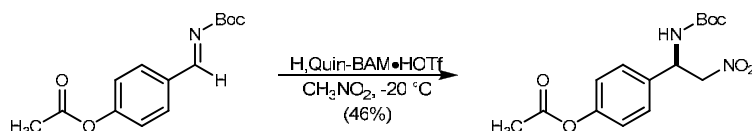
Acetic acid 4-(1-tert-butoxycarbonylamino-2-nitro-ethyl)-phenyl ester (168g). A solution of imine (25.0 mg, 100.0 μmol) and H,Quin-BAM•TfOH (5.2 mg, 10.0 μmol) in nitromethane (0.4 mL, 0.25M) was stirred at -20 °C. The solution was concentrated and purified by flash chromatography (SiO$_2$ Al$_2$O$_3$, 25% ethyl acetate in hexanes) to furnish the product as a white solid (15.0 mg, 46 %) and was determined to be *65% ee* by chiral HPLC analysis ([α]$_D$ -10.0 (*c* 1.0, CHCl$_3$) Chiralcel® AD, 90:10 hexanes:*i*-PrOH, 1 mL/min, t_r(major) = 17.6 min, t_r(minor) = 21.7 min). R$_f$ = 0.36 (50% EtOAc/hexanes); IR (film) 3367, 2985, 1747, 1678, 1551, 1522, 1511, 1368, 1217, 1161 cm^{-1}; ^{1}H NMR (400 MHz, CDCl$_3$) δ 7.30 (d, *J* = 8.2 Hz, 2H), 7.09 (d, *J* = 8.2 Hz, 2H), 5.36 (d, *J* = 5.8 Hz, 1H), 5.22 (bm, 1H), 4.80 (bm, 1H), 4.67 (ddd, *J* = 12.5, 5.5, 5.5 Hz, 1H), 2.27 (s, 3H), 1.41 (s, 9H); ^{13}C NMR (100 MHz, CDCl$_3$) ppm 169.4, 151.0, 134.7, 127.8, 122.6, 122.5, 81.0, 78.9, 52.5, 28.5, 21.3; HRMS (CI): Exact mass calcd for C$_{15}$H$_{21}$N$_2$O$_6$ [M+H]$^+$, 325.1399, found 325.1388.
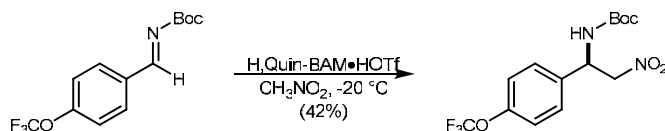
tert-butyl (*R*)-2-nitro-1-(4-(trifluoromethoxy)phenyl)ethylcarbamate (168h). A solution of imine (100.0 mg, 345.7 μmol) and H,Quin-BAM•TfOH (57.0 mg, 34.6 μmol) in CH$_3$NO$_2$ (0.4 mL, 0.25M) was stirred at -20 °C. The solution was concentrated and purified by flash chromatography (Al$_2$O$_3$, 40% ethyl acetate in hexanes) to furnish the product as a white solid (51.0 mg, 42 %) which was determined to be 67% ee by chiral HPLC analysis (Chiralcel® AD, 90:10 hexanes:*i*-PrOH, 1 mL / min, t_r(major) = 12.0 min, t_r(minor) = 9.0 min); Mp = 104-107 °C; R$_f$ = 0.25 (40% EtOAc/hexanes); IR (film) 3357, 2981, 2935, 1684, 1537, 1511, 1267, 1214, 1164 cm^{-1}; ^{19}F NMR (376 MHz, CDCl$_3$) δ -58.3; ^{1}H NMR (400 MHz, CDCl$_3$) δ 7.38 (d, *J* = 8.7 Hz, 2H), 7.24 (d, *J* = 8.5 Hz, 2H), 5.40-5.48 (m, 2H) 4.86 (m, 1H) 4.72 (dd, *J* = 12.5, 4.2 Hz, 1H) 1.45 (s, 9H); ^{13}C NMR (100 MHz, CDCl$_3$) ppm 154.9, 149.5, 135.9, 128.2, 121.8, 119.3, 81.2, 79.9, 52.4, 28.5; HRMS (CI): Exact mass calcd for C$_{14}$H$_{18}$F$_3$N$_2$O$_5$ [M+H]$^+$, 351.1168, found 351.1157.
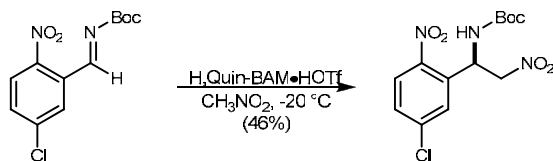
tert-butyl (R)-1-(5-chloro-2-nitrophenyl)-2-nitroethylcarbamate (168i). A solution of imine (28.5 mg, 100.0 μmol) and H,Quin-BAM•TfOH (5.2 mg, 10.0 μmol) in CH_3NO_2 (0.4 mL, 0.25M) was stirred at -20 °C. The solution was concentrated and purified by flash chromatography (Al_2O_3, 20% ethyl acetate in hexanes) to furnish the product as a white solid (16.0 mg, 46 %) which was determined to be 61% ee by chiral HPLC analysis (Chiralcel® OD, 90:10 hexanes:i-PrOH, 1 mL / min, t_r(major) = 13.8 min, t_r(minor) = 32.3 min); R_f = 0.14 (40% EtOAc/hexanes); IR (film) 3359, 2981, 1688, 1550, 1522, 1374, 1341, 1171 cm^{-1}; ^{1}H NMR (400 MHz, CDCl$_3$) δ 8.04 (d, J = 8.5 Hz, 1H), 7.54 (d, J = 2.1 Hz, 1H), 7.46 (dd, J = 2.1, 8.9 Hz, 1H) 5.85-5.91 (m, 2H) 4.86-4.92 (m, 2H) 1.40 (s, 9H); HRMS (CI): Exact mass calcd for $C_{13}H_{17}N_3O_6Cl$ [M+H]$^+$, 346.0806, found 346.0800.

tert-butyl (R)-1-(3,4-dichlorophenyl)-2-nitroethylcarbamate (168j). A solution of imine (100.0 mg, 364.8 μmol) and H,Quin-BAM•TfOH (18.9 mg, 36.5 μmol) in CH_3NO_2 (0.4mL, 0.25M) was stirred at -20 °C. The solution was concentrated and purified by flash chromatography (Al_2O_3, 20% ethyl acetate in hexanes) to furnish the product as a white solid (58.0 mg, 47 %) which was determined to be 76% ee by chiral HPLC analysis (Chiralcel® AD, 90:10 hexanes:i-PrOH, 1 mL / min, t_r(major) = 13.2 min, t_r(minor) = 9.4 min); Mp = 122-124 °C; R_f = 0.57 (40% EtOAc/hexanes); IR (film) 3346, 2978, 2928, 1689, 1549, 1520, 1170 cm^{-1}; ^{1}H NMR (400 MHz, CDCl$_3$) δ 7.43 (d, J = 8.2 Hz, 1H), 7.39 (d, J = 2.1 Hz, 1H), 7.13 (dd, J = 2.1, 8.2 Hz, 1H) 5.29-5.35 (m, 2H) 4.79 (m, 1H) 4.66 (dd, J = 12.8, 4.9 Hz, 1H) 1.41 (s, 9H); ^{13}C NMR (100 MHz, CDCl$_3$) ppm 154.8, 137.5, 133.7, 133.2, 131.4, 128.8, 125.9, 81.4, 78.6, 52.1, 28.5; HRMS (CI): Exact mass calcd for $C_{13}H_{17}N_2O_4Cl_2$ [M+H]$^+$, 335.0565, found 335.0574.

[1-(3,4-Difluoro-phenyl)-2-nitro-ethyl]-carbamic acid tert-butyl ester (168k). A solution of imine (25.0 mg, 100.0 μmol) and H,Quin-BAM•TfOH (5.2 mg, 10.0 μmol) in nitromethane (0.4 mL, 0.25M) was stirred at -20 °C. The solution was concentrated and purified by flash chromatography (Al$_2$O$_3$, 25% ethyl acetate in hexanes) to furnish the product as a white solid (24.2 mg, 80 %) and was determined to be 84% *ee* by chiral HPLC analysis ([α]$_D^{25}$ -9.4 (*c* 1.0, CHCl$_3$) Chiralcel® AD, 90:10 hexanes:*i*-PrOH, 1 mL/min, t_r(major) = 9.0 min, t_r(minor) = 12.5 min); Mp = 100-102 °C; R$_f$ = 0.47 (50% EtOAc/hexanes); IR (film) 3351, 2978, 2932, 1687, 1540, 1519, 1370, 1284, 1165 cm^{-1}; ^{1}H NMR (400 MHz, CDCl$_3$) δ 7.23-7.15 (m, 2H), 7.08-7.06 (m, 1H), 5.42 (d, *J* = 5.4 Hz, 1H), 4.83 (m, 1H), 4.70 (ddd, *J* = 12.8, 4.7, 4.7 Hz, 1H), 1.46 (s, 9H); ^{13}C NMR (100 MHz, CDCl$_3$) ppm 154.8, 151.7, 149.3, 134.3, 122.7, 118.3, 115.9, 81.4, 78.8, 52.1, 28.5; HRMS (CI): Exact mass calcd for C$_{13}$H$_{16}$F$_2$N$_2$O$_4$ [M+H]$^+$, 303.1156, found 303.1153.
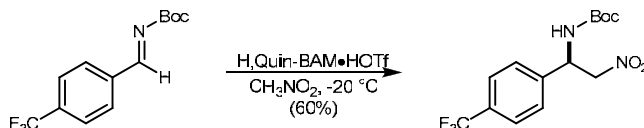
tert-butyl (*R*)-1-(4-(trifluoromethyl)phenyl)-2-nitroethylcarbamate (168l). A solution of imine (100.0 mg, 366.0 μmol) and H,Quin-BAM•TfOH (19.0 mg, 36.6 μmol) in CH$_3$NO$_2$ (0.4 mL, 0.25M) was stirred at -20 °C. The solution was concentrated and purified by flash chromatography (Al$_2$O$_3$, 40% ethyl acetate in hexanes) to furnish the product as a white solid (73 mg, 60 %) which was determined to be 78% ee by chiral HPLC analysis (Chiralcel® AD, 90:10 hexanes:*i*-PrOH, 1 mL / min, t_r(major) = 15.4 min, t_r(minor) = 10.3 min); Mp = 124-126 °C; R$_f$ = 0.25 (40% EtOAc/hexanes); IR (film) 3354, 2978, 1687, 1542, 1527, 1328, 1169, 1128, 1069 cm^{-1}; ^{19}F NMR (376 MHz, CDCl$_3$) δ -63.2; ^{1}H NMR (400 MHz, CDCl$_3$) δ 7.66 (d, *J* = 8.2 Hz, 2H), 7.47 (d, *J* = 8.2 Hz, 2H), 5.46-5.53 (m, 2H) 4.87 (m, 1H) 4.75 (d, *J* = 9.1 Hz, 1H) 1.45 (s, 9H); ^{13}C NMR (100 MHz, CDCl$_3$) ppm 154.9, 141.2, 131.2, 127.0, 126.4, 122.6, 81.3, 78.8, 52.6, 28.5; HRMS (CI): Exact mass calcd for C$_{14}$H$_{18}$F$_3$N$_2$O$_4$ [M+H]$^+$, 335.1219, found 335.1220.
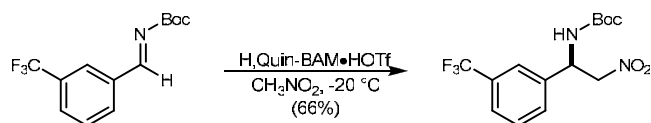
[2-Nitro-1-(3-trifluoromethyl-phenyl)-ethyl]-carbamic acid *tert*-butyl ester (168m).
A solution of imine (25.0 mg, 100.0 μmol) and H,Quin-BAM•TfOH (5.2 mg, 10.0 μmol)
in nitromethane (0.4 mL, 0.25M) was stirred at -20 °C. The solution was concentrated
and purified by flash chromatography (Al$_2$O$_3$, 25% ethyl acetate in hexanes) to furnish
the product as a white solid (22.0 mg, 66 %) and was determined to be 71*% ee* by chiral
HPLC analysis ([α]$_D^{25}$ -21.0 (*c* 1.0, CHCl$_3$) Chiralcel® AD, 90:10 hexanes:*i*-PrOH, 1
mL/min, t_r(major) = 6.8 min, t_r(minor) = 8.3 min). Mp = 90-92 °C; R$_f$ = 0.47 (50%
EtOAc/hexanes); IR (film) 3357, 2985, 2935, 1690, 1557, 1520, 1330, 1167, 1126 cm^{-1};
^{1}H NMR (400 MHz, CDCl$_3$) δ 7.63-7.59 (m, 2H), 7.54-7.53 (m, 2H), 5.47 (bm, 2H), 4.88
(bm, 1H), 4.76 (d, *J* = 12.9 Hz, 1H), 1.46 (s, 9H); ^{13}C NMR (100 MHz, CDCl$_3$) ppm
154.9, 138.4, 131.8, 130.0, 130.0, 125.8, 123.4, 81.4, 78.8, 52.7, 28.4; HRMS (CI): Exact
mass calcd for C$_{14}$H$_{18}$F$_3$N$_2$O$_4$ [M+H]$^+$, 335.1219, found 335.1202.
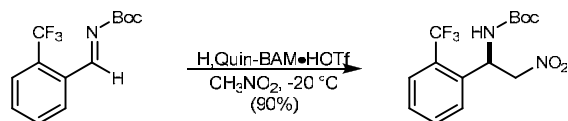
**[2-Nitro-1-(2-trifluoromethyl-phenyl)-ethyl]-carbamic acid tert-butyl ester (168n).** A
solution of imine (25.0 mg, 100.0 μmol) and H,Quin-BAM•TfOH (5.2 mg, 10.0 μmol) in
nitromethane (0.4 mL, 0.25M) was stirred at -20 °C. The solution was concentrated and
purified by flash chromatography (Al$_2$O$_3$, 25% ethyl acetate in hexanes) to furnish the
product as a white solid (30.0 mg, 90 %) and was determined to be 73*% ee* by chiral
HPLC analysis ([α]$_D^{25}$ -9.8 (*c* 1.0, CHCl$_3$) Chiralcel® AD, 90:10 hexanes:*i*-PrOH, 1
mL/min, t_r(major) = 9.2 min, t_r(minor) = 16.2 min); Mp = 97-99 °C; R$_f$ = 0.45 (50%
EtOAc/hexanes); IR (film) 3311, 2981, 2928, 1695, 1557, 1368, 1314, 1164, 1125, 1037
cm^{-1}; ^{1}H NMR (400 MHz, CDCl$_3$) δ 7.74 (d, *J* = 7.8 Hz, 1H), 7.63-7.54 (m, 2H), 7.48
(dd, *J* = 7.7, 7.4 Hz, 1H), 5.80 (ddd, *J* = 7.0, 6.3, 6.3 Hz, 1H), 5.58 (m, 1H), 4.75 (m, 2H),
1.41 (s, 9H); ^{13}C NMR (100 MHz, CDCl$_3$) ppm 154.6, 132.9, 129.0, 127.7, 127.0, 125.6,
122.9, 81.2, 79.0, 64.3, 49.8, 28.4; HRMS (CI): Exact mass calcd for C$_{14}$H$_{18}$F$_3$N$_2$O$_4$
[M+H]$^+$, 335.1219, found 335.1209.
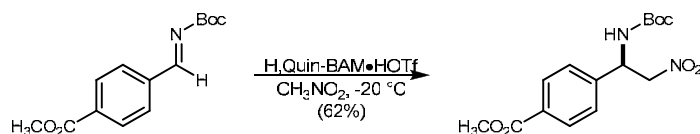
4-(1-tert-Butoxycarbonylamino-2-nitro-ethyl)-benzoic acid methyl ester (168o). A solution of imine (25.0 mg, 100.0 μmol) and H,Quin-BAM•TfOH (5.2 mg, 10.0 μmol) in nitromethane (0.4 mL, 0.25M) was stirred at -20 °C. The solution was concentrated and purified by flash chromatography (Al$_2$O$_3$, 25% ethyl acetate in hexanes) to furnish the product as a white solid (20.0 mg, 62 %) and was determined to be 80*% ee* by chiral HPLC analysis ([α]$_D^{25}$ -23.3 (*c* 1.0, CHCl$_3$) Chiralcel® AD, 90:10 hexanes:*i*-PrOH, 1 mL/min, *t*$_r$(major) = 19.8 min, *t*$_r$(minor) = 25.6 min). Mp = 166-168 °C; R$_f$ = 0.40 (50% EtOAc/hexanes); IR (film) 3364, 2978, 1717, 1684, 1553, 1522, 1281, 1168, 1110 cm^{-1}; ^{1}H NMR (400 MHz, CDCl$_3$) δ 8.03 (d, *J* = 8.5 Hz, 2H), 7.37(d, *J* = 8.2 Hz, 2H), 5.40 (bm, 2H), 4.83 (bm, 1H), 4.71 (d, *J* = 11.3 Hz, 1H), 3.89 (s, 3H), 1.41 (s, 9H); ^{13}C NMR (100 MHz, CDCl$_3$) ppm 166.6, 154.9, 142.0, 130.7, 130.6, 126.5, 81.1, 78.8, 52.7, 52.5, 28.4; HRMS (CI): Exact mass calcd for C$_{15}$H$_{21}$N$_2$O$_6$ [M+H]$^+$, 325.1400, found 325.1399.
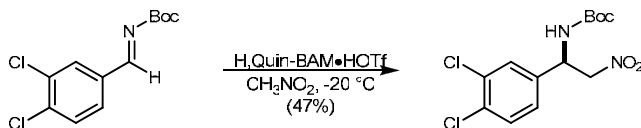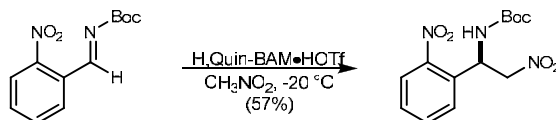

***tert*-butyl (*R*)-2-nitro-1-(2-nitrophenyl)ethylcarbamate (168p).** A solution of imine (100.0 mg, 400.0 μmol) and H,Quin-BAM•TfOH (20.7 mg, 40.0 μmol) in CH$_3$NO$_2$ (0.4 mL, 0.25M) was stirred at -20 °C. The solution was concentrated and purified by flash chromatography (Al$_2$O$_3$, 50% ethyl acetate in hexanes) to furnish the product as a white solid (71.0 mg, 57 %) which was determined to be 70% ee by chiral HPLC analysis (Chiralcel® OD, 90:10 hexanes:*i*-PrOH, 1 mL / min, *t*$_r$(major) = 16.4 min, *t*$_r$(minor) = 18.7 min); Mp = 158-160 °C; R$_f$ = 0.5 (80% EtOAc/hexanes); IR (film) 3367, 2974, 1684, 1550, 1521, 1275, 763 cm^{-1}; ^{1}H NMR (400 MHz, CDCl$_3$) δ 8.09 (d, *J* = 7.7 Hz, 1H), 7.69 (dd, *J* = 7.9, 7.3 Hz, 1H), 7.60 (d, *J* = 6.7 Hz, 1H), 7.54 (ddd, *J* = 7.1, 7.0, 1.3, 1H) 5.92 (m, 2H) 4.90-4.99 (m, 2H) 1.42 (s, 9H); ^{13}C NMR (100 MHz, CDCl$_3$) ppm 154.7, 148.2, 134.4, 133.1, 129.8, 129.6, 126.0, 81.2, 78.5, 50.2, 28.4; HRMS (CI): Exact mass calcd for C$_{13}$H$_{18}$N$_3$O$_6$ [M+H]$^+$, 312.1196, found 312.1186.
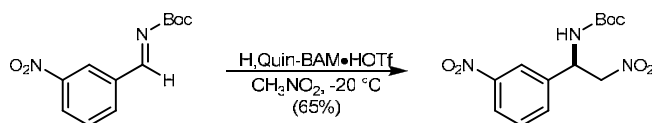
***tert*-butyl (*R*)-2-nitro-1-(3-nitrophenyl)ethylcarbamate (168q).** A solution of imine (25.0 mg, 100.0 μmol) and H,Quin-BAM•TfOH (5.2 mg, 10.0 μmol) in CH_3NO_2 (0.4 mL, 0.25M) was stirred at -20 °C. The solution was concentrated and purified by flash chromatography (Al_2O_3, 60% ethyl acetate in hexanes) to furnish the product as a white solid (20.1 mg, 65 %) which was determined to be 95% ee by chiral HPLC analysis (Chiralcel® AD, 90:10 hexanes:*i*-PrOH, 1 mL / min, t_r(major) = 19.0min, t_r(minor) = 13.1 min); Mp = 140-142 °C; R_f = 0.38 (80% EtOAc/hexanes); IR (film) 3356, 2978, 1681, 1551, 1524, 1351 cm^{-1}; ^{1}H NMR (400 MHz, CDCl$_3$) δ 8.21-8.23 (m, 2H), 7.70 (d, *J* = 7.8 Hz, 1H), 7.60 (dd, *J* = 7.9, 8.6 Hz, 1H), 5.61 (d, *J* = 7.5 Hz, 1H) 5.50 (d, *J* = 5.2 Hz, 1H) 4.92 (m, 1H) 4.80 (dd, *J* = 13.0, 4.3 Hz, 1H) 1.46 (s, 9H); ^{13}C NMR (100 MHz, CDCl$_3$) ppm 154.9, 148.9, 139.6, 132.7, 130.5, 123.9, 121.6, 81.6, 78.6, 52.3, 28.5; HRMS (CI): Exact mass calcd for $C_{13}H_{17}N_3O_6$ [M]$^+$, 311.1117, found 311.1118.
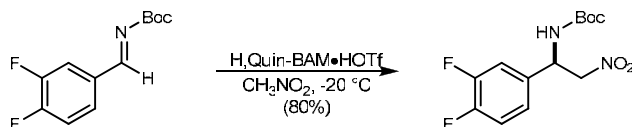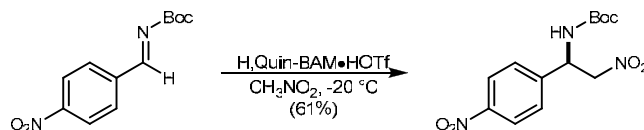

***tert*-butyl (*R*)-2-nitro-1-(4-nitrophenyl)ethylcarbamate (168r).** A solution of imine (50.1 mg, 200.0 μmol) and H,Quin-BAM•TfOH (10.4 mg, 20.0 μmol) in CH_3NO_2 (0.4 mL, 0.25M) was stirred at -20 °C. The solution was concentrated and purified by flash chromatography (Al_2O_3, 40% ethyl acetate in hexanes) to furnish the product as a yellow solid (38.1 mg, 61 %) which was determined to be 82% ee by chiral HPLC analysis (Chiralcel® AD, 90:10 hexanes:*i*-PrOH, 1 mL / min, t_r(major) = 45.3 min, t_r(minor) = 22.4 min); Mp = 132-134 °C; R_f = 0.38 (60% EtOAc/hexanes); IR (film) 3353, 2924, 2850, 1701, 1560, 1523 cm^{-1}; ^{1}H NMR (400 MHz, CDCl$_3$) δ 8.25 (d, *J* = 8.5 Hz, 2H), 7.52 (d, *J* = 8.5 Hz, 2H), 5.54 (bs, 1H), 5.47 (m, 1H), 4.89 (m, 1H), 4.77 (dd, *J* = 13.1, 4.3 Hz, 1H), 1.44 (s, 1H); ^{13}C NMR (100 MHz, CDCl$_3$) ppm 148.2, 144.3, 127.5, 124.6, 81.5, 78.5, 52.3, 28.4; HRMS (EI): Exact mass calcd for $C_{13}H_{17}N_3O_6$ [M]$^+$, 311.1117, found 311.1116.
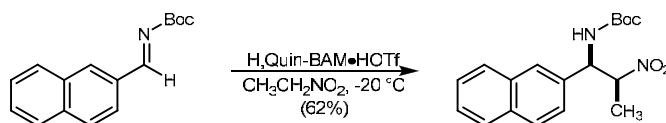
(1-Naphthalen-2-yl-2-nitro-propyl)-carbamic acid tert-butyl ester (169c). A solution of imine (25.0 mg, 100.0 μmol) and H,Quin-BAM•TfOH (5.2 mg, 10.0 μmol) in nitroethane (0.4 mL, 0.25M) was stirred at -20 °C. The solution was concentrated and purified by flash chromatography (SiO$_2$, 20% ethyl acetate in hexanes) to furnish the product as a white solid (20.1 mg, 62 %) and a 9:1 mixture of diastereomers; the major diastereomer was determined to be 44% ee by chiral HPLC analysis (Chiralcel® AD, 95:5 hexanes:i-PrOH, 1 mL/min, t_r(major) = 25.3 min, t_r(minor) = 22.7 min); Mp = 136-138 °C; R$_f$ = 0.78 (40% EtOAc/hexanes); IR (film) 3368, 3058, 2978, 2932, 1701 cm^{-1}; ^{1}H NMR (400 MHz, CDCl$_3$) δ 7.82-7.86 (m, 3H), 7.71 (s, 1H), 7.48-7.53 (m, 2H), 7.34 (dd, J = 8.5, 1.5 Hz, 1H), 5.36-5.43 (m, 2H), 5.02 (bs, 1H)1.57 (d, J = 6.7 Hz, 3H), 1.44 (s, 9H); ^{13}C NMR (100 MHz, CDCl$_3$) ppm 155.1, 134.0, 133.3 (2), 129.2, 128.2, 127.9, 126.9, 126.8, 126.5, 124.3, 85.9, 80.8, 57.8, 28.5, 15.4; HRMS (EI): Exact mass calcd for C$_{18}$H$_{22}$N$_2$O$_4$ [M]$^+$, 330.1580, found 330.1572.
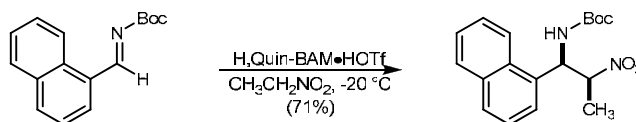
(1-Naphthalen-1-yl-2-nitro-propyl)-carbamic acid tert-butyl ester (169d). A solution of imine (25.0 mg, 100.0 μmol) and H,Quin-BAM•TfOH (5.2 mg, 10.0 μmol) in nitroethane (0.4 mL, 0.25M) was stirred at -20 °C. The solution was concentrated and purified by flash chromatography (SiO$_2$, 20% ethyl acetate in hexanes) to furnish the product as a colorless oil (23.1 mg, 71 %) and a 6:1 mixture of diastereomers; the major diastereomer was determined to be 56% ee by chiral HPLC analysis (Chiralcel® AD, 90:10 hexanes:i-PrOH, 1 mL/min, t_r(major) = 11.7 min, t_r(minor) = 10.8 min); R$_f$ = 0.73 (40% EtOAc/hexanes); IR (film) 3347, 3052, 2979, 2933, 1701 cm^{-1}; ^{1}H NMR (400 MHz, CDCl$_3$) δ 8.24 (d, J = 8.5 Hz, 1H), 7.89 (d, J = 7.9 Hz, 1H), 7.84 (d, J = 7.9 Hz, 1H), 7.62 (dd, J = 7.6, 7.0 Hz, 1H), 7.54 (dd, J = 7.3, 7.3 Hz, 1H), 7.40-7.48 (m, 2H), 6.43 (d, J = 7.3 Hz, 1H), 6.29 (dd, J = 8.5, 6.1 Hz, 1H), 5.15 (bs, 1H), 1.57 (d, J = 7.3 Hz, 3H), 1.43 (s, 9H); ^{13}C NMR (100 MHz, CDCl$_3$) ppm 155.2, 134.2, 133.4, 130.8, 129.5,

129.4, 127.5, 126.4, 125.4, 123.3, 122.8, 84.6, 80.8, 53.1, 28.4, 14.9; HRMS (EI): Exact mass calcd for $C_{18}H_{22}N_2O_4$ [M]$^+$, 330.1580, found 330.1571.
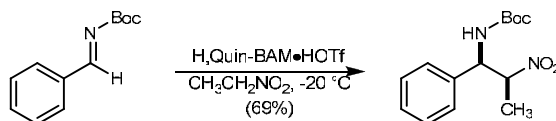
tert-butyl (1R,2S)-2-nitro-1-phenylpropylcarbamate (169e). A solution of imine (100.0 mg, 487 μmol) and H,Quin-BAM•TfOH (25.3 mg, 48.7 μmol) in $CH_3CH_2NO_2$ (1.6 mL, 0.25M) was stirred at -20 °C. The solution was concentrated and purified by flash chromatography (SiO$_2$, 20% ethyl acetate in hexanes) to furnish the product as a white solid (93.7 mg, 69 %) and a 14:1 mixture of diastereomers , the major of which was determined to be 59% ee by chiral HPLC analysis (Chiralcel® AD, 90:10 hexanes:i-PrOH, 1 mL / min, t_r(major) = 10.1 min, t_r(minor) = 9.3 min); Mp = 143-145 °C; R$_f$ = 0.61 (40% EtOAc/hexanes); IR (film) 3383, 2975, 2938, 1684, 1544 cm^{-1}; ^{1}H NMR (400 MHz, CDCl$_3$) δ 7.28-7.32 (m, 3H), 7.20-7.23(m, 2H), 5.35 (bs, 1H), 5.18 (dd, J = 8.5, 6.1 Hz, 1H), 4.89 (bs, 1H), 1.49 (d, J = 6.7 Hz, 3H), 1.39 (s, 9H); ^{13}C NMR (100 MHz, CDCl$_3$) ppm 155.2, 136.7, 129.2, 128.8, 127.1, 86.0, 80.7, 57.7, 28.4, 15.5; HRMS (EI): Exact mass calcd for $C_{14}H_{21}N_2O_4$ [M+H]$^+$, 281.1501, found 281.1491.
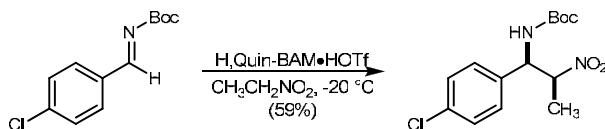
tert-butyl (1R,2S)-1-(4-chlorophenyl)-2-nitropropylcarbamate (169f). A solution of imine (100.0 mg, 417 μmol) and H,Quin-BAM•TfOH (21.6 mg, 41.7 μmol) in $CH_3CH_2NO_2$ (0.8 mL, 0.25M) was stirred at -20 °C. The solution was concentrated and purified by flash chromatography (SiO$_2$, 20% ethyl acetate in hexanes) to furnish the product as a white solid (77.8 mg, 59 %) and a 17:1 mixture of diastereomers , the major of which was determined to be 82% ee by chiral HPLC analysis (Chiralcel® AD, 95:5 hexanes:i-PrOH, 1 mL / min, t_r(major) = 25.5 min, t_r(minor) = 16.7 min); Mp = 142-144 °C; R$_f$ = 0.66 (40% EtOAc/hexanes); IR (film) 3393, 2981, 2935, 1682, 1524 cm^{-1}; ^{1}H NMR (400 MHz, CDCl$_3$) δ 7.32 (d, J = 8.5 Hz, 2H), 7.18 (d, J = 7.6 Hz, 2H), 5.39 (bs, 1H), 5.15 (dd, J = 8.9, 5.8 Hz, 1H), 4.89 (bs, 1H), 1.52 (d, J = 7.0 Hz, 3H), 1.42 (s, 9H); ^{13}C NMR (100 MHz, CDCl$_3$) ppm 155.0, 135.1, 134.8, 129.3, 128.5, 85.8, 81.0, 57.1,

28.4, 15.5; HRMS (EI): Exact mass calcd for $C_{14}H_{20}ClN_2O_4$ [M+H]$^+$, 315.1112, found 315.1117.
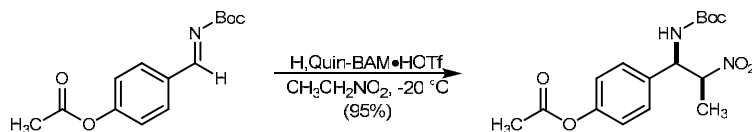
Acetic acid 4-(1-tert-butoxycarbonylamino-2-nitro-propyl)-phenyl ester (169g). A solution of imine (25.0 mg, 100.0 µmol) and H,Quin-BAM•TfOH (5.2 mg, 10.0 µmol) in nitroethane (0.4 mL, 0.25M) was stirred at -20 °C. The solution was concentrated and purified by flash chromatography (SiO$_2$, 20% ethyl acetate in hexanes) to furnish the product as a white solid (30.6 mg, 95 %) and a 13:1 mixture of diastereomers; the major diastereomer was determined to be 77% ee by chiral HPLC analysis ([α]$_D^{25}$ -11.0 (*c* 1.0, CHCl$_3$) Chiralcel® AD, 90:10 hexanes:*i*-PrOH, 1 mL/min, t_r(major) = 15.5 min, t_r(minor) = 14.1 min). Mp = 115-117 °C; R$_f$ = 0.51 (40% EtOAc/hexanes); IR (film) 3374, 2980, 2934, 1770, 1699 cm^{-1}; ^{1}H NMR (400 MHz, CDCl$_3$) δ 7.25 (d, *J* = 7.0 Hz, 2H), 7.10(d, *J* = 6.7 Hz, 2H), 5.29 (bs, 1H), 5.20 (dd, *J* = 8.9, 5.8 Hz, 1H), 4.90 (bs, 1H), 2.29 (s, 3H), 1.53 (d, *J* = 6.7 Hz, 3H), 1.42 (s, 9H); ^{13}C NMR (100 MHz, CDCl$_3$) ppm 169.4, 155.0, 151.0, 134.2, 128.2, 122.4, 85.8, 80.9, 57.1, 28.5, 21.3, 15.5; HRMS (CI): Exact mass calcd for $C_{16}H_{23}N_2O_6$ [M+H]$^+$, 339.1556, found 339.1540.
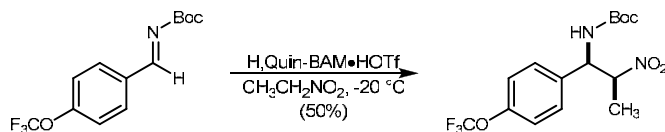
tert-butyl (1R,2S)-2-nitro-1-(4-(trifluoromethoxy)phenyl)propylcarbamate (169h). A solution of imine (100.0 mg, 346 µmol) and H,Quin-BAM•TfOH (19.0 mg, 34.5 µmol) in CH$_3$CH$_2$NO$_2$ (1.6 mL, 0.25M) was stirred at -20 °C. The solution was concentrated and purified by flash chromatography (SiO$_2$, 20% ethyl acetate in hexanes) to furnish the product as a white solid (62.5 mg, 50 %) and a 19:1 mixture of diastereomers , the major of which was determined to be 81% ee by chiral HPLC analysis (Chiralcel® AD, 95:5 hexanes:*i*-PrOH, 1 mL / min, t_r(major) = 19.7 min, t_r(minor) = 12.1 min); Mp = 113-115 °C; R$_f$ = 0.22 (20% EtOAc/hexanes); IR (film) 3373, 2989, 2941, 1680, 1518 cm^{-1}; ^{1}H NMR (400 MHz, CDCl$_3$) δ 7.26 (d, *J* = 8.2 Hz, 2H), 7.17(d, *J* = 8.2 Hz, 2H), 5.35 (bs, 1H), 5.17 (dd, *J* = 8.5, 5.8 Hz, 1H), 4.88 (bs, 1H) 1.51 (d, *J* = 6.7 Hz, 3H), 1.39 (s, 9H); ^{13}C NMR (100 MHz, CDCl$_3$) ppm 155.0, 149.5, 148.3, 128.6, 121.5, 85.7, 81.0, 57.0,

28.4, 15.5; HRMS (EI): Exact mass calcd for $C_{15}H_{20}F_3N_2O_5[M+H]^+$, 365.1324, found 365.1315.
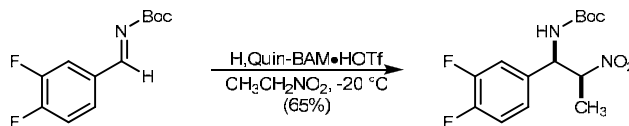
**[1-(3,4-Difluoro-phenyl)-2-nitro-propyl]-carbamic acid tert-butyl ester (169k).** A solution of imine (25.0 mg, 100.0 μmol) and H,Quin-BAM•TfOH (5.2 mg, 10.0 μmol) in nitroethane (0.4 mL, 0.25M) was stirred at -20 °C. The solution was concentrated and purified by flash chromatography (SiO$_2$, 20% ethyl acetate in hexanes) to furnish the product as a white solid (21.4 mg, 65 %) and a 18:1 mixture of diastereomers; the major diastereomer was determined to be 86% ee by chiral HPLC analysis ($[\alpha]_D^{25}$ -17.8 (*c* 1.0, CHCl$_3$) Chiralcel® AD, 90:10 hexanes:*i*-PrOH, 1 mL/min, t_r(major) = 9.6 min, t_r(minor) = 7.2 min); Mp = 136-138 °C; R$_f$ = 0.68 (40% EtOAc/hexanes); IR (film) 3363, 2986, 2941, 1678 cm^{-1}; ^{1}H NMR (400 MHz, CDCl$_3$) δ 7.16 (ddd, *J* = 8.5, 8.2, 8.2 Hz, 1H), 7.08 (ddd, *J* = 9.8, 7.3, 2.1 Hz, 1H), 6.97-7.00 (m, 1H) 5.36 (d, *J* = 8.5 Hz, 1H), 5.12 (dd, *J* = 8.5, 5.8 Hz, 1H), 4.88 (bs, 1H), 1.53 (d, *J* = 6.7 Hz, 3H), 1.43 (s, 9H); ^{13}C NMR (100 MHz, CDCl$_3$) ppm 154.9, 151.8, 149.3, 133.8, 123.4, 118.2, 116.3, 85.6, 81.2, 56.8, 28.4, 15.6; HRMS (CI): Exact mass calcd for $C_{14}H_{19}F_2N_2O_4$ [M+H]$^+$, 317.1313, found 317.1324.
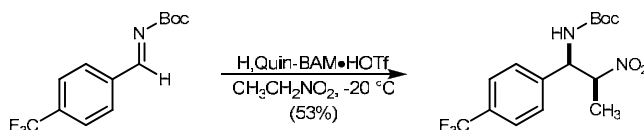
tert-butyl (1R,2S)-1-(4-(trifluoromethyl)phenyl)-2-nitropropylcarbamate (169l). A solution of imine (100.0 mg, 366 μmol) and H,Quin-BAM•TfOH (19.0 mg, 36.6 μmol) in CH$_3$CH$_2$NO$_2$ (1.6 mL, 0.25M) was stirred at -20 °C. The solution was concentrated and purified by flash chromatography (SiO$_2$, 20% ethyl acetate in hexanes) to furnish the product as a white solid (67.5 mg, 53 %) and a 19:1 mixture of diastereomers , the major of which was determined to be 84% ee by chiral HPLC analysis (Chiralcel® OD, 90:10 hexanes:*i*-PrOH, 1 mL / min, t_r(major) = 11.8 min, t_r(minor) = 7.6 min); Mp = 137-139 °C; R$_f$ = 0.65 (40% EtOAc/hexanes); IR (film) 3373, 2987, 1682, 1544 cm^{-1}; ^{1}H NMR (400 MHz, CDCl$_3$) δ 7.63 (d, *J* = 8.2 Hz, 2H), 7.37(d, *J* = 8.2 Hz, 2H), 5.39 (bs, 1H), 5.24 (dd, *J* = 8.5, 5.8 Hz, 1H), 4.93 (bs, 1H), 1.54 (d, *J* = 6.7 Hz, 3H), 1.43 (s, 9H); ^{13}C

NMR (100 MHz, CDCl$_3$) ppm 155.0, 140.1, 131.1, 127.6, 157.4, 122.6, 85.6, 57.2, 28.4, 15.4; HRMS (EI): Exact mass calcd for C$_{15}$H$_{20}$F$_3$N$_2$O$_4$ [M+H]$^+$, 349.1375, found 349.1375.
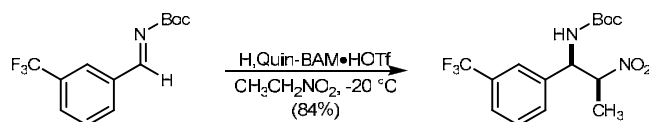
[2-Nitro-1-(3-trifluoromethyl-phenyl)-ethyl]-carbamic acid *tert*-butyl ester (169m).
A solution of imine (25.0 mg, 100.0 μmol) and H,Quin-BAM•TfOH (5.2 mg, 10.0 μmol) in nitroethane (0.4 mL, 0.25M) was stirred at -20 °C. The solution was concentrated and purified by flash chromatography (SiO$_2$, 20% ethyl acetate in hexanes) to furnish the product as a white solid (26.9 mg, 84 %) and a 12:1 mixture of diastereomers; the major diastereomer was determined to be 69% ee by chiral HPLC analysis ([α]$_D^{25}$ -7.1 (*c* 1.0, CHCl$_3$) Chiralcel® AD, 90:10 hexanes:*i*-PrOH, 1 mL/min, t_r(major) = 6.1 min, t_r(minor) = 5.6 min). Mp = 96-98 °C; R$_f$ = 0.67 (40% EtOAc/hexanes); IR (film) 3328, 2982, 2937, 1704 cm^{-1}; ^{1}H NMR (400 MHz, CDCl$_3$) δ 7.60 (d, *J* = 7.9 Hz, 1H), 7.48-7.52 (m, 2H), 7.44 (d, *J* = 7.9 Hz, 1H), 5.42 (bs, 1H), 5.26 (dd, *J* = 8.2, 5.8 Hz, 1H), 4.93 (bs, 1H), 1.54 (d, *J* = 6.7 Hz, 3H), 1.43 (s, 9H); ^{13}C NMR (100 MHz, CDCl$_3$) ppm 154.9, 137.8, 135.4, 131.4, 130.5, 129.8, 125.7, 123.9, 85.6, 81.2, 57.3, 28.4, 15.7; HRMS (CI): Exact mass calcd for C$_{15}$H$_{20}$F$_3$N$_2$O$_4$ [M+H]$^+$, 349.1375, found 349.1368.
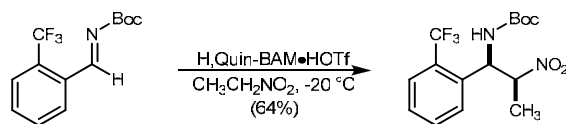
[2-Nitro-1-(2-trifluoromethyl-phenyl)-propyl]-carbamic acid tert-butyl ester (169n).
A solution of imine (25.0 mg, 100.0 μmol) and H,Quin-BAM•TfOH (5.2 mg, 10.0 μmol) in nitroethane (0.4 mL, 0.25M) was stirred at -20 °C. The solution was concentrated and purified by flash chromatography (SiO$_2$, 20% ethyl acetate in hexanes) to furnish the product as a white solid (20.4 mg, 64 %) and a 6:1 mixture of diastereomers; the major diastereomer was determined to be 83% ee by chiral HPLC analysis ([α]$_D^{25}$ -10.0° (*c* 1.0, CHCl$_3$) Chiralcel® AD, 90:10 hexanes:*i*-PrOH, 1 mL/min, t_r(major) = 12.9 min, t_r(minor) = 15.7 min); Mp = 88-90 °C; R$_f$ = 0.58 (40% EtOAc/hexanes); IR (film) 3272, 2982, 2935, 1704 cm^{-1}; ^{1}H NMR (400 MHz, CDCl$_3$) δ 7.71 (d, *J* = 7.6 Hz, 1H), 7.56-7.59 (m, 2H), 7.45 (dd, *J* = 7.9, 7.6 Hz, 1H), 5.69 (bs, 1H), 5.02-5.10 (m, 2H), 1.60 (d, *J* = 6.7 Hz,

3H), 1.41 (s, 9H); ^{13}C NMR (100 MHz, CDCl$_3$) ppm 154.7, 132.6, 128.9, 128.1, 127.0, 125.5, 122.8, 87.1, 84.6, 81.0, 53.5, 28.3, 15.6; HRMS (CI): Exact mass calcd for C$_{15}$H$_{20}$F$_3$N$_2$O$_4$ [M+H]$^+$, 349.1375, found 349.1389.
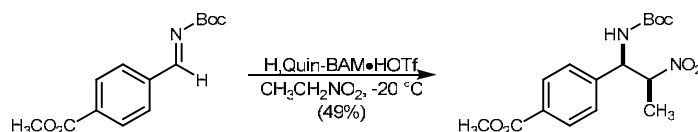

4-(1-tert-Butoxycarbonylamino-2-nitro-propyl)-benzoic acid methyl ester (169o). A solution of imine (25.0 mg, 100.0 μmol) and H,Quin-BAM•TfOH (5.2 mg, 10.0 μmol) in nitroethane (0.4 mL, 0.25M) was stirred at -20 °C. The solution was concentrated and purified by flash chromatography (SiO$_2$, 20% ethyl acetate in hexanes) to furnish the product as a white solid (15.6 mg, 49 %) and a 20:1 mixture of diastereomers; the major diastereomer was determined to be 88% ee by chiral HPLC analysis ([α]$_D^{25}$ -17.9 (c 1.0, CHCl$_3$) Chiralcel® AD, 90:10 hexanes:i-PrOH, 1 mL/min, t$_r$(major) = 18.4 min, t$_r$(minor) = 15.4 min). Mp = 121-123 °C; R$_f$ = 0.57 (40% EtOAc/hexanes); IR (film) 3362, 2980, 1718 cm^{-1}; ^{1}H NMR (400 MHz, CDCl$_3$) δ 8.03 (d, J = 8.5 Hz, 2H), 7.32(d, J = 8.2 Hz, 2H), 5.41 (d, J = 8.9 Hz, 1H), 5.25 (dd, J = 8.9, 5.5 Hz, 1H), 4.92 (bs, 1H), 3.91 (s, 3H), 1.52 (d, J = 7.0 Hz, 3H), 1.42 (s, 9H); ^{13}C NMR (100 MHz, CDCl$_3$) ppm 166.6, 155.0, 141.6, 130.7, 130.4, 127.2, 85.6, 81.0, 57.4, 52.5, 28.4, 15.3; HRMS (CI): Exact mass calcd for C$_{16}$H$_{23}$N$_2$O$_6$ [M+H]$^+$, 339.1556, found 339.1544.
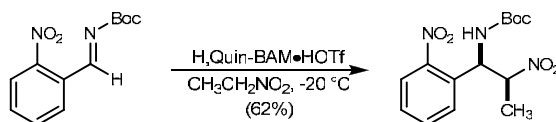
tert-butyl (1R,2S)-2-nitro-1-(2-nitrophenyl)propylcarbamate (169p). A solution of imine (50.0 mg, 200 μmol) and H,Quin-BAM•TfOH (10.4 mg, 20.1 μmol) in CH$_3$CH$_2$NO$_2$ (0.8 mL, 0.25M) was stirred at -20 °C. The solution was concentrated and purified by flash chromatography (SiO$_2$, 20% ethyl acetate in hexanes) to furnish the product as a colorless oil (40.4 mg, 62 %) and a 7:1 mixture of diastereomers , the major of which was determined to be 82% ee by chiral HPLC analysis (Chiralcel® OJ, 90:10 hexanes:i-PrOH, 1 mL / min, t$_r$(major) = 11.7 min, t$_r$(minor) = 13.4 min); R$_f$ = 0.43 (40% EtOAc/hexanes); IR (film) 3340, 2980, 1703, 1553 cm^{-1}; ^{1}H NMR (400 MHz, CDCl$_3$) δ 8.06 (d, J = 7.6 Hz, 1H), 7.63(dd, J = 7.6, 6.7 Hz, 1H), 7.49-7.53 (m 2H), 5.66-5.74 (m, 2H), 5.24 (bs, 1H), 1.64 (d, J = 6.7 Hz, 3H), 1.40 (s, 9H); ^{13}C NMR (100 MHz, CDCl$_3$)

140

ppm 155.1, 148.4, 134.6, 132.2, 130.1, 129.7126.4, 84.6, 81.1, 56.4, 28.5, 16.4; HRMS (EI): Exact mass calcd for $C_{14}H_{2}0N_{3}O_{6}$ [M+H]$^+$, 326.1352, found 326.1357.
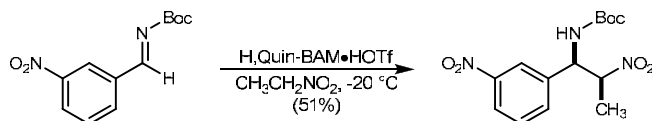

tert-butyl (1R,2S)-2-nitro-1-(3-nitrophenyl)propylcarbamate (169q). A solution of imine (100.0 mg, 400 μmol) and H,Quin-BAM•TfOH (20.7 mg, 39.9 μmol) in $CH_3CH_2NO_2$ (1.6 mL, 0.25M) was stirred at -20 °C. The solution was concentrated and purified by flash chromatography (SiO_2, 20% ethyl acetate in hexanes) to furnish the product as a white solid (66.3 mg, 51 %) and a 11:1 mixture of diastereomers , the major of which was determined to be 89% ee by chiral HPLC analysis (Chiralcel® AD, 90:10 hexanes:_i_-PrOH, 1 mL / min, t_r(major) = 11.9 min, t_r(minor) = 9.7 min); Mp = 146-148 °C; R_f = 0.61 (40% EtOAc/hexanes); IR (film) 3369, 2985, 1683, 1517 cm^{-1}; ^{1}H NMR (400 MHz, CDCl$_3$) δ 8.20 (ddd, _J_ = 7.8, 1.7, 1.6 Hz, 1H), 8.15 (s, 1H), 7.54-7.62 (m, 2H), 5.52(bs, 1H), 5.30 (dd, J = 8.5, 8.5 Hz, 1H), 4.95 (bs, 1H), 1.58 (d, _J_ = 6.8 Hz, 3H), 1.43 (s, 9H); ^{13}C NMR (100 MHz, CDCl$_3$) ppm 154.9, 148.7, 148.6, 133.4, 130.3, 123.9, 122.1, 85.5, 81.4, 57.0, 28.4, 15.5; HRMS (EI): Exact mass calcd for $C_{14}H_{19}N_3O_6$[M]$^+$, 325.1274, found 325.1269.
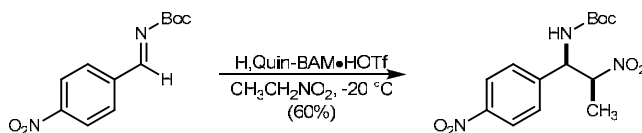
tert-butyl (1R,2S)-2-nitro-1-(4-nitrophenyl)propylcarbamate (169r). A solution of imine (50.0 mg, 200 μmol) and H,Quin-BAM•TfOH (10.4 mg, 20.1 μmol) in $CH_3CH_2NO_2$ (0.4 mL, 0.25M) was stirred at -20 °C. The solution was concentrated and purified by flash chromatography (SiO_2, 20% ethyl acetate in hexanes) to furnish the product as a yellow oil (38.9 mg, 60 %) and a 7:1 mixture of diastereomers , the major of which was determined to be 90% ee by chiral HPLC analysis (Chiralcel® AD, 80:20 hexanes:_i_-PrOH, 1 mL / min, t_r(major) = 13.1 min, t_r(minor) = 7.5 min); R_f = 0.60 (40% EtOAc/hexanes); IR (film) 3385, 2981, 2935, 1699, 1557 cm^{-1}; ^{1}H NMR (400 MHz, CDCl$_3$) δ 8.23 (d, _J_ = 8.7 Hz, 2H), 7.44 (d, _J_ = 8.7 Hz, 2H), 5.49 (bs, 1H), 5.27 (dd, _J_ =7.1,6.2 Hz, 1H), 4.94 (bs, 1H), 1.55 (d, _J_ = 6.7 Hz, 3H), 1.43 (s, 9H); ^{13}C NMR (100

MHz, CDCl$_3$) ppm 154.9, 148.3, 128.3, 124.4, 123.7, 85.4, 81.4, 57.2, 28.4, 18.3; HRMS (EI): Exact mass calcd for C$_{14}$H$_{20}$N$_3$O$_6$ [M+H]$^+$, 326.1352, found 326.1351.
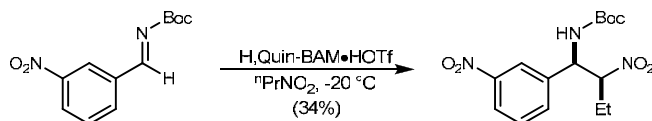
***tert*-Butyl (1*R*,2*S*)-2-nitro-1-(3-nitrophenyl)butylcarbamate.** A solution of imine (25.0 mg, 100 μmol) and H,Quin-BAM·TfOH (5.2 mg, 10.0 μmol) in 1-nitropropane (0.4 mL, 0.25 M) was stirred at -20 °C. The solution was concentrated and purified by flash chromatography (SiO$_2$, 20% ethyl acetate in hexanes) to furnish the product as a white solid (10.1 mg, 34%) and a 10:1 mixture of diastereomers; the major diastereomer was determined to be 89% *ee* by chiral HPLC analysis ([α]$_D^{25}$ -14.9 (*c* 1.0, acetone) (Chiralcel® AD, 95:5 hexanes:^{i}PrOH, 1 mL/min, t_r(major) = 19.1 min, t_r(minor) = 17.7 min); mp = 143-145 °C; R$_f$ = 0.61 (40% EtOAc/hexanes); IR (film) 3370, 2979, 2935, 1683 cm^{-1}; ^{1}H NMR (400 MHz, CDCl$_3$) δ 8.20 (d, *J* = 7.7 Hz, 1H), 8.14 (s, 1H), 7.60-7.53 (m, 2H), 5.30-5.25 (m, 2H), 4.76 (bs, 1H), 2.04-2.10 (m, 1H), 1.94-1.88 (m, 1H), 1.43 (s, 9H), 1.02 (t, *J* = 7.3 Hz, 3H); ^{13}C NMR (100 MHz, CDCl$_3$) ppm 154.8, 148.7, 144.1, 133.5, 130.3, 124.0, 122.1, 92.7, 81.9, 56.4, 28.5, 23.7, 10.6; HRMS (ESI): Exact mass calcd for C$_{15}$H$_{21}$N$_3$O$_6$Na [M+Na]$^+$ 362.1323. Found 362.1326.
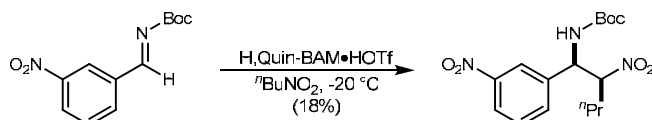
***tert*-Butyl (1*R*,2*S*)-2-nitro-1-(3-nitrophenyl)pentylcarbamate.** A solution of imine (25.0 mg, 100 μmol) and H,Quin-BAM·TfOH (5.2 mg, 10.0 μmol) in 1-nitrobutane (0.4 mL, 0.25 M) was stirred at -20 °C. The solution was concentrated and purified by flash chromatography (SiO$_2$, 20% ethyl acetate in hexanes) to furnish the product as a white solid (5.0 mg, 18%) and a 13:1 mixture of diastereomers; the major diastereomer was determined to be 90% *ee* by chiral HPLC analysis ([α]$_D^{25}$ -17.9 (*c* 1.0, acetone) (Chiralcel® AD, 90:10 hexanes:^{i}PrOH, 1 mL/min, t_r(major) = 8.6 min, t_r(minor) = 7.8 min); mp = 130-132 °C; R$_f$ = 0.59 (40% EtOAc/hexanes); IR (film) 3328, 2970, 2934, 2877, 1702 cm^{-1}; ^{1}H NMR (400 MHz, CDCl$_3$) δ 8.20 (d, *J* = 7.9 Hz, 1H), 8.14 (s, 1H), 7.53-7.60 (m, 2H), 5.30 (bs, 1H), 5.25 (bs, 1H), 4.84 (bs, 1H), 2.09-2.00 (m, 1H), 1.76-1.79 (m, 1H), 1.56-1.31 (m, 2H), 1.43 (s, 9H), 0.95 (t, *J* = 7.5 Hz, 3H); ^{13}C NMR (100 MHz, CDCl$_3$)

ppm 130.2, 123.9, 122.0, 90.9, 32.0, 28.4, 19.4, 13.6; HRMS (ESI): Exact mass calcd for $C_{16}H_{23}N_3O_6Na$ [M+Na]$^+$ 376.1479. Found 376.1480.
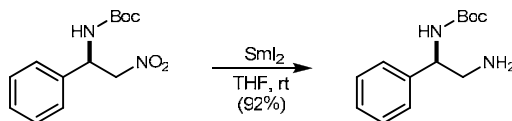
***tert*-Butyl (*R*)-2-amino-1-phenylethylcarbamate.** A solution of 1,2-diodoethane (137.6 mg, 488 µmol) in THF (1 mL) was added dropwise to samarium powder (79.1 mg, 526 µmol) in a flame-dried, argon purged round bottom flask. The suspension was stirred for an additional 2 h at room temperature resulting in a color change to a deep blue color. A solution of carbamate (20.0 mg, 75.1 µmol) in MeOH/H$_2$O (1 mL, 1:1) was then added all at once. After 4 h, a solution of oxalic acid (133 mg) in H$_2$O (2 mL) was added which immediately formed a brown precipitate. Filtration and addition of 1 M NaOH (1 mL), followed by extraction with ethyl acetate, drying (Na$_2$SO$_4$) and concentration gave the desired amine as a yellow oil (16.3 mg, 92%). The optical rotation $[\alpha]_D^{25}$ -16.8 (*c* 0.6, CHCl$_3$) is consistent with the (*R*)-enantiomer reported previously.[162]
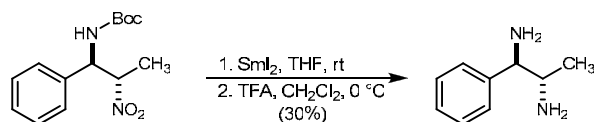
(1*R*,2*S*)-1-Phenylpropane-1,2-diamine. A solution of 1,2-diodoethane (522.9 mg, 1.86 mmol) in THF (3 mL) was added dropwise to samarium powder (300.4 mg, 2.0 mmol) in a flame-dried, argon purged round bottom flask. The suspension was stirred for an additional 2 h at room temperature resulting in a color change to a deep blue color. A solution of carbamate (80.0 mg, 285 µmol) in MeOH/H$_2$O (3 mL, 1:1) was then added all at once. After 4 h, a solution of oxalic acid (400 mg) in H$_2$O (2 mL) was added which immediately formed a brown precipitate. Filtration and addition of 1 M NaOH (4 mL) followed by extraction with ethyl acetate, drying (Na$_2$SO$_4$) and concentration gave the protected diamine as a yellow oil. To a solution of the diamine in CH$_2$Cl$_2$ at 0 °C was added TFA (0.2 mL) and the solution was allowed to warm to room temperature overnight. Addition of 1 M NaOH (5 ml) followed by extraction with CH$_2$Cl$_2$, drying of the organic phase, and concentration furnished the desired diamine as a yellow oil (12.7

[162] O'Brien, P. M.; Sliskovic, D. R.; Blankley, C. J.; Roth, B. D.; Wilson, M. W.; Hamelehle, K. L.; Krause, B. R.; Stanfield, R. L. *J. Med. Chem.* **1994**, *37*, 1810-1822.

mg, 30% over two steps). The ^{1}H NMR spectrum and optical rotation ($[\alpha]_D^{25}$ +7.4 (*c* 1.0, 1 M HCl)) were consistent with literature values.[163]
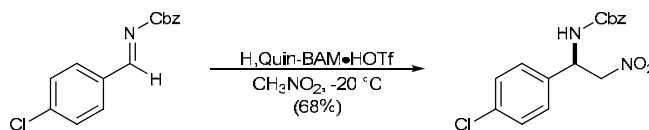
(*R*)-Benzyl 1-(4-chlorophenyl)-2-nitroethylcarbamate. A solution of imine (13.7 mg, 50.0 μmol) and H,Quin-BAM·TfOH (2.6 mg, 5.0 μmol) in nitromethane (0.2 mL, 0.25 M) was stirred at -20 °C for 12 days. The solution was concentrated and purified by flash chromatography (Al$_2$O$_3$, 20% ethyl acetate in hexanes) to furnish the carbamate as a yellow oil (11.4 mg, 68%), which was determined to be 62% *ee* by chiral HPLC analysis (Chiralcel® AD, 90:10 hexanes:*i*PrOH, 1 mL/min, t_r(major) = 42.9 min, t_r(minor) = 27.8 min); R$_f$ = 0.32 (20% EtOAc/hexanes); IR (film) 3319, 3036, 2960, 2922, 2856, 1707, 1555, 1489, 1380, 1261, 1135, 1054, 825, 743, 694 cm^{-1}; ^{1}H NMR (400 MHz, CDCl$_3$) δ 7.38-7.33 (m, 7H), 7.27-7.25 (m, 2H), 5.68 (d, *J* = 6.4 Hz, 1H), 5.43 (dd, *J* = 6.4, 6.0 Hz, 1H), 4.86 (s, 1H), 4.71 (dd, *J* = 13.2, 13.2 Hz, 1H), 3.74 (d, *J* = 14.0 Hz, 1H), 3.72 (d, *J* = 14.0 Hz, 1H); ^{13}C NMR (100 MHz, CDCl$_3$) ppm 155.6, 136.0, 135.1, 132.7, 131.1, 129.7, 128.9, 128.5, 128.0, 78.6, 68.4, 52.8; HRMS (EI): Exact mass calcd for C$_{16}$H$_{15}$ClN$_2$O$_4$ [M+H]$^+$ 335.0793. Found 335.0795.
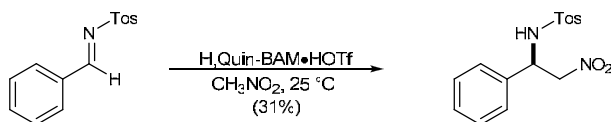
(*R*)-Benzyl 1-(4-chlorophenyl)-2-nitroethylcarbamate. A solution of imine (25.0 mg, 96.0 μmol) and H,Quin-BAM·TfOH (5.0 mg, 10.0 μmol) in nitromethane (0.4 mL, 0.25 M) was stirred at 25 °C for 4 days. The solution was concentrated and purified by flash chromatography (Al$_2$O$_3$, 20% ethyl acetate in hexanes) to furnish the sulfonamide as a white solid (9.7 mg, 31%), which was determined to be 57% *ee* by chiral HPLC analysis (Chiralcel® OD, 90:10 hexanes:*i*PrOH, 1 mL/min, t_r(major) = 45.2 min, t_r(minor) = 38.3 min); R$_f$ = 0.32 (20% EtOAc/hexanes); IR (film) 3243, 2355, 1555 cm^{-1}; ^{1}H NMR (400 MHz, CDCl$_3$) δ 7.85 (d, *J* = 8.2 Hz, 2H), 7.47-7.41 (m, 5H), 7.31-7.28 (m, 2H), 5.77 (d, *J* = 7.8 Hz, 1H), 5.20 (ddd, *J* = 6.7, 6.7, 6.7 Hz, 1H), 5.07-5.00 (m, 1H), 4.90-4.83 (m, 1H);

[163] Gust, R.; Gelbcke, M.; Angermaier, B.; Bachmann, H.; Krauser, R; Schoneneberger, H. *Inorganica Chimica Acta* **1997**, *264*, 145-160.

^{13}C NMR (100 MHz, CDCl$_3$) ppm 144.3, 136.7, 135.5, 130.0, 129.4, 129.2, 127.4, 126.7, 79.2, 55.7, 21.8; HRMS (EI): Exact mass calcd for C$_{15}$H$_{16}$N$_2$O$_4$S [M+H]$^+$ 321.0904. Found 321.0903.
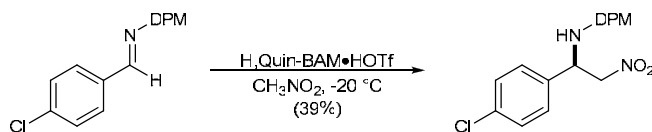
**(*R*)-*N*-Benzhydryl-1-(4-chlorophenyl)-2-nitroethanamine.** A solution of imine (30.6 mg, 100.0 μmol) and H,Quin-BAM·TfOH (5.2 mg, 10.0 μmol) in nitromethane (0.4 mL, 0.25 M) was stirred at -20 °C. The solution was concentrated and purified by flash chromatography (Al$_2$O$_3$, 20% ethyl acetate in hexanes) to furnish the carbamate as a yellow oil (14.3 mg, 39%), which was determined to be 7% *ee* by chiral HPLC analysis (Chiralcel® AD, 90:10 hexanes:^{i}PrOH, 1 mL/min, t_r(major) = 6.1 min, t_r(minor) = 7.1 min); R$_f$ = 0.36 (20% EtOAc/hexanes); IR (film) 3025, 2845, 1555, 1495, 1380, 1092, 825, 700 cm^{-1}; ^{1}H NMR (400 MHz, CDCl$_3$) δ 7.39 (d, *J* = 8.0 Hz, 2H), 7.35 (d, *J* = 7.2 Hz, 2H), 7.26 (m, 5H), 7.21 (d, *J* = 8.0 Hz, 1H), 4.60 (dd, *J* = 13.2, 12.0 Hz, 2H), 4.49 (dd, J = 12.4, 12.0 Hz, 1H), 4.33 (dd, J = 9.6, 9.2 Hz, 1H); ^{13}C NMR (100 MHz, CDCl$_3$) ppm 143.7, 141.9, 136.6, 129.7, 129.0, 128.8, 127.8, 127.3, 80.7, 63.8, 57.8; HRMS (EI): Exact mass calcd for C$_{21}$H$_{19}$ClN$_2$O$_2$ [M+H]$^+$ 367.1208. Found 367.1200.
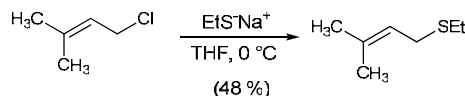
Ethyl(3-methylbut-2-enyl)sulfane (245). To a suspension of NaH (426 mg, 18 mmol) in tetrahydrofuran (20 mL) at 0 °C was added ethanethiol (1.32 mL, 18 mmol) and the mixture was stirred until H$_2$ evolution subsided (20-30 min). Neat 1-chloro-3-methyl-2-butene (2.0 mL, 18 mmol) was then added dropwise to the solution of sodium mercaptan and the solution was warmed to room temperature over the course of 1 h. Dilution with water (~5 mL) and extraction with dichloromethane gave, after drying with Na$_2$SO$_4$ and concentration, a yellow liquid. Purification by distillation (67 °C at 20 mm Hg) furnished the product as a colorless liquid (1.1124g, 48%).[164]

---

[164] Piras, P.; Stirling, C. *J. Chem. Soc. Perkin Trans. II* **1987**, *9*, 1265.

(9%)
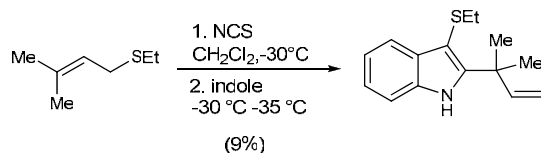
Ethyl(3-methylbut-2-enyl)sulfane (247). To a solution of NCS (4.8 g, 36.1 mmol) in dichloromethane (180 mL) at -40 °C[165] was added sulfide (5.6 mL, 36.1 mmol). After 15 min indole (1.06 g, 9.0 mmol) was added all at once, resulting in the solution to change to a bright yellow color. The solution was slowly warmed to room temperature over the course of 1 h, then heated at 35 °C for an additional 1 h. Concentration and purification by flash chromatography (SiO$_2$, 40% benzene in hexanes) furnished the product as a colorless oil (2.88 mg, 33%).

(56%)
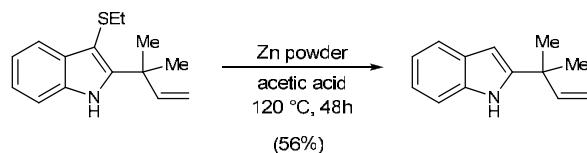
2-(2-Methylbut-3-en-2-yl)-1H-indole (248). To a solution of sulfide **247** (10 mg, 41 µmol) in acetic acid was added zinc dust (50 mg, 760 µmol) and the suspension was heated to 120 °C for 25 h. Concentration and purification by flash chromatography (SiO$_2$, 5% ethyl acetate in hexanes) furnished the product as a yellow oil (4.2 mg, 56%).[3]

(76%)
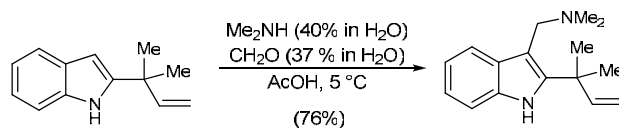
N,N-Dimethyl(2-(2-methylbut-3-en-2-yl)-1H-indol-3-yl)methanamine (237). To a cooled (5 °C) solution of dimethylamine (275 µL of 40% aqueous solution, 2.2 mmol) in acetic acid (0.5 mL) was added formaldehyde (163 µL of 37% aqueous solution, 2.2 mmol). The solution was swirled several times and added to a new argon-purged flask containing indole **248**. The solution was stirred at room temperature overnight, then quenched with 3M NaOH (10 mL). Extraction with dichloromethane followed by drying with Na$_2$SO$_4$ and concentration gave the crude product as a brown oil (402.2 mg, 76%).[166]

---

[165] A temperature of -40 ºC during sulfide addition is crucial, as -30 ºC led to appreciably lower yields.
[166] Houghton, E.; Saxton, J. E. *J. Chem. Soc. C* **1969**, 1003.

PhCH₂OCOCl
NaOH, H₂O, 0 °C
(68%)
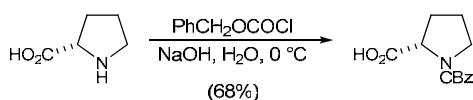
Pyrrolidine-1,2-dicarboxylic acid 1-benzyl ester (249). To a solution of (*S*)-proline (1.0 g, 8.7 mmol) in 2M NaOH (4.3 mL) at 0 °C was added simultaneously benzylchloroformate (976 µL, 8.7 mmol) and 2M NaOH (4.3 mL). The reaction was stirred at 0 °C for 3h, then allowed to warm to room temperature. After washing with diethyl ether (10 mL), the aqueous layer was acidified using 2 M HCl. Extraction with ethyl acetate (3 x 20 mL), drying with Na₂SO₄, and concentration gave the product as a colorless oil (1.48 g, 68%). No further purification was performed.[167]

EDC, DMAP, Et₃N
H₂NCH(CO₂Me)₂·HCl
CH₂Cl₂, 0 °C
(85%)
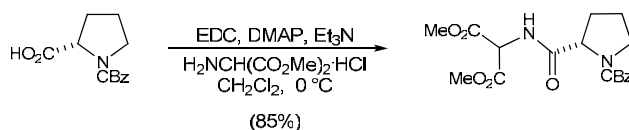
2-[(1-Benzyloxycarbonyl-pyrrolidine-2-carbonyl)-amino]-malonic acid dimethyl ester (250). To a solution of the acid (2.17 g, 8.7 mmol) and dimethylaminomalonate·hydrochloride salt (1.60 g, 8.7 mmol) in dichloromethane (90 mL) was added triethylamine (1.82 mL) and the solution was cooled to 0 °C for 30 m. EDC (2.0 g, 10.4 mmol) and DMAP (255 mg, 2.1 mmol) were then added all at once and the solution was allowed to warm to room temperature overnight. Dilution of the crude reaction mixture with dichloromethane, washing with water, drying (MgSO₄), concentration and purification by flash chromatography (SiO₂, 60% ethyl acetate in hexanes) furnished the malonic acid as a white solid (2.8 g, 85%); mp = 67-69 °C; R_f = 0.50 (80% EtOAc/hexanes); IR (film) 3297, 2955, 2881, 1745, 1709, 1656, 1540 cm⁻¹; ¹H NMR (400 MHz, CDCl₃) δ 7.66 (s, 1H), 7.31-7.35 (m, 5H), 5.18-5.08 (m, 3H), 4.44-4.36 (m, 1H), 3.78 (s, 6H), 3.59-3.44 (m, 2H), 2.33-1.88 (m, 4H); ¹³C NMR (100 MHz, CDCl₃) ppm 171.9, 166.6, 156.1, 136.7, 128.6, 128.1, 127.9, 67.4, 60.4, 56.4, 53.5, 47.1, 28.8, 24.6; HRMS (CI): Exact mass calcd for C₁₈H₂₂N₂O₇ [M]⁺ 378.1422. Found 378.1412.

[167] Corey, E. J.; Shibata, S.; Bakshi, R. K. *J. Org. Chem.* **1988**, *53*, 2861.
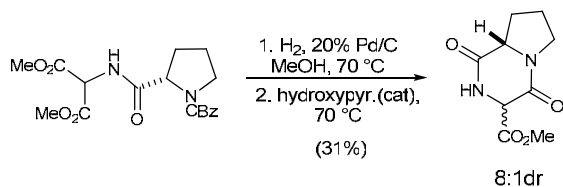
1,4-Dioxo-octahydro-pyrrolo[1,2-a]pyrazine-3-carboxylic acid methyl ester (236). To a solution of **250** (100 mg, 0.26 mmol) in methanol (14 mL) was added 10% Pd/C (60 mg). The flask was purged with H_2 and the mixture was stirred at 70 °C under an atomosphere of H_2 for 3h. The product was filtered throught celite, quenched with sat. $NaHCO_3$ and extracted with chloroform. Drying with Na_2SO_4 and concentration gave a yellow oil which was dissolved in toluene and stirred with 2-hydroxypyridine (cat. amt.) at 100 °C. Concentration and purification by flash chromatography (SiO_2, 80% ethyl acetate in hexanes) furnished the product as a colorless oil (17.6 mg, 31%).[168]
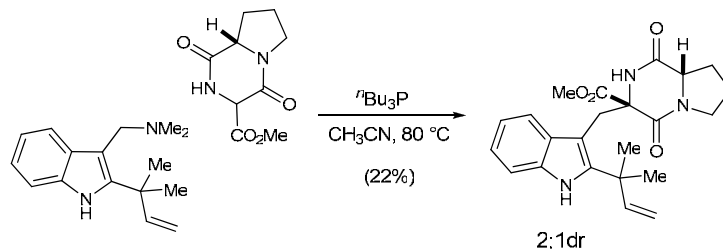
(S)-Methyl 3-((2-(2-methylbut-3-en-2-yl)-1H-indol-3-yl)methyl)-1,4-dioxo-octahydropyrrolo[1,2-a]pyrazine-3-carboxylate (251). To a solution of indole **237** (402.2 mg, 2.2 mmol) and piperazinedione **236** (460.6 mg, 2.2 mmol) in acetonitrile (10 mL) was added tri-*n*-butyl phosphine (541 μL). The solution was heated to 80 °C for 20h, then concentrated, taken up in 0.5M HCl, and extracted with dichloromethane. Drying with Na_2SO_4 followed by concentration and purification by flash chromatography (SiO_2, 60% ethyl acetate in hexanes) furnished the product as an off-white solid and a 2:1 mixture of diastereomers (127.5 mg, 22%).[2]

---
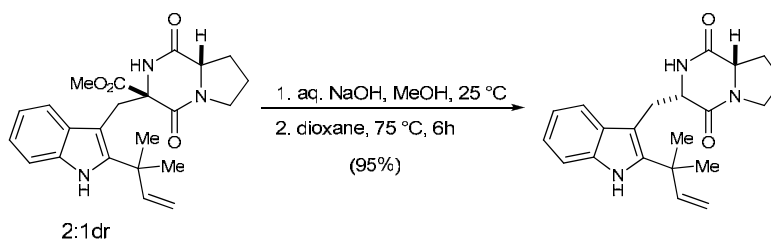
[168] Kardassis, G.; Brungs, P.; Steckhan, E. *Tetrahedron* **1998**, *54*, 3471.

epi-**Deoxybrevianamide E (205).** To a solution of **251** (118 mg, 0.29 mmol) in methanol (1 mL) was added 3M NaOH (143 µL, 0.43 mmol). The solution was stirred at room temperature for 2 days, then concentrated and several drops of 3M HCl added, which afforded a white precipitate. Extraction with dichloromethane, drying with Na_2SO_4 and concentration gave the product as a colorless oil which was taken up in dioxane (1 mL) and heated at 75 °C for 6 h. Concentration of the reaction mixture furnished the crude product as an oil (96 mg, 95%) and a 9:1 mixture of diastereomers.[169]
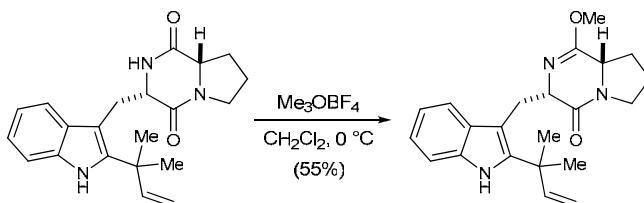
(3R,8aS)-1-Methoxy-3-((2-(2-methylbut-3-en-2-yl)-1H-indol-3-yl)methyl)-6,7,8,8a-tetrahydropyrrolo[1,2-a]pyrazin-4(3H)-one (222). A solution of **205** (134.4 mg, 380 µmol) in dichloromethane (3 mL) was stirred at 0 °C for 10 m. Me_3OBF_4 (169.8 mg, 1.2 mmol) was then added and the suspension was stirred at 0 °C for 12 h. The crude product was partitioned between dichloromethane and aq. $NaHCO_3$ and extracted with dichloromethane. Drying with Na_2SO_4, concentration, and purification by pipette column (SiO_2. ethyl acetate) furnished the product as a yellow oil (40.5 mg, 55%).[1b]
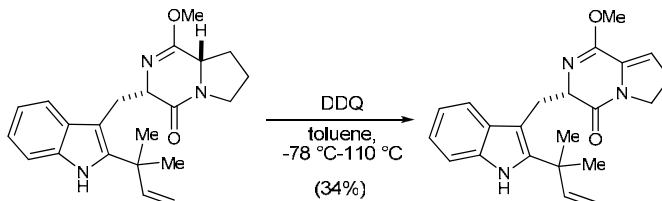
(S)-1-Methoxy-3-((2-(2-methylbut-3-en-2-yl)-1H-indol-3-yl)methyl)-6,7-dihydropyrrolo[1,2-a]pyrazin-4(3H)-one (223). To a solution of **222** (75.6 mg, 210 µmol) in toluene (5 mL) at -78 °C was added a solution of DDQ (57.1 mg, 250 µmol) in toluene (2 mL). The solution was stirred at -78 °C for 8 h, then was allowed to warm to room temperature overnight, followed by heating at 95 °C for 3 h. Concentration and purification by pipette column (SiO_2, 25% ethyl acetate in dichloromethane) furnished the product as a yellow oil (26.1 mg, 34%).[1b]

[169] Ritchie, R.; Saxton, J. E.; *Tetrahedron* **1981**, *37*, 4295.
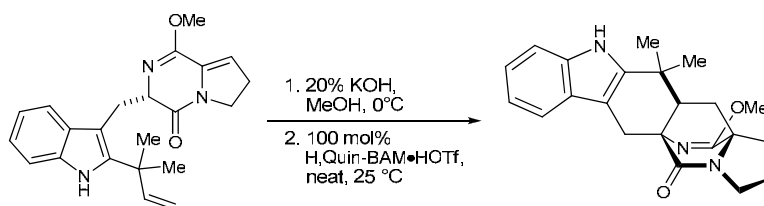
225. To a solution of amidate **223** (3.0 mg, 7 μmol) in methanol (0.5 mL) at 0 ºC was added 20% aqueous KOH (125 μL). The solution was stirred at 0 ºC for 30 min, then warmed to room temperature for an additional 30 min, monitoring by TLC to confirm consumption of amidate. The solution was concentrated, extracted with dichloromethane and the organic layers dried (Na$_2$SO$_4$) to give crude azadiene in solution. H,3-Quin-BAM·HOTf (4.3 mg, 7 μmol) was added and the solution was concentrated to remove all traces of solvent. The neat reaction mixture was allowed to stand at room temperature until the azadiene was fully consumed as determined by ^{1}H NMR. (~48 h) The product was then quenched with 1 M NaOH, extracted with dichloromethane and dried (Na$_2$SO$_4$). Concentration gave a 2.1:1 mixture of two diastereomers that were purified, but not separated, by flash chromatography (SiO$_2$, 20% ethyl acetate in dichloromethane); the major diastereomer was determined to be 35% *ee* by chiral HPLC analysis (Chiralcel® OD-H, 80:20 hexanes:^{i}PrOH, 1 mL/min, t_r(d$_1$e$_1$) = 9.6 min, t_r(d$_1$e$_2$) = 18.0 min).

Appendices

Appendix 1

R^1,R^2-BAM (**115**)

H,^{3}Me-BAM (**115a**)

H,^{5}Me-BAM (**115b**)

H,^{6}Me-BAM (**115c**)

H,^{1}Isoquin-BAM (**115d**)

H,Quin-BAM (**115e**)

H,Lep-BAM (**115f**)

Me,Quin-BAM (**115g**)

H,^{6}MeO-BAM (**115h**)

H(Me),^{6}Me-BAM (**115i**)

H(Bz),^{6}Me-BAM (**115j**)

Me,^{6}Me-BAM (**115k**)

H,Pyrazine-BAM (**115l**)

H,Pyrimidine-BAM (**115m**)

H,Quinox-BAM (**115n**)

H,Quin(^{2}Nap)-BAM (**115o**)

H,^{3}Quin-BAM (**115p**)

H,^{2}Quin(^{3}Quin)-BAM (**115q**)

H,^{6}(Ph$_2$COH)-BAM (**115r**)

2,6-di((*S*)-$^{\alpha Me}$Bn-amino)pyridine (**115s**)
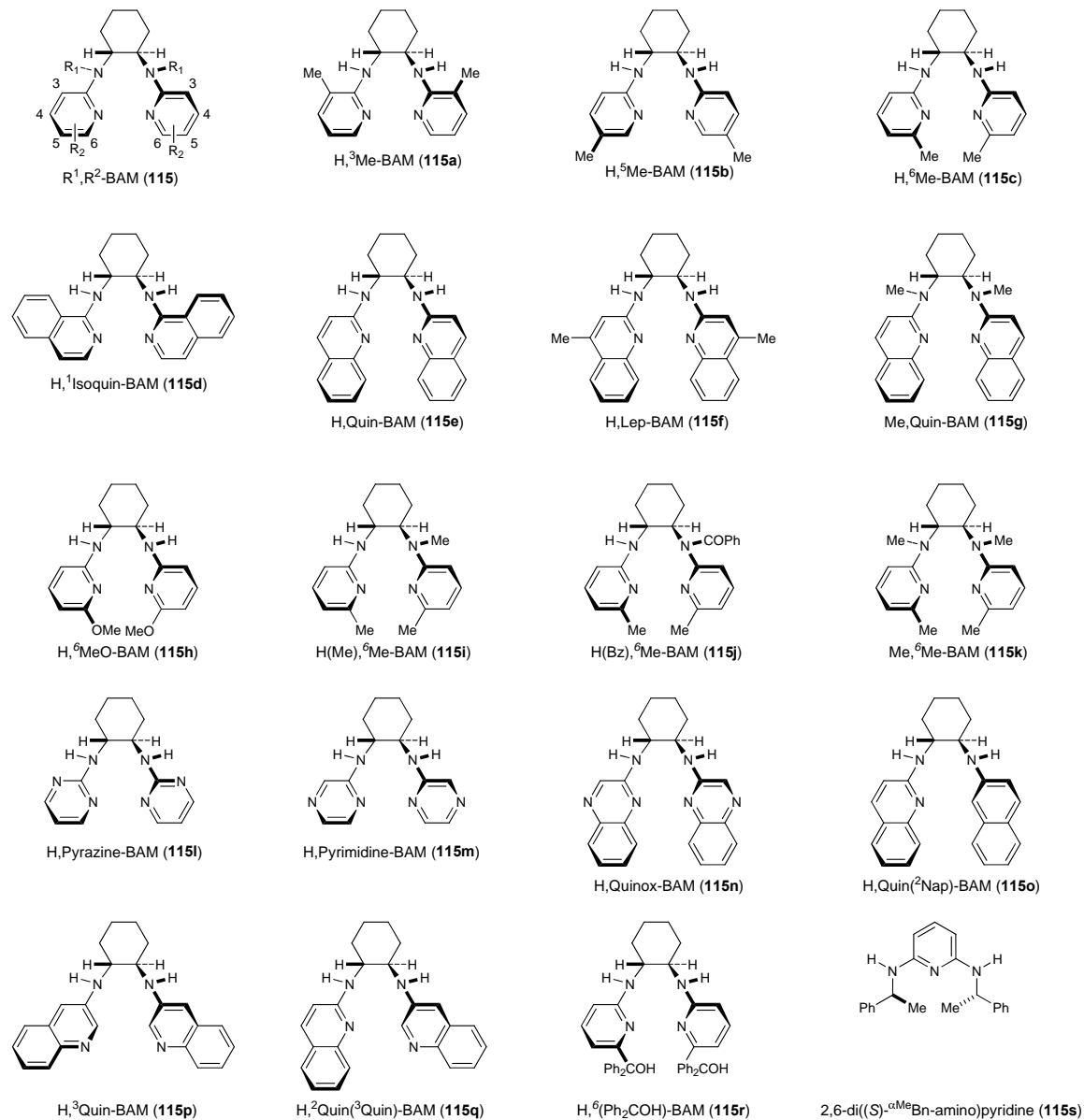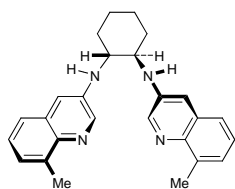
H,^{8}Me^{3}Quin-BAM (**115t**)

H,Quinox(^{3}Quin)-BAM (**115u**)
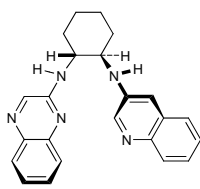
H,Quinox(^{2}Quin)-BAM (**115v**)
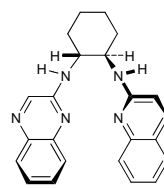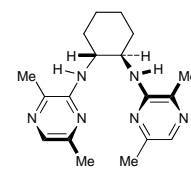
H,^{3,6}Me$_2$^{2}Pyrimidine-BAM (**115w**)
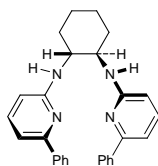
H,^{6}Ph-BAM (**115x**)
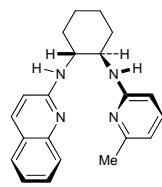
H,^{2}Quin(^{6}Me)-BAM (**115y**)
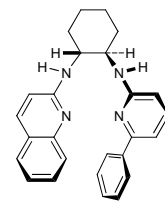
H,Quin(^{6}Ph)-BAM (**115z**)
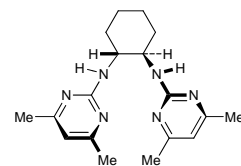
H,^{4,6}Me$_2$Pyrazine-BAM (**115aa**)
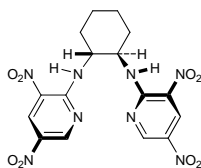
H,^{3,5}(NO$_2$)$_2$-BAM (**115bb**)
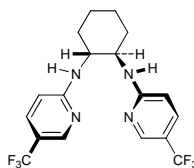
H,^{5}CF$_3$-BAM (**115cc**)
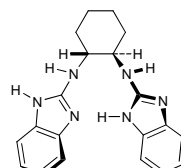
H,^{2}Imidazole-BAM (**115dd**)
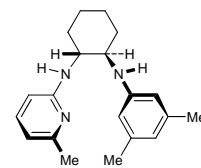
H,^{5}Xyl(^{6}Me)-BAM (**115ee**)
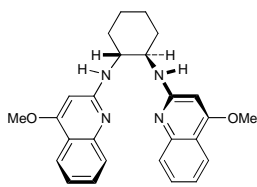
H,^{4}MeOQuin-BAM (**115ii**)
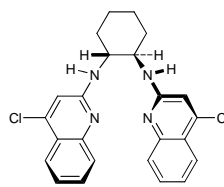
H,^{4}ClQuin-BAM (**115jj**)
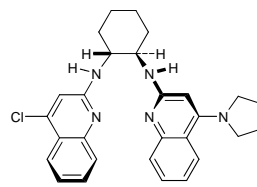
H,^{4}ClQuin(^{4}PyrrolidineQuin)-BAM (**115kk**)
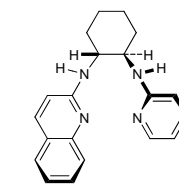
H,Quin(^{2}Pyr)-BAM (**115ll**)
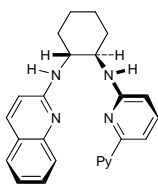
H,Quin(^{6}Pyrene)-BAM (**115ff**)
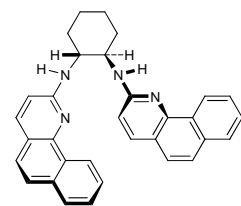
H,^{2}(^{7,8}benzoQuin)-BAM (**115gg**)
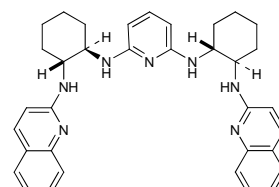
loss of all rational design-BAM (**115hh**)
or
miracle-BAM™ (**115hh**)

H,^{4,6}Me₂²Pyr-BAM (115mm)

H,Quin(⁶(¹Np)²Pyr)-BAM (115nn)

H,Quin(⁶(⁹Anth)²Pyr)-BAM (115oo)

H,Quin(EtO₂C)-BAM (115pp)

H,Quin(⁶BnOPyr)-BAM (115qq)

H,Quin(⁶Pyridone)-BAM (115rr)

H,⁶BnO-BAM (115ss)

H,⁶Pyridone-BAM (115tt)

H,Quin(²(⁴Quinolinone)-BAM (115uu)

H,Quin(⁴BnOQuin)-BAM (115vv)

H,⁴BnOQuin-BAM (115ww)

H,³Quin,Phen-BAM (115xx)
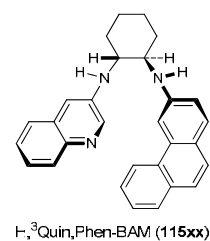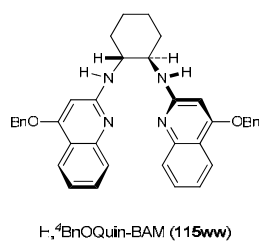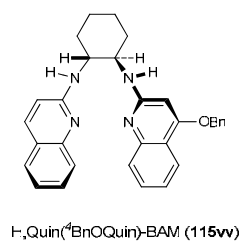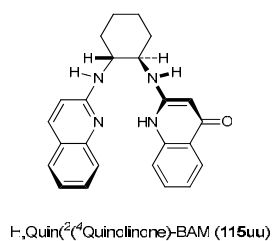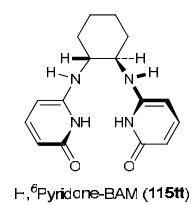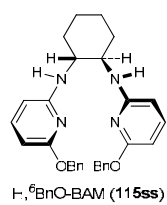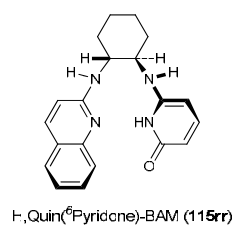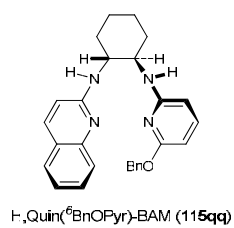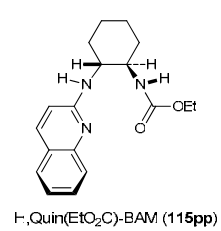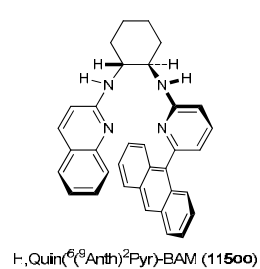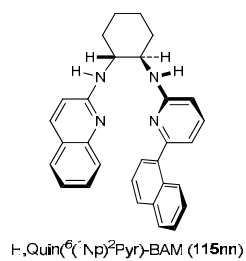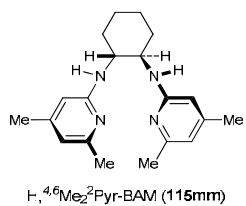
Appendix 2

Figure 39. Numbering System for **118c**
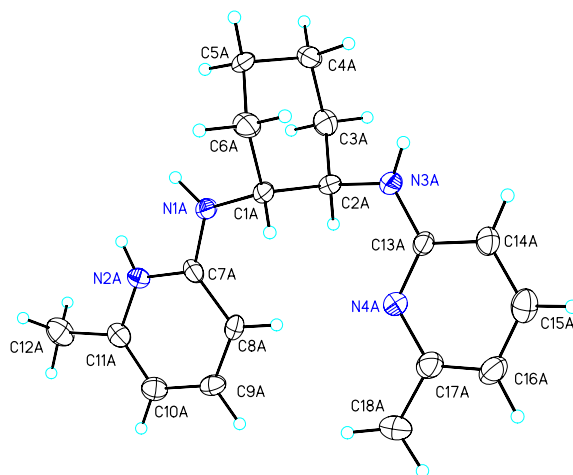
Note: Data were collected on a Bruker SMART 6000 sealed-tube system comprising a three-circle platform goniostat, an HOG crystal monochromator, a four kilopixel by four kilopixel single-chip CCD-based detector, a K761 high voltage generator, and a PC interface running Bruker's SMART software.

Table 28. Fractional Coordinates and Isotropic Thermal Parameters for **118c**

Atom	x	y	z	Uiso
S(1)	1000(1)	2352(1)	-2688(1)	28(1)
O(1)	2036(3)	1739(1)	-2701(2)	36(1)
O(2)	1357(3)	2961(1)	-1935(2)	35(1)
O(3)	452(3)	2594(2)	-3716(2)	51(1)
C(19)	-451(4)	1858(2)	-2094(3)	35(1)
F(1)	-821(2)	1225(1)	-2663(2)	50(1)
F(2)	-144(3)	1632(2)	-1100(2)	55(1)
F(3)	-1577(2)	2310(2)	-2076(2)	58(1)
S(2)	4531(1)	-327(1)	8104(1)	25(1)
O(4)	4102(3)	-909(1)	7324(2)	35(1)
O(5)	4894(3)	-596(2)	9162(2)	38(1)
O(6)	3656(3)	361(1)	8085(2)	33(1)
C(20)	6156(4)	29(2)	7613(3)	31(1)
F(4)	6016(3)	261(1)	6604(2)	49(1)
F(5)	6635(2)	632(1)	8199(2)	50(1)
F(6)	7142(2)	-522(1)	7665(2)	46(1)
N(1A)	2245(3)	402(2)	281(2)	27(1)
N(2A)	3338(3)	1519(2)	-248(2)	24(1)
N(3A)	-761(3)	-338(2)	1765(2)	28(1)

154

N(4A)	−454(3)	782(2)	2780(2)	28(1)
C(1A)	1508(3)	−83(2)	1032(3)	23(1)
C(2A)	−84(3)	8(2)	864(2)	22(1)
C(3A)	−593(4)	−351(2)	−198(3)	30(1)
C(4A)	−127(4)	−1193(2)	−340(3)	32(1)
C(5A)	1441(4)	−1268(2)	−180(3)	32(1)
C(6A)	1940(4)	−926(2)	906(3)	30(1)
C(7A)	2523(3)	1162(2)	457(3)	23(1)
C(8A)	2016(3)	1599(2)	1299(3)	24(1)
C(9A)	2436(3)	2356(2)	1395(3)	25(1)
C(10A)	3328(4)	2703(2)	676(3)	29(1)
C(11A)	3766(3)	2277(2)	−154(3)	26(1)
C(12A)	4687(4)	2561(2)	−991(3)	36(1)
C(13A)	−921(3)	49(2)	2705(3)	22(1)
C(14A)	−1574(3)	−313(2)	3552(3)	28(1)
C(15A)	−1792(4)	103(2)	4462(3)	32(1)
C(16A)	−1345(4)	876(2)	4527(3)	32(1)
C(17A)	−688(4)	1187(2)	3679(3)	30(1)
C(18A)	−167(4)	2014(2)	3691(3)	42(1)
N(1B)	3733(3)	1347(2)	5499(2)	25(1)
N(2B)	2190(3)	373(2)	5893(2)	23(1)
N(3B)	5294(3)	2414(2)	3258(2)	30(1)
N(4B)	5375(3)	1176(2)	2533(2)	25(1)
C(1B)	4843(3)	1706(2)	4906(3)	24(1)
C(2B)	4218(3)	2204(2)	3975(2)	24(1)
C(3B)	3522(4)	2940(2)	4397(3)	27(1)
C(4B)	4511(4)	3409(2)	5137(3)	31(1)
C(5B)	5043(4)	2919(2)	6083(3)	31(1)
C(6B)	5777(3)	2189(2)	5673(3)	28(1)
C(7B)	3082(3)	681(2)	5206(3)	22(1)
C(8B)	3276(3)	286(2)	4242(3)	25(1)
C(9B)	2550(3)	−389(2)	4059(3)	27(1)
C(10B)	1653(4)	−696(2)	4789(3)	30(1)
C(11B)	1480(3)	−311(2)	5718(3)	28(1)
C(12B)	592(4)	−572(2)	6592(3)	39(1)
C(13B)	5779(4)	1928(2)	2488(3)	24(1)
C(14B)	6658(4)	2205(2)	1723(3)	30(1)
C(15B)	7087(4)	1699(2)	955(3)	34(1)
C(16B)	6646(4)	933(2)	968(3)	29(1)
C(17B)	5830(3)	692(2)	1771(3)	25(1)
C(18B)	5383(4)	−140(2)	1867(3)	32(1)
H(1NA)	267(4)	19(2)	−35(3)	41(11)
H(2NA)	354(4)	121(2)	−79(3)	24(9)
H(3NA)	−93(4)	−83(2)	172(3)	29(10)
H(1A)	178	9	178	5(7)
H(2A)	−31	57	85	14(8)
H(3A)	−25	−4	−79	25(9)
H(3B)	−162	−33	−25	15(8)
H(4A)	−58	−153	18	37(10)
H(4B)	−42	−137	−107	29(10)
H(5A)	190	−99	−76	28(9)
H(5B)	171	−182	−21	59(13)
H(6A)	155	−124	149	41(11)
H(6B)	297	−96	98	16(8)
H(8A)	140	138	179	29(9)
H(9A)	211	266	197	21(8)
H(10A)	362	323	77	41(11)
H(12A)	495	310	−84	110(20)
H(12B)	419	253	−169	110(20)
H(12C)	552	224	−100	110(20)
H(14A)	−186	−84	350	12(8)
H(15A)	−224	−13	504	48(12)

H(16A)	-150	118	515	61(13)
H(18A)	84	202	360	89(18)
H(18B)	-37	226	437	62(13)
H(18C)	-64	230	310	62(14)
H(1NB)	353(4)	151(2)	611(3)	29(10)
H(2NB)	210(3)	57(2)	647(3)	17(9)
H(3NB)	545(3)	281(2)	318(2)	5(8)
H(1BA)	542	129	460	22(9)
H(2BA)	350	189	357	34(10)
H(3BA)	320	327	378	37(10)
H(3BB)	270	279	479	29(9)
H(4C)	531	359	473	41(11)
H(4D)	402	387	540	24(9)
H(5C)	426	276	652	29(9)
H(5D)	570	323	654	39(11)
H(6C)	662	235	530	23(8)
H(6D)	608	186	629	36(10)
H(8B)	389	48	373	15(8)
H(9B)	266	-66	341	21(8)
H(10B)	117	-117	464	30(9)
H(12D)	-6	-16	676	71(16)
H(12E)	118	-69	723	76(16)
H(12F)	7	-104	636	40(11)
H(14B)	695	273	173	70(15)
H(15B)	768	187	42	40(11)
H(16B)	691	58	43	17(8)
H(18D)	558	-42	121	49(12)
H(18E)	438	-16	198	38(11)
H(18F)	590	-38	248	37(10)

Notes:
1) Fractional coordinates are X 10**4 for non-hydrogen
atoms and X 10**3 for hydrogen atoms. Uiso values are all
X 10**3.
2) Isotropic values for those atoms refined anisotropically
are calculated as one third of the trace of the
orthogonalized
Uij tensor.
3) Parameters without standard deviations were not varied.

Table 29. Anisotropic Thermal Parameters for **118c**

Atom	U11	U22	U33	U23	U13	U12
S(1)	35(1)	22(1)	27(1)	-1(1)	5(1)	0(1)
O(1)	38(2)	26(1)	45(2)	-5(1)	11(1)	2(1)
O(2)	41(2)	21(1)	42(2)	-6(1)	0(1)	2(1)
O(3)	76(2)	46(2)	31(2)	8(1)	-9(1)	-7(2)
C(19)	33(2)	36(2)	36(2)	-3(2)	8(2)	-3(2)
F(1)	50(1)	35(1)	66(2)	-14(1)	12(1)	-15(1)
F(2)	62(2)	59(2)	44(1)	14(1)	17(1)	-6(1)
F(3)	31(1)	48(1)	95(2)	-14(1)	13(1)	7(1)
S(2)	26(1)	20(1)	28(1)	-2(1)	5(1)	2(1)
O(4)	35(1)	22(1)	46(2)	-10(1)	3(1)	-1(1)
O(5)	51(2)	31(1)	33(1)	6(1)	8(1)	4(1)
O(6)	34(1)	29(1)	37(1)	-9(1)	1(1)	12(1)
C(20)	35(2)	27(2)	33(2)	-1(2)	7(2)	2(2)
F(4)	58(2)	55(2)	37(1)	11(1)	17(1)	-2(1)
F(5)	46(1)	41(1)	62(2)	-12(1)	11(1)	-21(1)

```
F(6)      29(1)     51(2)     57(1)     -5(1)      3(1)     12(1)
N(1A)     32(2)     19(1)     32(2)     -6(1)     14(1)     -6(1)
N(2A)     26(2)     17(1)     29(2)     -3(1)      1(1)     -2(1)
N(3A)     32(2)     23(2)     28(2)     -4(1)      9(1)     -6(1)
N(4A)     28(2)     28(2)     27(2)     -6(1)      3(1)     -2(1)
C(1A)     26(2)     17(2)     28(2)     -3(1)      7(2)     -2(1)
C(2A)     26(2)     18(2)     23(2)     -5(1)      3(1)     -1(1)
C(3A)     26(2)     31(2)     33(2)     -2(2)      0(2)     -3(2)
C(4A)     39(2)     27(2)     29(2)     -8(2)      8(2)    -11(2)
C(5A)     35(2)     19(2)     42(2)    -11(2)     15(2)     -4(2)
C(6A)     27(2)     17(2)     45(2)     -1(2)      2(2)      2(1)
C(7A)     20(2)     20(2)     29(2)      2(1)      0(1)     -3(1)
C(8A)     20(2)     25(2)     26(2)      0(1)      3(1)      3(1)
C(9A)     32(2)     17(2)     27(2)     -3(1)     -2(1)      3(2)
C(10A)    34(2)     21(2)     32(2)      1(2)     -3(2)      0(2)
C(11A)    24(2)     23(2)     31(2)      3(2)     -2(1)     -4(2)
C(12A)    40(2)     29(2)     39(2)      9(2)      2(2)     -9(2)
C(13A)    19(2)     25(2)     22(2)     -2(1)      1(1)      1(1)
C(14A)    22(2)     30(2)     31(2)     -2(2)      2(1)      1(2)
C(15A)    25(2)     42(2)     29(2)      3(2)      1(2)      1(2)
C(16A)    28(2)     43(2)     25(2)    -11(2)      1(2)      2(2)
C(17A)    24(2)     35(2)     30(2)     -7(2)     -3(2)      3(2)
C(18A)    46(2)     36(2)     45(2)    -15(2)      5(2)     -9(2)
N(1B)     32(2)     22(2)     21(2)      1(1)      7(1)     -2(1)
N(2B)     25(2)     21(1)     21(2)     -2(1)      3(1)     -2(1)
N(3B)     44(2)     14(2)     34(2)      4(1)     14(1)     -2(1)
N(4B)     26(2)     24(1)     26(2)      0(1)      3(1)      1(1)
C(1B)     26(2)     24(2)     24(2)      3(1)      6(1)     -2(1)
C(2B)     26(2)     21(2)     25(2)     -1(1)      4(1)      2(1)
C(3B)     32(2)     19(2)     31(2)      1(1)     10(2)      2(2)
C(4B)     36(2)     22(2)     36(2)     -6(2)     12(2)     -1(2)
C(5B)     35(2)     29(2)     30(2)     -3(2)      5(2)    -13(2)
C(6B)     26(2)     28(2)     31(2)      4(2)      0(2)     -8(2)
C(7B)     20(2)     20(2)     25(2)      3(1)     -1(1)      5(1)
C(8B)     28(2)     23(2)     25(2)      1(1)      3(2)      2(2)
C(9B)     32(2)     20(2)     28(2)     -3(1)     -2(1)      7(2)
C(10B)    29(2)     19(2)     41(2)     -3(2)     -4(2)     -2(2)
C(11B)    23(2)     25(2)     34(2)      5(2)     -2(1)     -2(2)
C(12B)    37(2)     31(2)     49(2)      1(2)     10(2)    -13(2)
C(13B)    26(2)     26(2)     21(2)      1(1)      4(1)      4(1)
C(14B)    34(2)     28(2)     29(2)      5(2)      7(2)      2(2)
C(15B)    32(2)     37(2)     32(2)      7(2)     13(2)      8(2)
C(16B)    26(2)     30(2)     32(2)     -3(2)      4(2)      9(2)
C(17B)    19(2)     30(2)     25(2)     -4(1)     -2(1)      5(1)
C(18B)    31(2)     30(2)     34(2)     -8(2)      1(2)     -6(2)
```

Form of the anisotropic thermal parameter:
  exp{ -2 pi**2 [h**2 (a*)**2 U11 + ... + 2 h k (a*) (b*) U12] }
All values are X 10**3

Table 30. Bond distances for **118c**

```
    A              B            Distance

   S(1)           O(3)          1.429(3)
   S(1)           O(2)          1.442(2)
   S(1)           O(1)          1.453(3)
   S(1)           C(19)         1.824(4)
   C(19)          F(2)          1.323(4)
   C(19)          F(3)          1.336(4)
```

157

C(19)	F(1)	1.341(4)
S(2)	O(5)	1.430(3)
S(2)	O(4)	1.445(3)
S(2)	O(6)	1.454(2)
S(2)	C(20)	1.814(4)
C(20)	F(4)	1.326(4)
C(20)	F(6)	1.341(4)
C(20)	F(5)	1.342(4)
N(1A)	C(7A)	1.353(4)
N(1A)	C(1A)	1.465(4)
N(1A)	H(1NA)	0.98(4)
N(2A)	C(7A)	1.357(4)
N(2A)	C(11A)	1.373(4)
N(2A)	H(2NA)	0.90(4)
N(3A)	C(13A)	1.367(4)
N(3A)	C(2A)	1.456(4)
N(3A)	H(3NA)	0.86(4)
N(4A)	C(13A)	1.343(4)
N(4A)	C(17A)	1.352(4)
C(1A)	C(6A)	1.522(4)
C(1A)	C(2A)	1.544(5)
C(1A)	H(1A)	1.0000
C(2A)	C(3A)	1.526(4)
C(2A)	H(2A)	1.0000
C(3A)	C(4A)	1.532(5)
C(3A)	H(3A)	0.9900
C(3A)	H(3B)	0.9900
C(4A)	C(5A)	1.518(5)
C(4A)	H(4A)	0.9900
C(4A)	H(4B)	0.9900
C(5A)	C(6A)	1.538(5)
C(5A)	H(5A)	0.9900
C(5A)	H(5B)	0.9900
C(6A)	H(6A)	0.9900
C(6A)	H(6B)	0.9900
C(7A)	C(8A)	1.401(4)
C(8A)	C(9A)	1.371(5)
C(8A)	H(8A)	0.9500
C(9A)	C(10A)	1.406(5)
C(9A)	H(9A)	0.9500
C(10A)	C(11A)	1.356(5)
C(10A)	H(10A)	0.9500
C(11A)	C(12A)	1.486(5)
C(12A)	H(12A)	0.9800
C(12A)	H(12B)	0.9800
C(12A)	H(12C)	0.9800
C(13A)	C(14A)	1.404(5)
C(14A)	C(15A)	1.369(5)
C(14A)	H(14A)	0.9500
C(15A)	C(16A)	1.402(5)
C(15A)	H(15A)	0.9500
C(16A)	C(17A)	1.370(5)
C(16A)	H(16A)	0.9500
C(17A)	C(18A)	1.511(5)
C(18A)	H(18A)	0.9800
C(18A)	H(18B)	0.9800
C(18A)	H(18C)	0.9800
N(1B)	C(7B)	1.351(4)
N(1B)	C(1B)	1.466(4)
N(1B)	H(1NB)	0.84(4)
N(2B)	C(7B)	1.352(4)
N(2B)	C(11B)	1.376(4)
N(2B)	H(2NB)	0.80(3)

```
N(3B)          C(13B)          1.374(4)
N(3B)          C(2B)           1.447(4)
N(3B)          H(3NB)          0.70(3)
N(4B)          C(17B)          1.354(4)
N(4B)          C(13B)          1.356(4)
C(1B)          C(6B)           1.530(5)
C(1B)          C(2B)           1.547(4)
C(1B)          H(1BA)          1.0000
C(2B)          C(3B)           1.539(4)
C(2B)          H(2BA)          1.0000
C(3B)          C(4B)           1.528(5)
C(3B)          H(3BA)          0.9900
C(3B)          H(3BB)          0.9900
C(4B)          C(5B)           1.523(5)
C(4B)          H(4C)           0.9900
C(4B)          H(4D)           0.9900
C(5B)          C(6B)           1.542(5)
C(5B)          H(5C)           0.9900
C(5B)          H(5D)           0.9900
C(6B)          H(6C)           0.9900
C(6B)          H(6D)           0.9900
C(7B)          C(8B)           1.405(4)
C(8B)          C(9B)           1.371(5)
C(8B)          H(8B)           0.9500
C(9B)          C(10B)          1.391(5)
C(9B)          H(9B)           0.9500
C(10B)         C(11B)          1.355(5)
C(10B)         H(10B)          0.9500
C(11B)         C(12B)          1.489(5)
C(12B)         H(12D)          0.9800
C(12B)         H(12E)          0.9800
C(12B)         H(12F)          0.9800
C(13B)         C(14B)          1.392(5)
C(14B)         C(15B)          1.376(5)
C(14B)         H(14B)          0.9500
C(15B)         C(16B)          1.387(5)
C(15B)         H(15B)          0.9500
C(16B)         C(17B)          1.369(5)
C(16B)         H(16B)          0.9500
C(17B)         C(18B)          1.505(5)
C(18B)         H(18D)          0.9800
C(18B)         H(18E)          0.9800
C(18B)         H(18F)          0.9800
```

Table 31. Bond Angles for **118c**

A	B	C	Angle
O(3)	S(1)	O(2)	116.22(17)
O(3)	S(1)	O(1)	115.22(16)
O(2)	S(1)	O(1)	113.21(15)
O(3)	S(1)	C(19)	104.26(18)
O(2)	S(1)	C(19)	103.74(16)
O(1)	S(1)	C(19)	101.82(16)
F(2)	C(19)	F(3)	107.6(3)
F(2)	C(19)	F(1)	107.6(3)
F(3)	C(19)	F(1)	106.7(3)
F(2)	C(19)	S(1)	112.2(3)
F(3)	C(19)	S(1)	111.8(3)
F(1)	C(19)	S(1)	110.6(3)
O(5)	S(2)	O(4)	116.69(16)
O(5)	S(2)	O(6)	113.28(15)

O(4)	S(2)	O(6)	114.09(15)
O(5)	S(2)	C(20)	104.22(17)
O(4)	S(2)	C(20)	103.27(16)
O(6)	S(2)	C(20)	103.13(16)
F(4)	C(20)	F(6)	107.5(3)
F(4)	C(20)	F(5)	107.6(3)
F(6)	C(20)	F(5)	107.3(3)
F(4)	C(20)	S(2)	111.9(3)
F(6)	C(20)	S(2)	111.3(2)
F(5)	C(20)	S(2)	110.9(2)
C(7A)	N(1A)	C(1A)	123.0(3)
C(7A)	N(1A)	H(1NA)	114(2)
C(1A)	N(1A)	H(1NA)	123(2)
C(7A)	N(2A)	C(11A)	123.9(3)
C(7A)	N(2A)	H(2NA)	112(2)
C(11A)	N(2A)	H(2NA)	124(2)
C(13A)	N(3A)	C(2A)	122.6(3)
C(13A)	N(3A)	H(3NA)	120(2)
C(2A)	N(3A)	H(3NA)	116(2)
C(13A)	N(4A)	C(17A)	118.4(3)
N(1A)	C(1A)	C(6A)	109.6(3)
N(1A)	C(1A)	C(2A)	111.3(3)
C(6A)	C(1A)	C(2A)	110.9(3)
N(1A)	C(1A)	H(1A)	108.3
C(6A)	C(1A)	H(1A)	108.3
C(2A)	C(1A)	H(1A)	108.3
N(3A)	C(2A)	C(3A)	111.8(3)
N(3A)	C(2A)	C(1A)	109.3(3)
C(3A)	C(2A)	C(1A)	110.7(3)
N(3A)	C(2A)	H(2A)	108.3
C(3A)	C(2A)	H(2A)	108.3
C(1A)	C(2A)	H(2A)	108.3
C(2A)	C(3A)	C(4A)	113.7(3)
C(2A)	C(3A)	H(3A)	108.8
C(4A)	C(3A)	H(3A)	108.8
C(2A)	C(3A)	H(3B)	108.8
C(4A)	C(3A)	H(3B)	108.8
H(3A)	C(3A)	H(3B)	107.7
C(5A)	C(4A)	C(3A)	111.1(3)
C(5A)	C(4A)	H(4A)	109.4
C(3A)	C(4A)	H(4A)	109.4
C(5A)	C(4A)	H(4B)	109.4
C(3A)	C(4A)	H(4B)	109.4
H(4A)	C(4A)	H(4B)	108.0
C(4A)	C(5A)	C(6A)	110.6(3)
C(4A)	C(5A)	H(5A)	109.5
C(6A)	C(5A)	H(5A)	109.5
C(4A)	C(5A)	H(5B)	109.5
C(6A)	C(5A)	H(5B)	109.5
H(5A)	C(5A)	H(5B)	108.1
C(1A)	C(6A)	C(5A)	112.5(3)
C(1A)	C(6A)	H(6A)	109.1
C(5A)	C(6A)	H(6A)	109.1
C(1A)	C(6A)	H(6B)	109.1
C(5A)	C(6A)	H(6B)	109.1
H(6A)	C(6A)	H(6B)	107.8
N(1A)	C(7A)	N(2A)	116.7(3)
N(1A)	C(7A)	C(8A)	124.8(3)
N(2A)	C(7A)	C(8A)	118.5(3)
C(9A)	C(8A)	C(7A)	117.8(3)
C(9A)	C(8A)	H(8A)	121.1
C(7A)	C(8A)	H(8A)	121.1
C(8A)	C(9A)	C(10A)	122.4(3)

C(8A)	C(9A)	H(9A)	118.8
C(10A)	C(9A)	H(9A)	118.8
C(11A)	C(10A)	C(9A)	118.8(3)
C(11A)	C(10A)	H(10A)	120.6
C(9A)	C(10A)	H(10A)	120.6
C(10A)	C(11A)	N(2A)	118.5(3)
C(10A)	C(11A)	C(12A)	125.4(3)
N(2A)	C(11A)	C(12A)	116.1(3)
C(11A)	C(12A)	H(12A)	109.5
C(11A)	C(12A)	H(12B)	109.5
H(12A)	C(12A)	H(12B)	109.5
C(11A)	C(12A)	H(12C)	109.5
H(12A)	C(12A)	H(12C)	109.5
H(12B)	C(12A)	H(12C)	109.5
N(4A)	C(13A)	N(3A)	117.9(3)
N(4A)	C(13A)	C(14A)	121.7(3)
N(3A)	C(13A)	C(14A)	120.3(3)
C(15A)	C(14A)	C(13A)	119.1(3)
C(15A)	C(14A)	H(14A)	120.5
C(13A)	C(14A)	H(14A)	120.5
C(14A)	C(15A)	C(16A)	119.2(3)
C(14A)	C(15A)	H(15A)	120.4
C(16A)	C(15A)	H(15A)	120.4
C(17A)	C(16A)	C(15A)	118.6(3)
C(17A)	C(16A)	H(16A)	120.7
C(15A)	C(16A)	H(16A)	120.7
N(4A)	C(17A)	C(16A)	122.9(3)
N(4A)	C(17A)	C(18A)	115.3(3)
C(16A)	C(17A)	C(18A)	121.9(3)
C(17A)	C(18A)	H(18A)	109.5
C(17A)	C(18A)	H(18B)	109.5
H(18A)	C(18A)	H(18B)	109.5
C(17A)	C(18A)	H(18C)	109.5
H(18A)	C(18A)	H(18C)	109.5
H(18B)	C(18A)	H(18C)	109.5
C(7B)	N(1B)	C(1B)	124.2(3)
C(7B)	N(1B)	H(1NB)	114(3)
C(1B)	N(1B)	H(1NB)	122(3)
C(7B)	N(2B)	C(11B)	124.2(3)
C(7B)	N(2B)	H(2NB)	120(2)
C(11B)	N(2B)	H(2NB)	116(2)
C(13B)	N(3B)	C(2B)	124.0(3)
C(13B)	N(3B)	H(3NB)	114(3)
C(2B)	N(3B)	H(3NB)	119(3)
C(17B)	N(4B)	C(13B)	117.2(3)
N(1B)	C(1B)	C(6B)	109.5(3)
N(1B)	C(1B)	C(2B)	110.4(3)
C(6B)	C(1B)	C(2B)	111.5(3)
N(1B)	C(1B)	H(1BA)	108.5
C(6B)	C(1B)	H(1BA)	108.5
C(2B)	C(1B)	H(1BA)	108.5
N(3B)	C(2B)	C(3B)	110.1(3)
N(3B)	C(2B)	C(1B)	110.0(3)
C(3B)	C(2B)	C(1B)	111.1(3)
N(3B)	C(2B)	H(2BA)	108.6
C(3B)	C(2B)	H(2BA)	108.6
C(1B)	C(2B)	H(2BA)	108.6
C(4B)	C(3B)	C(2B)	112.0(3)
C(4B)	C(3B)	H(3BA)	109.2
C(2B)	C(3B)	H(3BA)	109.2
C(4B)	C(3B)	H(3BB)	109.2
C(2B)	C(3B)	H(3BB)	109.2
H(3BA)	C(3B)	H(3BB)	107.9

161

C(5B)	C(4B)	C(3B)	110.8(3)
C(5B)	C(4B)	H(4C)	109.5
C(3B)	C(4B)	H(4C)	109.5
C(5B)	C(4B)	H(4D)	109.5
C(3B)	C(4B)	H(4D)	109.5
H(4C)	C(4B)	H(4D)	108.1
C(4B)	C(5B)	C(6B)	109.7(3)
C(4B)	C(5B)	H(5C)	109.7
C(6B)	C(5B)	H(5C)	109.7
C(4B)	C(5B)	H(5D)	109.7
C(6B)	C(5B)	H(5D)	109.7
H(5C)	C(5B)	H(5D)	108.2
C(1B)	C(6B)	C(5B)	112.8(3)
C(1B)	C(6B)	H(6C)	109.0
C(5B)	C(6B)	H(6C)	109.0
C(1B)	C(6B)	H(6D)	109.0
C(5B)	C(6B)	H(6D)	109.0
H(6C)	C(6B)	H(6D)	107.8
N(1B)	C(7B)	N(2B)	117.5(3)
N(1B)	C(7B)	C(8B)	124.5(3)
N(2B)	C(7B)	C(8B)	118.0(3)
C(9B)	C(8B)	C(7B)	117.9(3)
C(9B)	C(8B)	H(8B)	121.1
C(7B)	C(8B)	H(8B)	121.1
C(8B)	C(9B)	C(10B)	122.7(3)
C(8B)	C(9B)	H(9B)	118.7
C(10B)	C(9B)	H(9B)	118.7
C(11B)	C(10B)	C(9B)	118.9(3)
C(11B)	C(10B)	H(10B)	120.6
C(9B)	C(10B)	H(10B)	120.6
C(10B)	C(11B)	N(2B)	118.4(3)
C(10B)	C(11B)	C(12B)	125.5(3)
N(2B)	C(11B)	C(12B)	116.1(3)
C(11B)	C(12B)	H(12D)	109.5
C(11B)	C(12B)	H(12E)	109.5
H(12D)	C(12B)	H(12E)	109.5
C(11B)	C(12B)	H(12F)	109.5
H(12D)	C(12B)	H(12F)	109.5
H(12E)	C(12B)	H(12F)	109.5
N(4B)	C(13B)	N(3B)	116.5(3)
N(4B)	C(13B)	C(14B)	122.8(3)
N(3B)	C(13B)	C(14B)	120.7(3)
C(15B)	C(14B)	C(13B)	118.4(3)
C(15B)	C(14B)	H(14B)	120.8
C(13B)	C(14B)	H(14B)	120.8
C(14B)	C(15B)	C(16B)	119.6(3)
C(14B)	C(15B)	H(15B)	120.2
C(16B)	C(15B)	H(15B)	120.2
C(17B)	C(16B)	C(15B)	118.9(3)
C(17B)	C(16B)	H(16B)	120.5
C(15B)	C(16B)	H(16B)	120.5
N(4B)	C(17B)	C(16B)	123.1(3)
N(4B)	C(17B)	C(18B)	115.3(3)
C(16B)	C(17B)	C(18B)	121.6(3)
C(17B)	C(18B)	H(18D)	109.5
C(17B)	C(18B)	H(18E)	109.5
H(18D)	C(18B)	H(18E)	109.5
C(17B)	C(18B)	H(18F)	109.5
H(18D)	C(18B)	H(18F)	109.5
H(18E)	C(18B)	H(18F)	109.5

Table 32. Torsion Angles for **118c**

A	B	C	D	Torsion Angle
O(3)	S(1)	C(19)	F(2)	-176.3(3)
O(2)	S(1)	C(19)	F(2)	-54.2(3)
O(1)	S(1)	C(19)	F(2)	63.6(3)
O(3)	S(1)	C(19)	F(3)	-55.3(3)
O(2)	S(1)	C(19)	F(3)	66.8(3)
O(1)	S(1)	C(19)	F(3)	-175.4(3)
O(3)	S(1)	C(19)	F(1)	63.5(3)
O(2)	S(1)	C(19)	F(1)	-174.4(2)
O(1)	S(1)	C(19)	F(1)	-56.6(3)
O(5)	S(2)	C(20)	F(4)	176.3(2)
O(4)	S(2)	C(20)	F(4)	53.9(3)
O(6)	S(2)	C(20)	F(4)	-65.1(3)
O(5)	S(2)	C(20)	F(6)	56.0(3)
O(4)	S(2)	C(20)	F(6)	-66.4(3)
O(6)	S(2)	C(20)	F(6)	174.5(2)
O(5)	S(2)	C(20)	F(5)	-63.5(3)
O(4)	S(2)	C(20)	F(5)	174.1(2)
O(6)	S(2)	C(20)	F(5)	55.1(3)
C(7A)	N(1A)	C(1A)	C(6A)	-153.3(3)
C(7A)	N(1A)	C(1A)	C(2A)	83.6(4)
C(13A)	N(3A)	C(2A)	C(3A)	-153.9(3)
C(13A)	N(3A)	C(2A)	C(1A)	83.2(4)
N(1A)	C(1A)	C(2A)	N(3A)	-167.3(3)
C(6A)	C(1A)	C(2A)	N(3A)	70.4(3)
N(1A)	C(1A)	C(2A)	C(3A)	69.2(3)
C(6A)	C(1A)	C(2A)	C(3A)	-53.1(4)
N(3A)	C(2A)	C(3A)	C(4A)	-69.1(4)
C(1A)	C(2A)	C(3A)	C(4A)	53.0(4)
C(2A)	C(3A)	C(4A)	C(5A)	-54.1(4)
C(3A)	C(4A)	C(5A)	C(6A)	54.1(4)
N(1A)	C(1A)	C(6A)	C(5A)	-67.4(4)
C(2A)	C(1A)	C(6A)	C(5A)	55.9(4)
C(4A)	C(5A)	C(6A)	C(1A)	-56.5(4)
C(1A)	N(1A)	C(7A)	N(2A)	173.3(3)
C(1A)	N(1A)	C(7A)	C(8A)	-7.6(5)
C(11A)	N(2A)	C(7A)	N(1A)	-177.0(3)
C(11A)	N(2A)	C(7A)	C(8A)	3.9(5)
N(1A)	C(7A)	C(8A)	C(9A)	177.5(3)
N(2A)	C(7A)	C(8A)	C(9A)	-3.4(4)
C(7A)	C(8A)	C(9A)	C(10A)	0.9(5)
C(8A)	C(9A)	C(10A)	C(11A)	1.3(5)
C(9A)	C(10A)	C(11A)	N(2A)	-1.0(5)
C(9A)	C(10A)	C(11A)	C(12A)	178.9(3)
C(7A)	N(2A)	C(11A)	C(10A)	-1.6(5)
C(7A)	N(2A)	C(11A)	C(12A)	178.5(3)
C(17A)	N(4A)	C(13A)	N(3A)	175.8(3)
C(17A)	N(4A)	C(13A)	C(14A)	-3.2(5)
C(2A)	N(3A)	C(13A)	N(4A)	1.3(5)
C(2A)	N(3A)	C(13A)	C(14A)	-179.6(3)
N(4A)	C(13A)	C(14A)	C(15A)	2.7(5)
N(3A)	C(13A)	C(14A)	C(15A)	-176.3(3)
C(13A)	C(14A)	C(15A)	C(16A)	-0.6(5)
C(14A)	C(15A)	C(16A)	C(17A)	-0.8(5)
C(13A)	N(4A)	C(17A)	C(16A)	1.8(5)
C(13A)	N(4A)	C(17A)	C(18A)	-178.4(3)
C(15A)	C(16A)	C(17A)	N(4A)	0.2(5)
C(15A)	C(16A)	C(17A)	C(18A)	-179.6(3)
C(7B)	N(1B)	C(1B)	C(6B)	-153.3(3)
C(7B)	N(1B)	C(1B)	C(2B)	83.6(4)
C(13B)	N(3B)	C(2B)	C(3B)	-157.2(3)

```
C(13B)      N(3B)      C(2B)      C(1B)         80.1(4)
N(1B)       C(1B)      C(2B)      N(3B)       -167.3(3)
C(6B)       C(1B)      C(2B)      N(3B)         70.8(3)
N(1B)       C(1B)      C(2B)      C(3B)         70.6(3)
C(6B)       C(1B)      C(2B)      C(3B)        -51.3(4)
N(3B)       C(2B)      C(3B)      C(4B)        -67.9(4)
C(1B)       C(2B)      C(3B)      C(4B)         54.1(4)
C(2B)       C(3B)      C(4B)      C(5B)        -58.0(4)
C(3B)       C(4B)      C(5B)      C(6B)         57.7(4)
N(1B)       C(1B)      C(6B)      C(5B)        -69.1(4)
C(2B)       C(1B)      C(6B)      C(5B)         53.3(4)
C(4B)       C(5B)      C(6B)      C(1B)        -56.3(4)
C(1B)       N(1B)      C(7B)      N(2B)        172.7(3)
C(1B)       N(1B)      C(7B)      C(8B)         -7.0(5)
C(11B)      N(2B)      C(7B)      N(1B)       -178.3(3)
C(11B)      N(2B)      C(7B)      C(8B)          1.4(5)
N(1B)       C(7B)      C(8B)      C(9B)        179.5(3)
N(2B)       C(7B)      C(8B)      C(9B)         -0.1(5)
C(7B)       C(8B)      C(9B)      C(10B)        -0.7(5)
C(8B)       C(9B)      C(10B)     C(11B)         0.5(5)
C(9B)       C(10B)     C(11B)     N(2B)          0.7(5)
C(9B)       C(10B)     C(11B)     C(12B)      -178.2(3)
C(7B)       N(2B)      C(11B)     C(10B)        -1.6(5)
C(7B)       N(2B)      C(11B)     C(12B)       177.4(3)
C(17B)      N(4B)      C(13B)     N(3B)        179.2(3)
C(17B)      N(4B)      C(13B)     C(14B)        -1.9(5)
C(2B)       N(3B)      C(13B)     N(4B)        -10.9(5)
C(2B)       N(3B)      C(13B)     C(14B)       170.1(3)
N(4B)       C(13B)     C(14B)     C(15B)         2.7(5)
N(3B)       C(13B)     C(14B)     C(15B)      -178.5(3)
C(13B)      C(14B)     C(15B)     C(16B)        -0.5(5)
C(14B)      C(15B)     C(16B)     C(17B)        -2.3(5)
C(13B)      N(4B)      C(17B)     C(16B)        -1.0(5)
C(13B)      N(4B)      C(17B)     C(18B)       178.6(3)
C(15B)      C(16B)     C(17B)     N(4B)          3.1(5)
C(15B)      C(16B)     C(17B)     C(18B)      -176.5(3)
```

Table 33. Summary of X-Ray Crystallographic Data for **118c**

```
Empirical Formula                 C19 H25 F3 N4 O3 S

Color of Crystal:                 colorless

Crystal Dimensions were:          0.20 x 0.20 x 0.10 mm.

Space Group:                      P2(1)

Cell Dimensions (at 128(2) K; 5820 reflections)
                 a =          9.6256(10)
                 b =         17.2404(17)
                 c =         12.5115(13)
             alpha =         90
              beta =         92.696(2)
             gamma =         90

Z (Molecules/cell):                4

Volume:                          2074.0(4)
```

```
Calculated Density:              1.430

Wavelength:                      0.71073

Molecular Weight:                446.49

F(000):                          936

Linear Absorption Coefficient:   0.211
```

Figure 40. Numbering System for **118e**
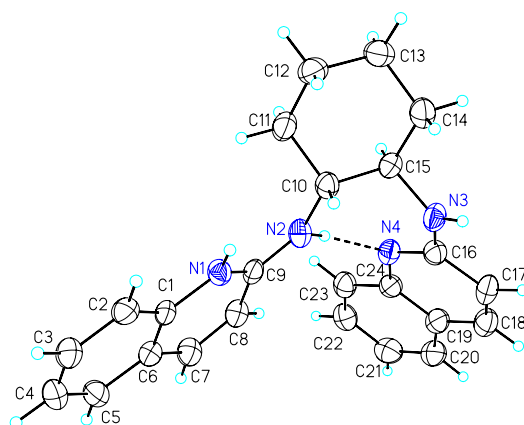
Note: Data were collected on a Bruker SMART 6000 sealed-tube system comprising a three-circle platform goniostat, an HOG crystal monochromator, a four kilopixel by four kilopixel single-chip CCD-based detector, a K761 high voltage generator, and a PC interface running Bruker's SMART software.

Table 34. Fractional Coordinates and Isotropic Thermal Parameters for **118e**

Atom	x	y	z	Uiso
N(1)	253(1)	4431(3)	3529(3)	29(1)
N(2)	-702(1)	4753(3)	2199(3)	32(1)
N(3)	-1296(1)	6041(3)	-256(3)	34(1)
N(4)	-1655(1)	4111(3)	74(2)	31(1)
C(1)	709(2)	3649(3)	4243(3)	28(1)
C(2)	1244(2)	4178(4)	4990(3)	33(1)
C(3)	1675(2)	3371(4)	5690(3)	40(1)
C(4)	1603(2)	2072(4)	5674(4)	42(1)
C(5)	1083(2)	1548(4)	4934(3)	38(1)
C(6)	625(2)	2337(4)	4199(3)	32(1)
C(7)	73(2)	1852(4)	3414(3)	35(1)
C(8)	-361(2)	2643(3)	2765(3)	33(1)

C(9)	-273(1)	3989(3)	2828(3)	27(1)
C(10)	-689(1)	6144(3)	2123(3)	30(1)
C(11)	-687(2)	6760(4)	3368(3)	38(1)
C(12)	-687(2)	8200(4)	3290(3)	39(1)
C(13)	-1210(2)	8659(4)	2163(4)	41(1)
C(14)	-1239(2)	8021(4)	906(3)	39(1)
C(15)	-1234(2)	6588(3)	1008(3)	31(1)
C(16)	-1550(2)	4934(4)	-713(3)	32(1)
C(17)	-1704(2)	4647(4)	-2072(3)	39(1)
C(18)	-1951(2)	3526(4)	-2534(4)	40(1)
C(19)	-2069(1)	2622(4)	-1713(3)	36(1)
C(20)	-2295(2)	1414(4)	-2115(3)	40(1)
C(21)	-2375(2)	575(4)	-1254(4)	45(1)
C(22)	-2225(2)	930(4)	40(4)	39(1)
C(23)	-1999(2)	2101(4)	465(3)	37(1)
C(24)	-1905(1)	2967(4)	-396(3)	31(1)
S(1)	917(1)	7919(1)	3095(1)	37(1)
O(1)	958(2)	7748(4)	1868(3)	86(1)
O(2)	637(1)	9036(3)	3240(3)	46(1)
O(3)	770(1)	6801(3)	3624(3)	67(1)
C(25)	1661(2)	8172(4)	4186(4)	48(1)
F(1)	1880(1)	9188(4)	3841(4)	98(1)
F(2)	1698(1)	8372(4)	5370(3)	79(1)
F(3)	1991(1)	7185(3)	4196(3)	71(1)
C(1S)	0	4378(7)	0	59(2)
C(2S)	0	2958(7)	0	44(1)
C(3S)	-499(2)	2271(5)	-625(4)	51(1)
C(4S)	-500(2)	971(5)	-618(4)	59(1)
C(5S)	0	292(8)	0	61(2)
H(1N)	36(2)	525(5)	353(5)	60(14)
H(2N)	-109(2)	442(5)	162(5)	61(14)
H(3N)	-120(2)	648(5)	-71(4)	48(13)
H(2)	131	507	501	40
H(3)	204	372	621	47
H(4)	191	154	617	50
H(5)	103	66	492	46
H(7)	1	96	335	42
H(8)	-73	231	226	40
H(10)	-34	642	195	36
H(11A)	-103	648	354	45
H(11B)	-34	648	410	45
H(12A)	-33	849	318	46
H(12B)	-69	856	410	46
H(13A)	-119	959	208	50
H(13B)	-156	846	233	50
H(14A)	-159	829	20	46
H(14B)	-91	830	69	46
H(15)	-157	633	121	37
H(17)	-163	524	-263	47
H(18)	-205	334	-342	48
H(20)	-239	117	-299	48
H(21)	-253	-24	-153	54
H(22)	-228	35	63	47
H(23)	-191	233	134	44
H(1SA)	39	469	49	88
H(1SB)	-26	469	40	88
H(1SC)	-13	469	-89	88
H(3SA)	-85	271	-107	62
H(4SA)	-85	53	-104	70
H(5S)	0	-70(9)	0	73

Notes:

166

1) Fractional coordinates are X 10**4 for non-hydrogen
atoms and X 10**3 for hydrogen atoms. Uiso values are all
X 10**3.
2) Isotropic values for those atoms refined anisotropically
are calculated as one third of the trace of the
orthogonalized
Uij tensor.
3) Parameters without standard deviations were not varied.

Table 35. Anisotropic displacement parameters for **118e**

Atom	U11	U22	U33	U23	U13	U12
N(1)	27(1)	29(2)	26(1)	-1(1)	5(1)	0(1)
N(2)	28(2)	36(2)	27(1)	3(1)	6(1)	-2(1)
N(3)	43(2)	35(2)	25(1)	5(1)	14(1)	-2(2)
N(4)	30(1)	38(2)	25(1)	1(1)	8(1)	0(1)
C(1)	27(2)	37(2)	18(2)	-2(1)	5(1)	4(1)
C(2)	33(2)	36(2)	30(2)	-6(1)	9(1)	1(2)
C(3)	31(2)	51(2)	29(2)	-6(2)	3(2)	4(2)
C(4)	36(2)	46(2)	34(2)	0(2)	3(2)	10(2)
C(5)	40(2)	34(2)	35(2)	-3(2)	6(2)	8(2)
C(6)	34(2)	37(2)	24(2)	0(1)	11(1)	4(2)
C(7)	41(2)	29(2)	32(2)	2(1)	11(2)	-4(2)
C(8)	34(2)	36(2)	26(2)	0(1)	8(1)	-3(2)
C(9)	29(2)	35(2)	18(1)	2(1)	9(1)	0(2)
C(10)	26(2)	35(2)	27(2)	1(1)	7(1)	1(2)
C(11)	37(2)	49(2)	25(2)	-1(2)	8(1)	4(2)
C(12)	37(2)	42(2)	35(2)	-8(2)	11(2)	4(2)
C(13)	43(2)	36(2)	42(2)	-4(2)	13(2)	6(2)
C(14)	39(2)	40(2)	32(2)	3(2)	8(2)	3(2)
C(15)	33(2)	34(2)	24(2)	-2(1)	8(1)	1(2)
C(16)	30(2)	36(2)	29(2)	2(1)	10(1)	3(2)
C(17)	42(2)	49(2)	25(2)	5(2)	11(2)	-1(2)
C(18)	36(2)	50(2)	29(2)	0(2)	8(2)	0(2)
C(19)	26(2)	47(2)	30(2)	-3(2)	5(1)	3(2)
C(20)	35(2)	45(2)	35(2)	-7(2)	6(2)	-2(2)
C(21)	39(2)	40(2)	50(2)	-9(2)	10(2)	-3(2)
C(22)	28(2)	44(2)	42(2)	5(2)	9(2)	-2(2)
C(23)	29(2)	45(2)	33(2)	3(2)	8(2)	1(2)
C(24)	25(2)	36(2)	31(2)	-1(2)	9(1)	2(2)
S(1)	43(1)	31(1)	32(1)	-3(1)	9(1)	3(1)
O(1)	111(3)	109(3)	37(2)	-3(2)	27(2)	57(3)
O(2)	44(2)	43(2)	47(2)	-8(1)	14(1)	2(1)
O(3)	44(2)	45(2)	83(2)	15(2)	-10(2)	-13(2)
C(25)	42(2)	43(3)	64(3)	-5(2)	26(2)	-6(2)
F(1)	58(2)	76(2)	166(4)	17(2)	50(2)	-17(2)
F(2)	45(2)	127(3)	49(2)	-26(2)	-3(1)	2(2)
F(3)	48(2)	67(2)	90(2)	-13(2)	14(1)	15(1)
C(1S)	67(4)	59(4)	69(4)	0	46(4)	0
C(2S)	39(3)	65(4)	33(2)	0	20(2)	0
C(3S)	37(2)	72(3)	44(2)	-5(2)	14(2)	5(2)
C(4S)	45(2)	68(3)	58(3)	-10(2)	13(2)	-6(2)
C(5S)	56(4)	53(4)	70(5)	0	18(3)	0

Form of the anisotropic thermal parameter:
   exp{ -2 pi**2 [h**2 (a*)**2 U11 + ... + 2 h k (a*) (b*) U12] }
All values are X 10**3

Table 36. Bond lengths [Å] for **118e**

A	B	Distance
N(1)	C(9)	1.348(4)
N(1)	C(1)	1.399(4)
N(1)	H(1N)	0.91(6)
N(2)	C(9)	1.322(5)
N(2)	C(10)	1.473(5)
N(2)	H(2N)	1.01(5)
N(3)	C(16)	1.339(5)
N(3)	C(15)	1.480(4)
N(3)	H(3N)	0.80(5)
N(4)	C(16)	1.331(4)
N(4)	C(24)	1.374(5)
C(1)	C(6)	1.399(5)
C(1)	C(2)	1.410(5)
C(2)	C(3)	1.373(5)
C(2)	H(2)	0.9500
C(3)	C(4)	1.383(6)
C(3)	H(3)	0.9500
C(4)	C(5)	1.378(6)
C(4)	H(4)	0.9500
C(5)	C(6)	1.412(5)
C(5)	H(5)	0.9500
C(6)	C(7)	1.436(5)
C(7)	C(8)	1.353(5)
C(7)	H(7)	0.9500
C(8)	C(9)	1.436(5)
C(8)	H(8)	0.9500
C(10)	C(11)	1.533(5)
C(10)	C(15)	1.544(4)
C(10)	H(10)	1.0000
C(11)	C(12)	1.524(6)
C(11)	H(11A)	0.9900
C(11)	H(11B)	0.9900
C(12)	C(13)	1.525(5)
C(12)	H(12A)	0.9900
C(12)	H(12B)	0.9900
C(13)	C(14)	1.534(5)
C(13)	H(13A)	0.9900
C(13)	H(13B)	0.9900
C(14)	C(15)	1.516(6)
C(14)	H(14A)	0.9900
C(14)	H(14B)	0.9900
C(15)	H(15)	1.0000
C(16)	C(17)	1.453(5)
C(17)	C(18)	1.347(6)
C(17)	H(17)	0.9500
C(18)	C(19)	1.429(5)
C(18)	H(18)	0.9500
C(19)	C(20)	1.402(6)
C(19)	C(24)	1.420(4)
C(20)	C(21)	1.376(6)
C(20)	H(20)	0.9500
C(21)	C(22)	1.403(5)
C(21)	H(21)	0.9500
C(22)	C(23)	1.370(6)
C(22)	H(22)	0.9500
C(23)	C(24)	1.409(5)
C(23)	H(23)	0.9500
S(1)	O(2)	1.414(3)
S(1)	O(1)	1.422(3)
S(1)	O(3)	1.429(4)
S(1)	C(25)	1.836(4)

```
C(25)          F(2)          1.308(5)
C(25)          F(1)          1.327(5)
C(25)          F(3)          1.331(5)
C(1S)          C(2S)         1.500(10)
C(1S)          H(1SA)        0.9800
C(1S)          H(1SB)        0.9800
C(1S)          H(1SC)        0.9800
C(2S)          C(3S)         1.393(6)
C(2S)          C(3S)#1       1.393(6)
C(3S)          C(4S)         1.373(7)
C(3S)          H(3SA)        0.9500
C(4S)          C(5S)         1.389(6)
C(4S)          H(4SA)        0.9500
C(5S)          C(4S)#1       1.389(6)
C(5S)          H(5S)         1.05(9)
```

Symmetry transformations used to generate equivalent atoms:
   #1 -x,y,-z

Table 37. Bond Angles for **118e**

A	B	C	Angle
C(9)	N(1)	C(1)	123.3(3)
C(9)	N(1)	H(1N)	125(3)
C(1)	N(1)	H(1N)	112(3)
C(9)	N(2)	C(10)	127.5(3)
C(9)	N(2)	H(2N)	122(3)
C(10)	N(2)	H(2N)	110(3)
C(16)	N(3)	C(15)	124.9(3)
C(16)	N(3)	H(3N)	119(3)
C(15)	N(3)	H(3N)	116(3)
C(16)	N(4)	C(24)	119.7(3)
N(1)	C(1)	C(6)	118.9(3)
N(1)	C(1)	C(2)	120.4(3)
C(6)	C(1)	C(2)	120.7(3)
C(3)	C(2)	C(1)	118.1(4)
C(3)	C(2)	H(2)	121.0
C(1)	C(2)	H(2)	121.0
C(2)	C(3)	C(4)	122.4(4)
C(2)	C(3)	H(3)	118.8
C(4)	C(3)	H(3)	118.8
C(5)	C(4)	C(3)	119.8(4)
C(5)	C(4)	H(4)	120.1
C(3)	C(4)	H(4)	120.1
C(4)	C(5)	C(6)	120.0(4)
C(4)	C(5)	H(5)	120.0
C(6)	C(5)	H(5)	120.0
C(1)	C(6)	C(5)	119.0(3)
C(1)	C(6)	C(7)	118.3(3)
C(5)	C(6)	C(7)	122.7(4)
C(8)	C(7)	C(6)	120.9(3)
C(8)	C(7)	H(7)	119.6
C(6)	C(7)	H(7)	119.6
C(7)	C(8)	C(9)	120.4(3)
C(7)	C(8)	H(8)	119.8
C(9)	C(8)	H(8)	119.8
N(2)	C(9)	N(1)	122.1(3)
N(2)	C(9)	C(8)	119.8(3)
N(1)	C(9)	C(8)	118.1(3)
N(2)	C(10)	C(11)	111.3(3)
N(2)	C(10)	C(15)	108.6(3)
C(11)	C(10)	C(15)	107.9(3)

N(2)	C(10)	H(10)	109.7
C(11)	C(10)	H(10)	109.7
C(15)	C(10)	H(10)	109.7
C(12)	C(11)	C(10)	111.9(3)
C(12)	C(11)	H(11A)	109.2
C(10)	C(11)	H(11A)	109.2
C(12)	C(11)	H(11B)	109.2
C(10)	C(11)	H(11B)	109.2
H(11A)	C(11)	H(11B)	107.9
C(11)	C(12)	C(13)	110.3(3)
C(11)	C(12)	H(12A)	109.6
C(13)	C(12)	H(12A)	109.6
C(11)	C(12)	H(12B)	109.6
C(13)	C(12)	H(12B)	109.6
H(12A)	C(12)	H(12B)	108.1
C(12)	C(13)	C(14)	110.6(3)
C(12)	C(13)	H(13A)	109.5
C(14)	C(13)	H(13A)	109.5
C(12)	C(13)	H(13B)	109.5
C(14)	C(13)	H(13B)	109.5
H(13A)	C(13)	H(13B)	108.1
C(15)	C(14)	C(13)	111.9(3)
C(15)	C(14)	H(14A)	109.2
C(13)	C(14)	H(14A)	109.2
C(15)	C(14)	H(14B)	109.2
C(13)	C(14)	H(14B)	109.2
H(14A)	C(14)	H(14B)	107.9
N(3)	C(15)	C(14)	108.8(3)
N(3)	C(15)	C(10)	113.6(3)
C(14)	C(15)	C(10)	110.1(3)
N(3)	C(15)	H(15)	108.0
C(14)	C(15)	H(15)	108.0
C(10)	C(15)	H(15)	108.0
N(4)	C(16)	N(3)	120.1(3)
N(4)	C(16)	C(17)	120.8(3)
N(3)	C(16)	C(17)	119.1(3)
C(18)	C(17)	C(16)	119.4(3)
C(18)	C(17)	H(17)	120.3
C(16)	C(17)	H(17)	120.3
C(17)	C(18)	C(19)	121.1(3)
C(17)	C(18)	H(18)	119.5
C(19)	C(18)	H(18)	119.5
C(20)	C(19)	C(24)	119.6(3)
C(20)	C(19)	C(18)	123.9(3)
C(24)	C(19)	C(18)	116.4(3)
C(21)	C(20)	C(19)	120.6(3)
C(21)	C(20)	H(20)	119.7
C(19)	C(20)	H(20)	119.7
C(20)	C(21)	C(22)	119.7(4)
C(20)	C(21)	H(21)	120.2
C(22)	C(21)	H(21)	120.2
C(23)	C(22)	C(21)	121.2(4)
C(23)	C(22)	H(22)	119.4
C(21)	C(22)	H(22)	119.4
C(22)	C(23)	C(24)	120.1(3)
C(22)	C(23)	H(23)	120.0
C(24)	C(23)	H(23)	120.0
N(4)	C(24)	C(23)	118.5(3)
N(4)	C(24)	C(19)	122.5(3)
C(23)	C(24)	C(19)	118.9(4)
O(2)	S(1)	O(1)	115.6(2)
O(2)	S(1)	O(3)	115.2(2)
O(1)	S(1)	O(3)	114.6(3)

```
O(2)          S(1)          C(25)         103.33(19)
O(1)          S(1)          C(25)         103.9(2)
O(3)          S(1)          C(25)         101.67(19)
F(2)          C(25)         F(1)          106.3(4)
F(2)          C(25)         F(3)          107.9(4)
F(1)          C(25)         F(3)          108.1(3)
F(2)          C(25)         S(1)          111.7(3)
F(1)          C(25)         S(1)          110.9(3)
F(3)          C(25)         S(1)          111.7(3)
C(2S)         C(1S)         H(1SA)        109.5
C(2S)         C(1S)         H(1SB)        109.5
H(1SA)        C(1S)         H(1SB)        109.5
C(2S)         C(1S)         H(1SC)        109.5
H(1SA)        C(1S)         H(1SC)        109.5
H(1SB)        C(1S)         H(1SC)        109.5
C(3S)         C(2S)         C(3S)#1       117.2(7)
C(3S)         C(2S)         C(1S)         121.4(3)
C(3S)#1       C(2S)         C(1S)         121.4(3)
C(4S)         C(3S)         C(2S)         121.4(5)
C(4S)         C(3S)         H(3SA)        119.3
C(2S)         C(3S)         H(3SA)        119.3
C(3S)         C(4S)         C(5S)         121.0(5)
C(3S)         C(4S)         H(4SA)        119.5
C(5S)         C(4S)         H(4SA)        119.5
C(4S)#1       C(5S)         C(4S)         117.9(7)
C(4S)#1       C(5S)         H(5S)         121.1(4)
C(4S)         C(5S)         H(5S)         121.1(4)


Symmetry transformations used to generate equivalent atoms:
   #1 -x,y,-z
```

Table 38. Torsion Angles for **118e**

A	B	C	D	Torsion Angle
C(9)	N(1)	C(1)	C(6)	2.2(5)
C(9)	N(1)	C(1)	C(2)	-177.9(3)
N(1)	C(1)	C(2)	C(3)	178.9(3)
C(6)	C(1)	C(2)	C(3)	-1.2(5)
C(1)	C(2)	C(3)	C(4)	0.7(6)
C(2)	C(3)	C(4)	C(5)	0.0(7)
C(3)	C(4)	C(5)	C(6)	-0.2(6)
N(1)	C(1)	C(6)	C(5)	-179.1(3)
C(2)	C(1)	C(6)	C(5)	1.0(5)
N(1)	C(1)	C(6)	C(7)	0.4(5)
C(2)	C(1)	C(6)	C(7)	-179.5(3)
C(4)	C(5)	C(6)	C(1)	-0.2(5)
C(4)	C(5)	C(6)	C(7)	-179.7(4)
C(1)	C(6)	C(7)	C(8)	-2.1(5)
C(5)	C(6)	C(7)	C(8)	177.4(3)
C(6)	C(7)	C(8)	C(9)	1.3(5)
C(10)	N(2)	C(9)	N(1)	1.2(5)
C(10)	N(2)	C(9)	C(8)	-178.2(3)
C(1)	N(1)	C(9)	N(2)	177.6(3)
C(1)	N(1)	C(9)	C(8)	-3.0(5)
C(7)	C(8)	C(9)	N(2)	-179.4(3)
C(7)	C(8)	C(9)	N(1)	1.2(5)
C(9)	N(2)	C(10)	C(11)	-76.4(4)
C(9)	N(2)	C(10)	C(15)	165.0(3)
N(2)	C(10)	C(11)	C(12)	-178.7(3)
C(15)	C(10)	C(11)	C(12)	-59.7(4)
C(10)	C(11)	C(12)	C(13)	58.3(4)
C(11)	C(12)	C(13)	C(14)	-54.5(4)

171

```
     C(12)      C(13)      C(14)      C(15)         55.5(4)
     C(16)      N(3)       C(15)      C(14)       -149.3(3)
     C(16)      N(3)       C(15)      C(10)         87.6(4)
     C(13)      C(14)      C(15)      N(3)         176.8(3)
     C(13)      C(14)      C(15)      C(10)        -58.0(4)
     N(2)       C(10)      C(15)      N(3)         -58.1(4)
     C(11)      C(10)      C(15)      N(3)        -178.9(3)
     N(2)       C(10)      C(15)      C(14)        179.5(3)
     C(11)      C(10)      C(15)      C(14)         58.8(4)
     C(24)      N(4)       C(16)      N(3)        -178.7(3)
     C(24)      N(4)       C(16)      C(17)          1.0(5)
     C(15)      N(3)       C(16)      N(4)         -14.9(5)
     C(15)      N(3)       C(16)      C(17)        165.4(3)
     N(4)       C(16)      C(17)      C(18)         -0.8(5)
     N(3)       C(16)      C(17)      C(18)        178.9(4)
     C(16)      C(17)      C(18)      C(19)          0.7(6)
     C(17)      C(18)      C(19)      C(20)       -176.3(4)
     C(17)      C(18)      C(19)      C(24)         -0.8(5)
     C(24)      C(19)      C(20)      C(21)          1.9(5)
     C(18)      C(19)      C(20)      C(21)        177.3(4)
     C(19)      C(20)      C(21)      C(22)         -0.5(6)
     C(20)      C(21)      C(22)      C(23)          0.0(6)
     C(21)      C(22)      C(23)      C(24)         -1.0(5)
     C(16)      N(4)       C(24)      C(23)        178.5(3)
     C(16)      N(4)       C(24)      C(19)         -1.2(5)
     C(22)      C(23)      C(24)      N(4)        -177.2(3)
     C(22)      C(23)      C(24)      C(19)          2.4(5)
     C(20)      C(19)      C(24)      N(4)         176.8(3)
     C(18)      C(19)      C(24)      N(4)           1.0(5)
     C(20)      C(19)      C(24)      C(23)         -2.9(5)
     C(18)      C(19)      C(24)      C(23)       -178.6(3)
     O(2)       S(1)       C(25)      F(2)          57.7(4)
     O(1)       S(1)       C(25)      F(2)         178.8(3)
     O(3)       S(1)       C(25)      F(2)         -62.0(4)
     O(2)       S(1)       C(25)      F(1)         -60.7(3)
     O(1)       S(1)       C(25)      F(1)          60.4(4)
     O(3)       S(1)       C(25)      F(1)         179.6(3)
     O(2)       S(1)       C(25)      F(3)         178.6(3)
     O(1)       S(1)       C(25)      F(3)         -60.3(4)
     O(3)       S(1)       C(25)      F(3)          58.9(3)
     C(3S)#1    C(2S)      C(3S)      C(4S)          0.4(3)
     C(1S)      C(2S)      C(3S)      C(4S)       -179.6(3)
     C(2S)      C(3S)      C(4S)      C(5S)         -0.9(6)
     C(3S)      C(4S)      C(5S)      C(4S)#1        0.4(3)

     Symmetry transformations used to generate equivalent atoms:
        #1 -x,y,-z
```

Table 39. Summary of X-Ray Crystallographic Data for **118e**

```
Empirical Formula                 C28.50 H29 F3 N4 O3 S

Color of Crystal:                 colorless

Crystal Dimensions were:          0.17 x 0.13 x 0.11 mm.

Space Group:                      C2

Cell Dimensions (at 130(2) K; 1487 reflections)
                  a =             25.147(4)
```

```
               b =              10.5601(16)
               c =              11.1691(17)
           alpha =              90
            beta =             111.682(8)
           gamma =              90

Z (Molecules/cell):             4

Volume:                        2756.1(7)

Calculated Density:            1.361

Wavelength:                    0.71073

Molecular Weight:              564.62

F(000):                        1180

Linear Absorption Coefficient: 0.175
```

Ryan A. Yoder

603 Mattern Orchard Dr Apt 2A
Hollidaysburg, PA 16648
ryanayoder@gmail.com
(615) 495-2063

Professional and Research Experience:

2007-present   **Senior Research and Development Chemist**
Albemarle Corporation, Tyrone, Pennsylvania
*Duties include new process route selection and optimization,
introducing process into plant, and process troubleshooting*

2002-2007   **Graduate Research Fellow with Prof. Jeffrey N. Johnston**
Indiana University, Bloomington, Indiana
*Chiral Proton Catalysis: Design and Development of
Enantioselective Aza-Henry and Diels-Alder Reactions*

2000-2002   **Undergraduate Research with Prof. Jeffrey N. Johnston**
Indiana University, Bloomington, Indiana
*Development of Axially Chiral β-Diketimines for Asymmetric
Synthesis*

Education:

2002-2007   Ph.D. Studies in Synthetic Organic Chemistry, Indiana University,
Bloomington, Indiana

1998-2002   B.S. Chemistry, Indiana University, Bloomington, Indiana

Honors and Awards:

2007-2008   Albemarle Technology Award for Spiro-Dione Process
2007   Albemarle Technology Award for Green Bromination Process
2005-2006   ACS Division of Organic Chemistry Fellowship
2004   McCormick Science Grant
2002-2003   Indiana University Graduate Fellowship
2002   GAANN Summer Fellowship
2001   Eli Lilly Undergraduate Research in Organic Chemistry Fellowship
1998-2000   Indiana University Scholarship

Publications and Presentations:

"Chiral Proton Catalysis: Enantioselective Brønsted Acid Catalyzed Additions of Nitroacetic Acid Derivatives as Glycine Equivalents " Singh, A.; Yoder, R. A.; Shen, B.; Johnston, J. N. *J. Am. Chem. Soc.* **2007**, *129*, 3466.

"Chiral Proton Catalysis: pK_a Determination for a BAM-HX Brønsted Acid" Hess, A.; Yoder, R. A.; Johnston, J. N. *SynLett* **2006**, *1*, 147.

"A Case Study in Biomimetic Total Synthesis: Polyolefin Carbocyclizations to Terpenes and Steroids" Yoder, R. A.; Johnston, J. N. *Chem. Rev.* **2005**, *105*, 4730.

"Chiral Proton Catalysis: A Catalytic Enantioselective Direct aza-Henry Reaction" Nugent, B. M.; Yoder, R. A.; Johnston, J. N. *J. Am. Chem. Soc.* **2004**, *126*, 3418-3419.

(Highlighted in Science Concentrates, *Chemical & Engineering News*, March 22, 2004)

"IAN Amines: Chiral C_2-Symmetric Zirconium(IV) Complexes from Readily Modified Axially Chiral C_1-Symmetric β-Diketimines" Cortright, S. B.; Huffman, J. C.; Yoder, R. A.; Coalter III, J. N.; Johnston, J. N. *Organometallics* **2004**, *23*, 2238-2250.

"IAN-Amines: Determination of the Atropisomerization Barrier" Cortright, S. B.; Yoder, R. A.; Johnston, J. N. Heterocycles (Special Issue in Honor of Leo A. Paquette's 70th Birthday), **2004**, *62,* 223-227.

"Chiral Proton Catalysis: Design and Development of an Enantioselective Aza-Henry Reaction," Ryan A. Yoder, Jeffrey N. Johnston. Presented at the Organic Reactions & Processes Gordon Research Conference, July 31-August 05, 2005 in Providence, Rhode Island.

"Chiral Proton Catalysis: Design and Development of an Enantioselective Aza-Henry Reaction," Ryan A. Yoder, Jeffrey N. Johnston. Presented at the 40th National Organic Symposium, June 3-7, 2007 in Durham, North Carolina.

References:

Jeffrey N. Johnston
Department of Chemistry
Vanderbilt University
7962 Stevenson Center
Station B 351822
Nashville, TN 37235
(615) 322-7376;
jeffrey.n.johnston@vanderbilt.edu

John Pascavage
Research and Development Manager
Albemarle Corporation
2 Adams Avenue,
Tyrone, PA 16686
(814) 684-7223;
john.pascavage@albemarle.com